



UNIVERSITÀ DEGLI STUDI DI PALERMO

Dottorato di Ricerca in Scienze Chimiche
Dipartimento di Fisica e Chimica
S.S.D. – CHIM/06

SINTESI E PROPRIETÀ DI SALI ORGANICI POLICATIONICI UTILIZZATI COME MEZZI DI REAZIONE

Synthesis and properties of policationic organic salts
used as reaction media

IL DOTTORE
Carla Rizzo

IL COORDINATORE
Prof. Paolo Lo Meo

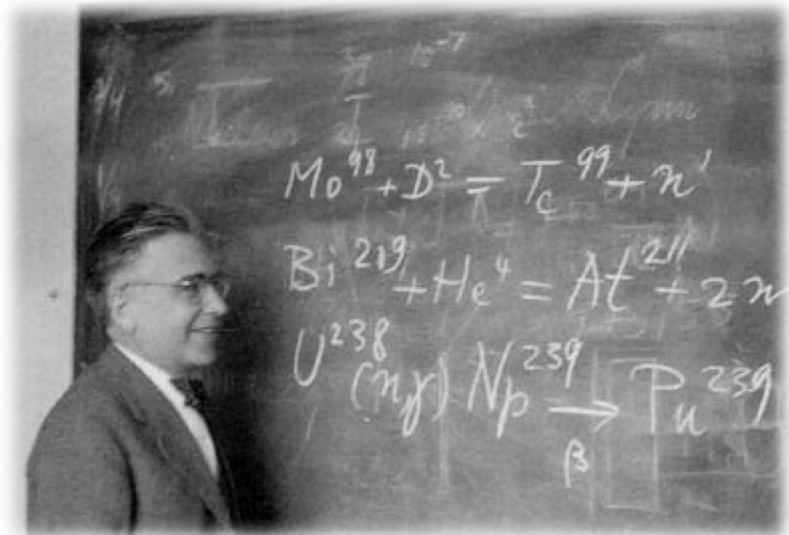
IL TUTOR
Prof.ssa Francesca D'Anna

IL CO-TUTOR
Prof. Renato Noto

CICLO XXVI
Anno 2016

*The science of today is
the technology of tomorrow.*

Edward Teller



da *A mind always in motion* di Emilio Segrè

1937, via Archirafi, Palermo.
In una città definita "penurious" viene scoperto
il primo elemento artificiale nel mondo
e l'unico in Italia.

Table of contents

Abstract	
Introduction	1
1. <i>Monocationic Organic Salts: Ionic Liquids</i>	2
2. <i>Imidazolium Salts</i>	5
3. <i>Dicationic Organic Salts (DOSs)</i>	9
4. <i>Tricationic Organic Salts (TOSs)</i>	12
Chapter 1: Task Specific Ionic liquids	15
Results and discussion	23
1. <i>Synthesis of functionalised dicationic organic salts</i>	25
2. <i>Solution behaviour of functionalised DOSs: presence of conformational equilibria</i>	28
3. <i>Thermal properties of functionalised DOSs</i>	33
4. <i>Catalytic ability of TSILs studied.</i>	38
4. 1. <i>The mononuclear rearrangement of heterocycles of (Z)-phenylhydrazone of 3-benzoyl-5-phenyl-1,2,4-oxadiazole into the corresponding triazole</i>	38
4. 2. <i>The Michael addition of trans-chalcone to malononitrile</i>	46
Experimental section	
1. <i>Materials and methods</i>	58
2. 1. <i>General procedure for the synthesis of the neutral precursor bti</i>	61
2. 2. <i>General procedure for the synthesis of the dicationic bromide salt [2C₈bti][Br]₂</i>	61
2. 3. <i>General procedure for the classical anion exchange</i>	62
2. 4. <i>General procedure for anionic exchange on basic resin</i>	62
Chapter 2: Low-Molecular Weight Gelators	68
Results and discussion	77
1. <i>Functionalised dicationic organic salts: gelators of ionic liquids</i>	77
1. 1. <i>Synthesis of organic salts as gelators</i>	79
1. 2. <i>Thermal stability of dipyrrolidinium salts</i>	80
1. 3. <i>Gelation tests</i>	81
1. 4. <i>Thermal stability of gel phases</i>	85
1. 5. <i>Kinetic of gel formation</i>	86
1. 6. <i>Self-healing ability of ionogels</i>	89
1. 7. <i>Conductivity of ionogels</i>	91
2. <i>Gel phases formed by non-stoichiometric organic salts</i>	94
2. 1. <i>Synthesis of DOSs</i>	95

2. 2. <i>Thermal stability of DOSs</i>	96
2. 3. <i>Gelation tests and thermal stability of DOSs</i>	98
2. 4. <i>Morphology of gel phases</i>	103
2. 5. <i>Mechanical properties</i>	106
2. 6. <i>Self-healing ability of gel phases</i>	111
2. 7. <i>Kinetic formation of gel phases: rheology measurements</i>	114
2. 8. <i>Kinetic formation of gel phases: RLS and UV-vis</i>	116
2. 9. <i>Powder X-ray diffraction (XRD)</i>	119
3. <i>Two-component hydrogels formed by cyclodextrins and DOSs</i>	122
3. 1. <i>Gelation tests</i>	124
3. 2. <i>Investigation on the role of CDs in hydrogel formation</i>	125
3. 3. <i>Thermal stability of hydrogels</i>	131
3. 4. <i>Kinetic of formation of hydrogels</i>	132
3. 5. <i>Self-healing ability of hydrogels</i>	134
3. 6. <i>Morphology of hydrogels</i>	134
4. <i>DOSs and gels exerting antimicrobial activity</i>	137
4. 1. <i>Melting process of DOSs</i>	139
4. 2. <i>Gelation tests and thermal stability of gel phases</i>	140
4. 3. <i>Self-healing ability of gel phases</i>	142
4. 4. <i>Morphology of gel phases</i>	142
4. 5. <i>Kinetic of gel formation</i>	144
4. 6. <i>Application of the gels: test of antimicrobial activity</i>	145
Experimental section	
1. <i>Materials and methods</i>	153
2. 1. <i>General procedure for the synthesis of the neutral precursor btp</i>	159
2. 2. <i>General procedure for the synthesis of the dipyrrolidinium dibromide salt</i>	160
2. 3. <i>General procedure for anion exchange on resin as reported in Chapter 1</i>	160
3. 1. <i>Procedure for the synthesis of neutral precursors diimidazole-methylenbenzene</i>	161
3. 2. <i>Procedure for the synthesis of bromide salts precursors</i>	162
3. 3. <i>General procedure for anion exchange on resin as reported in Chapter 1</i>	163
4. 1. <i>DOS for two-component hydrogels</i>	166
5. 1. <i>Aminoacid based DOSs</i>	166
Conclusions	168
List of abbreviations and acronyms	172
Acknowledgements	I
Curriculum vitae	II

Abstract

La sintesi e lo studio delle proprietà di nuovi sali organici policationici rappresentano il fulcro della presente tesi di dottorato. In particolar modo è stato possibile dimostrare come la diversa combinazione fra cationi e anioni moduli le proprietà dei sali organici e ne permetta l'applicazione in diversi ambiti.

Sono stati sintetizzati sali dicationici formati da una struttura cationica comprensiva di uno spaziatore aromatico che porta due cationi di diottilimidazolio e un imidazolo neutro come funzionalità basica, e da mono- e dianioni che differiscono per forma dimensione e abilità coordinante. Una peculiarità dei sali è la presenza in soluzione di tre isomeri conformazionali attribuita all'alta flessibilità della struttura cationica; la presenza di questi conformeri così come le proprietà termiche dei sali sono fortemente influenzate dalla natura dell'anione associato al catione. Inoltre, i sali, presentando temperature di fusione inferiori a 100 °C, rientrano nella classe dei liquidi ionici funzionalizzati, cosiddetti *Task Specific Ionic liquids* (TSILs). Questa caratteristica ha permesso di utilizzarli come mezzi di reazione per lo studio di due reazioni organiche base-catalizzate: la reazione di trasposizione eterociclica mononucleare dello (*Z*)-fenilidrazone del 3-benzoil-5-fenil-1,2,4-ossadiazolo nel corrispondente triazolo e la reazione di addizione di Michael del malononitrile al *t*-calcone. I TSILs risultano essere degli ottimi mezzi di reazione in termini di tempi e rese di reazione; inoltre, la diversa natura dell'anione ha un ruolo determinante anche sul decorso delle reazioni base-catalizzate studiate. Queste ultime risultano favorite dalla presenza di dianioni aventi spaziatori alifatici, mentre quelli aventi spaziatori aromatici hanno mostrato una spiccata abilità a gelificare in soluzione di liquidi ionici. Pertanto sono state studiate le proprietà di questi materiali *soft* che rappresentano una nuova classe di gel supramolecolari in forte espansione grazie all'elevata stabilità termica e conduttività. In questo caso, si è visto come le proprietà degli ionogel siano influenzate sia dall'anione sia dal catione del *gelator*, dato che sono studiati anche ionogel formati da sali di dipirrolidinio aventi come funzionalità neutra la pirrolidina. Inoltre, grazie alla presenza della funzionalità basica nella struttura del *gelator*, i materiali *soft* ottenuti potranno essere utilizzati per condurre reazioni in ambiente confinato.

La formazione di gel supramolecolari è stata studiata prendendo in considerazione anche sali dicationici non funzionalizzati come *gelator*. In particolare, sali di diimidazolio *meta* e *para* sostituiti con di-, tri- e tetranioni sono stati sintetizzati per valutare un possibile effetto della differente stechiometria fra cationi e anioni sull' "impacchettamento" del *gelator* nel gel. Questi sali hanno portato alla formazione di organo- e ionogel con buone proprietà meccaniche e termiche.

La formazione di idrogel, invece, è stata ottenuta dall'interazione tra sali dicationici monoanionici con α - o β -ciclodestrina non modificata. In questo caso, oltre allo studio delle proprietà dei materiali *soft*, è stato dimostrato che la formazione dei gel deriva dalla precedente interazione fra il sale e la ciclodestrina, attraverso interazioni supramolecolari di tipo *host-guest*.

Infine, sali dicationici di imidazolio associati ad alcuni derivati di amminoacidi o dipeptidi hanno portato alla formazione sia di idrogel che di ionogel con spiccata attività antimicrobica, attribuibile non soltanto ai *gelator* ma al sistema supramolecolare nel suo complesso.

I sali organici, ottenuti con semplici procedure sintetiche, presentano un'ampia varietà di cationi e anioni e sono caratterizzati da proprietà molto diverse tra di loro che ne permettono l'utilizzo in catalisi, in sistemi elettrochimici, in biologia e in preparazioni farmaceutiche.

Introduction

The interest of the scientific research in the synthesis of new compounds is continuously increasing both for enhancing the general knowledge in the field of basic science and for designing new molecules useful for several applications.

Over the years organic chemists have built and are still developing a huge library of new molecules, comprehensive of both neutral and charged organic compounds.

This dissertation will be mainly focused on charged organic compounds or “organic salts” (OSs), salts formed by organic cations and organic or inorganic anions. Even if this class of molecules have been extensively investigated since the last decades of 19th century, its knowledge dates back to the 18th century when M. V. Regnault draft the first accurate analysis of organic salts in the “*Nouvelles Recherches sur la Composition des Alcalis Organiques*” in 1838.¹ It represents an analytical study on the composition of organic salts derived from natural bases such as quinine, cinchonine and urea. After several experiments of neutralization between these organic bases and inorganic acids he stated, in his conclusion, that: “all salts formed from organic bases with oxacids, include one molecule of water necessary to their composition, and of which they cannot be deprived without undergoing decomposition. These bases, therefore, present a complete analogy with ammonia in its mode of action with acids. They combine directly with the hydracids without decomposition, forming hydrochlorates and not chlorides, like the mineral oxybases; and with oxacids dissolved in water, the vegetable bases unit by fixing one atom of water which enters into their intimate composition”.

So, it was clear since the past that, analogously to inorganic salts, organic ones could be easily synthesized with the common acid-base neutralization and that their properties vary in relation to the charges and the symmetry of the ions considered. In addition in the case of OSs, properties can be modulated introducing small structural change in the structure of the ions.² For this reason the attention of the scientific community in the synthesis of new OSs is growing drastically.

[1] M. V. Regnault, *Compte Rendus* **1838**, 6, 113-160.

[2] F. D'Anna and R. Noto, *Eur. J. Org. Chem.* **2014**, 4201- 4223.

Coulombic interactions represent the primary interactions between ions of OSs as well as in common inorganic salts, however in dependence on ions structure of the OSs they can be held by strong secondary interactions, such as hydrogen bonds, π - π or cation- π interactions. Furthermore, while inorganic salts are mainly soluble in water, OSs can be soluble in an extended range of solvents. According to solvent properties for example the polarity, in solution, OSs can be presented as intimate ion pair, ion pair separated by the solvent and free ion pair.³

1. Monocationic Organic Salts: Ionic Liquids

Ionic liquids (ILs) represent the most studied class of monocationic OSs. They are defined as salts already liquid at low temperatures (<100 °C) with no measurable vapour pressure and low flammability.⁴ In particular, the low vapour pressure of ILs facilitates the separation of solvents and reaction products deleting the problem of azeotrope formation. These properties have allowed using ILs as alternative solvents to the common organic ones.⁵ On the basis of Green Chemistry principles,⁶ they were also defined as "green solvents" indeed ILs can be recycled for several catalytic cycles both as reaction media or catalysts. In this way the production of dangerous wastes is minimized.⁷ Seddon *et al.* diffused the study of ILs working first with chloroaluminates ILs as nonaqueous, polar solvents for the investigation of transition metal complexes.⁸ The progression of this first class of ILs brought to the most widely studied class of the "room temperature ionic liquids" (RTILs). These monocationic OSs are liquid at room temperature and their properties vary in dependence on the nature of the cation and anion used.⁹

The most reported cations used for the formation of ILs are imidazolium, tiazolium, pyridinium, ammonium, phosphonium, pyrrolidinium and chinolinium ions. They are easily synthesized by quaternization of the select heterocycle, amine or phosphate and

[3] H. K. Stassen, R. Ludwig, A. Wulf and J. Dupont, *Chem. Eur. J.* **2015**, *21*, 8324-8335.

[4] P. Wasserscheid and T. Welton, *Ionic Liquids in Synthesis*, Weinheim, Germany, **2008**, p. 1-355.

[5] J. Dupont, *Acc. Chem. Res.* **2011**, *44*, 1223-1231.

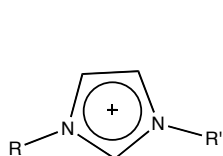
[6] S. L. Y. Tang, R. L. Smith and M. Poliakoff, *Green Chem.* **2005**, *7*, 761-762.

[7] C.-J. Li and P. T. Anastas, *Chem. Soc. Rev.* **2012**, *41*, 1413-1414.

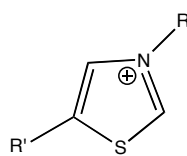
[8] a) A. J. Dent, K. R. Seddon and T. Welton, *J. Chem. Soc., Chem. Commun.* **1990**, 315-316, b) P. B. Hitchcock, T. J. Mohammed, K. R. Seddon, J. A. Zora, C. L. Hussey and E. Haynes Ward, *Inorg. Chim. Acta* **1986**, *113*, L25-L26.

[9] P. Wasserscheid and W. Keim, *Angew. Chem., Int. Ed.* **2000**, *39*, 3772-3789.

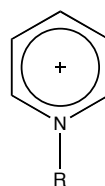
they differ in the structure that can be aromatic or aliphatic. The anions can be varied by anion exchange reactions; the most common anions present in ILs are chloride, tetrafluoroborate, hexafluorophosphate, hexafluoroantimonate, nitrate, *N*-bis(trifluoromethanesulfonyl)imide and acetate. In Figure 1 structures of the most representative cations and anions forming ILs are reported.

Common cations:

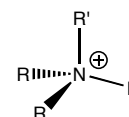
Imidazolium ion



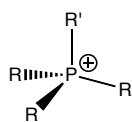
Tiazolium ion



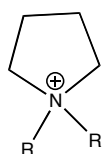
Pyridinium ion



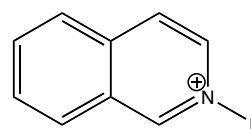
Ammonium ion



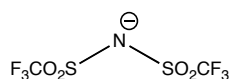
Phosphonium ion



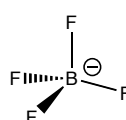
Pyrrolidinium ion



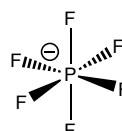
Isochinolinium ion

Common anions:

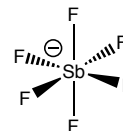
N-bis(trifluoromethanesulfonyl)imide



tetrafluoroborate



hexafluorophosphate



hexafluoroantimonate

Figure 1: structures of the most representative cations and anions forming ILs.

As already mentioned the relationship between structure and chemical-physical properties of ILs is really tight.

First of all, melting point is the peculiar criterion for the evaluation of ILs as they are defined on the base of it. Usually cations with low symmetry, weak intermolecular interactions and good distribution of charge contribute for the formation of low-melting salts. A decrease of salts melting point is also reported with an increase of the anion size. The melting process of OSs follows the same principle of inorganic salts, ions with larger

size and small charge require a small amount of energy to break bonds and this phenomenon causes the decreasing of melting point.

It is worth mentioning that, instead of simple molten salts, a non-symmetrical disposition of molecules into at least one of the ions of the RTILs prevents their normal crystallization.¹⁰

Moreover, the thermal stability varies in dependence on heteroatom-carbon and heteroatom-hydrogen bonds strength of ILs. In general aromatic ILs present a greater thermal stability than the aliphatic ones, thermal stabilities range from 145 up to 185 °C.¹¹ On the other hand the density decreases with the increasing of alkyl chain and of the bulkiness the organic cations. The viscosity is another important property of ILs and it is usually higher compared to common solvents. This is due to the IL tendency to form hydrogen bonding and by the strength of the van der Waals interactions. However the viscosity, especially influenced by anion structure and symmetry, can be drastically reduced increasing the working temperature or adding small amount of organic cosolvents.¹²

The ILs solubilisation ability has supported their large employment as reaction media, in particular this property depends above all on the polarity of the cation. In the wide range of cations presenting different polarities, the dissolution of several substrates becomes easy. On the other hand, the fact that ILs are usually immiscible with both water and nonpolar organic solvents can cause the formation of micelles. An exhaustive review on the nanostructure of neat ILs, their solvent cohesive energy density and their solvophobic effect has been recently reported. In particular, the review focused on strong correlation between the nanostructure of the ionic liquids and their characteristics as amphiphile self-assembly solvents. ILs are considered as amphiphile self-assembly media and their behaviour in relation with common solvents is analytically studied considering some thermodynamic parameters.¹³

Finally, the coordination ability and the acidity are mostly determined by the nature of the anion. Basic anions are strongly coordinating, while acid anions are weakly or non

[10] J. Dupont and P. A. Z. Suarez, *Phys. Chem. Chem. Phys.* **2006**, *8*, 2441-2452.

[11] M. L. Mutch and J. S. Wilkes, *Proc. Electrochem. Soc.* **1998**, *98*, 254-260.

[12] P. Bonhôte, A.-P. Dias, N. Papageorgiou, K. Kalyanasundaram and M. Grätzel, *Inorg. Chem.* **1996**, *35*, 1168-1178.

[13] T. L. Greaves and C. J. Drummond, *Chem. Soc. Rev.* **2013**, *42*, 1096-1120.

coordinating. For the acidity of ILs, it is common to refer to “latent acidity” or “superacidity” of protons in ILs.¹⁴

2. Imidazolium Salts

Imidazolium salts represent one of the most studied classes of OSs, as their structural organisation involves the formation of supramolecular aggregates in which weak interactions generate a high degree of directionality.¹⁵ In dependence on the reactions, this supramolecular structure may give a high catalytic ability to the ILs, indeed the introduction of other molecules occurs with the formation of inclusion-type compounds, for this reason imidazolium ILs seem to be suitable reaction media.³ This pronounced self-organization in solid, liquid and gas phase is peculiar of imidazolium ILs.¹⁶

In particular X-ray studies on 1,3-dialkylimidazolium salts evidenced the formation in solid state of an extended network of cations and anions connected together by hydrogen bonds. A two-dimensional simplified model of the supramolecular structure consists of one imidazolium cation surrounded by three anions and in turn each anion is surrounded by at least three imidazolium cations (Figure 2).

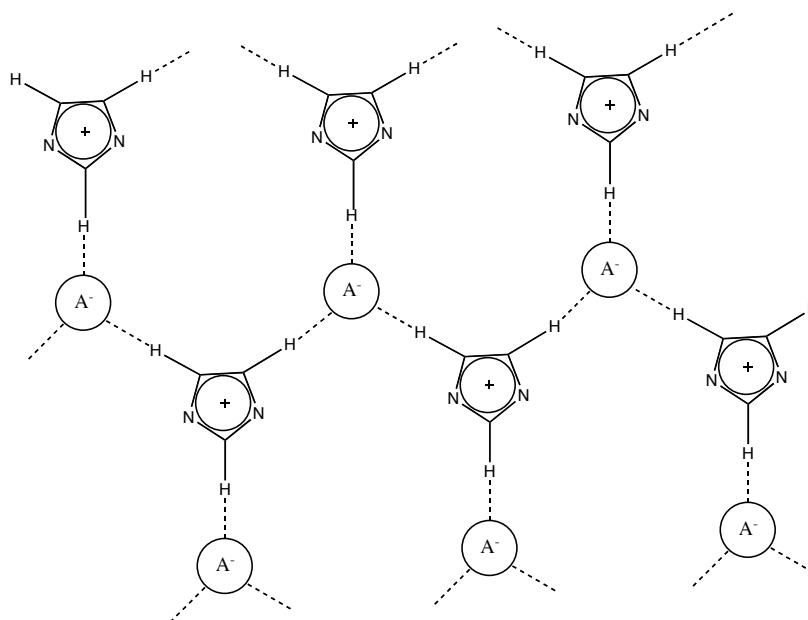


Figure 2: two-dimensional schematization of supramolecular polymeric structure of 1,3-dialkyl imidazolium ILs, showing hydrogen bonds between cations and anions.

[14] C. Scordilis-Kelley, J. Fuller, R. T. Carlin and J. S. Wilkes, *J. Electrochem. Soc.* **1992**, *139*, 694-699.

[15] J. Dupont, *Acc. Chem. Res.* **2011**, *44*, 1223-1231.

[3] H. K. Stassen, R. Ludwig, A. Wulf and J. Dupont, *Chem. Eur. J.* **2015**, *21*, 8324-8335.

[16] F. C. Gozzo, L. S. Santos, R. Augusti, C. S. Consorti, J. Dupont and M. N. Eberlin, *ibid.* **2004**, *10*, 6187-6193.

The H2 imidazolium proton, being the most acidic, forms the strongest hydrogen bond. This general arrangement can change in relation of anion size and type of *N*-alkyl imidazolium substituent.¹⁷

Furthermore, in a tridimensional view of the supramolecular structure of imidazolium salts, cations stack one above the other thanks to π - π interactions connecting aromatic rings; in this way they arrange in a sort of "pile" forming channels in which spherical anions are hosted. Two schematic representations of this model are reported in Figure 3.

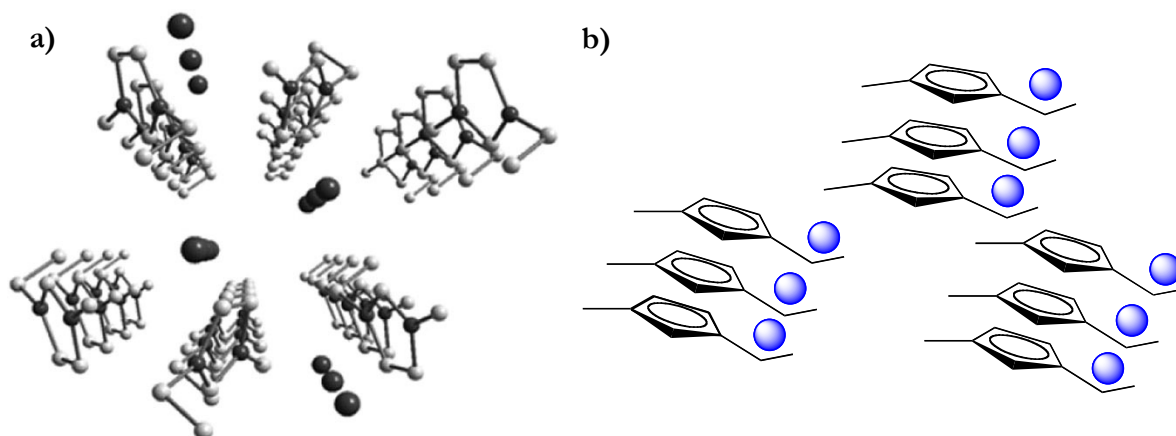


Figure 3: schematic representation of the supramolecular polymer of ILs showing π - π stacking among imidazolium rings and channels in which spherical anions are incorporated, **a)** tridimensional and **b)** two-dimensional views.

As above mentioned these IL structures are adaptable to many species, as the formation of hydrophobic or hydrophilic region and high directional polarizability of the IL well includes different species. In addition to this, the low interface tension of ILs makes them suitable media to interact with other phases. Therefore, the introduction of other molecules in IL network causes the disruption of some hydrogen bonds generating nanostructures with polar and non-polar region where the external molecule can well adapt. This phenomenon involves ions,¹⁸ macromolecules,¹⁹ molecules and nanoparticles that can be stabilized in this media.²⁰

In literature many examples of catalysts, metal-nanoparticles, semisolid catalysts are reported to be stabilized in ILs structure. The same stabilization process of reactants

[17] J. Dupont, *J. Braz. Chem. Soc.* **2004**, *15*, 341-350.

[18] R. P. J. Bronger, S. M. Silva, P. C. J. Kamer and P. W. N. M. v. Leeuwen, *Chem. Commun.* **2002**, 3044-3045.

[19] R. P. Swatloski, S. K. Spear, J. D. Holbrey and R. D. Rogers, *J. Am. Chem. Soc.* **2002**, *124*, 4974-4975.

[20] M. Deetlefs, C. Hardacre, M. Nieuwenhuyzen, O. Sheppard and A. K. Soper, *J. Phys. Chem. B* **2005**, *109*, 1593-1598.

molecules, or transition state reaction, occurs when ILs are utilized as reaction media, for this reason in most cases higher yields in minor reaction times are reported. Finally ILs can be used also in presence of small amount of cosolvents, so in diluted ionic liquids the organic salts ion-pair principle operates. In Figure 4 is reported the schematization of this concept as in Dupont’s review.³

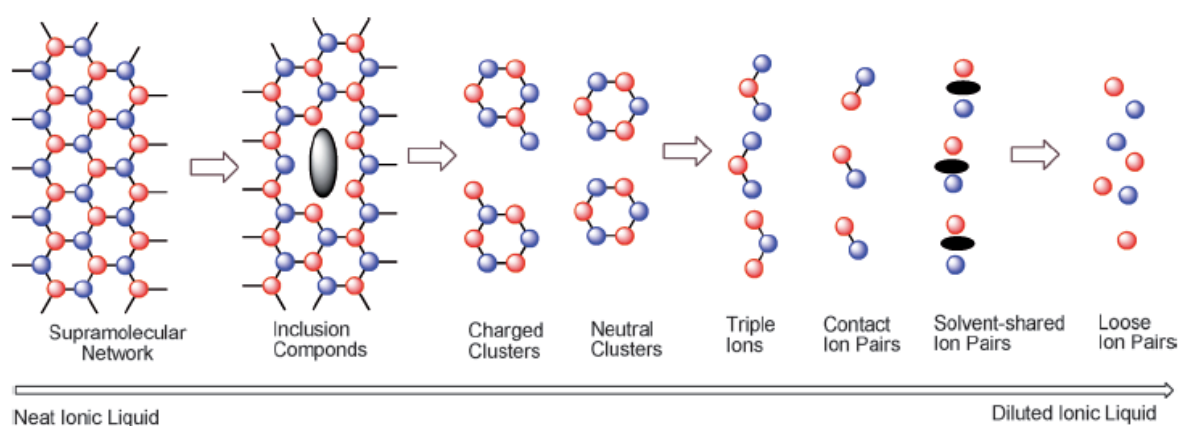


Figure 4: two-dimensional representation of the structure of a neat ionic liquid to its infinite dilution in the presence of other organic species (red spheres=anions, blue spheres=cations, black spots=solvent molecules and the lines represent the hydrogen bonds and/or other weaker interactions).

Thanks to all these properties, ILs have been widely applied as alternative solvents in almost all kind of organic reactions and they have been applied in industrial processes.²¹ In addition to this, their high electrical conductivity and low corrosiveness has allowed their use in electrochemical field in order to design new devices.²² Over the years ILs properties and applications have been reviewed several times, indeed thanks to their tunable characteristics they can be used in multiple applications fields.

Even if the most widely studied class of monocationic organic salts fall in ILs one, other examples of monocationic organic salts are reported. Imidazolium salts have been applied as ligands for transition metal catalysis and Lewis base catalysts thanks to their easy

[3] H. K. Stassen, R. Ludwig, A. Wulf and J. Dupont, *Chem. Eur. J.* **2015**, *21*, 8324-8335.

[21] a) T. Welton, *Coord. Chem. Rev.* **2004**, *248*, 2459-2477, b) N. V. Plechkova and K. R. Seddon, *Chem. Soc. Rev.* **2008**, *37*, 123-150, c) J. P. Hallett and T. Welton, *Chem. Rev. (Washington, DC, U. S.)* **2011**, *111*, 3508-3576, d) B. Masciocchi, C. Chiappe and C. S. Pomelli in *Ionic Liquids Applied to CO₂ Fixation and Conversion*, Vol. Eds.: M. D. Falco, G. Iaquaniello and G. Centi), Springer London, **2013**, pp. 81-94, e) F. D’Anna, S. Marullo, P. Vitale, C. Rizzo, P. Lo Meo and R. Noto, *Applied Catalysis A: General* **2014**, *482*, 287-293, f) S. Marullo, F. D’Anna, C. Rizzo and R. Noto, *Ultrason. Sonochem.* **2015**, *23*, 317-323.

[22] D. R. MacFarlane, N. Tachikawa, M. Forsyth, J. M. Pringle, P. C. Howlett, G. D. Elliott, J. H. Davis, M. Watanabe, P. Simon and C. A. Angell, *Energy Environ. Sci.* **2014**, *7*, 232-250.

formation of *N*-heterocyclic carbenes (NHCs). NHCs imidazolium derived are preferred to triazolium ones for their success in organocatalytical transformation. In this context a “sandwich complex” of iron among chiral imidazopyridinium salts has proven to be highly competent as both Lewis base catalysts and as ligand for transition-metal complexes. Significantly, the planar chiral NHCs give high levels of stereoselectivity for asymmetric reactions.²³ Another example of imidazolium derived NHCs and Fe complex has been recently synthesized and performed for the cross-coupling reaction of alkyl halides.²⁴ Obviously these metal-NHCs complexes are really common with several metals and in particular with Pd thanks to the promotion of Suzuki and Heck reactions and the possibility of catalyst recycle.²⁵

The use of unsymmetric aryl(mesityl)iodonium arylating reagents for the coupling of aliphatic alcohol pronucleophiles is described to generate industrially important alkyl-aryl ethers with a metal-free reaction.²⁶ Others OSs involved as catalysts and reaction media are *o*-Boronato- and *o*-Trifluoroborato-Phosphonium salts supported by L- α -amino acid side chain. These salts showed promising properties for their applications in synthesis and radiolabeling of peptides.²⁷

Finally aspartic acid derived cationic polymers and cellulose ammonium salts have been used for the removal of water pollutants such as toxic metal ions and humic acid.²⁸ In the last case ammonium salts present the double function to entrap the humic acid and to form “soil-mimicking” porous foams having good capacity to capture Cu(II) ions and positive dyes from contaminated water.

[23] C. T. Check, K. P. Jang, C. B. Schwamb, A. S. Wong, M. H. Wang and K. A. Scheidt, *Angew. Chem., Int. Ed.* **2015**, *54*, 4264-4268.

[24] X. Wang, J. Zhang, L. Wang and L. Deng, *Organometallics* **2015**, *34*, 2775-2782.

[25] a) S. Navalón, M. Álvaro and H. García, *ChemCatChem* **2013**, *5*, 3460-3480, b) K. V. S. Ranganath, S. Onitsuka, A. K. Kumar and J. Inanaga, *Catal. Sci. Technol.* **2013**, *3*, 2161-2181.

[26] S. K. Sundalam and D. R. Stuart, *J. Org. Chem.* **2015**, *80*, 6456-6466.

[27] J. Bernard, R. Malacea-Kabbara, G. S. Clemente, B. P. Burke, M.-J. Eymin, S. J. Archibald and S. Jugé, *ibid.* 4289-4298.

[28] a) Z. A. Jamiu, H. A. Al-Muallem and S. A. Ali, *React. Funct. Polym.* **2015**, *93*, 120-129, b) H. Sehaqui, U. Perez de Larraya, P. Tingaut and T. Zimmermann, *Soft Matter* **2015**, *11*, 5294-5300.

3. Dicationic Organic Salts (DOSs)

It is clear that the high structural order of aromatic organic salts defined them as "supramolecular fluids". Their properties have been tuned especially in dependence on the anion indeed, as already mentioned, imidazolium cation is the most widely applied as changing cationic structure means the obtainment of less structured salts. In order to extend the variety of aromatic cationic unit, Armstrong *et al.* introduced in 2005 a new class of organic salts.²⁹ He studied the relationship between the structure and properties of 39 dicationic organic salts. These salts, having melting points below 100 °C and presenting two identical cationic unit, were named as geminal dicationic ionic liquids (DILs).

An aliphatic chain of different length is the linker between the cationic heads, such as imidazolium, 2-methylimidazolium and pyrrolidinium. The length of alkyl chains attached to the cations and the nature of the anions were also varied. In Figure 5 a schematic representation of the structures is presented.

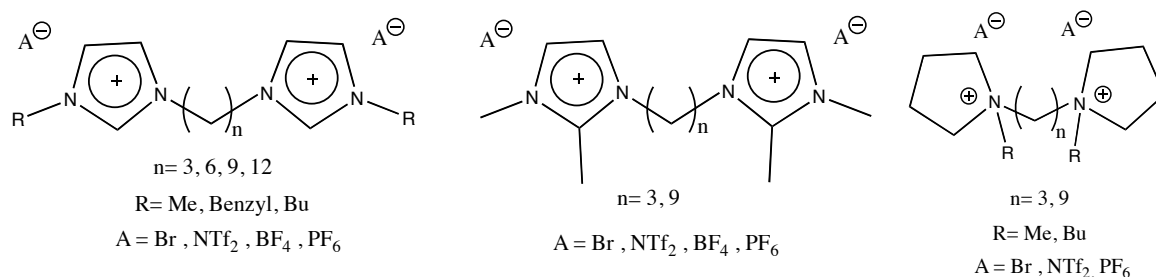


Figure 5: geminal dicationic ionic liquids studied by Armstrong *et al.*

Density, viscosity and melting point depend on the length of alkyl chain of the cations and the length of the linker joining them. A longer alkyl chain of the linker causes a decrease in melting point and density, and an increase in the viscosity. In general, they follow the same trend of imidazolium monocationic ILs as well as they are insolubles in water and in heptane. The interest in DILs stands also in a thermal stability higher than monocationic ones. Indeed, MacFarlane *et al.* using thermogravimetric analysis have demonstrated that the maximum operational temperature limit of imidazolium ILs was lower than the reported decomposition temperature;³⁰ while the new class of divalent ILs showed a decomposition temperature that varies from 330 up to 400 °C. As a

[29] J. L. Anderson, R. Ding, A. Ellern and D. W. Armstrong, *J. Am. Chem. Soc.* **2005**, *127*, 593-604.

[30] K. J. Baranyai, G. B. Deacon, D. R. MacFarlane, J. M. Pringle and J. L. Scott, *Aust. J. Chem.* **2004**, *57*, 145-147.

consequence they exhibited a very large liquid range (-4 to 400 °C), important for their application as reaction media for high-temperature organic reactions such as isomerization, Claisen rearrangement and Diels Alder reaction.³¹

Also the conductivity of the DILs can be related to their structure, Pitawala *et al.* studying thermal and conductive properties of similar DILs, have demonstrated that the length of the alkyl chain on the cation has weak influence on the glass transition temperature, T_g , whereas the presence of rigid aromatic side groups has a strong influence on T_g . The highest ionic conductivity was evaluated for an IL with a long chain linker and a methyl group on each imidazolium ring. As the conductivity results correlate well with the glass transition temperatures, the flexibility of the geminal cations is a key factor for the obtainment of high conductivity. For this reason the presence of rigid aromatic side groups on the imidazolium ring decreases the flexibility and hence the mobility.³² In general the ionic conductivity is lower than the one of the corresponding monocationic ILs.

With the aim of enhancing the DILs properties, the nature of cation, linker and the alkyl chains have been modified. For example, geminal diimidazolium ILs with linker namely polyalkyl ether, polyfluoroalkyl, 1,4-bismethylenebenzene or 1,4-bismethylene-2,3,5,6-tetrafluorobenzene have been synthesized and analysed. The DILs with polyfluoroalkyl chain linker presented the highest densities and viscosities. The presence of the aromatic linkers and the longer alkyl substituents on the imidazolium rings increase the apolar character of the IL and as consequence the solubility in solvent such as toluene increases as well. The salts studied exhibit also higher conductivities and tribological properties at 300 °C, thus they seem to be good candidates as high-temperature lubricants.³³

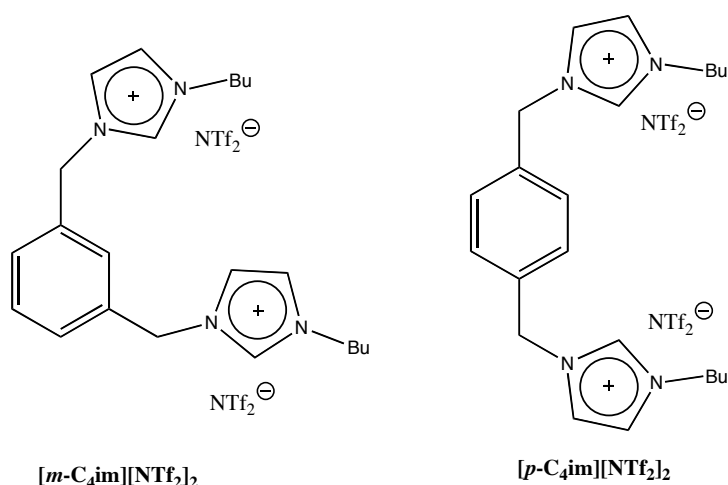
The presence of an aromatic ring as spacer between the two cationic heads of DOSs has attracted the attention of our research group. Indeed, comparing data with the corresponding monocationic IL, it has been demonstrated that the increase of the π -surface gives high degree of order to the solvent system, thanks to the formation of a thick network of π - π interactions.

[31] X. Han and D. W. Armstrong, *Org. Lett.* **2005**, 7, 4205-4208.

[32] J. Pitawala, A. Matic, A. Martinelli, P. Jacobsson, V. Koch and F. Croce, *J. Phys. Chem. B* **2009**, 113, 10607-10610.

[33] Z. Zeng, B. S. Phillips, J.-C. Xiao and J. M. Shreeve, *Chem. Mater.* **2008**, 20, 2719-2726.

Furthermore, a different isomeric substitution on the aromatic spacer generates a different three-dimensional packing of the DOSs and subsequently different properties (Figure 6). In particular, it has been shown, by NMR, RLS (Resonance Light Scattering) and computational analysis, that *meta* isomer presents a lower degree of order than *para* one, probably due to the interaction of the anion with both the imidazolium units of the same cation as consequence of its geometry.³⁴ This is evident also from their state at



room temperature the first presents a liquid like behaviour and second one is a solid. The analysis of these properties has allowed understanding their possible use in applications such as reaction media, organogelators and anion recognition.³⁵

Figure 6: DOSs with a different isomeric substitution.

According to some applications, the necessity is to modulate the melting point and other physical chemical properties, in these cases a lower symmetry of the cation can be required. For this reason, also unsymmetrical DOSs have been studied, they can incorporate a hydrophilic and a hydrophobic anion for each positive charge, cations with different nature, such as one imidazolium unit and one triethylammonium or different alkyl chain on the cationic heads.³⁶

DOSs as well as monocationic OSs have been widely used as reaction media. In addition to the higher thermal stability already evidenced, DOSs present a lower miscibility with conventional solvents so that the product recovery and reuse of the reaction media becomes easier. Moreover the immobilization of metal catalyst with DOSs is more stable

[34] F. D'Anna, F. Ferrante and R. Noto, *Chem. Eur. J.* **2009**, *15*, 13059-13068.

[35] a) F. D'Anna, S. Marullo, P. Vitale and R. Noto, *Eur. J. Org. Chem.* **2011**, *2011*, 5681-5689, b) F. D'Anna, P. Vitale, F. Ferrante, S. Marullo and R. Noto, *ChemPlusChem* **2013**, *78*, 331-342, c) S. Marullo, F. D'Anna, M. Cascino and R. Noto, *J. Org. Chem.* **2013**, *78*, 10203-10208.

[36] a) J.-C. Chang, W.-Y. Ho, I. W. Sun, Y.-L. Tung, M.-C. Tsui, T.-Y. Wu and S.-S. Liang, *Tetrahedron* **2010**, *66*, 6150-6155, b) T. Payagala, J. Huang, Z. S. Breitbach, P. S. Sharma and D. W. Armstrong, *Chem. Mater.* **2007**, *19*, 5848-5850, c) R. Wang, C.-M. Jin, B. Twamley and J. M. Shreeve, *Inorg. Chem.* **2006**, *45*, 6396-6403.

thanks to the stronger interactions between metal and DOSs cations, in this way a lower leaching of the system has been observed during the recovery cycles. The use of the proper DOS as solvent media for organic reactions is influenced especially by the nature of the cationic head and the geometry of the system.²

An important application of DOSs is their use in biomass pretreatment processes and its transformation into products of industrial interest such as 5-(hydroxymethyl)furfural.³⁷

Obviously, also the formation of heterocycles carbene from diimidazolium OSs is favoured. Many examples of DOSs derivative carbene complex with metals are reported either as free complexes or as supported complexes in solid matrix such as silica.³⁸

According to the structure of the spacer joining the positive charge, the geometry, the length and nature of alkyl chain and the anion nature, DOSs can behave also as Ionic Liquid Crystals, organogelators or fluorescent materials.³⁹

4. Tricationic Organic Salts (TOSs)

If the study of DOSs is recent and in continuing expansion, the accurate analysis of TOSs can be considered at an early stage. It has been proved that as the number of charged groups and the molecular weight of OSs increases, they are usually solid and they can be applied as ionic crystals, antimicrobial agents or fluorescent materials more than reaction media as traditional ILs. TOSs properties can be further tuned than DOSs however the synthetic pathway is sometimes more complex especially for unsymmetrical TOSs.

A first analysis on the physico-chemical properties of trigeminal imidazolium and pyridinium salts has been studied by Pernak *et al.*. The TOSs were characterized by the presence of glycerol as cationic spacer and different monoanions. They resulted very viscous liquids with a consequent lower conductivity compared to DOSs. The presence of oxygen atoms in the spacer causes also a decrease in their thermal stability.⁴⁰ A different

[2] F. D'Anna and R. Noto, *Eur. J. Org. Chem.* **2014**, 4201- 4223.

[37] A. H. Jadhav, H. Kim and I. T. Hwang, *Catal. Commun.* **2012**, *21*, 96-103.

[38] a) M. Gruttadauria, L. A. Bivona, P. Lo Meo, S. Riela and R. Noto, *Eur. J. Org. Chem.* **2012**, *2012*, 2635-2642, b) Q.-X. Liu, L.-X. Zhao, X.-J. Zhao, Z.-X. Zhao, Z.-Q. Wang, A.-H. Chen and X.-G. Wang, *J. Organomet. Chem.* **2013**, *731*, 35-48.

[39] a) Y. Gao, J. M. Slattery and D. W. Bruce, *New J. Chem.* **2011**, *35*, 2910-2918, b) B. Dong, T. Sakurai, Y. Bando, S. Seki, K. Takaishi, M. Uchiyama, A. Muranaka and H. Maeda, *J. Am. Chem. Soc.* **2013**, *135*, 14797-14805, c) F. D'Anna, S. Marullo, G. Lazzara, P. Vitale and R. Noto, *Chem. Eur. J.* **2015**, *21*, 14780-14790, d) P. Vitale, F. D'Anna, F. Ferrante, C. Rizzo and R. Noto, *Phys. Chem. Chem. Phys.* **2015**, *17*, 26903-26917.

[40] J. Pernak, A. Skrzypczak, G. Lota and E. Frackowiak, *Chem. Eur. J.* **2007**, *13*, 3106-3112.

situation was reported by Armstrong *et al.* who analysed the properties of four different spacers (trimethyl mesitylene, mesitylene, diethylamine and tri(2-hexanamido)ethylamine) with nine different types of cationic heads (Figure 7).

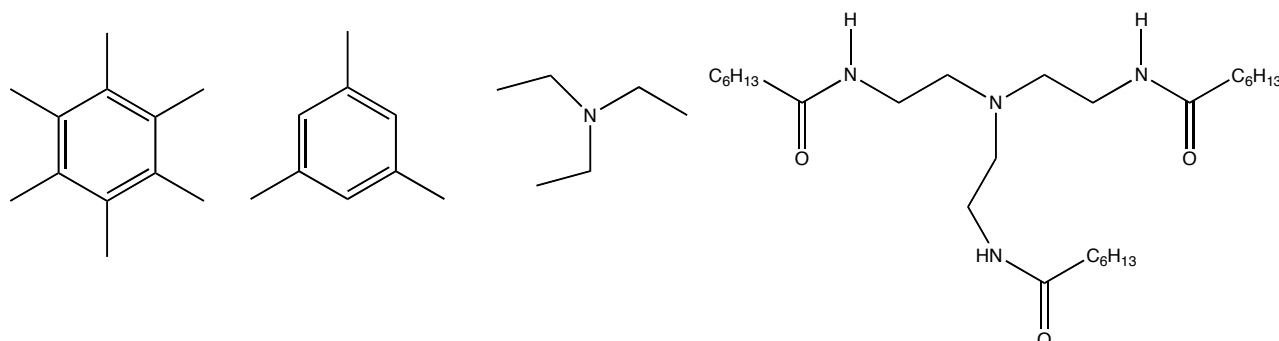


Figure 7: structures of spacers used to synthesise TOSs.

TOSs with more rigid spacer present the highest melting temperatures. The high thermal stability and viscosity of these salts allow their use as stationary phases chromatography.⁴¹ A series of TOSs formed by mesitylene and stilbazolium moieties exhibited interestingly photophysical properties in addition to the high thermal stability. They present a positive solvatochromism effect in dependence on the polarity of the organic solvents. They showed blue lights emission in solution, but emitted green light in a narrow range of wavelengths in the solid states, displaying a bathochromic shift.⁴²

The presence of TOSs seems also really important in order to enhance magnetic properties. Tricationic magnetic ILs containing three $[\text{FeCl}_3\text{Br}^-]$ anions exhibited the highest effective magnetic moment value reported for magnetic ILs and they also represent an inexpensive alternative to magnetic ILs based on lanthanides. These salts showed good properties for application in liquid–liquid extraction and catalytic studies where the magnetic IL can be easily removed or in microfluidic applications where the magnetic IL can be manipulated by an external field.⁴³

[41] P. S. Sharma, T. Payagala, E. Wanigasekara, A. B. Wijeratne, J. Huang and D. W. Armstrong, *Chem. Mater.* **2008**, *20*, 4182-4184.

[42] T. S. Jo, W. L. McCurdy, O. Tanthmanatham, T. K. Kim, H. Han, P. K. Bhowmik, B. Heinrich and B. Donnio, *J. Mol. Struct.* **2012**, *1019*, 174-182.

[43] O. Nacham, K. D. Clark, H. Yu and J. L. Anderson, *Chem. Mater.* **2015**, *27*, 923-931.

In this context the research developed during the PhD is well set. Indeed, a new class of dicationic ILs functionalised with a neutral base has been synthesized and studied in relation to different modification of cationic and anionic structures. These ILs fall in a specific class called task-specific ionic liquids (TSILs), ILs that can incorporate neutral functionality in order to pursue a specific goal. The functionalised DILs have been subsequently used as reaction media for two organic reactions evidencing their catalytic ability that is really influenced by the ILs nature.

Some of the DILs taken into account were more structured than others and present a poor catalytic ability for the studied reactions. In these cases, they were tested as gelators and it has been demonstrated that they can act as low molecular weight gelators (LMWGs) in IL solution.

Another class of DOSs with imidazolium cation was considered in order to study their gelation ability in water, organic solvents and IL solutions. In addition, two-component gels with macrocycles and gels exhibiting antimicrobial activity have been studied.

In summary several kind of DOSs have been studied, they present different properties in dependence on their structure and as consequence they have been applied in the catalytic field or in the formation of soft material like supramolecular gels (Figure 8).

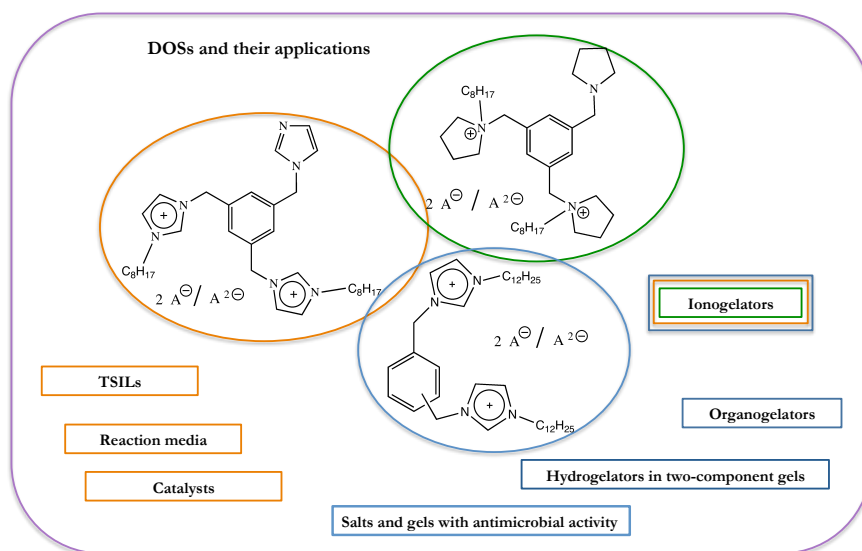


Figure 8: schematic representation of DOSs studied and their applications.

Chapter 1

Task-Specific Ionic Liquids

Some of the most common ILs properties and applications have been discussed in the introduction section as they represent the most studied class of organic salts. Since they have been deeply studied, nowadays they can be classified in several subgroups characterized by peculiar properties. For example, in addition to their use as catalyst, electrolytes and “green solvents” for synthesis and extraction processes, ILs have tickled researcher’s imagination thanks to their predisposition for structural modifications either in the cation or in the anion. This feature contributed to the development of functionalised ILs defined as “Task-Specific Ionic Liquids (TSILs)”.¹

TSILs incorporate in the cation or in the anion a functional group able to impart a particular capability to the IL; in this way they are tailored for a specific applicative task. The peculiarity of this class of ILs is the possibility to covalently tether the catalyst on the IL structure, so that one compound is comprehensive of both solvent and catalyst, for this reason they can be considered “rivals” of solid supported catalysts. Indeed, this IL structure increases the kinetic mobility and allows a large operational surface area.²

The incorporation of the functional groups minimizes the leakage of the catalyst in organic reactions and increases the recyclability of the solvent-catalyst media for several catalytic cycles.³ At the beginning, the definition of TSILs was applied only to these systems able to behave both as catalyst and solvents, but it has recently involved all organic salts with the typical properties of ionic liquids (melting point below 100 °C, negligible vapour pressure and wide liquid range) containing a specific functional group although they may not necessarily behave as reaction media.⁴

In general, they are applied as catalyst or as reactive precursors and the functional group can be a metal, an acid or a base; but ILs formed by basic (carboxylates), acidic

[1] J. J. H. Davis, *Chem. Lett.* **2004**, *33*, 1072-1077.

[2] A. D. Sawant, D. G. Raut, N. B. Darvatkar and M. M. Salunkhe, *Green Chem. Lett. Rev.* **2011**, *4*, 41-54.

[3] S.-G. Lee, *Chem. Commun.* **2006**, 1049-1063.

[4] C. Chiappe and C. S. Pomelli, *Eur. J. Org. Chem.* **2014**, *2014*, 6120-6139.

(halometallates, hydrogen sulfate), reducing (nitrite) or oxidizing anions are also considered TSILs.

The vast majority of reviews and manuscripts on this topic focus once again on imidazolium ionic liquids (Figure 1), even if some examples of ammonium and phosphonium TSILs are present in literature.

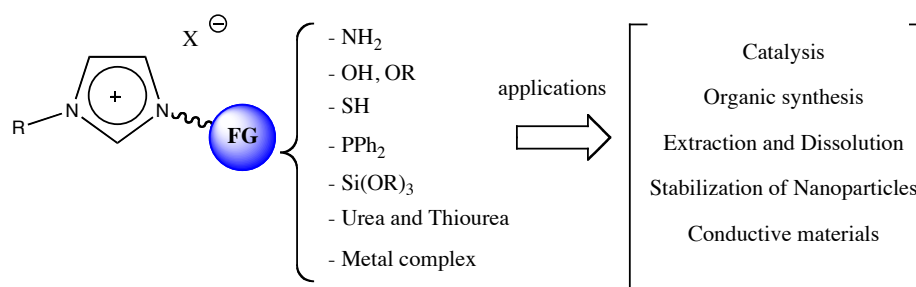


Figure 1: schematic representation of imidazolium TSILs according to their first definition.

In particular, one of the first IL catalysts was a phosphonium sulfonate salt that showed its ability to catalyse the most common acid-catalyzed reaction such as esterification, dehydration reactions and pinacol rearrangements.⁵ Recently, an azole-based phosphonium IL, applied for the chemisorption of CO₂, has demonstrated to overcome the drastically increase of the TSILs viscosity after CO₂ absorption, that usually causes the transition from viscous liquids to gel and leads to a very low reaction rate. A combined approach of MD calculation and experimental data allowed the authors to assert that the asymmetry of anions influences the dynamics of the system and affects the viscosity in a consequent decrease after absorbing CO₂.⁶

On the other hand, ammonium bifunctional ionic liquids, thanks to their thermoregulated properties in aqueous and common organic solvents, have been used for catalytic oxidative desulfurization of fuels.⁷ While, Binnemans *et al.* have synthesised a range of ammonium sulfonic acid ILs that exert great skills as solvents extraction of metal ions and as dissolving agents of metal oxides.⁸ In Figure 2 phosphonium and ammonium TSILs discussed are shown.

[5] A. C. Cole, J. L. Jensen, I. Ntai, K. L. T. Tran, K. J. Weaver, D. C. Forbes and J. H. Davis, *J. Am. Chem. Soc.* **2002**, *124*, 5962-5963.

[6] A. Li, Z. Tian, T. Yan, D. Jiang and S. Dai, *J. Phys. Chem. B* **2014**, *118*, 14880-14887.

[7] F.-L. Yu, Y.-Y. Wang, C.-Y. Liu, C.-X. Xie and S.-T. Yu, *Chem. Eng. J. (Lausanne)* **2014**, *255*, 372-376.

[8] D. Dupont, S. Raiguel and K. Binnemans, *Chem. Commun.* **2015**, *51*, 9006-9009.

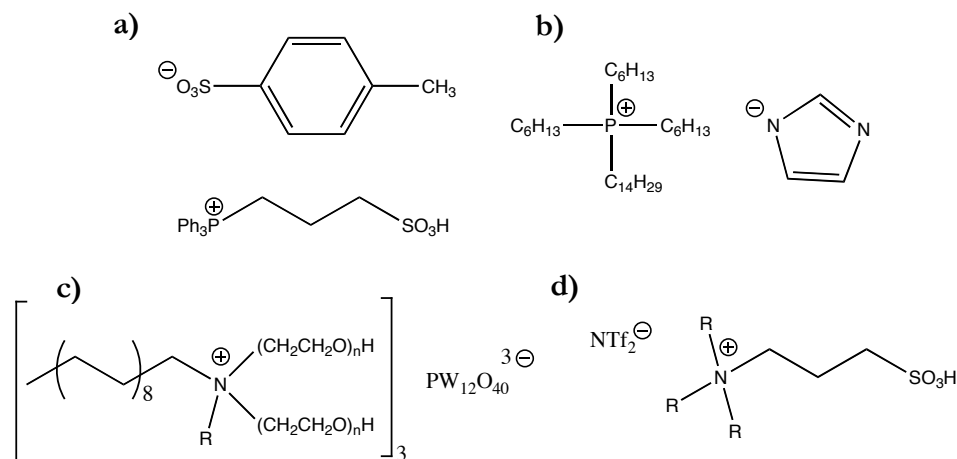


Figure 2: structures of TSILs corresponding to references: **a)** 5; **b)** 6; **c)** 7 and **d)** 8.

A brief overview on the physical-chemical properties of TSILs can be especially comprehensive of data collected for imidazolium TSILs.

In general, the functionalization dramatically affects all the peculiar ILs properties starting from the melting point. For example, the presence of electron-withdrawing groups (NO_2 , Cl, Br, COOEt) in *para*-substituted 1-phenyl-3-alkylimidazolium bromides increases the melting point, whereas electron-donating substituents (Me, EtO, MeO) have the opposite effect.⁹ Furthermore, the functionalization causes an increase of the aggregation properties attributed to the presence of new hydrogen-bonding sites for hydrophilic groups or to a different charge distribution for aprotic groups. On the other hand, a higher viscosity and a lower conductivity than the corresponding alkyl-substituted salts have been normally reported for TSILs. Of course acidity, basicity and the anion coordination ability of ILs are also drastically affected by the functional groups, *i.e.* NTf₂-based ILs in presence of OH groups keep the high polarity of the functionality.⁴

As already evidenced the peculiarity of the functionalised ILs is their design for a specific application, for this reason in order to better understand their properties it is essential to analyse some of the most common applications in which they have been used.

First of all, TSILs have been widely employed in catalysis and in organic synthesis, in this context they can be divided in dependence on the functionality (metal, acid or base).

[9] T. Schulz, S. Ahrens, D. Meyer, C. Allolio, A. Peritz and T. Strassner, *Chem.-Asian J.* **2011**, *6*, 863-867.

[4] C. Chiappe and C. S. Pomelli, *Eur. J. Org. Chem.* **2014**, *2014*, 6120-6139.

Metals coordinated to the ILs represent a big improvement to perform metal catalysed reaction. Indeed, the limited solubilisation of inorganic salts and the poor coordination ability of some anions of unfunctionalised ILs have limited their use in this field. This issue has been overcome exploiting the stabilization of metal nanoparticles in ILs, due to the ability of charged components to interact with the metal surface. The weak interactions between non-functionalised ILs and metal nanoparticles generally assure a high catalytic activity. Nevertheless, neither anion nor cation can prevent nanoparticles agglomeration, causing a poor stability and recyclability of nanoparticles. The use of TSILs has enhanced the efficiency of these reactions, increasing inorganic salt solubility and improving metal catalyst performance, although the higher viscosity of TSILs have brought to their use in mixture of other ILs.

In most cases ILs act as ligand for the transition-metal catalyst, for example phosphine ligands linked to the cation or anion of imidazolium salts have been synthesised to coordinate Rh salts for the hydroformylation of alkenes.¹⁰ While imidazolium-, pyridinium- and pyrrolidinium-based ILs with nitrile functionalities have been studied as solvents and stabilizers in palladium-catalysed C–C cross-coupling reactions. They have stabilized nanoparticles and active Pd^{II} species, formed after the oxidative addition of the aryl halide substrate starting from Pd⁰, in this way also the formation of inactive palladium black deposits was avoided.¹¹ However, the nitrile-functionalised ILs should present non-coordinating anion otherwise Pd^{II} preferentially reacts with the anion forming a stable and inactive species such as [PdCl₄]²⁻. Analogously to nitrile-functionalised ILs, the OH function is able to stabilize both the Pd nanoparticles and the monometallic Pd⁰ species and in addition they are able to guarantee the Pd catalytic activity when chlorides or bromides are the IL counter anions, or are present as impurities arising from the metathesis reaction.¹²

[10] a) D. J. Brauer, K. W. Kottsieper, C. Liek, O. Stelzer, H. Waffenschmidt and P. Wasserscheid, *J. Organomet. Chem.* **2001**, *630*, 177-184, b) M. F. Sellin, P. B. Webb and D. J. Cole-Hamilton, *Chem. Commun.* **2001**, 781-782.

[11] Z. Fei, D. Zhao, D. Pieraccini, W. H. Ang, T. J. Geldbach, R. Scopelliti, C. Chiappe and P. J. Dyson, *Organometallics* **2007**, *26*, 1588-1598.

[12] F. Bellina, A. Bertoli, B. Melai, F. Scalesse, F. Signori and C. Chiappe, *Green Chem.* **2009**, *11*, 622-629.

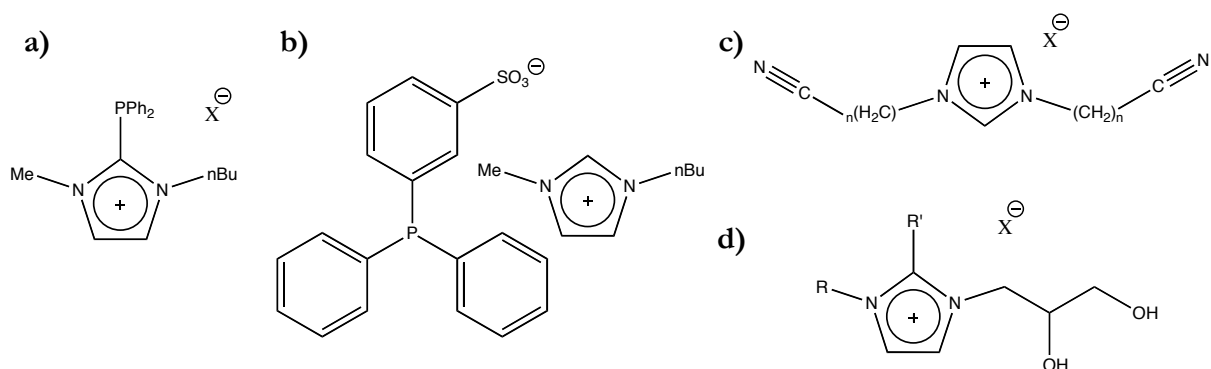


Figure 3: structures of some TSILs linked to metals, **a)** and **b)** Rh ref. 10; **c)** and **d)** Pd ref. 11 and 12.

Nucleophile functionalised ILs have been used for the synthesis in mild conditions of aryl-azide, useful intermediates for the synthesis of heterocyclic compounds. [bmim][N₃] was the TSIL taken into account and, forming a binary mixture with ILs such as [bmim][BF₄], [bmim][NTf₂] and others, it reveals a suitable source of nucleophile to obtain the desired products.¹³ Another example of base-TSIL is a polymer supported ascorbate TSIL that, easily coordinating the Cu salt, showed an excellent catalytic effect in the 1,3-dipolar cycloaddition for the formation of triazoles.¹⁴ On the other hand, sulfonic-TSILs have been widely applied for the dissolution and conversion of sugars. For example 1-allyl-3-methylimidazolium chloride and 1-(4-sulfobutyl)-3-methylimidazolium chloride have been used for the depolymerisation of starch-based industrial waste into high reducing sugars. These systems represent a green way to reduce organic waste in important industrial products.¹⁵

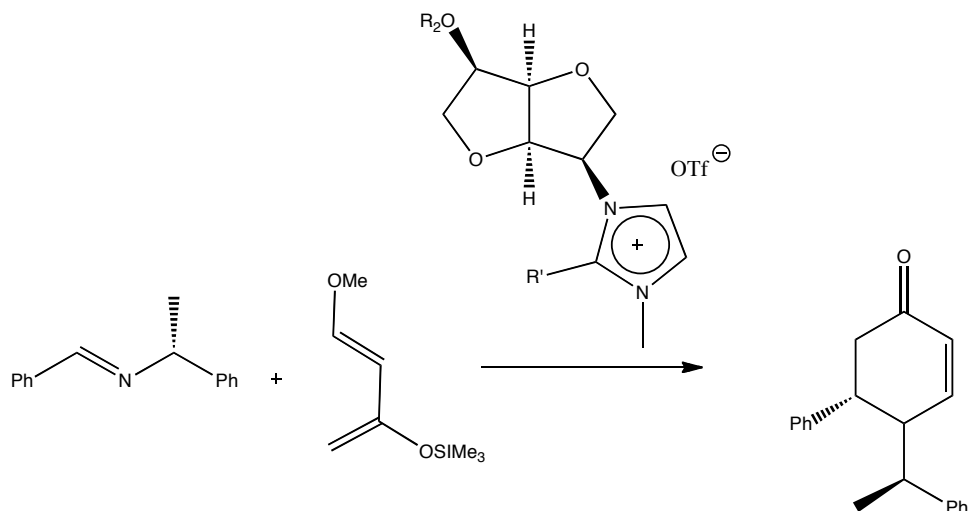
Functionalised chiral ILs have been also used in asymmetric organic synthesis as new chiral solvents or catalyst. The simpler way to prepare enantiomerically pure ILs is to use precursors derived from the chiral source either for the generation of the chiral ILs anion or cation. Simple ILs such as derivative of tartaric, lactic acid and aminoacids have been synthesised, but also more complex structure, such as polymeric chiral silanes or chiral

[13] a) F. D'Anna, S. Marullo and R. Noto, *J. Org. Chem.* **2010**, *75*, 767-771, b) F. D'Anna, S. Marullo, P. Vitale and R. Noto, *Ultrason. Sonochem.* **2012**, *19*, 136-142.

[14] J. D. Patil, S. A. Patil and D. M. Pore, *RSC Adv.* **2015**, *5*, 21396-21404.

[15] A. Hernoux-Villière, J.-M. Lévêque, J. Kärkkäinen, N. Papaiconomou, M. Lajunen and U. Lassi, *Catal. Today* **2014**, *223*, 11-17.

moiety derived from isosorbide as a biorenewable substrate, have been prepared (Scheme 1).²



Scheme 1: Aza-Diel Alder reaction catalyzed by a chiral imidazolium-based ILs.

Furthermore, imidazolium TSILs, as already discussed for ammonium and phosphonium ones, are widely applied for decontamination of matrixes and air thanks to their ability to entrap CO₂ and metals. One of the most promising strategies to capture CO₂ considers its conversion into industrially useful chemicals, so it has a dual importance in view of environmental protection and sustainable chemistry. In this field, Zn-based ionic liquids have proved to be highly efficient catalysts for the chemical fixation of carbon dioxide to epoxides through a cycloaddition reaction.¹⁶

One of the main challenges of chemists is the recovery of organic compounds and the separation of chemically toxic or radiotoxic metal ions from aqueous media, for this reason a tributyl phosphate imidazole-TSIL has been designed to extract U^{VI} from nitric acid.¹⁷ While new hydrophilic ILs functionalised with 8-hydroxyquinoline and ammonium pyrrolidine dithiocarbamate have been successfully used as chelation agents to form complexes with Cr^{III} and Cr^{VI} ions. In the last study the presence of a hydrophobic anion (PF₆) allowed the separation of the chelated ionic liquid phase from aqueous solution in the sedimented phase for the subsequent analysis of the Cr species.¹⁸

[2] A. D. Sawant, D. G. Raut, N. B. Darvatkar and M. M. Salunkhe, *Green Chem. Lett. Rev.* **2011**, *4*, 41-54.

[16] M. Liu, F. Wang, L. Shi, L. Liang and J. Sun, *RSC Adv.* **2015**, *5*, 14277-14284.

[17] H. Li, B. Wang, L. Zhang and L. Shen, *J. Radioanal. Nucl. Chem.* **2015**, *303*, 433-440.

[18] S. Sadeghi and A. Z. Moghaddam, *RSC Adv.* **2015**, *5*, 60621-60629.

One of the limitations of TSILs can be their use at high temperature and their low conductivity respect to ILs, to overcome this problem the combination of TSILs and di- or polycationic organic salts may form an innovative class of ILs.

This new efficient class of organic salts is not widely explored yet, however some examples in the application fields, just described, have been reported. Among metal-functionalised ILs, Wang *et al.* have synthesised and studied a series of Ag^I, Pd^{II}, and Hg^{II} complexes with *N*-imidazolium heterocyclic carbene (NHC) linked with a mesitylene core. In particular, the NHC Pd^{II} complex has been applied to catalyse the Suzuki–Miyaura reaction of aryl halides with phenylboronic acid in good yields, using MeOH/H₂O as solvent and KOH as base in air.¹⁹ For the study of the same reaction, Knoevenagel reaction and one-pot condensation of benzopyranes, Luo *et al.* have developed a series of PEG-bridged dicationic ILs tethered to the appropriate functionality (Figure 4) that can be used in thermoregulated catalytic systems.²⁰ Indeed, thanks to their low solubility at room temperature in conventional organic solvents, it is possible to perform reactions at high temperature recycling the dicationic ILs at the end of the process.

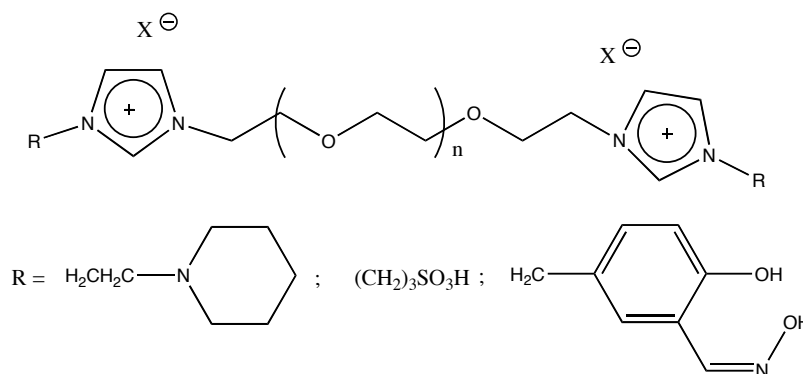


Figure 4: functionalised PEG-bridged dicationic ILs synthesised and applied in catalysis by Luo *et al.*

Dicationic acidic or basic TSILs have also been used for biomass transformation in industry products.²¹ An imidazolium based catalysed system was the homogeneous

[19] Q.-X. Liu, L.-X. Zhao, X.-J. Zhao, Z.-X. Zhao, Z.-Q. Wang, A.-H. Chen and X.-G. Wang, *J. Organomet. Chem.* **2013**, 731, 35-48.

[20] a) H. Zhi, C. Lu, Q. Zhang and J. Luo, *Chem. Commun.* **2009**, 2878-2880, b) J. Luo, T. Xin and Y. Wang, *New J. Chem.* **2013**, 37, 269-273, c) Y. Wang, J. Luo and Z. Liu, *Appl. Organomet. Chem.* **2013**, 27, 601-605.

[21] a) D. Fang, J. Yang and C. Jiao, *ACS Catal.* **2011**, 1, 42-47, b) H.-F. Liu, F.-X. Zeng, L. Deng, B. Liao, H. Pang and Q.-X. Guo, *Green Chem.* **2013**, 15, 81-84.

reaction media in the transesterification reaction for biodiesel production from soybean oil with several alcohols.²²

These salts have been also applied in supported catalysis, for example a diimidazolium ionic liquid with a radical functionality was absorbed on different types of silica supports and on fullerene. It presents an enhanced catalytic ability in the oxidation of primary and secondary alcohols.²³

Having in mind all the peculiarities and the advantages of DOSs and TSILs, we studied a new class of functionalised diimidazolium salts. In particular the new series of DOSs present the 1,3,5-tris(methylen)benzene as spacer, the 1-octylimidazolium ion as the cationic head group and a neutral imidazole as functionality. As counter ions mono- and dianions were chosen. A combined approach of TGA, DSC and NMR investigation has allowed the evaluation of the solution and thermal behaviour of the DOSs, demonstrating a tight relationship between physical-chemical properties and structure of these systems.

The new class of the DOSs presents melting temperature below 100 °C, so they can be defined as TSILs. Indeed after an accurate analysis of their properties, they have been applied as both reaction media and catalysts to perform two base-catalysed reaction: the mononuclear rearrangement of heterocycles of (*Z*)-phenylhydrazone of 3-benzoyl-5-phenyl-1,2,4-oxadiazole into the corresponding triazole and Michael addition of malononitrile to *t*-chalcone. In order to test the catalytic ability of the TSILs, we firstly selected the mononuclear rearrangement, as it is a well known base-catalysed reaction in conventional and ILs solution; while the choice of the Michael addition lies in the formation of an important precursor for pharmaceutical products.

[22] M. Fan, J. Yang, P. Jiang, P. Zhang and S. Li, *RSC Adv.* **2013**, *3*, 752-756.

[23] a) H. A. Beejapur, F. Giacalone, R. Noto, P. Franchi, M. Lucarini and M. Gruttadauria, *ChemCatChem* **2013**, *5*, 2991-2999, b) H. A. Beejapur, V. Campisciano, F. Giacalone and M. Gruttadauria, *Adv. Synth. Catal.* **2015**, *357*, 51-58.

Results and discussion

The synthesis and characterization of new policationic organic salts and their applications represent the central aims of the PhD dissertation.

For this purpose, on the grounds of the efficiency reported for DOSs and functionalised OSs, a novel series of functionalised DOSs have been synthesised. In particular, they were formed by 1-(1-imidazolylmethyl)-3,5-di[1-(3'-octylimidazolylmethyl)]benzene cation, namely [2C₈bti], where bti indicates the benzene-tris-imidazole unit bearing two octyl alkyl chains (2C₈) on two different imidazole rings (Figure 5).

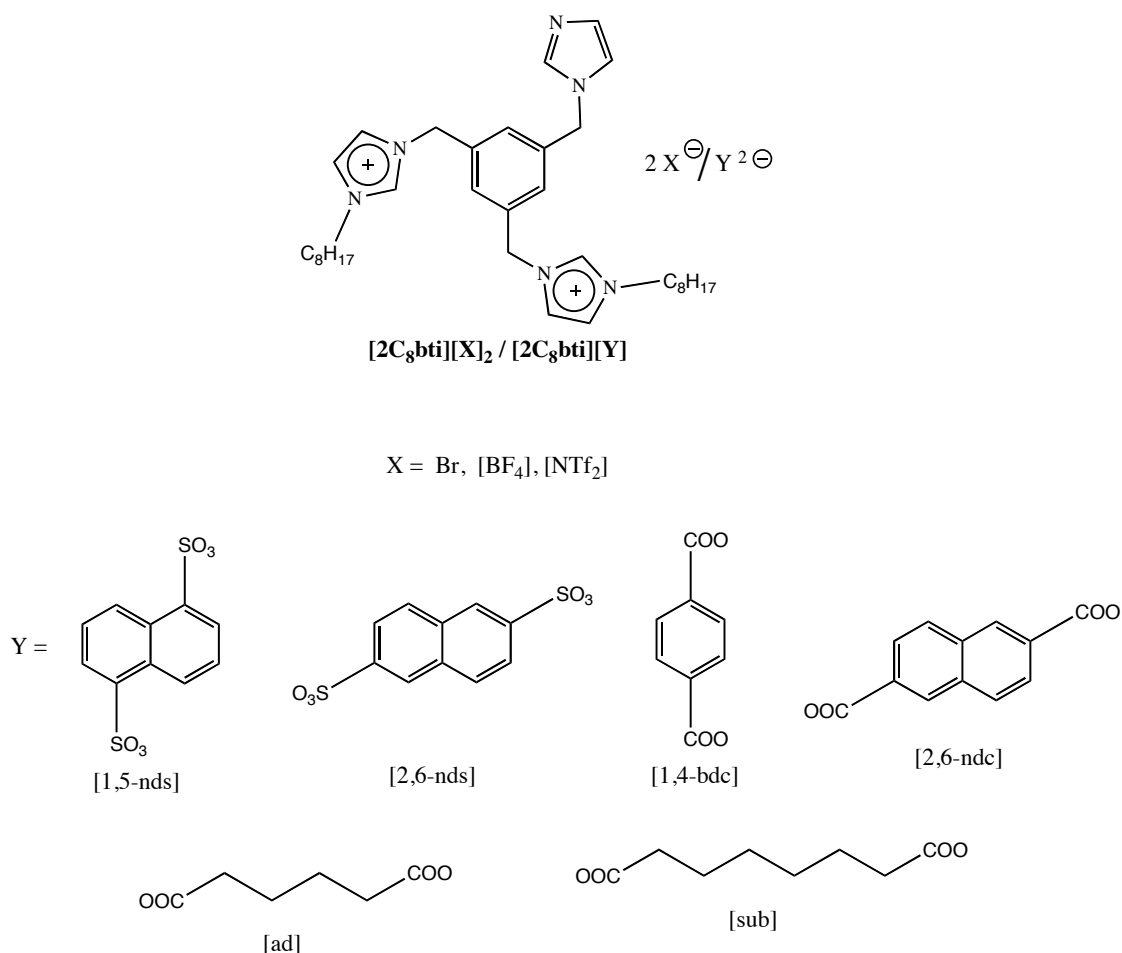


Figure 5: structures of functionalised DOSs studied.

The choice of 1,3,5-tris(methylen)benzene as spacer stands on the fact that a rigid unit awards a high structural order to the ILs. Indeed for geminal diimidazolium ILs it has been demonstrated that the presence of π - π interactions between imidazolium rings and

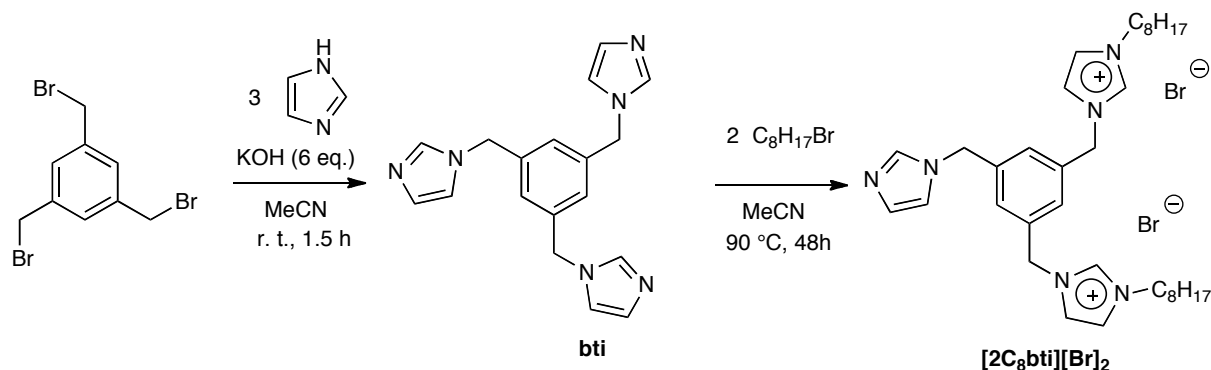
phenyl spacer gives rise to highly structured fluids able to impart a positive directionality to some organic reactions.²⁴ In addition aromatic cationic units such as imidazolium ones strongly support the supramolecular interactions described and the formation of a thick network between cations and anions (see Introduction section 2). On the other hand octyl alkyl chains should favour a liquid like behaviour of DOSs as they should be applied as reaction media. Finally a neutral imidazole represents the base functionality of the DOSs.

In order to modulate DOSs properties several anions have been taken into account, in particular both mono and dianions have been used. Bromide, tetrafluoroborate and *N*-bis(trifluoromethylsulfonyl)imide [NTf₂] were chosen as monoanions since they are the most widely used anions in ILs and they differ for size, shape and coordination ability. On the other hand, dianions present the two charged head groups on the same spacer and this could affect the spatial arrangement of cation–anion pairs and so the three-dimensional structure of ILs. It is worth of mentioning that dianion effect on ILs properties has been rarely analysed. At this aim dianions differing on nature of charged heads (sulfonate, carboxylate) and flexibility of the spacer have been selected. For this reason both aromatic and aliphatic dianions have been used. Among aromatic ones, differences on the isomeric substitution and on π -surface extension have been considered (1,5-naphthalendisulfonate [1,5-nds], 2,6-naphthalendisulfonate [2,6-nds] and 1,4-benzenedicarboxylate [1,4-bdc] and 2,6-naphthalenedicarboxylate [2,6-ndc] respectively). Finally, among aliphatic dianions, carboxylates with hexyl and octyl alkyl chain (adipate [ad] and suberate [sub] respectively) as spacers have been used in order to compare their flexibility with the rigidity of the corresponding aromatic dianions. Indeed, chains of four or six carbon atoms separate the charged heads as well as in the aromatic ones ([1,4-bdc], [1,5-nds], [ad] and [2,6-nds], [2,6-ndc], [sub] respectively).

[24] F. D'Anna, F. Ferrante and R. Noto, *Chem. Eur. J.* **2009**, *15*, 13059-13068.

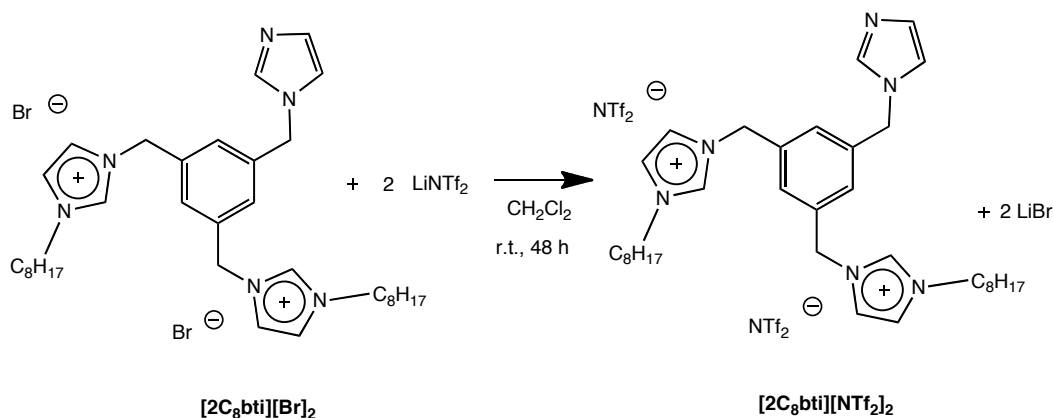
1. Synthesis of functionalised dicationic organic salts

The bromide DOSs studied were obtained after the dialkylation reaction on the neutral precursor 1,3,5-tris(imidazolyl)benzene (**bti**) as shown in Scheme 2. For the synthesis of this precursor, a previous procedure reported in literature was modified as explained in the experimental section.²⁵



Scheme 2: two-step synthesis for the bromide functionalised DOS.

In order to obtain all the salts previously described, two anion-exchange protocols were performed. The first is the classical one applied in ILs synthesis and it has been used for the formation of $[2C_8bti][NTf_2]_2$, Scheme 3 shows the synthetic pathway.²⁶



Scheme 3: synthetic procedure for classical anion exchange.

The anion substitution is established on the double exchange principle operating in presence of inorganic salts or in acid-base reactions. This procedure is favoured for

[25] H.-K. Liu, W.-Y. Sun, H.-L. Zhu, K.-B. Yu and W.-X. Tang, *Inorg. Chim. Acta* **1999**, *295*, 129-135.

[26] L. Cammarata, S. G. Kazarian, P. A. Salter and T. Welton, *Phys. Chem. Chem. Phys.* **2001**, *3*, 5192-5200.

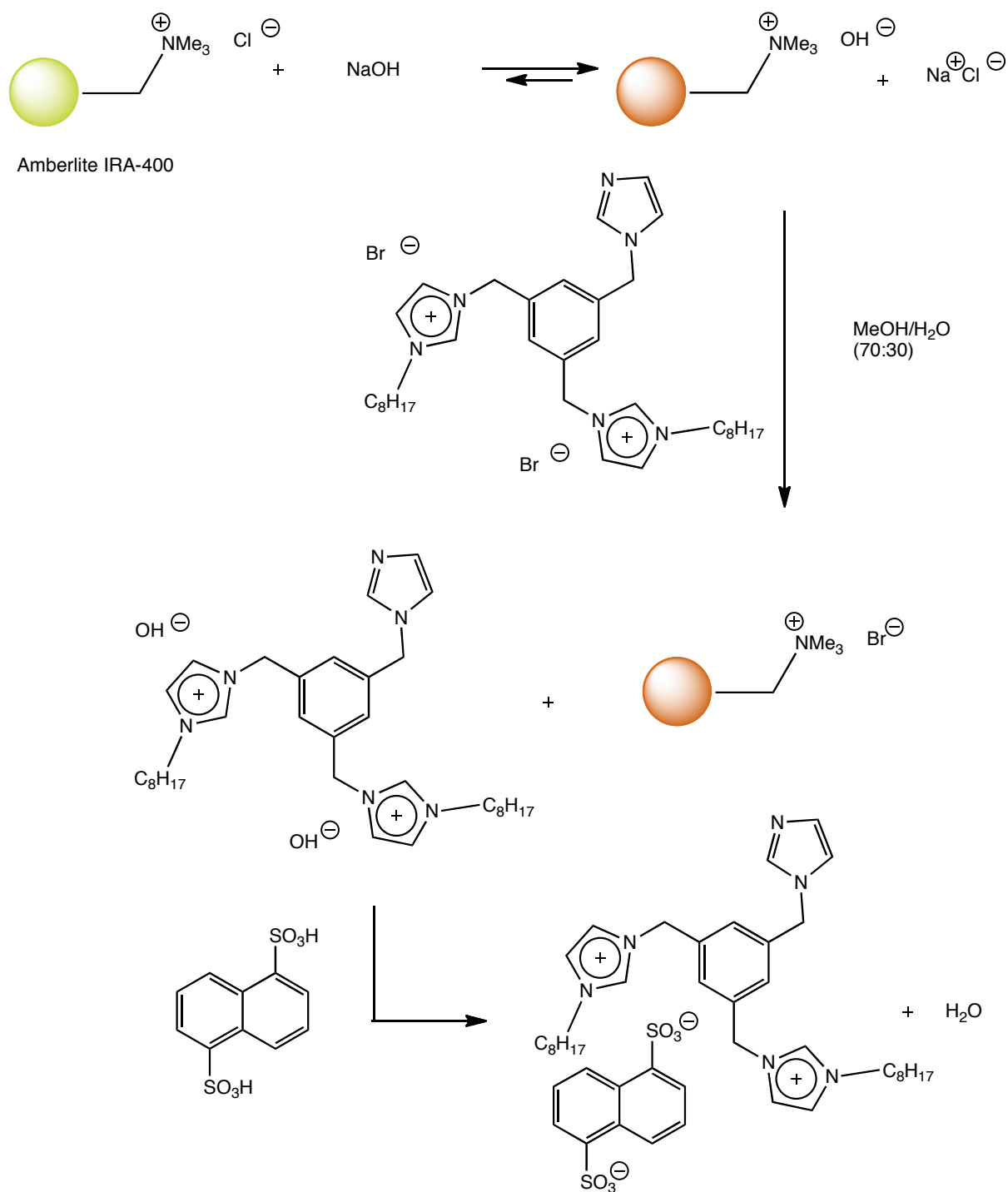
common ILs as they are highly soluble in solvent like dichloromethane while the inorganic salts formed during the anion exchange are soluble in water; consequently the separation of ILs from by-products becomes extremely simple.

The principle is not valid when the anion desired renders the final product soluble in water as the by-products. To avoid this problem, acid-base neutralization has been proposed by Earle and Seddon; however it requires the formation of intermediates like carbenes, as imidazolium or pyrrolidinium cations are usually less acid than the acid forms of the anions desired.²⁷ For this reason, Dinares *et al.* developed an excellent anion exchange protocol in agreement with the synthetic Green Chemistry principles.²⁸ The procedure requires a basic resin (Amberlite) charged in the oxydrilic form that is able to exchange the OH⁻ ion with the selected bromide salt; subsequently the latter one reacts with the conjugate acid of the anion wanted. The exchange is performed in water solution and does not form any by-products; finally the resin can be reused several times.

The explained procedure is reported in Scheme 4 for the obtainment of product **[2C₈bti][1,5-nds]**.

[27] M. J. Earle and K. R. Seddon in *Imidazole carbenes*, Vol. Google Patents, **2001**.

[28] I. Dinares, C. Garcia de Miguel, A. Ibanez, N. Mesquida and E. Alcalde, *Green Chem.* **2009**, *11*, 1507-1510.



Scheme 4: schematic representation of resin anion exchange procedure for product $[2C_8bti][1,5-nds]$.

2. Solution behaviour of functionalised DOSs: presence of conformational equilibria²⁹

The spectroscopic analysis, ¹H NMR, of TSILs synthesised showed an unexpected signal shape for benzylic and aromatic protons (5–9.5 ppm). In Figure 6, the ¹H NMR spectrum of [2C₈bti][Br]₂ in DMSO-d₆ solution, recorded at 300 K, is reported. The predicted singlets were split into three signals of different intensities, however their integrals were in agreement with the salt structure. In addition ¹³C NMR, HPLC, ESI-MS and elemental analysis confirmed the purity of the compound.

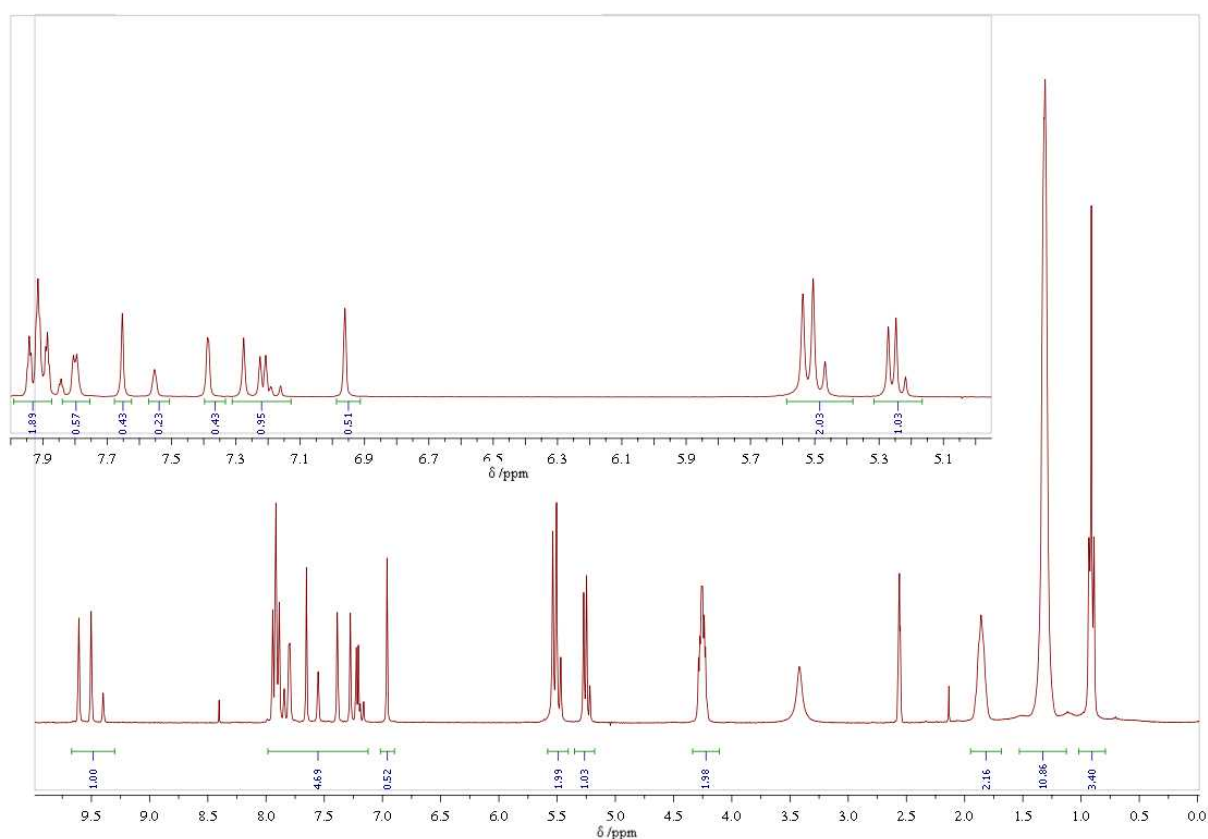


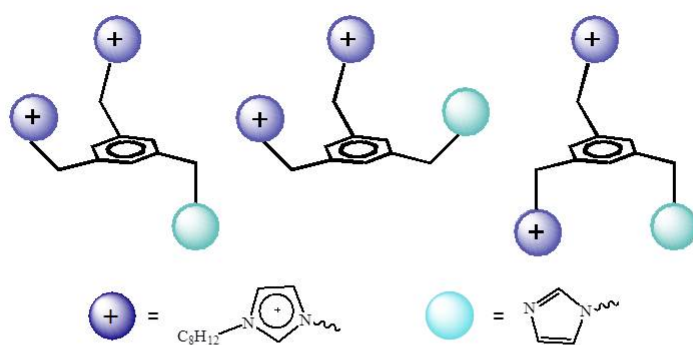
Figure 6: 400 MHz ¹H NMR spectrum of [2C₈bti][Br]₂ in DMSO-d₆ solution (0.038 M) at 300 K (inset: the expanded region 5–8 ppm comprehensive of benzylic and aromatic signals).

On the light of data collected it was hypothesized the presence of conformational equilibria in solution. The hypothesis was first supported by a similarity in structure with

[29] F. D'Anna, H. Q. N. Gunaratne, G. Lazzara, R. Noto, C. Rizzo and K. R. Seddon, *Org. Biomol. Chem.* **2013**, *11*, 5836-5846.

the coelenterands that usually possess three different conformational isomers around the aryl ring.³⁰

The possible conformational isomers in solution are shown in Figure 7. Considering the



aryl ring as a plane, they can present the charged heads on one side, all the three functionalities on the same side or one charged head together with the neutral functionality on one side.

Figure 7: possible conformational isomers in solution.

A further support came from the ^1H NMR study as function of temperature in the range between 300 and 390 K. The temperature range was limited from the freezing point of DMSO- d_6 and the maximum operational temperature of the instrument. Unfortunately the coalescence temperature was out of this range; however significant changes of chemical shifts and shape of the signals were recorded at different temperatures. Steed *et al.* have applied a similar approach studying the behaviour of aminopyridinium hosts for anion recognition, indeed they have reported splits of ^1H NMR signals at low temperature and ascribed this behaviour to the presence of conformational equilibria.³¹

This solution behaviour was detected for all the organic salts synthesised so it was also possible to compare data focusing in the signals at 5.0–5.5 ppm and 9.0–10.0 ppm that present “clean” regions. In Figure 8 ^1H NMR spectra corresponding to **[2C₈bti][1,5-nds]** as a function of temperature are reported.

[30] a) S. Koeller, G. Bernardinelli, B. Bocquet and C. Piguet, *Chem. Eur. J.* **2003**, *9*, 1062-1074, b) M. H. Filby and J. W. Steed, *Coord. Chem. Rev.* **2006**, *250*, 3200-3218.

[31] K. J. Wallace, W. J. Belcher, D. R. Turner, K. F. Syed and J. W. Steed, *J. Am. Chem. Soc.* **2003**, *125*, 9699-9715.

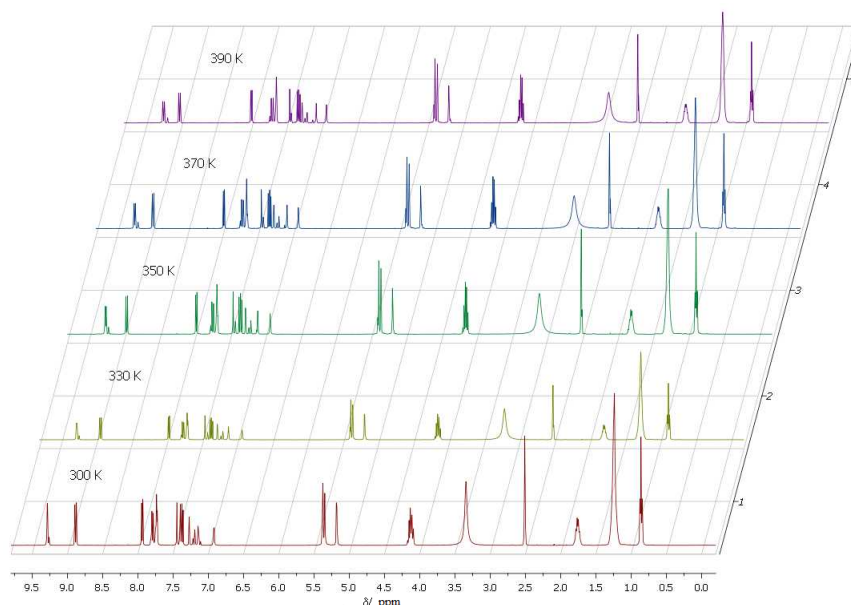


Figure 8: ^1H NMR spectra of $[\text{2C}_8\text{bti}][\text{1,5-nds}]$ in DMSO-d_6 solution (0.038 M) in the range 300-390 K.

With the temperature increase, the H(2) proton of the imidazolium ion (~ 9.5 ppm) undergoes an up-field shift on the contrary the benzylic protons (~ 5.5 ppm) undergo a down-field shift. In general, signals of H(2) of the imidazolium ion have more significant variation than benzylic ones ($\Delta\delta_{\text{Hi}} \sim -0.09$ and $+0.05$ ppm for H(2) of the imidazolium ion and benzylic protons, respectively). See also slope values of Table 1 reported below). In order to better understand the chemical shift variations as function of the temperature and to compare them for all salts taken into account, differences in chemical shifts were plotted as $\Delta\delta_{\text{Hi}}(T)$, where $\Delta\delta_{\text{Hi}}(T) = \delta_{\text{Hi}}(T) - \delta_{\text{Hi}}(300 \text{ K})$.

Table 1: correlation parameters of $\Delta\delta_{\text{Hi}}(T)$ for the H(2) of imidazolium and CH_2 benzylic, according to equations (1) and (2), *R= correlation coefficient.

Organic Salt	Imidazolium ring H(2) protons			CH_2 group attached to imidazolium		
	$(m_1 \pm \delta m_1)/10^{-4}$	$m_2 \pm \delta m_2$	R^*	$(m_3 \pm \delta m_3)/10^{-4}$	$m_4 \pm \delta m_4$	R^*
$[\text{2C}_8\text{bti}][\text{Br}]_2$	5.03 ± 0.90	-0.144 ± 0.031	0.955	5.16 ± 0.55	-0.151 ± 0.019	0.983
$[\text{2C}_8\text{bti}][\text{BF}_4]_2$	-8.77 ± 0.61	0.267 ± 0.021	0.992	3.05 ± 0.89	-0.091 ± 0.003	0.998
$[\text{2C}_8\text{bti}][\text{NTf}_2]_2$	-7.32 ± 0.85	0.225 ± 0.029	0.980	3.94 ± 0.54	-0.115 ± 0.099	0.973
$[\text{2C}_8\text{bti}][\text{1,5-nds}]$	-5.09 ± 0.17	0.154 ± 0.006	0.998	1.07 ± 0.17	-0.0314 ± 0.006	0.963
$[\text{2C}_8\text{bti}][\text{2,6-nds}]$	-3.91 ± 0.47	0.117 ± 0.002	0.999	1.99 ± 0.13	-0.060 ± 0.005	0.993
$[\text{2C}_8\text{bti}][\text{1,4-bdc}]$	-8.74 ± 0.40	0.260 ± 0.014	0.996	2.75 ± 0.04	-0.082 ± 0.001	0.999
$[\text{2C}_8\text{bti}][\text{2,6-ndc}]$	-9.28 ± 0.92	0.279 ± 0.003	0.999	3.02 ± 0.56	-0.087 ± 0.002	0.952
$[\text{2C}_8\text{bti}][\text{ad}]$	-	-	-	5.62 ± 0.11	-0.167 ± 0.004	0.999
$[\text{2C}_8\text{bti}][\text{sub}]$	-	-	-	5.20 ± 0.55	-0.156 ± 0.002	0.999

In Table 1, correlation parameters of $\Delta\delta_{\text{Hi}}(T)$ derived from the linear fit of following equations are reported:

$$\Delta\delta_{\text{H2}} = m_1 * T + m_2 \quad (1)$$

$$\Delta\delta_{\text{CH2}} = m_3 * T + m_4 \quad (2)$$

In Figure 9 the chemical shift variations for the analysed signals as a function of the temperature and the different nature of the anion are reported.

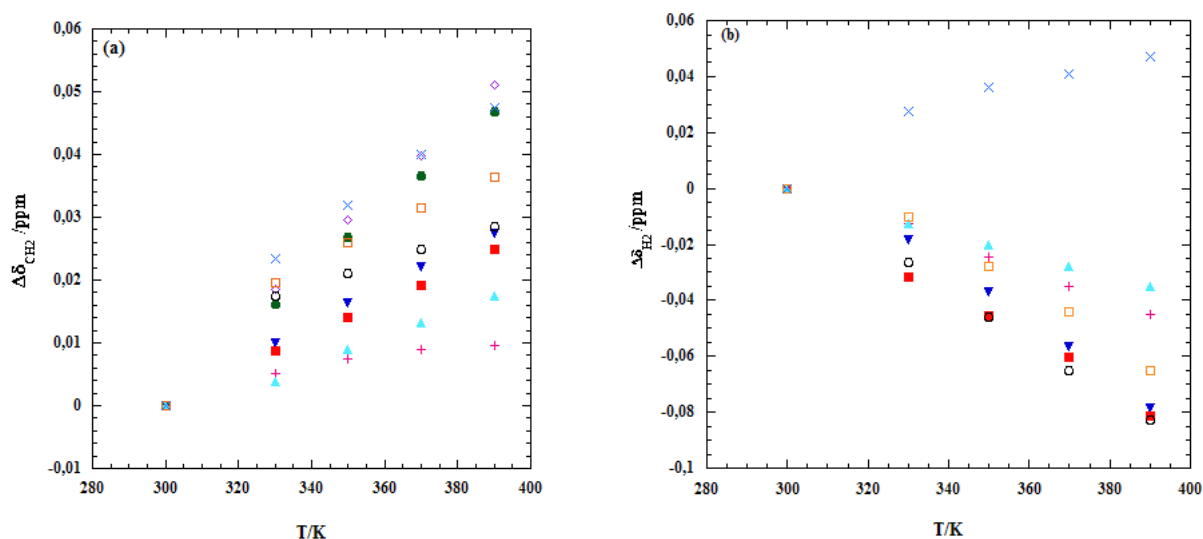


Figure 9: plots of $\Delta\delta_{\text{Hi}}(T)$ as a function of temperature corresponding to: (a) benzylic protons (~ 5.5 ppm) and (b) H(2) of imidazolium ion (~ 9.5 ppm).

Legend: \times [2C₈bti][Br]₂; \blacktriangledown [2C₈bti][BF₄]₂; \square [2C₈bti][NTf₂]₂; $+$ [2C₈bti][1,5-nds]; \blacktriangle [2C₈bti][2,6-nds]; \blacksquare [2C₈bti][1,4-bdc]; \circ [2C₈bti][2,6-ndc]; \diamond [2C₈bti][ad]; \bullet [2C₈bti][sub].

It is noteworthy that in the case of [2C₈bti][ad] and [2C₈bti][sub] a significant decrease

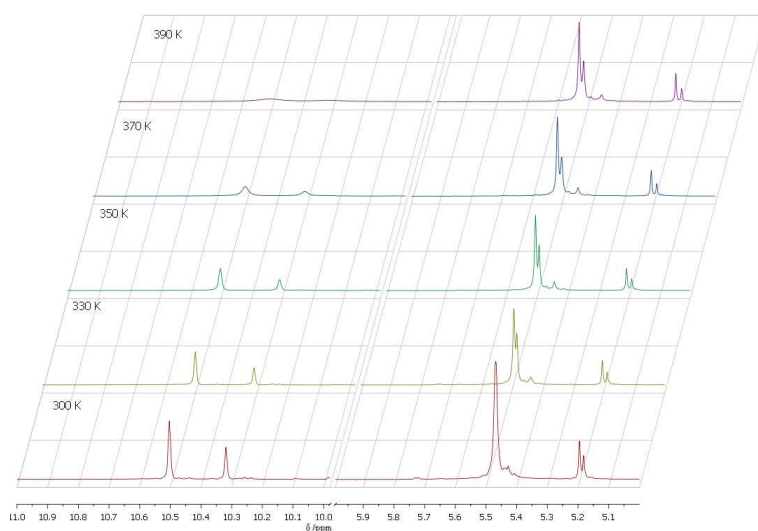


Figure 10: expanded region of ¹H NMR spectra of [2C₈bti][ad] in DMSO-d₆ solution (0.038 M) in the range 300-390 K.

in the H(2) signal at 370 K was observed (Figure 10). This phenomenon can be ascribed to the acid–base reaction probably occurring between the carboxylate and the H(2) proton of the imidazolium ion.

Indeed, it has been demonstrated that aliphatic amines are able to extract the H(2) by the imidazolium ion, accounting for its acidic nature.³² Moreover, the reaction with carboxylate anions has been widely used to favour carbene complexes formation.³³

However, this behaviour has not been evidenced for the aromatic carboxylate [1,4-bdc] and [2,6-ndc], therefore the influence of the temperature is really affected by anion structure.

Considering the chemical shift variations of benzylic protons, the highest $\Delta\delta_{\text{H}}$ were detected for the bromide ion and the flexible anions such as [ad] and [sub], followed by the others monoanions. While the lowest variations both in H(2) and benzylic protons were evidenced in the presence of naphthalenedisulfonate anions.

$\Delta\delta \text{ CH}_2$: [Br] \approx [ad] \approx [sub] > [NTf₂] > [1,4-bdc] \approx [2,6-ndc] > [BF₄] > [2,6-nds] > [1,5-nds]

Since significant changes in chemical shifts should depend on significant changes in the spatial arrangement of the cation structure, it is clear from the above trend that anion nature affects the distribution in solution of conformational isomers. In particular, the naphthalenedisulfonate anions seem to induce the formation of the most tight ion pairs in which only small variations in the cation conformation are allowed; on the other hand flexible dianions and monoanions give more freedom of conformational interconversion to the cation.

This hypothesis can be supported by some calculation previously performed on the geometry of the interactions between the 3,3'-dioctyl-1,1'-(1,3-phenylenedimethylene)diimidazolium cation and the 1,5-naphthalenedisulfonate anion.³⁴ In the optimised geometry, the anion is included in a kind of close cage formed by two aromatic rings of the cation and the sulfonate groups of the anion form hydrogen bond interactions with two imidazolium rings of different cations.

By the way to ascertain experimentally these cation–anion interactions 2D NOESY spectra were recorded (Figure 11a).

[32] F. D'Anna, V. Frenna, R. Noto, V. Pace and D. Spinelli, *J. Org. Chem.* **2006**, *71*, 9637-9642.

[33] a) S. A. Forsyth, H. Q. N. Gunaratne, C. Hardacre, A. McKeown, D. W. Rooney and K. R. Seddon, *J. Mol. Catal. A: Chem.* **2005**, *231*, 61-66, b) A. Biffis, L. Gazzola, C. Tubaro and M. Basato, *ChemSusChem* **2010**, *3*, 834-839.

[34] F. D'Anna, P. Vitale, F. Ferrante, S. Marullo and R. Noto, *ChemPlusChem* **2013**, *78*, 331-342.

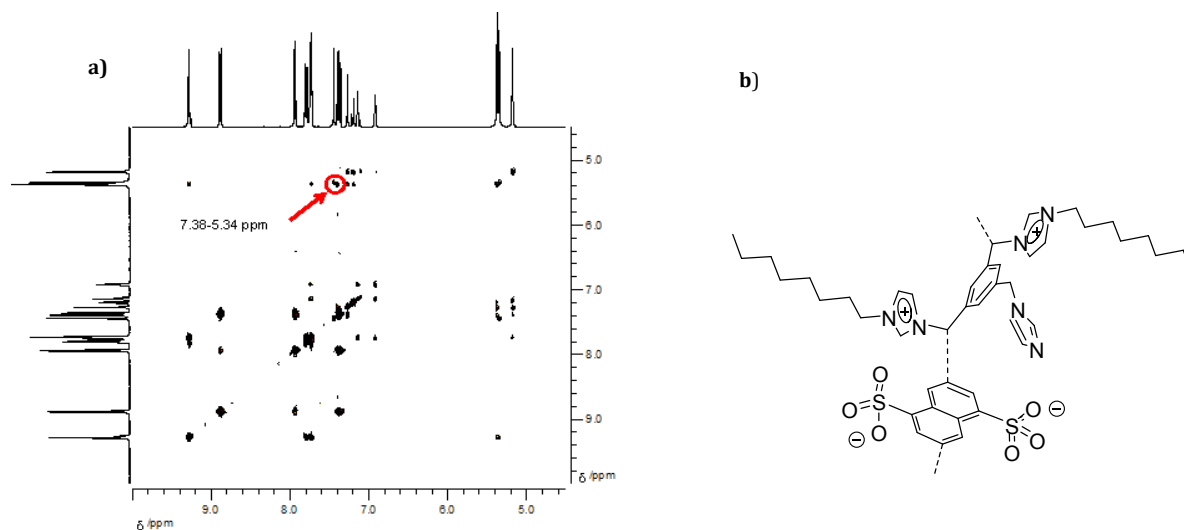


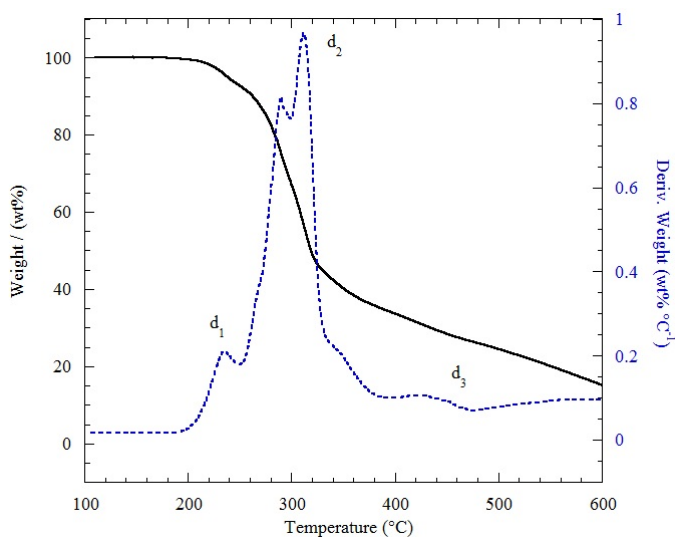
Figure 11: a) 2D NOESY spectrum of **[2C₈bti][1,5-nds]**; b) schematic representation of the possible cation-anion interactions.

The 2D NOESY spectra reveal the presence of cross-correlations peaks for TSILs having aromatic dianions. For example, in the case of naphthalenedisulfonate salts **[2C₈bti][1,5-nds]** and **[2C₈bti][2,6-nds]**, interactions between benzylic protons of the cation and anion protons (5.34–7.38 ppm for **[2C₈bti][1,5-nds]** and 5.14–7.71 ppm for **[2C₈bti][2,6-nds]** respectively) were evidenced. For **[2C₈bti][1,4-bdc]** in addition to this interaction (5.41–7.77 ppm), a cross correlation peak between the H(2) proton of the imidazolium ion and anion protons (10.24–7.77 ppm) was also detected. In Figure 11b, a schematic representation of possible cation-anion interactions occurring in presence of aromatic dianions is reported. From the data discussed, it is evident that the rigidity or flexibility of the anions affects cation-anion interactions and subsequently the distribution of conformational isomers in solution.

3. Thermal properties of functionalised DOSs

The thermal behaviour of the TSILs synthesised was studied by TGA (thermogravimetric analysis) and DSC (differential scanning calorimetry) measurements. With the first analysis degradation temperature, *i.e.* the thermal stability, and the degradation pathway of TSILs were determined. While with the second analysis the melting point, the enthalpy and the entropy variations relating to the melting process were obtained.

A typical TGA thermogram is shown in Figure 12. The percentage of loss weight (black line) represents the TGA trace; by



the way the degradation temperature of the TSILs was determined considering the first maximum (T_{d1}) of the TGA trace derivative (blue dotted line). This value has been considered as the maximum operational limit of the salts.

Figure 12: TGA (black) and DTGA (blue) traces of $[2C_8bti][Br]_2$.

In Table 2 decomposition temperatures and the percentage of loss in weight corresponding to the degradation steps are reported.

Table 2: experimental decomposition temperatures (T_{dn}) and percentage of loss in weight (in brackets) determined by TGA measurements.

TSILs	T_{d1} /°C	T_{d2} /°C	T_{d3} /°C
$[2C_8bti][Br]_2$	235.4 (7.3)	311.8 (56.3)	422.9 (19.2)
$[2C_8bti][BF_4]_2$	283.3 (18.1)	380.8 (53.7)	461.2 (8.7)
$[2C_8bti][NTf_2]_2$	283.6 (6.5)	436.0 (83.1)	
$[2C_8bti][1,5-nds]$	289.0 (11.8)	345.5 (56.2)	
$[2C_8bti][2,6-nds]$	236.2 (7.4)	316.7 (52.7)	485.9 (16.5)
$[2C_8bti][1,4-bdc]$	250.4 (38.9)	340.4 (23.4)	
$[2C_8bti][2,6-ndc]$	245.9 (64.3)		
$[2C_8bti][ad]$	228.8 (16)	244.3 (47.1)	351.4 (24.0)
$[2C_8bti][sub]$	233.6 (41.3)	373.6 (29.3)	

All salts analysed present at least two degradation steps with the only exception of $[2C_8bti][2,6-ndc]$. Data reported in the Table show that the operational limit for the dicationic TSILs ranges from

228.8 °C for $[2C_8bti][ad]$ up to 289.0 °C for $[2C_8bti][1,5-nds]$. Therefore the dicationic TSILs exhibit a high thermal stability that is lower than the one reported in literature for dicationic organic salts, but in agreement with the decreasing thermal stability observed for functionalised ILs.^{35,4} Furthermore, in our case in addition to a neutral functionality, the presence of different conformers could also affect the thermal stability.

The degradation process can be due to a nucleophilic attack of the anion to the imidazolium cations causing a reversible dealkylation.

[35] J. L. Anderson, R. Ding, A. Ellern and D. W. Armstrong, *J. Am. Chem. Soc.* **2005**, *127*, 593-604.

[4] C. Chiappe and C. S. Pomelli, *Eur. J. Org. Chem.* **2014**, *2014*, 6120-6139.

Values in the Table indicate once again an influence of the anion nature on the thermal stability of the TSILs. In general, with the only exception of **[2C₈bti][2,6-nds]**, monoanionic TSILs present a larger temperature range in the degradation process in respect to dianionic ones. In the series of monoanions, the lowest T_{d1} value is evidenced for **[2C₈bti][Br]₂**, indeed among the monoanions considered, the bromide presents the highest nucleophilicity. The same behaviour has been previously obtained for monocationic imidazolium salts.³⁶

The highest decomposition temperature is observed for **[2C₈bti][1,5-nds]**, probably due to the π - π interactions occurring in this salt. Interestingly, the thermal stability decreases in the case of a different isomeric substitution of the anion, from 289.0 °C to 236.2 °C for **[2C₈bti][2,6-nds]**. Furthermore, the comparison among naphthalendisulfonate and dicarboxylate salts shows that the different nature of the charged head substantially determines the thermal stability of the studied ionic liquids.

Concerning the dicarboxylate anions, aromatic ones give higher thermal stability to the salts than the aliphatic ones. However, an increase in π -surface extension of the anion aromatic spacers causes a negative effect on salt thermal stability (T_{d1} of [1,4-bdc] > T_{d1} [2,6-ndc]). On the contrary, a longer alkyl chain in the structure of flexible dianions increases the operational temperature of the salts (T_{d1} of [sub] > T_{d1} [ad]). Furthermore, it is worth noting a peculiar behaviour for the dicarboxylate salts. Indeed, their TGA traces showed a significant first loss in weight below 150 °C, this loss can be ascribed to a decarboxylation process.³⁷ In Table 3, temperatures, experimental and calculated weight loss corresponding to decarboxylation processes of these salts are reported.

Table 3: temperatures, experimental and calculated weight loss corresponding to decarboxylation processes of dicarboxylate salts.

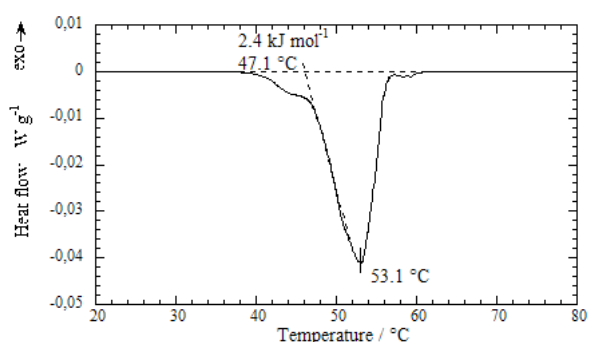
<i>Organic Salt</i>	<i>T / °C</i>	<i>Weight loss / %</i>	<i>Calc. weight loss / %</i>
[2C₈bti][1,4-bdc]	143.6	10.5	6.2
[2C₈bti][2,6-ndc]	92.7	8.7	5.8
[2C₈bti][ad]	99.1	11.6	6.4
[2C₈bti][sub]	92.0	11.8	6.1

[36] a) M. C. Kroon, W. Buijs, C. J. Peters and G.-J. Witkamp, *Thermochim. Acta* **2007**, *465*, 40-47, b) Y.-N. Hsieh, R. Horng, W.-Y. Ho, P.-C. Huang, C.-Y. Hsu, T.-J. Whang and C.-H. Kuei, *Chromatographia* **2008**, *67*, 413-420.

[37] K. Ma, K.-M. Lee, L. Minkova and R. G. Weiss, *J. Org. Chem.* **2009**, *74*, 2088-2098.

Analysis of data in Table 3 underlines that the lower difference detected between calculated and experimental percentages of loss in weight is observed for aliphatic dianions, so they present the highest tendency to decarboxylate. This phenomenon can also influence the loss of H(2) imidazolium proton evidenced by variable temperature ^1H NMR studies.

As previously disclosed, after this accurate analysis on the thermal stability of the TSILs, a calorimetric analysis on their melting temperatures has been performed. In general TSILs taken into account showed broad endothermic peaks, sometimes presenting small



shoulders, and no signal in the crystallization process. In Figure 13 a typical DSC trace is shown. This behaviour is not strange for ILs; indeed it could be a consequence of the high viscosity of the liquid phases obtained from the melting process.³⁵

Figure 13: DSC trace of functionalised dicationic ionic liquid $[\text{2C}_8\text{bti}][\text{Br}]_2$.

In addition, the different conformations derived by the high flexibility of the cation structure can lead to different energies of the crystal lattice and then to multistep transitions, further complicating the thermogram trace.³⁸ In Table 4 melting temperature (T_m) and the correlated thermodynamic parameters for TSILs are reported.

Table 4: melting temperatures and thermodynamic parameters determined by DSC measurements.

TSILs	$T_m / ^\circ\text{C}$	$\Delta H_m / \text{kJ mol}^{-1}$	$\Delta S_m / \text{J mol}^{-1}\text{K}$
$[\text{2C}_8\text{bti}][\text{Br}]_2$	53.1	2.4	7.3
$[\text{2C}_8\text{bti}][\text{BF}_4]_2$	51.1	5.3	16.4
$[\text{2C}_8\text{bti}][\text{NTf}_2]_2$	51.1	4.2	12.9
$[\text{2C}_8\text{bti}][1,5\text{-nds}]$	55.3	45.9	139.8
$[\text{2C}_8\text{bti}][2,6\text{-nds}]$	50.4	41.8	129.3
$[\text{2C}_8\text{bti}][1,4\text{-bdc}]$	55.9	5.4	16.2
$[\text{2C}_8\text{bti}][2,6\text{-ndc}]$	-	-	-
$[\text{2C}_8\text{bti}][\text{ad}]$	51.1	6.2	19.2
$[\text{2C}_8\text{bti}][\text{sub}]$	54.4	8.5	26.0

[35] J. L. Anderson, R. Ding, A. Ellern and D. W. Armstrong, *J. Am. Chem. Soc.* **2005**, *127*, 593-604.

[38] J. D. Holbrey, W. M. Reichert, M. Nieuwenhuyzen, S. Johnson, K. R. Seddon and R. D. Rogers, *Chem. Commun.* **2003**, 1636-1637.

On the grounds of melting temperatures, all the organic salts taken into account can be defined as ILs and considering the presence of the neutral functionality, as TSILs. Differently from thermal stability, melting temperatures were not highly influenced by anion nature of TSILs, indeed they ranged from 50.4 to 55.8 °C. However it is possible to make some considerations also about this property.

It is worth of noting that the melting process was not determined in the case of **[2C₈bti][2,6-ndc]** due to the small enthalpy variation associated to the process.

In the class of TSILs presenting monoanions, the bromide one has the highest T_m . This result recalls properties of ILs as the presence of fluorine in anion structure usually induces a decrease in melting temperature of ionic liquids.³⁹ On the other hand, the highest T_m among dianionic TSILs has been observed for **[2C₈bti][1,5-nds]** and **[2C₈bti][1,4-bdc]**, probably because the rigidity of the spacer induces the formation, also in the solid state, of tighter cation–anion interactions. The length of the alkyl chain of the spacer is also important, so that going from **[2C₈bti][ad]** to **[2C₈bti][sub]** an increase of T_m is observed.

A deeper analysis of the melting process can be performed considering the thermodynamic parameters (ΔH_m and ΔS_m) associated to the process. These parameters reflect results obtained from previous analysis, *i.e.* NMR and TGA measurements; therefore the highest energy required for the solid-liquid transition is recorded for naphthalendisulfonate salts. As this trend is in agreement with the lowest conformational freedom in solution detected for naphthalendisulfonate salts, we found a qualitative correspondence between melting parameters and conformational equilibria. In particular, a linear plot of the slope describing the temperature effect on benzylic chemical shifts (Table 1) and ΔH_m is reported in Figure 14. Indeed, with the only exception of **[2C₈bti][1,4-bdc]**, two distinct linear trends were observed for mono- and dianions. From this trend it is possible to assert that cation–anion interactions affect the thermal properties in similar way in solution and in the concentrated liquid phase.

[39] a) T. Payagala, Y. Zhang, E. Wanigasekara, K. Huang, Z. S. Breitbach, P. S. Sharma, L. M. Sidisky and D. W. Armstrong, *Anal. Chem.* **2009**, *81*, 160-173, b) T. S. Jo, W. L. McCurdy, O. Tanthmanatham, T. K. Kim, H. Han, P. K. Bhowmik, B. Heinrich and B. Donnio, *J. Mol. Struct.* **2012**, *1019*, 174-182.

As previously stated this reaction has been widely studied in solution of conventional solvent and ILs, as it is well known that the rearrangement is favoured in polar solvents.⁴¹ In particular, in order to study the effect of ILs on the reaction outcome, it has been studied in solution of both mono- and dicationic ILs in lack of a base catalyst.⁴² ILs used in a previous study are shown in Figure 15.

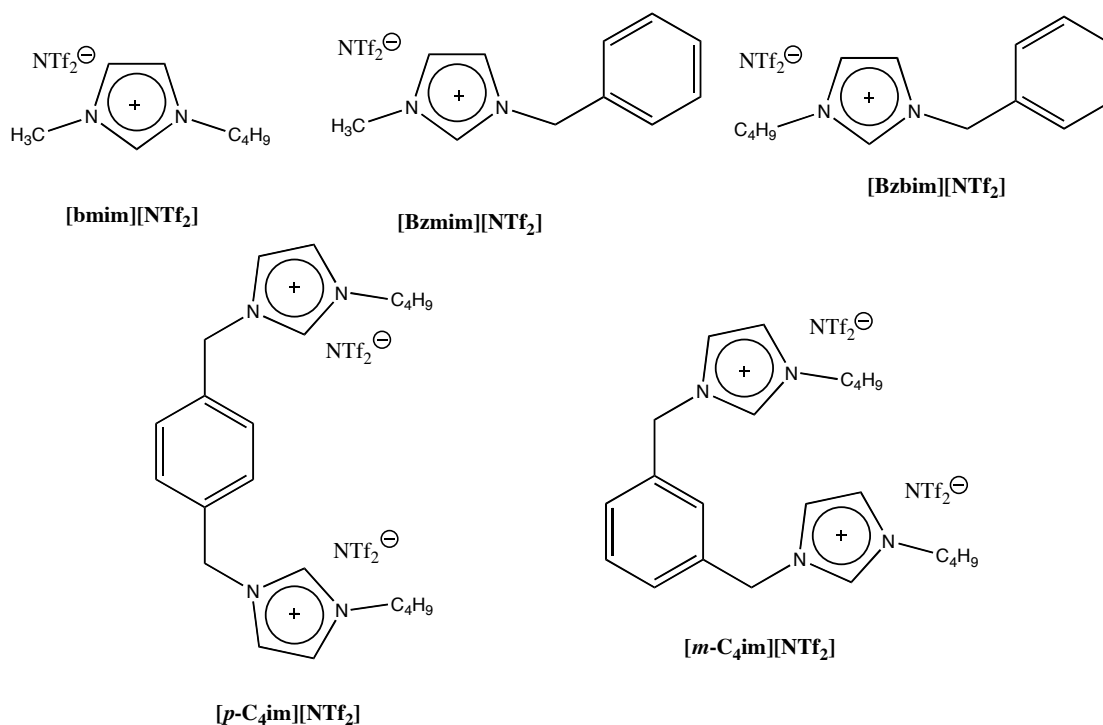


Figure 15: mono- and dicationic ILs used as reaction media for the mononuclear rearrangement, ref. 42.

Experimental data evidenced that benzylimidazolium and *para*-substituted diimidazolium ILs resulted the best reaction media obtaining higher percentage yields than in MeOH and DMF, even if in longer reaction times. These results indicate that solvents with high structural order establish π - π stacking interactions stabilizing the cyclic quasi-aromatic transition state of the reaction. The above hypothesis has been supported by a combined approach of different techniques evidencing that the outcome of the reaction is ruled by the structural order degree of ILs instead by the polarity effect normally occurring in conventional solvents. Furthermore the possibility to recycle the ILs and to use a small amount of solvent turns structured ILs as best reaction media for the reaction taken into account.

[41] F. D'Anna, V. Frenna, R. Noto, V. Pace and D. Spinelli, *ibid.* **2005**, *70*, 2828-2831.

[42] F. D'Anna, S. Marullo, P. Vitale and R. Noto, *Eur. J. Org. Chem.* **2011**, *2011*, 5681-5689.

On the grounds of this information, we decided to study the outcome of the rearrangement in solution of TSILs, as demonstrated above they possess a high structural degree and a base functionality that should favour the reaction selected.

The reaction has been performed at 90 °C in order to have a homogeneous reaction mixture and to compare results with the ones previously reported in ILs solution. The reaction outcome was monitored via TLC until the complete disappearance of the substrate. The reaction was carried out using a solvent/substrate molar ratio equal to 4.5 (0.48 mmol of TSIL and 0.105 mmol of substrate). In agreement with Green Chemistry principles, the amount of TSILs used was the smallest allowing the solubilisation of the substrate.

In Table 5 the reaction times as function of TSILs are reported. Table includes also results previously obtained for the same reaction to better understand the catalytic activity of the new salts.

Table 5: reaction times and yields in triazole obtained in different TSILs.

TSILs	Reaction time (h)	Yield (%) ^a
[2C ₈ bti][Br] ₂	2.75	77
[2C ₈ bti][BF ₄] ₂	1	96
[2C ₈ bti][NTf ₂] ₂	7	84
[2C ₈ bti][1,5-nds]	7	0
[2C ₈ bti][2,6-nds]	7	0
[2C ₈ bti][1,4-bdc]	5.5	86
[2C ₈ bti][2,6-ndc]	7	63
[2C ₈ bti][ad]	0.5	95
[2C ₈ bti][sub]	0.5	87
[bmim][NTf ₂] ^b	8	53
[Bzmim][NTf ₂] ^b	8	63
[Bzbim][NTf ₂] ^b	8	92
[<i>p</i> -C ₄ im][NTf ₂] ₂ ^b	8	96
[<i>m</i> -C ₄ im][NTf ₂] ₂ ^b	8	74

^aYields were reproducible within 4%. ^bSee reference 42.

Analysis of data in Table 5 evidences the highest efficiency of [2C₈bti][ad] and [2C₈bti][sub] as in these TSILs the reaction is completed in just 30 minutes and presents

good percentage yields. On the other hand, the reaction is not favoured in presence of TSILs with aromatic dianions. Reaction times increase drastically in aromatic dicarboxylate TSILs and in the case of naphthalendisulfonate ones the triazole was not detected even in traces. In the last case, the concentration of (*Z*)-phenylhydrazone in the reaction mixture did not show significant decrease, as evaluated using a UV-vis calibration curve (see Experimental Section). In general, data indicate that an increase in the spacer length of alkyl chain ([ad] and [sub]) or in the π -surface area of the spacer ([1,4-bdc] and [2,6-ndc]), induced a parallel increase in reaction time and a decrease in yields.

These results show that the catalytic ability of TSILs, as well as the properties previously described, is affected by anion nature of TSILs taken into account.

Among the TSILs studied, also **[2C₈bti][BF₄]₂** represents a good reaction media. In particular, reactivity results obtained in the series of monoanionic TSILs in terms of reaction times decrease as following: [NTf₂] > [Br] > [BF₄]. This trend seems to be dependent on the anion crosslinking ability that favours the formation of a highly organized three-dimensional network.⁴³ Moreover, considering the significantly difference in reaction times for **[2C₈bti][NTf₂]₂** and **[2C₈bti][Br]₂** (7 and 2.75 h, respectively), yields obtained in these TSILs can be considered almost equal (84% and 77%, respectively).

Results reported in the above Table underline the importance of the basic functionality in the cationic structure. This is shown by the comparison between reaction times obtained in **[2C₈bti][NTf₂]₂** and those previously collected using both mono- and dicationic [NTf₂]-based ILs. Indeed, lower yields in higher reaction times and using a higher solvent/substrate molar ratio (8/1) were obtained in solution of [bmim][NTf₂], [Bzmim][NTf₂] and [*m*-C₄im][NTf₂]₂. Above all, comparison with the *meta*-dicationic ionic liquid, presenting a similar cationic structure to TSILs, allowed us to evaluate the positive effect deriving from the anchoring of the basic catalyst on the structure of dicationic IL.

In order to compare homogeneously percentage yields in different TSILs, minimum and maximum reaction times have been selected on the grounds of reaction times obtained (30 minutes and 7 h, respectively). Data are reported in the histogram below.

[43] M. D. Joshi and J. L. Anderson, *RSC Adv.* **2012**, 2, 5470-5484.

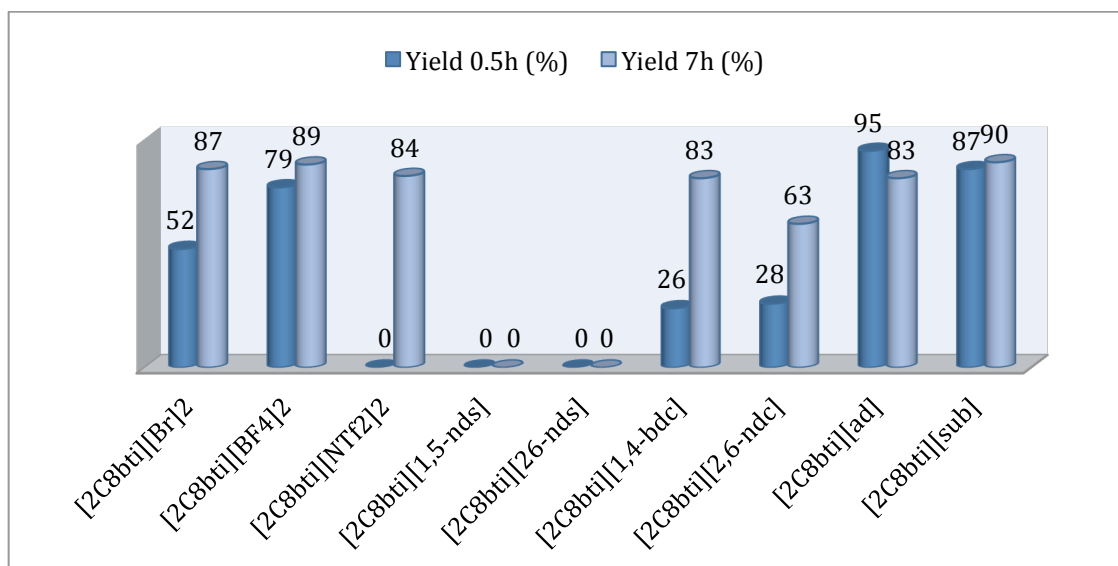


Figure 16: yields in triazole at equivalent reaction times (0.5 and 7 h) as a function of TSIL used.

Yields collected at equivalent reaction times confirmed the trend observed following the disappearance of the substrate. Once again TSILs with [ad] and [sub] anions present the highest yield at 0.5 h, followed by [BF₄]-based TSIL that is the best media among monoanionic ones. Results obtained at 7 h further supported the influence of the different anion nature on the reaction outcome. This dependence realizes in terms of different nature of anionic head, demonstrated by higher reactivity of [2,6-ndc] than [2,6-nds] derivative; extension of π -surface area of the anion, decreasing on going from [1,4-bdc] to [2,6-ndc]; flexibility of anion spacer, as testified by the high reactivity obtained in aliphatic dicarboxylate anions rather than in aromatic ones.

To explain which parameter ruled this reaction, we have further analysed TSILs properties. First of all, knowing that the mononuclear rearrangement is a base catalysed reaction, we have determined in methanol solution the TSILs basicity function, H_- , using the Hammett indicator method.^{22,44} Basic strength was expressed by the following equation 3:

$$H_- = pK_{HI} + \log\frac{[I^-]}{[HI]} \quad (3)$$

where pK_{HI} is the logarithm of the dissociation constant of the indicator used, and [HI] and [I⁻] are the concentration of the indicator and its conjugated base, respectively. The

[22] M. Fan, J. Yang, P. Jiang, P. Zhang and S. Li, *ibid.* **2013**, 3, 752-756.

[44] a) W. Xie, H. Peng and L. Chen, *Applied Catalysis A: General* **2006**, 300, 67-74, b) M. Kouzu, T. Kasuno, M. Tajika, Y. Sugimoto, S. Yamanaka and J. Hidaka, *Fuel* **2008**, 87, 2798-2806.

$[I^-]/[HI]$ ratio was determined spectrophotometrically after the evaluation of indicator ε value.

Even if the basicity detected in methanol solution could be different than the one of neat IL, determination of the H_- function should give general information about basic strength of solvent media able to promote the target reaction.

To this aim, H_- values were determined using two acidic indicators *p*-nitrophenol and bromocresol green because the nature of anions used gave rise to different basic strengths. The UV-vis spectra of two TSILs of different basicity strength are shown in Figure 17, while all collected data are reported in Table 6.

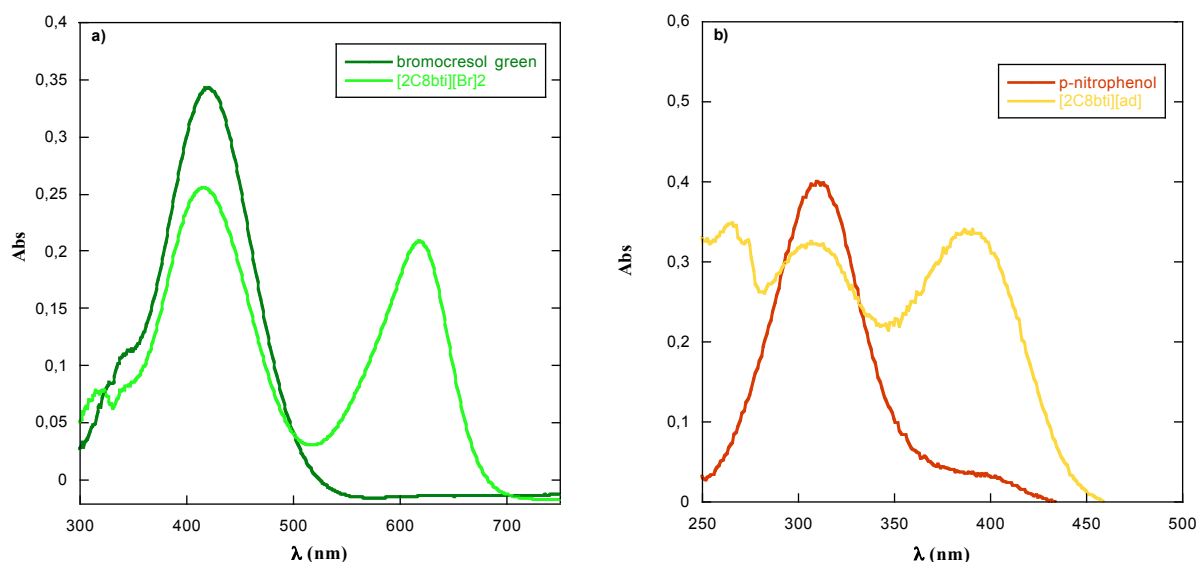


Figure 17: UV-vis spectra recorded at 25 °C for **a)** bromocresol green/[2C₈bti][Br]₂ and **b)** *p*-nitrophenol/[2C₈bti][ad] systems in methanol solution.

Table 6: H_- values determined for TSILs at 25 °C using the method of Hammett indicator.

Bromocresol Green ^a		<i>p</i> -nitrophenol ^b	
TSILs	H_-^c	TSILs	H_-^c
[2C ₈ bti][Br] ₂	9.3	[2C ₈ bti][1,4-bdc]	10.7
[2C ₈ bti][BF ₄] ₂	9.0	[2C ₈ bti][ad]	10.7
[2C ₈ bti][NTf ₂] ₂	8.5	[2C ₈ bti][sub]	10.5
[2C ₈ bti][1,5-nds]	8.9		
[2C ₈ bti][2,6-nds]	8.6		

^a pK_a (MeOH) = 9.80.⁴⁵ ^b pK_a (MeOH) = 11.30.⁴⁵ ^c H_- values were reproducible within ± 0.1 .

[45] F. Rived, M. Rosés and E. Bosch, *Anal. Chim. Acta* **1998**, 374, 309-324.

It is worth mentioning that **[2C₈bti][2,6-ndc]** presents a strong UV absorption band and it was not possible to measure the corresponding H_{-} value.

The highest basicity has been detected for **[2C₈bti][ad]**, **[2C₈bti][1,4-bdc]** and **[2C₈bti][sub]**, whereas the least one has been determined for **[2C₈bti][2,6-nds]** and **[2C₈bti][NTf₂]₂**. Even if these data indicate a certain influence of TSIL basic strength on the reaction outcome, it cannot be considered the driving force of the reaction. Indeed, even if the best reaction media, *i.e.* [ad]- and [sub]-based ILs, present the highest basicity values, the comparable basicity between [NTf₂] and [2,6-nds]-based ILs does not explain the triazole formation in **[2C₈bti][NTf₂]₂** solution. Moreover, also the basicity of **[2C₈bti][BF₄]₂** is lower than the ones reported for **[2C₈bti][Br]₂** and **[2C₈bti][1,4-bdc]**, in which the reaction proceeds in longer time obtaining lower reaction yields.

The correlation between acidity or basicity of TSILs and their reactivity has not always been reported as it depends on ILs nature and type of reaction. As in our case, this correlation was not observed in the study of catalytic performance of some acidic ILs in the Beckmann rearrangement and in the production of γ,γ -bishydroxyphenyl valeric acid from renewable levulinic acid.^{46,21b} Yields obtained in the biodiesel production, using basic DILs, have instead been explained as function of base amount.²²

Having in mind the above-mentioned effect of ILs structure on the outcome of the rearrangement and the influence of anion nature on TSILs properties, such as conformational equilibria in solution and thermal stability, we explained the reactivity results. Indeed, the geometry of the TSILs should hamper the inclusion of the transition state between two parallel planes of cations and consequently the formation of stabilizing $\pi-\pi$ interactions.²⁴ On the grounds of activation parameters, the occurrence of these interactions has been previously proved in solution of aromatic but not in aliphatic monocationic ILs.³²

Therefore, remembering that the formation of tightest ion pairs, for example in presence of [nds]- and [ndc]-based TSILs (see Figure 11), limits the conformational freedom of the cation in solution, it probably limits also the interactions with the transition state. On the

[46] X. Liu, L. Xiao, H. Wu, J. Chen and C. Xia, *Helv. Chim. Acta* **2009**, *92*, 1014-1021.

[21] b) H.-F. Liu, F.-X. Zeng, L. Deng, B. Liao, H. Pang and Q.-X. Guo, *Green Chem.* **2013**, *15*, 81-84.

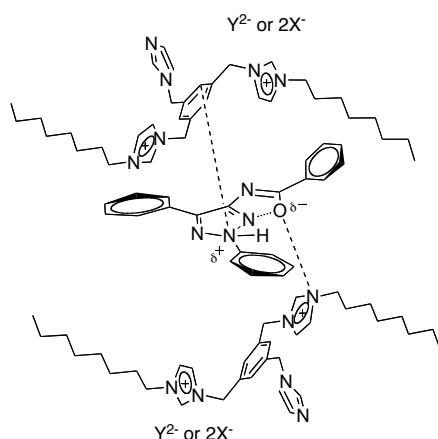
[22] M. Fan, J. Yang, P. Jiang, P. Zhang and S. Li, *RSC Adv.* **2013**, *3*, 752-756.

[24] F. D'Anna, F. Ferrante and R. Noto, *Chem. Eur. J.* **2009**, *15*, 13059-13068.

[32] F. D'Anna, V. Frenna, R. Noto, V. Pace and D. Spinelli, *J. Org. Chem.* **2006**, *71*, 9637-9642.

other hand, more flexible anions, such as [ad] and [sub] or monoanions, can easily allow the establishment of π - π interactions between cation and the transition as shown in Figure 18.

This hypothesis can better explain TSILs reactivity. In addition, this could also clarify the significant differences in yields and reaction times detected among [2C₈bti][1,4-bdc],



[2C₈bti][ad], and [2C₈bti][sub] notwithstanding comparable basicity. Furthermore, a different behaviour of mono- and dianionic TSILs has been observed. Indeed, the thick reticulation of solvent induced by the presence of the [BF₄] anion did not hamper cation-transition state interactions able to favour the outcome of the reaction.

Figure 18: schematic representation of interactions between cation and transition state.

Finally, as previously evidenced, one of the main advantages to use TSILs in catalysis is the possibility to recycle them for several catalytic cycles avoiding the catalyst leakage. For this reason the recyclability of the TSILs studied has been tested; interestingly in our case both the solvent and the catalyst could be employed again for a subsequent reaction.

The recycling of the TSILs has been performed reusing the solvent system after extraction of the reaction product in diethyl ether. This procedure was possible thanks to the low solubility of TSILs in diethyl ether; indeed after each recycle loss in weight of the IL was lower than 5%. It is worth noting that further recycling was avoided if drop in yields higher than 10% or loss in IL weight higher than 5% were detected.

Data reported in Table 7 show that all TSILs presenting catalytic activity were recyclable for at the least two times. The best reaction media, namely [2C₈bti][BF₄]₂, [2C₈bti][ad], and [2C₈bti][sub], have been reused with good percentage yields for 4 and 5 cycles in the case of [ad]-based TSIL.

On the other hand, longer reaction times and poor recyclability of [2C₈bti][NTf₂]₂ and [2C₈bti][2,6-ndc] deter from their use as solvent media for the reaction taken into account. In particular, the first one precluded the possibility of recycling, whereas in the second case a significant drop in yield was observed after the second cycle.

Table 7: yields in triazole, reaction times and catalytic cycles as a function of TSIL used.

TSILs	Catalytic cycle	Time (h)	Yield (%) ^a
[2C ₈ bti][Br] ₂	I	2.75	77
	II	2.75	84
	III	2.75	67
[2C ₈ bti][BF ₄] ₂	I	1	96
	II	1	90
	III	1	88
	IV	1	91
[2C ₈ bti][NTf ₂] ₂	I	7	84
[2C ₈ bti][1,5-nds]	I	7	0
[2C ₈ bti][2,6-nds]	I	7	0
[2C ₈ bti][1,4-bdc]	I	5.5	86
	II	5.5	90
	III	5.5	74
[2C ₈ bti][2,6-ndc]	I	7	63
	II	7	56
[2C ₈ bti][ad]	I	0.5	95
	II	0.5	83
	III	0.5	86
	IV	0.5	88
	V	0.5	78
[2C ₈ bti][sub]	I	0.5	87
	II	0.5	85
	III	0.5	88
	IV	0.5	76

^aYields were reproducible within 4%.

The catalytic and the recycling ability of the TSILs have been proved. Therefore the mononuclear rearrangement of heterocycles has been performed with good yields and reaction times. Finally, the reactivity of TSILs confirmed the influence of anion, in terms of flexibility, coordination ability or aromaticity, on the ILs properties.

These results encouraged us to test the catalytic ability of the best reaction media for another base-catalysed reaction.

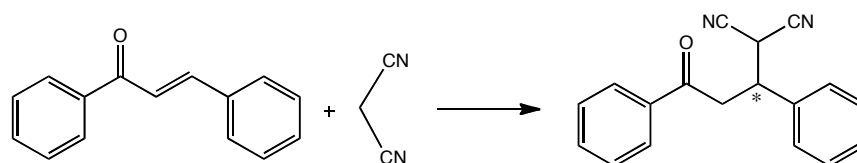
4. 2. *The Michael addition of trans-chalcone to malononitrile*

The Michael addition of nucleophiles to α,β -unsaturated carbonyl compounds represents one of the most studied reactions of the carbon-carbon bond formation in organic chemistry.⁴⁷

In particular, we took into account the reaction of *t*-chalcone with malononitrile (Scheme 6) as nucleophile because it has not been widely reported in comparison to those of other

[47] E. N. Jacobsen, A. Pfaltz and H. Yamamoto, *Comprehensive Asymmetric Catalysis*, Springer, New York, 1999, p. 1105-1143.

carbanion nucleophiles. In addition, the nitrile group of malononitrile is a useful functional group that could be conveniently transformed to other groups. The product reaction results, sure enough, as an intermediate for the formation of compounds of biochemical and pharmaceutical interest, such as 4H-pyran derivative.⁴⁸



Scheme 6: Michael addition of malononitrile to *t*-chalcone.

t-Chalcone is also an important compound in the fight against cancer, indeed it has been proved to be a chemotype able to suppress the invasive phenotype of malignant cells avoiding the attack of neighbouring tissues that causes metastases.⁴⁹ So, the possibility to generate small modification in the structure of chalcones could be also interesting in order to enhance their activity as chemotype.

Another reason that pushed us to study the above reaction is the fact that it has always been studied using strong base catalysts in conventional solvents, so it represents the perfect candidate to test the catalytic ability of some of the novel imidazolium TSILs studied with the addition of other anion structures (Figure 19).

In particular, it has been applied the cationic unit [2C₈bt⁺] with the imidazole as neutral functionality. While bromide, adipate and suberate were selected among the anions previously studied. The first one has been selected in order to homogenously compare the catalytic activity of the TSIL with the one of the corresponding unfunctionalised dicationic IL, 3,3'-di-*N*-octyl-1,1'-(1,3-phenylenedimethylene)diimidazolium dibromide [***m*-Csim**][Br]₂. The other ones, [ad] and [sub], have been chosen in consideration of the fact that they have awarded the best catalytic ability to the TSILs in the study of the mononuclear heterocyclic rearrangement.

Having in mind that the reaction product is chiral, we were also interested in testing the stereochemical aspects of the reaction. For this reason, chiral anions have been used as

[48] a) L. Jiarong, C. Xian, S. Daxin, M. Shuling, L. Qing, Z. Qi and T. Jianhong, *Org. Lett.* **2009**, *11*, 1193-1196, b) J. Shi, M. Wang, L. He, K. Zheng, X. Liu, L. Lin and X. Feng, *Chem. Commun.* **2009** 4711-4713.

[49] B. I. Roman, T. De Ryck, S. Verhasselt, M. E. Bracke and C. V. Stevens, *Bioorg. Med. Chem. Lett.* **2015**, *25*, 1021-1025.

counter ions of the cationic unit. TSILs presenting chiral dianions, D- and L-tartrate, were synthesised while chiral monoanions such as L-prolinate, L-phenylalaninate and (R)-(-)-1,1'-binaphthyl-2,2'-diyl phosphate have been used as they represent some of the chiral organocatalysts most applied in organic synthesis.

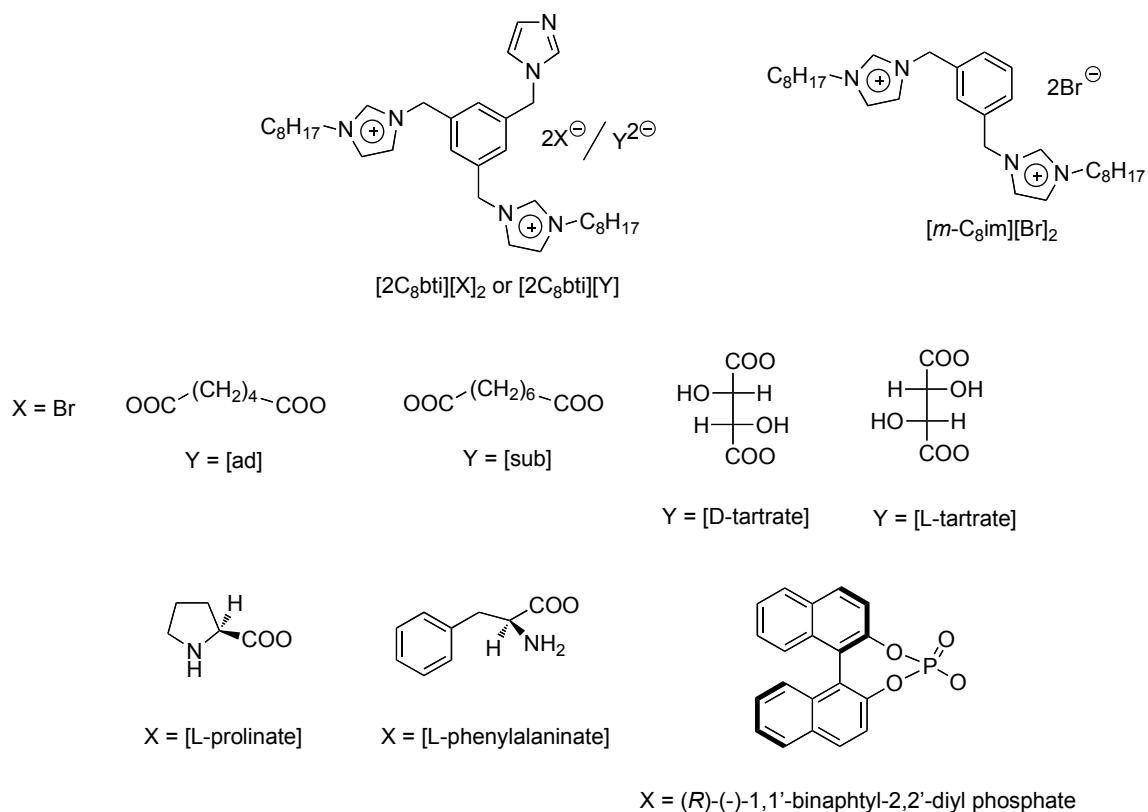


Figure 19: structure of ILs used for the study of Michael addition.

In order to apply the best reaction conditions, we first performed the Michael addition in a conventional solvent, tetrahydrofuran (THF), using as catalyst a strong base, K_2CO_3 . Indeed, the reaction is not favoured in highly polar solvents, while THF is one of the solvents most commonly used. On the other hand, it is well known that strong bases, like K_2CO_3 or KOH, catalyse the reaction. Nevertheless, we were interested in following Green Chemistry principles to perform this reaction, so that we applied also a weak base as catalyst. We chose 1-methylimidazole because it represents the same basic functionality of the TSILs and, in addition, its catalytic ability for the Michael addition has been proved in ILs solution.⁵⁰

[50] M. Mečiarová, M. Cigáň, Š. Toma and A. Gáplovský, *Eur. J. Org. Chem.* **2008**, 2008, 4408-4411.

The percentage yield has been evaluated varying also the stoichiometry between *t*-chalcone and malononitrile, the temperature and the time of reaction. Results are reported in the table below.

The final product has been isolated by flash chromatography and reaction times have been evaluated observing the total disappearance of *t*-chalcone from TLC.

Table 8: reaction conditions applied for the study of Michael addition in THF.

stoichiometric ratio <i>t</i> -chalcone/malononitrile	catalyst	T (°C)	time (h)	yield (%) ^a
1:1.3	K ₂ CO ₃	25	16	0
1:1.3	1-methylimidazole	25	16	0
1:1.3	1-methylimidazole	25 & US	1	12
1:1.3	1-methylimidazole	40	1	41
1:10	1-methylimidazole	25	22	43

^aYields were reproducible within 4%, product isolated by flash chromatography.

A little excess of nucleophile should favour the reaction outcome, however in a long reaction time (16 h) and at room temperature, no product formation has been detected in presence of both strong and weak base catalyst. As the result obtained with the two bases was the same, we decided to avoid the use of the strong base in favour of 1-methylimidazole in order to find the best reaction conditions. To this aim, other variables such as stoichiometry between reactants, time or temperature were changed.

In particular keeping constant *t*-chalcone/malononitrile ratio to 1/1.3, it was necessary to use ultrasound irradiation or a temperature of 40 °C to obtain a moderate yield in a short reaction time (1 h). Even though only 12 % and 41 % yields were respectively obtained, furthermore the increasing of the temperature caused the formation of some by-products. On the other hand, maintaining the temperature at 25 °C, the increase of stoichiometric ratio of *t*-chalcone/malononitrile from 1:1.3 to 1:10 brought to a higher yield but with a long reaction time (22 h) and using less green reaction conditions.

In general, results obtained in THF were not promising in terms of yields and reaction times but they gave us a clear help in the study of the reaction. For example, considering the little formation of the product in THF using a small excess of malononitrile, we have decided to test the catalytic ability of our TSILs in this condition, *i.e.* ratio of *t*-chalcone/malononitrile equal to 1:1.3, searching for a positive effect of the TSILs.

The solvent/substrate molar ratio used was equal to 1 (≈ 0.15 mmol), smaller than the one used for the mononuclear heterocyclic rearrangement (4.5).⁴⁰ However, as the reaction was performed at room temperature and at that temperature TSILs are solid like or waxy solids, it was required the use of a small amount of cosolvent in order to have a homogeneous reaction mixture. To respect green chemistry principles, we determined the lowest amount of cosolvent necessary.

Having in mind the results obtained in the mononuclear rearrangements of heterocycles, the reaction was first performed in TSILs presenting the best catalytic ability, *i.e.* **[2C₈bti][sub]** and **[2C₈bti][ad]**. So that, using the [sub]-based TSIL as reference solvent, we determined the right cosolvent for the Michael addition fixing the reaction time at 30 min and using 30 μ L of cosolvent. Table 9 summarizes results obtained in terms of percentage conversion of *t*-chalcone as function of cosolvent polarity and amount of cosolvent.

Table 9: influence of cosolvent in the reaction outcome.

cosolvent	[2C₈bti][sub]^a		[2C₈bti][ad]^a		
	ϵ	conversion ^b	μ L of MeOH	reaction times ^d	conversion ^{b,f}
1,4-dioxane	2.21	73%	0	3.25 h ^e	72%
toluene	2.40	98% ^c	10	0.5 h	85%
CHCl ₃	4.81	89% ^c	20	0.5 h	83%
THF	7.58	92% ^c	30	0.5 h	99%
1-PrOH	20.1	90% ^c			
MeOH	32.7	74%			
DMF	36.7	96%			
ACN	37.5	93%			

^areference TSIL; ^bconversion obtained at room temperature after 30 minutes, conversions were reproducible within 4%, product isolated by flash chromatography; ^cformation of by-products; ^dreactions performed at room temperature, reaction times determined after the disappearance of chalcone on TLC; ^ereaction performed at room temperature assisted by ultrasound irradiation; ^fconversions and yields were almost coincident.

The increase of the dielectric constant (ϵ), on going from 1,4-dioxane to 1-PrOH, positively affects substrate reactivity. Indeed, the conversion of the substrate is high also in solvents of low or medium polarity such as toluene, chloroform, THF and 1-propanol. However it is comprehensive of the presence of some by-products, which could not be easily separated from the product desired.

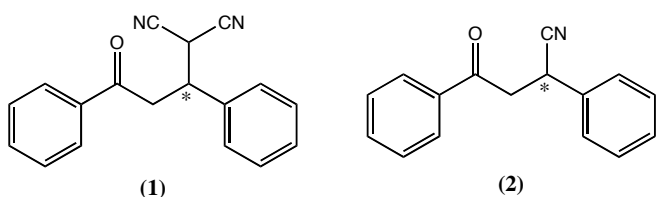
[40] C. Rizzo, F. D'Anna, S. Marullo and R. Noto, *J. Org. Chem.* **2014**, *79*, 8678-8683.

Considering the positive effect of the solvent polarity, we decided to use methanol as cosolvent as it gave rise to a good conversion allowing understanding TSILs effects. These effects could not be observed in DMF or ACN as they present almost the total conversion of the substrate in the desired product.

Decided the cosolvent, we tested the reaction in [2C₈btj][ad] using the same conditions - 25 °C, 30 min, 30 μL MeOH- and we obtained a surprising increase in yield (99% and 74 % in [ad]- and [sub]-based TSILs, respectively). This result encouraged us to perform the reaction using a smaller amount of cosolvent in order to fulfil green chemistry principles. By the way on the grounds of results obtained (Table 9), 30 μL of MeOH seemed the right amount of cosolvent; indeed it allowed having the highest percentage yield. Without cosolvent the yield was good, but it required a longer time of reaction and the use of ultrasound irradiation. On the grounds of above results, we thought it was more convenient the use of the cosolvent as the amount is really low. Furthermore, the use of energy source, in the absence of cosolvent, did not induce improvements both in terms of yield and reaction time.

Once determined the reaction conditions, the influence of TSILs anions on the Michael addition was studied. The reaction was followed via TLC until the disappearance of the *t*-chalcone in order to evaluate the catalytic ability of each TSIL, determining reaction times and percentage yields. In particular, in presence of the unfunctionalised IL the reaction was performed adding an amount of 1-methylimidazole equimolar to IL and *t*-chalcone. Reaction times and yields are displayed in the histogram of Figure 21 and reported in Table 10. It is worth of noting that in some cases ([D-tartrate], [L-tartrate], [L-prolinate], [L-phenylalaninate] and [R-binaphthylphosphate]) the reaction mixture presented two main products (Figure 20). Liang *et al.* have previously reported this behaviour, demonstrating the formation of a cyanated product as consequence of a cyanohydrin formation.⁵¹

[51] S. Lin, Y. Wei and F. Liang, *Chem. Commun.* **2012**, 48, 9879-9881.



The mechanism of formation probably entails dioxygen of air that in presence of a base oxidizes the tertiary proton of the principal product (1) giving product (2).

Figure 20: reaction products.

Table 10: percentage yields of products (1) and (2) at the reaction time reported in brackets.

TSIL	yield %(1) reaction time	yield %(2) reaction time	conversion %
[2C ₈ bti][Br] ₂	93 (5.5 h)	0 (5.5 h)	96
[2C ₈ bti][ad]	99 (30 min)	0 (30 min)	99
[2C ₈ bti][sub]	74 (30 min)	0 (30 min)	78
[2C ₈ bti][D-tartrate]	43 (24 h)	20 (24 h)	67
[2C ₈ bti][L-tartrate]	52 (24 h)	26 (24 h)	84
[2C ₈ bti][L-prolinate] ₂	63 (10 min)	25 (10 min)	92
[2C ₈ bti][L-phenylalaninate] ₂	56 (30 min)	35 (30 min)	94
[2C ₈ bti][R-binaphthylphosphate] ₂	78 (24 h)	0 (24 h)	83

Yields were reproducible within 4%, in presence of product (1) alone yield and conversion were almost coincident, products were isolated by flash chromatography and reaction times were determined observing the disappearance of chalcone by TLC.

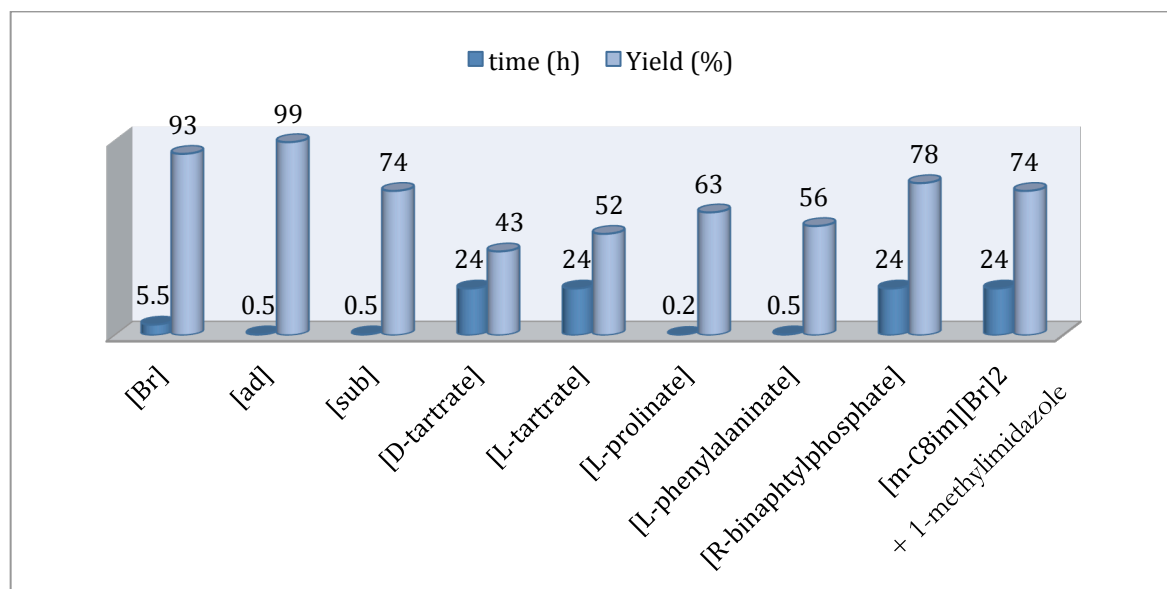


Figure 21: reaction times and yields as function of different TSILs used. Yields were reproducible within 4%, products were isolated by flash chromatography and reaction times were determined observing the disappearance of *t*-chalcone from TLC.

Analysis of data collected evidences the advantage of utilizing TSILs in respect to unfunctionalised dicationic IL with the addition of the base. Indeed, in **[2C₈bti][Br]₂**, the reaction is completed in 5.5 h reaching a 93 % yield, while in **[*m*-C₈im][Br]₂** it is necessary to wait 24 h (maximum reaction time) in order to have the 74 % yield. This test better supports the importance of the catalyst directly linked in the IL as already supposed in the study of the mononuclear rearrangement of heterocycles. Indeed, in this case the difference between the two systems of reactions is only the covalent bond of the imidazole to the cationic structure.

[2C₈bti][ad] and **[2C₈bti][sub]** seem to be the best reaction media also for the Michael addition in terms of both yield and time. On the other hand, the reaction is not really favoured in chiral tartrates and *R*-binaphthylphosphate based TSILs, even if it is important to underline that reaction times collected also in these cases represent a great challenge comparing to the ones reported in literature. For example Lattanzi *et al.* obtained high yields in reaction times in a range of 60–186 hours,⁵² North *et al.* in a minimum of 20 h up to 72 h,⁵³ that is the average reaction time used to perform this reaction.⁵⁴

TSILs with L-prolinate and L-phenylalaninate present good yield in short reaction time but it is worth noting that in these cases the reaction mixture presented two main products in good amount (Figure 20).

As the nature of TSILs anions influences their catalytic ability, we fixed reaction time once again at 30 minutes to better compare results obtained in different TSILs. Yields of products **(1)** and **(2)** at 30 minutes are reported in Table 11.

[52] A. Russo, A. Perfetto and A. Lattanzi, *Adv. Synth. Catal.* **2009**, *351*, 3067-3071.

[53] J. A. Castro-Osma, J. W. Comerford, S. Heath, O. Jones, M. Morcillo and M. North, *RSC Adv.* **2015**, *5*, 3678-3685.

[54] a) K. Yasuda, M. Shindo and K. Koga, *Tetrahedron Lett.* **1996**, *37*, 6343-6346, b) X. Li, L. Cun, C. Lian, L. Zhong, Y. Chen, J. Liao, J. Zhu and J. Deng, *Org. Biomol. Chem.* **2008**, *6*, 349-353.

Table 11: percentage yields of products (1) and (2) and conversions at 30 minutes.

TSIL	yield %(1) 30 min	yield %(2) 30 min	conversion %
[2C ₈ bti][Br] ₂	58	0	63
[2C ₈ bti][ad]	99	0	99
[2C ₈ bti][sub]	74	0	78
[2C ₈ bti][D-tartrate]	51	0	57
[2C ₈ bti][L-tartrate]	52	0	56
[2C ₈ bti][L-prolinate] ₂	32	39	76
[2C ₈ bti][L-phenylalaninate] ₂	56	35	94
[2C ₈ bti][R-binaphtylphosphate] ₂	40	0	46

Yields were reproducible within 4%, in presence of product (1) alone yield and conversion were almost coincident, products were isolated by flash chromatography and reaction times were determined observing the disappearance of chalcone by TLC.

Considering product (1), the percentage yields obtained were higher in non chiral TSILs, the highest values were detected for [ad] and [sub] based TSILs. The trend observed as function of different TSILs anions is the following one:

L-prolinate < R-binaphtylphosphate < D- and L-tartrate < L-phenylalaninate \approx Br < sub < ad

Data analysis seems to indicate that, in agreement with data obtained in the mononuclear rearrangement of heterocycles, the flexibility of the anion has a positive effect on the reaction outcome. Indeed the extended π -surface of the R-binaphtylphosphate, as previously observed for naphthalendisulfonate derivatives,⁴⁰ can easily interact through π - π stacking with the cationic unit blocking its conformational freedom and making it less disposable to interact with the substrate. While tartrates anions could probably interact with the cation by hydrogen bonds. In particular, the interaction between hydroxyl group in the anion and nitrogen of neutral imidazole unit could explain the loss of catalytic efficiency.

A different analysis has to support data obtained in L-prolinate and L-phenylalaninate based TSILs, indeed conversion values of *t*-chalcone (76% and 94% respectively) indicate an enhanced catalytic ability of the solvent systems that however brings to the formation of another product. Data collected at reaction times reveal that the formation of product (2) is favoured in longer time (tartrate anions) and in TSILs presenting aminoacid based anions.

[40] C. Rizzo, F. D'Anna, S. Marullo and R. Noto, *J. Org. Chem.* **2014**, *79*, 8678-8683.

To explain the latter results and considering the base catalysis acting on the reaction, we determined the basicity function of the new chiral TSILs using the Hammett indicator method previously applied (see pag. 43-44).

Table 12: H_- values determined for TSILs at 25 °C using the method of Hammett indicator.²²

Bromocresol Green ^a		<i>p</i> -nitrophenol ^b	
TSILs	H_-^c	TSILs	H_-^c
[2C ₈ bti][L-tartrate] ₂	9.6	[2C ₈ bti][L-prolinate] ₂	11.8
[2C ₈ bti][Br] ₂	9.3	[2C ₈ bti][L-phenylalaninate] ₂	10.9
[2C ₈ bti][R-binaphthylphosphate] ₂	8.6	[2C ₈ bti][ad]	10.7
		[2C ₈ bti][sub]	10.5

^ap*K*_a (MeOH) = 9.80.⁴⁵ ^bp*K*_a (MeOH) = 11.30.⁴⁵ ^c H_- values were reproducible within ± 0.1 .

Differently from what observed in the case of the *Z*-phenylhydrazone rearrangement, in this case the basicity of TSILs clearly affects their reactivity, indeed the reaction is faster and with higher conversion in more basic TSILs. The most basic TSIL, [2C₈bti][L-prolinate]₂, allowed the disappearance of the substrate in just 10 minutes, while the less basic [2C₈bti][R-binaphthylphosphate]₂ gave rise to the lowest percentage yield in the comparable reaction time of 30 min. By the way, it is worth of noting that thanks to the low solubility of [2C₈bti][R-binaphthylphosphate]₂ in acetone, it was possible to recover the 50 % of it; process not possible for the other TSILs.

An exception of this trend is the bromide TSIL that even if is less basic than tartrates TSILs, presents lower reaction time and higher conversion (5.5 h/93 % and 24 h/67% or 84% for bromide, D- and L-tartrate, respectively). So the outcome of the reaction is probably affected by a concomitant action of basicity and structure of TSILs anions.

Moreover, the high yield in product (2) obtained using [L-prolinate] and [L-phenylalaninate]-based TSILs seems to indicate that a higher basicity favours the substrate conversion but speeding up also the further transformation of the desired product.

Nevertheless the introduction of chiral anions, as already mentioned, was thought in order to study stereochemical aspects of the reaction. For this reason, after the purification by flash chromatography of the products obtained in chiral TSILs, they were

[22] M. Fan, J. Yang, P. Jiang, P. Zhang and S. Li, *RSC Adv.* **2013**, *3*, 752-756.

[45] F. Rived, M. Rosés and E. Bosch, *Anal. Chim. Acta* **1998**, *374*, 309-324.

submitted to the HPLC analysis with a chiral pack column to assess probable enantiomeric excesses.

Unfortunately our results were not promising to this aim, indeed a moderate enantiomeric excess was observed only in **[2C₈bti][R-binaphthylphosphate]₂** (10 % ee). In addition knowing that polar solvents and high temperature favour the formation of racemic mixtures, we used toluene as cosolvent and we lowered the temperature to 4 °C. By the way, we obtained the same percentage yields but only a slight increase of enantiomeric excess just in **[2C₈bti][R-binaphthylphosphate]₂** (35 % ee). This behaviour is probably due to the high polarity of TSILs and their organization as ionic pairs separated by cosolvent disfavour the stereoselective path of the reaction.

A similar behaviour has been detected in 2005 for the study of Michael addition of diethylmalonate to *t*-chalcone in chiral ILs presenting the chiral functionality in the cationic unit. Also in that case the maximum enantiomeric excess reached was 24 %, in addition, 1 mL of a cosolvent, K₂CO₃ as catalyst and a molar ratio substrate/ILs equal to 10 were used.⁵⁵

It is worth noting that high enantiomeric excess are reported for reactions performed in presence of organocatalysts with a proven enantioselectivity such as cinchona derivatives. In addition the reaction conditions used do not follow green chemistry principles, indeed organic solvents in non negligible amount have been applied,⁵¹ the atom economy of the reaction was not respected and really low temperature even -40 °C were required in some cases.⁵²

Considering that some TSILs allowed the outcome of the reaction in just 10 minutes, following the atom-economy of the reaction and utilizing the same solvent and catalyst, the systems studied can be considered a great challenge for the Michael addition taken into account. Especially remembering that results obtained in literature in terms of reaction times, addition of catalyst and additive are worst compared to our less reactive TSIL (67 % conversion in D-tartrate-based TSILs in 24 h).^{56, 53}

[55] Z. Wang, Q. Wang, Y. Zhang and W. Bao, *Tetrahedron Lett.* **2005**, *46*, 4657-4660.

[52] A. Russo, A. Perfetto and A. Lattanzi, *Adv. Synth. Catal.* **2009**, *351*, 3067-3071.

[53] J. A. Castro-Osma, J. W. Comerford, S. Heath, O. Jones, M. Morcillo and M. North, *RSC Adv.* **2015**, *5*, 3678-3685.

[56] J. Wang, H. Li, L. Zu, W. Jiang, H. Xie, W. Duan and W. Wang, *J. Am. Chem. Soc.* **2006**, *128*, 12652-12653.

Results obtained in TSILs underlined also the importance of the catalyst linked to the IL, indeed it has been reported that good yields were reached only after 22 h for the same reaction performed in 1 mL of monocationic IL with the addition of proline as catalyst.⁵⁷

Finally, we have demonstrated also in the study of this reaction how important is the combination between cation and anion in order to modulate the properties of ILs. In general the majority of salts synthesised present peculiar properties such as the presence of conformers in solution, high thermal stability and an enhanced catalytic ability for the base catalysed reactions.

[57] M. Mečiarová and Š. Toma, *Chem. Eur. J.* **2007**, *13*, 1268-1272.

Experimental section

1. Materials and methods

1,3,5-Tris(bromomethyl) benzene, 1-bromooctane, imidazole, sodium hydroxide, Amberlite IRA 400 resin, 1,5-naphthalenedisulfonic-4H₂O acid, terephthalic acid, 1,4-butanedicarboxylic acid, 1,6-hexanedicarboxylic acid, 2,6-naphthalenedicarboxylic acid, tetrafluoroboric acid (50% w/w), lithium bis(trifluoromethyl)sulfonylimide, IR 120 PLUS resin, sodium 2,6-naphthalenedisulfonate, α , α' -1,3-dibromoxylene, D-tartaric acid, L-tartaric acid, L-proline, L-phenylalanine, (R)-(-)-1,1'-binaphthyl-2,2'-diyl hydrogenphosphate, *t*-chalcone, malononitrile, potassium carbonate, 1-methyl-imidazole, *p*-nitrophenol, bromocresol green, 1-propanol, dimethylformamide, tetrahydrofuran, acetonitrile, diethyl ether, toluene and 1,4-dioxane were analytical reagents purchased from commercial sources and used as received. Dichloromethane and methanol were distilled prior to use.

For the study of the catalytic ability, (*Z*)-phenylhydrazone of 3-benzoyl-5-phenyl-1,2,4-oxadiazole was synthesised according to previous reports.⁵⁸

While for the study of Michael addition, [*m*-C₈im][Br]₂ was prepared as previously reported.⁵⁹

NMR studies. ¹H-NMR, ¹³C-NMR, 2D COSY-NMR and 2D NOESY-NMR spectra were recorded using Bruker 250, 300 and 400 MHz nuclear magnetic resonance spectrometers. ¹H-NMR spectra at variable temperature were recorded using a 400 MHz nuclear magnetic resonance spectrometer at the following temperatures: 300 K, 330 K, 350 K, 370 K, and 390 K.

Mass spectrometry analysis. ESI-MS spectra were recorded using a Waters LCT Premier ES-MS instrument with an Advion Nanomate infusion system.

[58] M. Ruccia and D. Spinelli, *Gazz. Chim. Ital.* **1959**, *89*, 1654.

[59] S. Marullo, F. D'Anna, M. Cascino and R. Noto, *J. Org. Chem.* **2013**, *78*, 10203-10208.

TGA analysis. The temperatures of decomposition, as well as the mass loss, were measured using a TA instrument TGA Q5000 thermogravimetric analyzer, at a heating rate of $5\text{ }^{\circ}\text{C min}^{-1}$ under nitrogen flow. For carboxylate salts a significant mass loss (ca. 10 %) observed at ca. $100\text{ }^{\circ}\text{C}$ was attributed to the thermally induced decarboxylation processes, while all other samples showed a very small mass loss ($<3.0\%$) in this range likely due to the moisture content. On this basis, non carboxylate salts were kept at $100\text{ }^{\circ}\text{C}$ until the time derivative of weight loss was less than $0.001\% \text{ min}^{-1}$ to ensure complete solvent evaporation before the heating ramp. The maximum values of the DTGA curves of each thermogram were used as a measure of the decomposition temperature. The mass loss was calculated from the area of the peaks exhibited by the DTG curves.

DSC analysis. The melting points were recorded using a TA Instrument DSC (2920 CE). The samples were sealed in TA Tzero aluminium pans with hermetic lids. The instrument was calibrated using indium as the standard. The temperature was ramped from 20 to $100\text{ }^{\circ}\text{C}$, at $10\text{ }^{\circ}\text{C min}^{-1}$. The melting temperature and melting enthalpy were determined respectively from the maximum of the signal and from its area. The DSC chamber was filled with dry nitrogen gas. The melting point of neutral compound **bti** was determined with a Kofler.

Spectrophotometric analysis. For the study of mononuclear heterocyclic rearrangement, product or substrate concentrations in the reaction mixture were determined with a common UV–vis spectrophotometer using calibration curves in 1,4-dioxane ($\lambda_{\text{max, (triazole)}} = 291\text{ nm}$; $\lambda_{\text{max, (Z-phenylhydrazone)}} = 367\text{ nm}$).

Polarimetric Measurements. Solutions of chiral TSILs were prepared in volumetric flasks ($C = 1.10^{-2}\text{ M}$). Optical rotations were measured using a glass polarimetric cell (light path 1 dm) and obtained as the average value over 50 readings.

HPLC analysis. HPLC was performed using a Chiralpak AS-H column with eluent 2-propanol/hexane = 30/70, flow rate 0.5 mL/min and $\lambda = 234\text{ nm}$: $t_{\text{monociane}} = 15.2\text{ min}$, $t_{\text{minor diciane}} = 19\text{ min}$, $t_{\text{major diciane}} = 22\text{ min}$.

Base Strength of TSILs. A suitable amount of TSIL was added to a methanol solution of the indicator. After the addition, colour change of the indicator solution was observed. The resulting solution was analysed by means of UV–vis spectroscopy. The indicators used, the relative concentrations, and the TSIL concentrations were as follows: *p*-nitrophenol ($pK_{\text{HI}} = 11.30$; $[\text{HI}] = 2 \times 10^{-4} \text{ M}$; $[\text{TSIL}] = 2 \times 10^{-3} \text{ M}$); bromocresol green ($pK_{\text{HI}} = 9.8$; $[\text{HI}] = 1 \times 10^{-4} \text{ M}$; $[\text{TSIL}] = 5 \times 10^{-4} \text{ M}$).

Reaction Conditions for the mononuclear heterocyclic rearrangement. All of the catalytic reactions were performed using a TSIL/substrate molar ratio of 4.5. In a typical experiment, 0.48 mmol of TSIL was weighed into a 4 mL screw capped vial, and its temperature was stabilized for 30 min at 90 °C. Subsequently (*Z*)-phenylhydrazone of 3-benzoyl-5-phenyl-1,2,4-oxadiazole (36 mg; 0.105 mmol) was added into the vial. The reaction was performed under magnetic stirring at 90 °C evaluating the disappearance of the substrate via TLC (eluent, petroleum ether/ethyl acetate 10/1). One milliliter of H₂O was added to the reaction mixture; then the reaction product was extracted with diethyl ether. The organic phase was concentrated in vacuum and solubilized in 1,4-dioxane to determine the percentage yields of the reaction. In order to recycle the TSIL, the water phase was concentrated in vacuum and reused several times.

Reaction Conditions for the Michael addition. The catalytic reactions were performed using a TSIL/*t*-chalcone molar ratio of 1 and a malononitrile/*t*-chalcone molar ratio of 1.13. In a typical experiment TSIL ($\approx 100 \text{ mg}$, 0.15 mmol), *t*-chalcone (30 mg, 0.15 mmol) and malononitrile ($\approx 11 \text{ mg}$, 0.17 mmol) were weighed into a 4 mL screw capped vial, then an appropriate amount of cosolvent was added. The reaction was performed under magnetic stirring at room temperature or at 4 °C evaluating the disappearance of the substrate via TLC (eluent, petroleum ether/ethyl acetate 5/1). Only for **[2C₈btj][R-binaphthylphosphate]₂** the reaction products were extract in acetone allowing the recovery of the TSIL. In the other cases MeOH was added to the mixture reaction in order to separate the products with silica flash chromatography (eluent, petroleum ether/ethyl acetate 10/1 and 5/1). The organic phase was concentrated in vacuum and solubilized in 2-propanol to determine the enantiomeric excess and percentage yields of reaction products by HPLC.

2. 1. General procedure for the synthesis of the neutral precursor **bti**

1,3,5-Tris(imidazolemethylen)benzene (**bti**). The compound was obtained by modifying a procedure reported in the literature.²⁵

Imidazole (2.88 g, 0.042 mol) and potassium hydroxide (4.71 g, 0.084 mol) were dissolved in acetonitrile (375 mL) and stirred for 2 h at room temperature. Then 1,3,5-tris(bromomethyl)benzene (5 g, 0.014 mol) was added to the mixture.

The reaction mixture was stirred at room temperature for 1.5 h. The mixture was filtered through a Hirsch funnel to remove insoluble salts and the filtrate was concentrated in vacuo at 40 °C. The residue was dissolved in CHCl₃ (1 L) and was washed with water (6 × 150 mL) until the aqueous layer was neutral to pH paper. The organic layer was dried over anhydrous Na₂SO₄ and was concentrated in vacuo. Yield 52%.

White powder. m.p.: 175.7-179.7 °C. ¹H-NMR (300 MHz; dms_o-d₆); δ/ppm: 5.25 (s, 6 H); 6.95 (s, 3 H); 7.16 (dd, J¹_{H-H} = 8.4 Hz, J²_{H-H} = 0.9 Hz, 6 H); 7.75 (s, 3 H). ¹³C-NMR (250 MHz; dms_o-d₆); δ/ppm: 49.3; 119.6; 126.3; 128.9; 137.5; 138.9. Elemental Anal. Calcd (%) for C₁₈H₁₈N₆ (318.38): C, 67.90; H, 5.70; N, 26.40. Found: C, 67.73; H, 5.65; N, 26.62.

2. 2. General procedure for the synthesis of the dicationic bromide salt [2C₈bti][Br]₂

To a stirred solution of 1,3,5-tris(imidazolemethylen)benzene, **bti** (2.33 g; 0.00733 mol) in CH₃CN (150 mL) was added dropwise a solution of 1-bromooctane (2.5 mL; 0.0146 mol or 3.5 mL) in CH₃CN (30 mL). The reaction mixture was stirred at 90 °C for 48 h under an Ar atmosphere. After concentration in vacuo at 40 °C, the residue was washed with diethyl ether (4 × 100 mL) under sonication.

1-[1'-Methyleneimidazole]-3,5-di[1'-methylene-3'-octylimidazolium]-benzene dibromide [2C₈bti][Br]₂.

Yield 92%. A white vitreous solid. m.p.: 53.1 °C. ¹H-NMR (300 MHz; dms_o-d₆); δ/ppm: 0.92 (t, J_{H-H} = 6.6 Hz, 6 H); 1.31 (m, 20 H); 1.85 (m, 4 H); 4.25 (m, 4 H); 5.25 (m, 2 H); 5.49 (m, 4 H); 6.96 (s, 1 H); 7.25 (m, 2 H); 7.58 (m, 3 H); 7.90 (m, 4 H); 9.46 (m, 2 H). ¹³C-NMR (250 MHz; dms_o-d₆); δ/ppm: 14.1; 22.2; 25.7; 28.5; 28.7; 29.5; 31.4; 43.9; 49.2; 51.6; 119.7; 122.7; 123.0; 126.8; 127.9; 128.7; 128.8; 129.1; 136.4; 137.5. ESI-MS: m/z (+):

[25] H.-K. Liu, W.-Y. Sun, H.-L. Zhu, K.-B. Yu and W.-X. Tang, *Inorg. Chim. Acta* **1999**, *295*, 129-135.

544; m/z (-): 79; 81. Elemental Anal. Calcd (%) for $C_{34}H_{58}Br_2N_6$ (710.67): C, 57.46; H, 8.23; N, 11.83. Found: C, 57.33; H, 8.04; N, 11.98.

2. 3. General procedure for the classical anion exchange

1-[1'-Methyleneimidazole]-3,5-di[1'-methylen-3'-octylimidazolium]-benzene

dibis(trifluoromethylsulfonyl)imide [**2C₈bti**][**NTf₂**]₂. The product was obtained using a procedure reported in the literature.²⁶

The dibromide salt (1.0 g, 1.95 mmol) was dissolved in dichloromethane (40 mL) and lithium bis(trifluoromethylsulfonyl)imide (1.12 g, 3.9 mmol) was added slowly to the solution. The reaction mixture was stirred at room temperature for 48 h. Then, the organic solution was washed with water, until the aqueous phase was halide free (by means of a silver nitrate test). The organic layer was concentrated in vacuo to obtain the salt.

Yield 54%. A yellow waxy solid. m.p.: 51.1 °C. ¹H-NMR (300 MHz; dmsO-d₆); δ/ppm: 0.85 (t, $J_{H-H} = 6.6$ Hz, 6 H); 1.25 (m, 20 H); 1.79 (m, 4 H); 4.15 (t, $J_{H-H} = 7.2$ Hz, 4 H); 5.18 (s, 2 H); 5.40 (s, 4 H); 6.90 (s, 1 H); 7.20 (m, 2 H); 7.58 (m, 3 H); 7.83 (m, 4 H); 9.22 (m, 2 H). ¹³C-NMR (250 MHz; dmsO-d₆); δ/ppm: 14.2; 22.4; 25.9; 28.7; 28.8; 29.7; 31.5; 49.4; 51.8; 55.2; 116.2; 117.7; 121.9; 122.8; 123.2; 123.4; 127.9; 128.9; 136.4; 137.6; 139.7. ESI-MS: m/z (+): 1103; total mass = 1105.2787; calculated mass = 1105.2678. Elemental Anal. Calcd (%) for $C_{38}H_{52}F_{12}N_8O_8S_4$ (1105.11): C, 41.30; H, 4.74; N, 10.14. Found: C, 41.07; H, 4.97; N, 9.98.

2. 4. General procedure for anionic exchange on basic resin

The compounds were obtained by modifying a procedure reported in literature.²⁸

Compound [**2C₈bti**][**Br**]₂ was subjected to anion exchange using a basic resin Amberlite IRA-400 with chloride sites. The resin (2 g for 0.0037 mol of [**2C₈bti**][**Br**]₂) was washed with water. Then it was washed with an aqueous solution of NaOH (10 mL, 10% w/v). The excess of the NaOH solution was removed by washing the resin with water until neutrality of pH. Compound [**2C₈bti**][**Br**]₂ (0.0037 mol) was dissolved in 25 mL of a

[26] L. Cammarata, S. G. Kazarian, P. A. Salter and T. Welton, *Phys. Chem. Chem. Phys.* **2001**, *3*, 5192-5200.

[28] I. Dinares, C. Garcia de Miguel, A. Ibanez, N. Mesquida and E. Alcalde, *Green Chem.* **2009**, *11*, 1507-1510.

binary mixture of methanol–water (70/30, v/v). The resin was washed with this binary mixture, so, for simple elution, the anion exchange of bromide with hydroxide was carried out. A new species of dihydroxide was formed and it reacted with the acid solution (0.0037 mol in 50 mL of methanol–water (70/30, v/v)) of the desired anion. The elution continued until neutrality of *pH*. After concentration in vacuo, the final product was washed with acetone (3 × 30 mL) irradiating with an ultrasonic bath.

1-[1'-Methyleneimidazole]-3,5-di[1'-methylen-3'-octylimidazolium]-benzene di tetrafluoroborate [2C₈bti][BF₄]₂. Yield 94%. A yellow waxy solid. m.p.: 51.1 °C. ¹H-NMR (300 MHz; dms_o-d₆); δ/ppm: 0.92 (t, J_{H-H} = 6.3 Hz, 6 H); 1.32 (m, 20 H); 1.85 (m, 4 H); 4.22 (t, J_{H-H} = 7.2 Hz, 4 H); 5.24 (m, 2 H); 5.47 (s, 4 H); 6.96 (s, 1 H); 7.30 (m, 2 H); 7.64 (m, 3 H); 7.89 (m, 4 H); 9.28 (m, 2 H). ¹³C-NMR (250 MHz; dms_o-d₆); δ/ppm: 14.1; 22.2; 25.7; 28.5; 28.6; 29.5; 31.3; 44.4; 49.2; 51.6; 119.6; 122.7; 123.0; 126.7; 127.7; 128.7; 128.9; 136.3; 137.5; 139.6. ESI-MS: m/z (+): 544; cation mass = 543.4178; calculated mass = 543.4175; total mass = 717.4282; calculated mass = 717.4234. Elemental Anal. Calcd (%) for C₃₄H₅₂B₂F₈N₆ (718.43): C, 56.84; H, 7.30; N, 11.70. Found: C, 56.63; H, 7.18; N, 12.04.

1-[1'-Methyleneimidazole]-3,5-di[1'-methylen-3'-octylimidazolium]-benzene 1,5-naphthalenedisulfonate [2C₈bti][1,5-nds]. Yield 96%. A white solid. m.p.: 55.3 °C. ¹H-NMR (300 MHz; dms_o-d₆); δ/ppm: 0.91 (t, J_{H-H} = 6.3 Hz, 6 H); 1.27 (m, 20 H); 1.80 (m, 4 H); 4.17 (m, 4 H); 5.23 (m, 2 H); 5.41 (m, 4 H); 6.97 (s, 1 H); 7.23 (m, 2 H); 7.44 (m, 3 H); 7.43 (dd, J¹_{H-H} = 8.1 Hz, J²_{H-H} = 7.8 Hz, 2 H); 7.79 (m, 4 H); 7.98 (d, J_{H-H} = 7.2 Hz, 2 H); 8.93 (d, J_{H-H} = 8.4 Hz, 2 H); 9.33 (m, 2 H). ¹³C-NMR (250 MHz; dms_o-d₆); δ/ppm: 14.1; 22.2; 25.7; 28.5; 28.6; 29.5; 31.3; 44.7; 49.1; 51.5; 119.6; 122.6; 122.9; 124.1; 124.2; 127.8; 128.9; 129.2; 129.7; 136.2; 136.3; 136.4; 136.5; 137.5; 144.0. ESI-MS: m/z (+): 544; m/2z (-): 142; total mass = 831.3937; calculated mass = 831.3938. Elemental Anal. Calcd (%) for C₄₄H₅₈N₆O₆S₂ (830.15): C, 63.13; H, 7.71; N, 10.04. Found: C, 62.98; H, 7.57; N, 10.17.

1-[1'-Methyleneimidazole]-3,5-di[1'-methylen-3'-octylimidazolium]-benzene 2,6-naphthalenedisulfonate [2C₈bti][2,6-nds]. Naphthalenedisulfonic acid is not commercially available. So, it was obtained from the corresponding sodium salt utilizing the acid resin IR 120 PLUS (15.4 g

for 0.0030 mol of salt). The cation exchange was carried out in the same way as the anion exchange. The resin was charged with an aqueous solution of HCl (775 mL, 10% v/v). When the naphthalenedisulfonic acid was obtained, the anion exchange was carried out utilising the general procedure described above.

Yield 98%. A white solid. m.p.: 50.4 °C. ¹H-NMR (300 MHz; dms_o-d₆); δ/ppm: 0.84 (m, 6 H); 1.21 (m, 20 H); 1.75 (m, 4 H); 4.13 (m, 4 H); 5.17 (s, 2 H); 5.40 (s, 4 H); 6.88 (s, 1 H); 7.13 (m, 2 H); 7.58 (m, 3 H); 7.71 (m, 2 H); 7.78 (m, 4 H); 7.88 (m, 2 H); 8.13 (s, 2 H); 9.38 (m, 2 H). ¹³C-NMR (250 MHz; dms_o-d₆); δ/ppm: 14.3; 22.4; 25.9; 28.7; 28.8; 29.6; 31.5; 44.7; 49.3; 51.8; 119.8; 122.8; 123.3; 124.1; 124.6; 128.0; 128.4; 129.1; 132.3; 136.4; 136.6; 137.7; 139.5; 139.8; 146.3. ESI-MS: m/2z (+): 272; m/z (-): 283. Elemental Anal. Calcd (%) for C₄₄H₅₈N₆O₆S₂ (830.15): C, 63.59; H, 7.03; N, 10.11. Found: C, 63.44; H, 7.24; N, 10.01.

1-[1'-Methyleneimidazole]-3,5-di[1'-methylen-3'-octylimidazolium]-benzene *1,4-benzendicarboxylate* **[2C₈bti][1,4-bdc]**. Terephthalic acid is insoluble in water and in methanol at room temperature. So, an aqueous suspension was generated and the anion exchange reaction was carried out stirring in suspension.

Yield 95%. A white solid. m.p.: 55.9 °C. ¹H-NMR (300 MHz; dms_o-d₆); δ/ppm: 0.87 (m, 6 H); 1.25 (m, 20 H); 1.81 (m, 4 H); 4.20 (m, 4 H); 5.20 (m, 2 H); 5.47 (m, 4 H); 6.92 (m, 1 H); 7.26 (m, 2 H); 7.38 (m, 3 H); 7.78 (s, 4 H); 7.87 (m, 4 H); 10.31 (m, 2 H). ¹³C-NMR (250 MHz; dms_o-d₆); δ/ppm: 19.1; 22.4; 27.2; 30.7; 33.5; 33.6; 34.5; 36.3; 54.1; 56.5; 124.6; 127.7; 127.8; 132.9; 133.1; 133.9; 134.5; 137.5; 142.5; 142.6; 146.4; 174.5. ESI-MS: m/z (+): 709; total mass = 709.4454; calculated mass = 709.4441. Elemental Anal. Calcd (%) for C₄₂H₅₆N₆O₄ (708.44): C, 71.16; H, 7.96; N, 11.85. Found: C, 71.32; H, 7.88; N, 11.68.

1-[1'-Methyleneimidazole]-3,5-di[1'-methylen-3'-octylimidazolium]-benzene *2,6-naphthalenedicarboxylate* **[2C₈bti][2,6-ndc]**. 2,6-Naphthalenedicarboxylic acid is insoluble in water and in methanol at room temperature. So an aqueous suspension was generated and the anion exchange reaction was carried out stirring in suspension.

Yield 98%. A light yellow hygroscopic solid. ¹H-NMR (300 MHz, dms_o-d₆); δ/ppm: 0.86 (m, 6 H); 1.20 (m, 20 H); 1.78 (m, 4 H); 4.18 (m, 4 H); 5.20 (s, 2 H); 5.53 (s, 4 H); 6.87 (s,

1 H); 7.16 (m, 2 H); 7.35 (m, 3 H); 7.72 (dd, 2 H); 7.80 (m, 2 H); 7.90 (m, 2 H); 8.01 (dd, 2 H); 8.34 (s, 2 H); 10.23 (m, 2 H). ^{13}C -NMR (250 MHz; dms o-d_6); δ /ppm: 14.3; 23.5; 27.1; 29.8; 29.9; 30.9; 32.6; 50.4; 52.8; 52.9; 120.9; 124.1; 128.3; 128.4; 129.4; 129.8; 130.2; 130.9; 134.4; 137.5; 137.8; 138.6; 138.8; 140.4; 140.7; 170.5. ESI-MS: m/z (+): 544; m/z (-): 214. Elemental Anal. Calcd (%) for $\text{C}_{46}\text{H}_{58}\text{N}_6\text{O}_4$ (758.45): C, 72.79; H, 7.70; N, 11.07. Found: C, 71.95; H, 7.44; N, 11.86.

1-[1'-Methyleneimidazole]-3,5-di[1'-methylen-3'-octylimidazolium]-benzene 1,4-butanedicarboxylate [2C₈bti][ad]. Yield 95%. A yellow waxy solid. m.p.: 51.1 °C. ^1H -NMR (300 MHz; dms o-d_6); δ /ppm: 0.89 (t, $J_{\text{H-H}} = 4.8$ Hz, 6 H); 1.28 (m, 24 H); 1.86 (m, 8 H); 4.23 (t, $J_{\text{H-H}} = 6.3$ Hz, 4 H); 5.23 (m, 2 H); 5.50 (m, 4 H); 6.94 (m, 1 H); 7.30 (m, 2 H); 7.60 (m, 3 H); 8.06 (m, 4 H); 10.50 (m, 2 H). ^{13}C -NMR (250 MHz; dms o-d_6); δ /ppm: 14.1; 22.2; 25.8; 27.2; 28.5; 28.6; 29.5; 31.3; 44.7; 48.7; 49.1; 51.4; 119.6; 122.6; 122.7; 122.8; 127.9; 128.9; 129.3; 136.5; 137.6; 137.9; 176.5. ESI-MS: m/z (+): 544; m/z (-): 145; cation mass = 543.4181; calculated mass = 543.4175; anion mass = 145.0484; calculated mass = 145.0501. Elemental Anal. Calcd (%) for $\text{C}_{40}\text{H}_{60}\text{N}_6\text{O}_4$ (688.94): C, 69.73; H, 8.78; N, 12.20. Found: C, 69.56; H, 8.58; N, 12.11.

1-[1'-Methyleneimidazole]-3,5-di[1'-methylen-3'-octylimidazolium]-benzene 1,6-hexanedicarboxylate [2C₈bti][sub]. Yield 94%. A yellow waxy solid. m.p.: 54.4 °C. ^1H -NMR (300 MHz; dms o-d_6); δ /ppm: 0.88 (m, 6 H); 1.28 (m, 28 H); 1.88 (m, 8 H); 4.24 (t, $J_{\text{H-H}} = 7.1$ Hz, 4 H); 5.23 (m, 2 H); 5.50 (m, 4 H); 6.93 (s, 1 H); 7.33 (m, 2 H); 7.63 (m, 3 H); 8.02 (m, 4 H); 10.50 (m, 2 H). ^{13}C -NMR (250 MHz; dms o-d_6); δ /ppm: 14.3; 22.4; 25.9; 26.9; 28.7; 28.8; 29.7; 29.9; 31.5; 48.9; 49.2; 51.6; 116.2; 119.8; 122.9; 127.2; 128.2; 129.1; 136.7; 137.7; 138.0; 139.4; 176.5. ESI-MS: m/z (+): 717; total mass = 717.5082; calculated mass = 717.5067. Elemental Anal. Calcd (%) for $\text{C}_{42}\text{H}_{64}\text{N}_6\text{O}_4$ (717.00): C, 70.36; H, 9.00; N, 11.72. Found: C, 69.98; H, 8.76; N, 11.96.

1-[1'-Methyleneimidazole]-3,5-di[1'-methylen-3'-octylimidazolium]-benzene D-tartrate [2C₈bti][D-tartrate]. Yield 94 %. A light yellow waxy solid. m.p.: 35-38 °C. $[\alpha] = -5.57$ (C=1.10 -^2 M in CH_3OH). ^1H -NMR (300 MHz; dms o-d_6); δ /ppm: 0.88 (t, $J_{\text{H-H}} = 8$ Hz, 6 H); 1.23 (m, 20 H); 1.83 (m, 4 H); 3.85 (s, 2 H); 4.23 (m, 4 H); 5.23 (m, 2H); 5.49 (m, 4 H); 6.94 (s,

1H); 7.26 (m, 2 H); 7.71 (m, 3 H); 7.88 (m, 4 H); 9.72 (m, 2 H). ¹³C-NMR (300 MHz; dms_o-d₆); δ/ppm: 14.0; 22.2; 25.7; 28.5; 28.6; 29.5; 31.3; 49.1; 51.5; 51.5; 72.0; 119.6; 122.8; 126.8; 127.9; 128.2; 128.9; 129.4; 136.7; 137.1; 137.5; 139.4; 174.9. Elemental Anal. Calcd (%) for C₃₈H₅₆N₆O₆ (692.89): C, 65.87; H, 8.15; N, 12.13. Found: C, 65.69; H, 8.12; N, 12.15.

1-[1'-Methyleneimidazole]-3,5-di[1'-methylen-3'-octylimidazolium]-benzene L-tartrate **[2C₈bti][L-tartrate]**. Yield 95 %. A light yellow waxy solid. m.p.: 35-38 °C. [α] = 5.59 (C=1.10⁻² M in CH₃OH). ¹H-NMR (300 MHz; dms_o-d₆); δ /ppm: 0.90 (t, J_{H-H}= 8 Hz, 6 H); 1.24 (m, 20 H); 1.84 (m, 4 H); 3.87 (s, 2 H); 4.24 (m, 4 H); 5.24 (m, 2 H); 5.50 (m, 4 H); 6.94 (s, 1 H); 7.24 (m, 2 H); 7.75 (m, 3 H); 7.90 (m, 4 H); 9.72 (m, 2 H). ¹³C-NMR (300 MHz; dms_o-d₆); δ/ppm: 14.0; 22.2; 25.7; 28.5; 28.6; 29.5; 31.3; 49.1; 51.5; 51.5; 72.1; 119.6; 122.8; 126.8; 128.0; 128.2; 128.9; 129.4; 136.3; 136.5; 137.1; 137.5; 175.0. Elemental Anal. Calcd (%) for C₃₈H₅₆N₆O₆ (692.89): C, 65.87; H, 8.15; N, 12.13. Found: C, 65.73; H, 8.17; N, 12.11.

1-[1'-Methyleneimidazole]-3,5-di[1'-methylen-3'-octylimidazolium]-benzene di-L-prolinate **[2C₈bti][L-prolinate]₂**. Yield 94 %. A yellow waxy solid. [α] = -19.80 (C=1.10⁻² M in CH₃OH). ¹H-NMR (400 MHz; dms_o-d₆); δ /ppm: 0.84 (t, J_{H-H}= 8 Hz, 6 H); 1.23 (m, 20 H); 1.50 (m, 8 H); 1.77 (m, 4 H); 2.95 (m, 4 H); 4.16 (m, 4 H); 5.16 (m, 2 H); 5.44 (m, 4 H); 6.87 (s, 1 H); 7.14 (m, 2 H); 7.63 (m, 3 H); 7.94 (m, 4 H); 9.92 (m, 2 H). ¹³C-NMR (300 MHz; dms_o-d₆); δ/ppm: 14.4; 22.5; 25.9; 28.8; 28.8; 29.0; 29.7; 31.8; 47.7; 49.4; 49.5; 51.7; 119.9; 122.9; 123.1; 127.1; 128.3; 129.2; 129.8; 136.8; 136.9; 137.4; 137.9; 139.5; 139.7; 172.1. Elemental Anal. Calcd (%) for C₄₄H₆₈N₈O₄ (772.03): C, 68.36; H, 8.87; N, 14.49. Found: C, 68.20; H, 8.89; N, 14.52.

1-[1'-Methyleneimidazole]-3,5-di[1'-methylen-3'-octylimidazolium]-benzene di-L-phenylalaninate **[2C₈bti][L-phenylalaninate]₂**. Yield 95 %. Orange oil. [α] = -6.48 (C=1.10⁻² M in CH₃OH). ¹H-NMR (400 MHz; dms_o-d₆); δ /ppm: 0.82 (t, J_{H-H}= 6 Hz, 6 H); 1.22 (m, 20 H); 1.77 (m, 4 H); 3.03 (dd, J¹_{H-H}= 9 Hz, J²_{H-H}= 6 Hz, 4 H); 4.14 (m, 4 H); 5.14 (m, 2 H); 5.42 (m, 4 H); 6.88 (s, 1 H); 7.12 (m, 2 H); 7.15 (m, 10 H); 7.71 (m, 3 H); 7.95 (m, 4H);

9.89 (m, 2 H). ^{13}C -NMR (300 MHz; dms o-d_6); δ/ppm : 14.4; 22.5; 26.0; 28.8; 29.0; 29.8; 30.2; 31.6; 49.4; 49.5; 119.9; 123.0; 127.3; 128.1; 129.2; 129.9; 136.8; 137.8; 139.54; 137.5; 140.7. Elemental Anal. Calcd (%) for $\text{C}_{52}\text{H}_{72}\text{N}_8\text{O}_4$ (873.18): C, 71.53; H, 8.31; N, 12.83. Found: C, 71.59; H, 8.29; N, 12.79.

1-[1'-Methyleneimidazole]-3,5-di[1'-methylen-3'-octylimidazolium]-benzene di-(R)-(-)-1,1'-binaphthyl-2,2'-diyl phosphate [2C₈bti][R-binaphthylphosphate]₂. Yield 97 %. A light yellow powder. m.p.: 134-136 °C. $[\alpha] = -386.36$ (C=1.10⁻² M in CH₃OH). ^1H -NMR (300 MHz; dms o-d_6); δ/ppm : 0.82 (t, $J_{\text{H-H}} = 6$ Hz, 6 H); 1.17 (m, 20 H); 1.62 (m, 4 H); 4.00 (m, 4 H); 5.26 (m, 2 H); 5.39 (m, 4 H); 7.38 (m, 20 H); 7.60 (s, 2 H); 7.76 (m, 4 H); 8.10 (dd, $J^1_{\text{H-H}} = 21$ Hz, $J^2_{\text{H-H}} = 9$ Hz, 8 H); 9.45 (m, 2 H). ^{13}C -NMR (300 MHz; dms o-d_6); δ/ppm : 14.1; 22.5; 26.0; 28.8; 28.9; 29.7; 31.6; 49.4; 51.9; 122.2; 122.2; 123.0; 123.1; 123.2; 124.8; 126.0; 126.5; 128.8; 130.1; 130.7; 132.4; 136.7; 136.7; 136.9; 150.6; 150.7. Elemental Anal. Calcd (%) for $\text{C}_{74}\text{H}_{76}\text{N}_6\text{O}_8\text{P}_2$ (1238.52): C, 71.71; H, 6.18; N, 6.78. Found: C, 71.60; H, 6.16; N, 6.76.

Chapter 2

Low-Molecular Weight Gelators

The easy synthetic pathway to obtain OSs and how little modifications in their structure can lead to different properties have been so far stressed to understand why OSs have been widely applied in several fields. In particular, these peculiarities have recently gained the attention of researchers in order to use OSs also as Low Molecular Weight Gelators (LMWGs) forming physical gels, better known as supramolecular gels.

In general, gels are viscoelastic solid-like materials formed by an elastic cross-linked network and a solvent, which is the major component. Gels have been widely applied in several fields like drug delivery, pharmacy, catalysis, electronics, conservation of arts and others.¹

LMWGs are molecules of low molecular weight able to trap solvents forming a three-dimensional network through a self-assembly process occurring by the instauration of supramolecular interactions among gelator molecules.² LMWGs possess zero-dimensional arrangement on the micrometer scale; by the way they must possess anisotropy on the molecular scale, which allows specific ways of packing within the fibrillar objects of their three-dimensional network.³ On the contrary, the formation of molecular gels proceeds from gelating species, like polymers, that are held together by covalent bonds arranged in at least one-dimension. In addition in molecular gels, networks immobilize the liquid component macroscopically by surface tension and capillary forces.⁴

In particular a hierarchical organization comprehensive of three different processes generates the three-dimensional network of supramolecular gels. Indeed, molecules of gelator can interact giving rise to fibrils after an initial nucleation process; these fibrils can

[1] a) B. Escuder, F. Rodriguez-Llansola and J. F. Miravet, *New J. Chem.* **2010**, *34*, 1044-1054, b) S. Das, S. L. de Rooy, A. N. Jordan, L. Chandler, I. I. Negulescu, B. El-Zahab and I. M. Warner, *Langmuir* **2012**, *28*, 757-765, c) Y. Fang, J. Zhang, X. Zhou, Y. Lin and S. Fang, *Electrochim. Acta* **2012**, *68*, 235-239, d) A. A. Sobczuk, Y. Tsuchiya, T. Shiraki, S.-I. Tamaru and S. Shinkai, *Chem. Eur. J.* **2012**, *18*, 2832-2838, e) R. G. Weiss, *J. Am. Chem. Soc.* **2014**, *136*, 7519-7530.

[2] N. M. Sangeetha and U. Maitra, *Chem. Soc. Rev.* **2005**, *34*, 821-836.

[3] M. George and R. G. Weiss, *Acc. Chem. Res.* **2006**, *39*, 489-497.

[4] Y. Jeong, K. Hanabusa, H. Masunaga, I. Akiba, K. Miyoshi, S. Sakurai and K. Sakurai, *Langmuir* **2005**, *21*, 586-594.

further grow and become fibers. Finally, fiber growth and branching kinetics govern the final structure of the fiber network.⁵ This process has been considered as an incomplete crystallization⁶ and it can be summarized as in Figure 1.

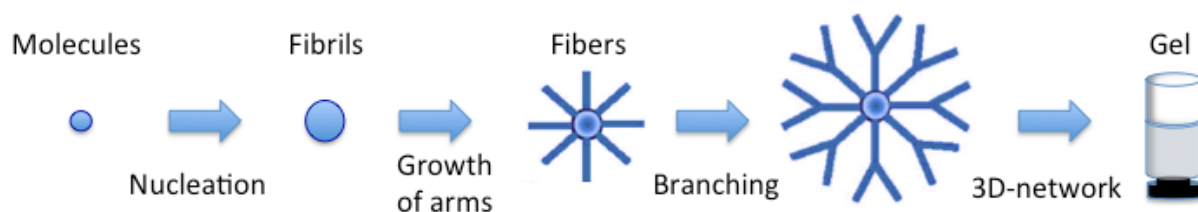


Figure 1: schematic illustration of fiber network formation through nucleation and growth of fibers.

It is worth of noting that the design of molecules able to induce the gelation process is the main difficulty in this research area. Indeed, especially during the first years of research in this field, supramolecular gels have been serendipitously found. Nevertheless, some research's groups have recently proposed a combined approach of experimental and computational X-RD data in order to predict the self-assembled fibrillar network in dependence on the gelator structure.⁷ So that, nowadays the design of the gelator can be thought considering the presence of functional groups or structures able to form supramolecular interactions.

In this framework several molecules have been modified to behave as LMWGs some examples are urea, hydroxystearic acid and aminoacids derivative. In particular, the ability of urea derivatives to form supramolecular gels is due to the presence of extended hydrogen bonded chains. During the years these derivatives have been widely modified, Steed *et al.* have recently introduced a neutral imidazole on phenyl urea and they have demonstrated that the molecule displays a switchable hydrogelation behaviour that can be turned off by metal ion coordination.⁸ On the other hand stearic acid, itself, is a very poor gelator, but the addition of functional groups attached to the end and in the middle position of the alkyl backbone can lead to good gelators such as (*R*)-12-hydroxystearic acid. An extended study of (*R*)-12-hydroxystearic acid and its derivatives was performed

[5] J.-L. Li and X.-Y. Liu, *Adv. Funct. Mater.* **2010**, *20*, 3196-3216.

[6] F. M. Menger and K. L. Caran, *J. Am. Chem. Soc.* **2000**, *122*, 11679-11691.

[7] a) V. A. Mallia, P. Terech and R. G. Weiss, *J. Phys. Chem. B* **2011**, *115*, 12401-12414, b) U. K. Das, V. G. Puranik and P. Dastidar, *Cryst. Growth Des.* **2012**, *12*, 5864-5868.

[8] S. J. James, A. Perrin, C. D. Jones, D. S. Yufit and J. W. Steed, *Chem. Commun.* **2014**, *50*, 12851-12854.

in order to demonstrate the possibility to predict the gelling ability of the molecules.⁹ Moreover, L-proline functionalised aminoacid hydrogelators exhibited catalytic activity in the gel phase formed.¹⁰

In this context also OSs perfectly match the characteristics to be applied as gelators even if, until now, they are not widely studied as neutral molecules. Ammonium salts first exerted a gelling ability in organic solutions¹¹ and organogels have been also obtained with a mixture of amine and acid components that produced an organic salt through acid-base reactions. The salts, generated *in situ*, created a three-dimensional network by entangling self-assembled nanofibers through hydrogen bonding and van der Waals interactions.¹² In addition, Dastidar *et al.*, following the supramolecular synthon approach, reported a combinatorial library of gelators obtained by simple acid-base reaction,¹³ while Steed explained how hydrogel properties are influenced by anion nature of the LMWG used.¹⁴ In Figure 2 some organogelators structures related to the studies just discussed are shown.

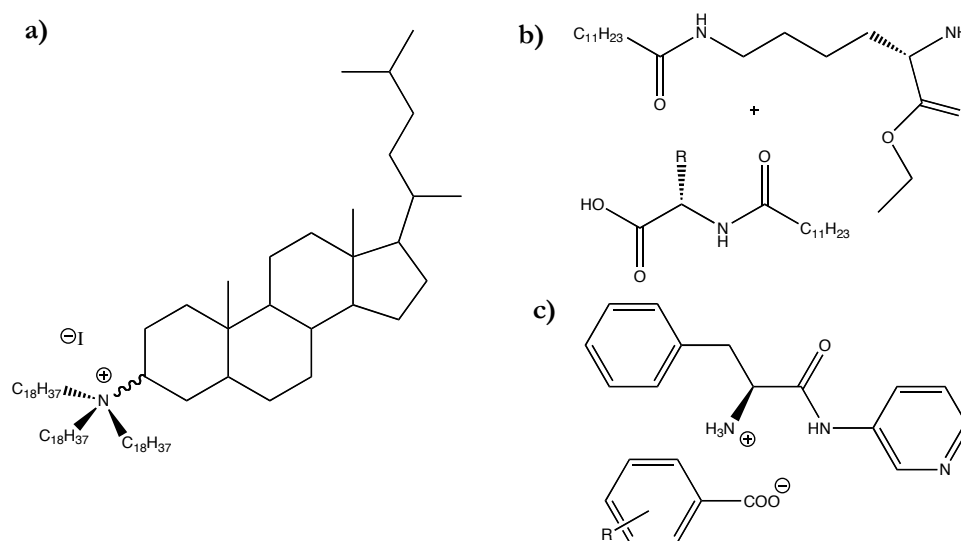


Figure 2: OSs exhibiting gelling ability in organic solvents: **a)** ref. 11, **b)** ref. 12 and **c)** ref. 13.

Gels formed by OSs have also been applied in biological field; in particular it was studied a novel cationic surfactant-based gelling system able to entrap laccase and horseradish

[9] V. A. Mallia and R. G. Weiss, *J. Phys. Org. Chem.* **2014**, *27*, 310-315.

[10] S. Diaz-Oltra, C. Berdugo, J. F. Miravet and B. Escuder, *New J. Chem.* **2015**, *39*, 3785-3791.

[11] L. Lu and R. G. Weiss, *Chem. Commun.* **1996**, 2029-2030.

[12] M. Suzuki, H. Saito and K. Hanabusa, *Langmuir* **2009**, *25*, 8579-8585.

[13] P. Sahoo, N. N. Adarsh, G. E. Chacko, S. R. Raghavan, V. G. Puranik and P. Dastidar, *ibid.* 8742-8750.

[14] G. O. Lloyd and J. W. Steed, *Soft Matter* **2011**, *7*, 75-84.

peroxidase biologically and/or electrochemically active. This gel shows also a great promise in green biocatalysis and biotransformation.¹⁵

Considering the strict relation between LMWG structure and its gelling ability, it was thought that the high structural degree present in DOSs¹⁶ could induce the formation of a three-dimensional network able to form gels. To this aim, it was tested the gelling ability of diimidazolium salts presenting long alkyl chain and monoanions, such as bromide and tetrafluoroborate,¹⁷ or aromatic dianions, such as naphthalenedisulphonate.¹⁸ The prediction of the gelling ability of some DOSs was correct indeed they were able to gel organic solvents.

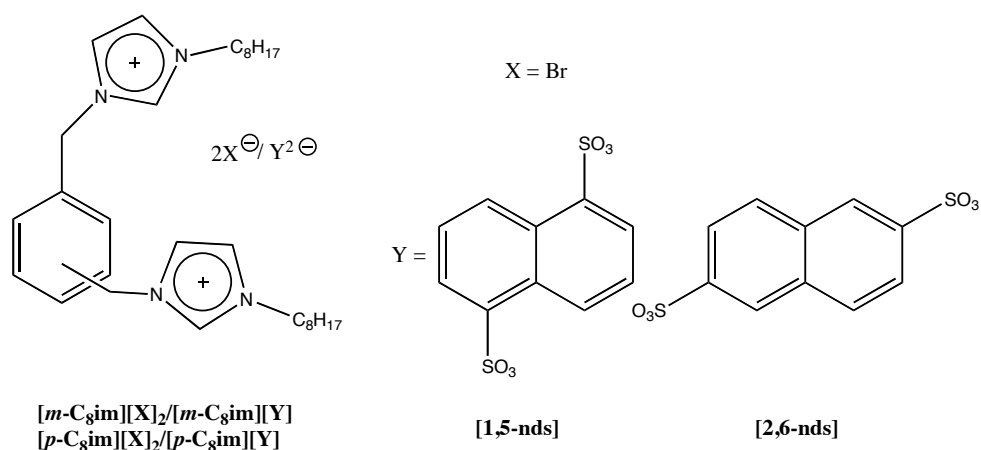


Figure 3: DOSs studied to form gels.

Even if DOSs are not so common to be used as gelator, few examples are present in literature: some DOSs, for example, have been used as gelators in a mixture of ethanol and water. The resulting material was an efficient drug delivery system thanks to the gelator ability of incorporating anionic drugs.¹⁹

The choice of a good gelator is a necessary but not sufficient condition to form a gel, as the solvent represents the major component of the material. In the discovery of the right

[15] Y. Sun and X. Huang, *Supramol. Chem.* **2014**, *27*, 21-27.

[16] F. D'Anna, F. Ferrante and R. Noto, *Chem. Eur. J.* **2009**, *15*, 13059-13068.

[17] F. D'Anna, P. Vitale, S. Marullo and R. Noto, *Langmuir* **2012**, *28*, 10849-10859.

[18] F. D'Anna, P. Vitale, F. Ferrante, S. Marullo and R. Noto, *ChemPlusChem* **2013**, *78*, 331-342.

[19] M. Rodrigues, A. C. Calpena, D. B. Amabilino, M. L. Garduno-Ramirez and L. Perez-Garcia, *J. Mater. Chem. B* **2014**, *2*, 5419-5429.

combination of gelator and solvent, many solvents have to be usually screened before succeeding in gel formation. To simplify this procedure the solvent–gelator specific (*i.e.*, hydrogen-bonding) and non specific (dipole–dipole, dipole-induced and instantaneous dipole induced forces) intermolecular interactions should be taken into account. As solvent properties could affect the self-assembly of molecular gelators into their self-assembled fibrillar networks, several solubility parameters of solvents have been correlated to the gelation ability of numerous classes of molecular gelators. Partition coefficients, Henry’s law constants, solvatochromic, Kamlet–Taft and Hansen solubility parameters allowed identifying which solvents will be gelled by molecular gelators.²⁰

The importance of the gelation solvent is evidenced also in the classification of supramolecular gels as organo-, hydro- or ionogels. Many organo- and hydrogels have been studied in the last decades, but the current approach to this topic is influenced by an analytical choice of gelator and solvents and a specific application of the gel. For example, a recent review analyses the gelling ability of dendrons and dendrimers, well-defined structures that can be precisely controlled at the molecular level. Thanks to their architectures and multiple functionalities, these molecules have shown a self-assembly behaviour that gives rise to organogels formation.²¹ This new approach in gel formation has been also applied in the development of a supramolecular gel with a self-delivery property for treating inflammation. The idea stands in building a supramolecular topical gel derived from a non steroidal anti-inflammatory drug in order to overcome the poor water solubility and the low bioavailability of these drugs. To this aim, strict criteria have to be followed and also the choice of biocompatible solvents, such as menthol and methylsalicylate, has a predominant role to the final design of the gel (TEM image of three-dimensional network of this organogel is reported in Figure 4c).²² Moreover, it has been demonstrated that highly polar solvents such as DMF can regulate the chiral twist of fibers usually formed in chiral organogels.²³ Photo of this chiral organogel and its fiber network are shown below (Figure 4).

[20] Y. Lan, M. G. Corradini, R. G. Weiss, S. R. Raghavan and M. A. Rogers, *Chem. Soc. Rev.* **2015**, *44*, 6035-6058.

[21] Y. Feng, Y.-M. He and Q.-H. Fan, *Chem. Asian J.* **2014**, *9*, 1724-1750.

[22] J. Majumder, P. Yedoti and P. Dastidar, *Org. Biomol. Chem.* **2015**, *13*, 2300-2309.

[23] W. Miao, D. Yang and M. Liu, *Chem. Eur. J.* **2015**, *21*, 7562-7570.

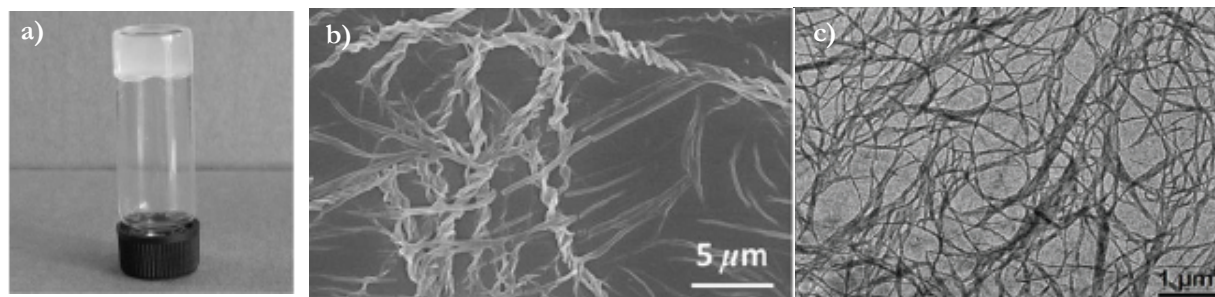


Figure 4: a) photograph of chiral organogel; b) SEM image of twisted fibers of chiral organogels, ref. 23; c) TEM of organogel exerting antiinflammatory activity, ref. 22.

Regarding hydrogels, this new approach can lead for example to design small molecules in which self-assembly and gelation processes are enzymatically controlled so that, these functional hydrogel can be applied in biological field. Hydrogels of Fmoc-tyrosine and histidine derivatives have shown an enzyme-like catalytic behaviour evidenced after the self-assembly process.²⁴

Currently the class of ionogels is not studied such as organo- and hydrogels, even though the interest in these new innovative materials is growing fast. The peculiarity of ionogels stands in their high thermal stability and conductivity,²⁵ typical properties derived from ILs. It has been shown that the ILs keep constant their properties, such as the conductivity, also in the soft materials obtained and in some cases they are even enhanced. The immobilization of ILs in a gel network can be required to use them in devices that need a solid like behaviour.²⁶ They can be used for example as conductive materials in dye-sensitized-solar-cells (DSSCs), avoiding the leakage problem that occurs using ILs.²⁷

[24] a) A. R. Hirst, B. Escuder, J. F. Miravet and D. K. Smith, *Angew. Chem., Int. Ed.* **2008**, *47*, 8002-8018, b) N. Singh, M. P. Conte, R. V. Ulijn, J. F. Miravet and B. Escuder, *Chem. Commun.* **2015**, *51*, 13213-13216.

[25] a) K. Hanabusa, H. Fukui, M. Suzuki and H. Shirai, *Langmuir* **2005**, *21*, 10383-10390, b) J. Le Bideau, L. Viau and A. Vioux, *Chem. Soc. Rev.* **2011**, *40*, 907-925.

[26] a) B. Y. Lim, J. Yoon, J. Yun, D. Kim, S. Y. Hong, S.-J. Lee, G. Zi and J. S. Ha, *ACS Nano* **2014**, *8*, 11639-11650, b) D. Kim, G. Lee, D. Kim and J. S. Ha, *ACS Appl. Mater. Interfaces* **2015**, *7*, 4608-4615.

[27] N. Mohmeyer, D. Kuang, P. Wang, H.-W. Schmidt, S. M. Zakeeruddin and M. Gratzel, *J. Mater. Chem.* **2006**, *16*, 2978-2983.

Since the first definition of ionogels, given by Kimizuka, referring to polymers that can gel in ILs solutions,²⁸ nowadays the research has gone beyond. Indeed several materials such as polymeric gels, hybrid materials comprehensive of inorganic species and supramolecular gels presenting ILs as liquid component fall in the class of ionogels.²⁹

The properties of supramolecular ionogels are surprising. Indeed, it has been demonstrated that ionogel formed by a chiral, crown-ether-functionalised bisurea gelator presents a thermal stability higher than 100 °C, a mechanical strength so high to be comparable to that of cross-linked protein fibres and a fast self-healing ability after mechanical deformation.³⁰ On the other hand, ionogel formed by (*S,S*)-bis(leucinol)oxalamide in [bmim][BF₄] possesses ionic conductivity higher than that of neat IL. This behaviour has been attributed to the higher affinity of gelator molecules towards IL's anions, which reduces the electrostatic attraction between [bmim⁺] and [BF₄⁻] and thus increases their mobility.³¹

Few examples of salts forming supramolecular ionogels have been reported until now. Some studies include an anisotropic thermal reversible ionogel of sodium laureate,³² an anticorrosive/antioxidant supramolecular gel having as LMWG an imidazolium type “ionic liquid” bearing a benzotriazole group³³ and more recently Yan's group has developed new conductive materials for DSSCs that involve ionogels formation by host-guest interaction between organic salts and β-cyclodextrins.³⁴

Another important factor that positively or negatively affect the gelation process can be the presence of a second component. These multi-component gels can be classified as following: gels that present one of the individual components usually forming a solution and the gelation process occurs only on addition of the second component; two gelators which can either co-assemble or self-sort into distinct assemblies and one gelator and one

[28] N. Kimizuka and T. Nakashima, *Langmuir* **2001**, *17*, 6759-6761.

[29] a) S. A. M. Noor, P. M. Bayley, M. Forsyth and D. R. MacFarlane, *Electrochim. Acta* **2013**, *91*, 219-226, b) K. Rawat, J. Pathak and H. B. Bohidar, *Soft Matter* **2014**, *10*, 862-872, c) T. M. Benedetti, T. Carvalho, D. C. Iwakura, F. Braga, B. R. Vieira, P. Vidinha, J. Gruber and R. M. Torresi, *Sol. Energy Mater. Sol. Cells* **2015**, *132*, 101-106.

[30] Z. Qi, N. L. Traulsen, P. Malo de Molina, C. Schlaich, M. Gradzielski and C. A. Schalley, *Org. Biomol. Chem.* **2014**, *12*, 503-510.

[31] A. Maršavelski, V. Smrečki, R. Vianello, M. Žinić, A. Mogaš-Milanković and A. Šantić, *Chem. Eur. J.* **2015**, *21*, 12121-12128.

[32] W. Jiang, J. Hao and Z. Wu, *Langmuir* **2008**, *24*, 3150-3156.

[33] M. Cai, Y. Liang, F. Zhou and W. Liu, *J. Mater. Chem.* **2011**, *21*, 13399-13405.

[34] a) W. Zhang, C. Yuan, J. Guo, L. Qiu and F. Yan, *ACS Appl. Mater. Interfaces* **2014**, *6*, 8723-8728, b) J. Zhang, W. Zhang, J. Guo, C. Yuan and F. Yan, *Electrochim. Acta* **2015**, *165*, 98-104.

non-gelling additive which can affect the assembly process of the gelator and therefore the gel's properties.³⁵

Hanabusa *et al.*, that reported a two-component gel based on the supramolecular interaction between barbituric acid and pyrimidine units, studied the first class of two-component gels for the first time in 1993.³⁶ The advantage of the two-component gels is the introduction of a higher degree of control in the gelation process, due to the presence of an additional level of hierarchical control, *i.e.* complex formation, in the self-assembly process (Figure 5).³⁷

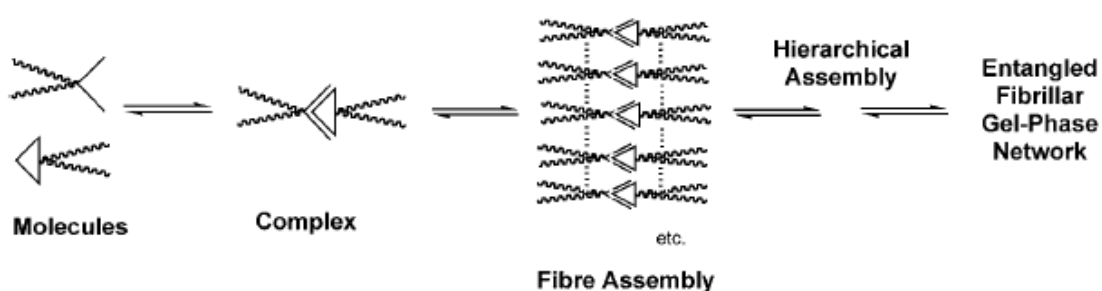


Figure 5: schematic representation of self-assembly process in two-component gels.

The two components can interact through host-guest interactions, metal coordination - if one of the components is a metal - or simple acid-base reaction. In particular, it has been reported a supramolecular hydrogel formed by guest recognition into a modified cyclodextrin. The modified β -CD initially aggregates in supramolecular fibrils through host-guest interactions and these fibrils are subsequently cross-linked via hydrogen bond occurring between cyclodextrins.³⁸ On the other hand, a modified steroid amine in presence of Zn^{II} , Cu^{II} and Ni^{II} generates an *in situ* gelation process; the gels obtained are multi-responsive as they are sensitive to stoichiometry and chemical stimuli in addition to the thermal stimulus.³⁹ For the last class of two-component gels, an acid-amine gelation system can be discussed. The study gives a complete thermodynamic explanation for the

[35] L. E. Buerkle and S. J. Rowan, *Chem. Soc. Rev.* **2012**, *41*, 6089-6102.

[36] K. Hanabusa, T. Miki, Y. Taguchi, T. Koyama and H. Shirai, *J. Chem. Soc., Chem. Commun.* **1993**, 1382-1384.

[37] A. R. Hirst and D. K. Smith, *Chem. Eur. J.* **2005**, *11*, 5496-5508.

[38] W. Deng, H. Yamaguchi, Y. Takashima and A. Harada, *Angew. Chem., Int. Ed.* **2007**, *46*, 5144-5147.

[39] H. Bunzen, Nonappa, E. Kalenius, S. Hietala and E. Kolehmainen, *Chem. Eur. J.* **2013**, *19*, 12978-12981.

assembly of two-component gels from complex mixtures. Indeed, they have demonstrated that the gelation occurs after complexes formation dependent by amine pK_a and fiber assembly.⁴⁰

Nevertheless as previously stated, the presence of a non gelling component in a successful combination of gelator and solvent can vary and modulate the properties of the resulting material. Gel properties as function of the introduction of different guests have been analysed, and it can be assessed that if the presence of guests poorly affects the thermal stability of the gel, it significantly influences the rate of gel phase formation, the size and the nature of the aggregates of the soft materials. In addition, the guest release process from the gelatinous matrix, considering the same extraction solvent, is slower with the increase in guest polarity and π -surface area, while, using different extraction solvents, the process is affected by their structure and ability of diffusing into the gel phase of the solvent, rather than their polarity.⁴¹

On the grounds of our interest in the study of dicationic organic salts properties, we have analysed the gelling ability of some of the novel functionalised DOSs in organic solvents and ionic liquid solutions.

The gelation process has been studied also using unfunctionalised DOSs, modulating structures of cation and anion of the salts in organic solvents and ILs. While hydrogel formation resulted from the host-guest interaction between DOSs and cyclodextrins. Finally, some hydro- and ionogels exhibited antimicrobial activity.

[40] W. Edwards and D. K. Smith, *J. Am. Chem. Soc.* **2013**, *135*, 5911-5920.

[41] P. Vitale, F. D'Anna, S. Marullo and R. Noto, *Soft Matter* **2015**, *11*, 6652-6662.

Results and Discussion

The study of the gelling ability of some of the OSs synthesised represents another important aspect of this dissertation; indeed, in addition to their use as reaction media they can also form gel phases in dependence on structural properties. In these cases properties of the soft materials obtained have been deeply analysed in terms of critical gelation concentration, thermal stability, mechanical properties, self-healing ability of the gels after submission to external stimuli, kinetic of gel formation, morphology and conductivity. Nevertheless, after the synthesis of the organic salts, the first step to understand soft material properties is the study of gelator ones, so that thermal properties of novel OSs have been analysed.

Furthermore, it is worth of noting that also gel phases can be used as confined media to perform organic reactions.

1. Functionalised DOSs: gelators of ionic liquids⁴²

The gelling ability of diimidazolium functionalised OSs presenting rigid dianions has been tested having in mind the fact that NOESY analysis evidenced strict interactions occurring between cations and dianions in these salts. In particular, it has been demonstrated that these interactions limited their use as reaction media in base catalysed reactions.⁴³ By the way, this high structural order, that prevents also the abundant presence of conformational isomers in solution, should favour the formation of the three-dimensional network able to trap solvents. Furthermore, base-catalysed reaction could be better catalysed in the new functional soft-materials rather than in solution, thanks to the presence of directionality conferred by the confined reaction media, as previously reported by Escuder *et al.*^{1a}

[42] F. D'Anna, C. Rizzo, P. Vitale, G. Lazzara and R. Noto, *ibid.* **2014**, *10*, 9281-9292.

[43] a) F. D'Anna, H. Q. N. Gunaratne, G. Lazzara, R. Noto, C. Rizzo and K. R. Seddon, *Org. Biomol. Chem.* **2013**, *11*, 5836-5846, b) C. Rizzo, F. D'Anna, S. Marullo and R. Noto, *J. Org. Chem.* **2014**, *79*, 8678-8683.

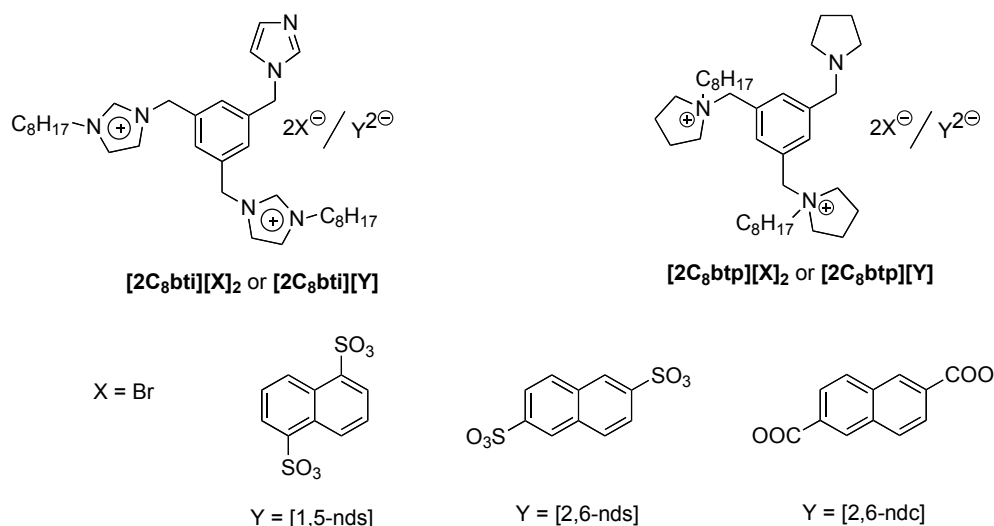
[1] a) B. Escuder, F. Rodriguez-Llansola and J. F. Miravet, *New J. Chem.* **2010**, *34*, 1044-1054.

For this reason we took into account salts with dianions having aromatic spacers, such as 1,5-, 2,6-naphthalenedisulfonate anions and 2,6-naphthalenedicarboxylate ([1,5-nds], [2,6-nds] and [2,6-ndc]). In particular, the use of isomeric anions, differing in the dipole moment and in the interactions through hydrogen bonds along different directions, might affect the properties of the materials. In addition, the different nature of negative charges (sulfonate and carboxylate) should cause changes in the anion coordination ability and subsequently in the gelling ability of the salts. Finally, in order to understand the importance of rigid anions of the salts in gelation process also a monoanionic salt – the bromide one- has been studied for comparison reasons.

Dipyrrolidinium salts bearing pyrrolidine as basic functionality have been also synthesised in order to study results obtained as function of aromatic or aliphatic cationic units. In particular, the aliphatic unit used was 1-(*N*-pyrrolidylmethyl)-3,5-di-(*N,N*-octylpyrrolidylmethyl)-benzene [**2C₈btp**].

The gelling ability of the above mentioned salts has been tested in organic and ILs solutions. Structures of functionalised OSs and ionic liquids applied for this study are shown in Figure 6.

Gelators structures:



Ionic Liquids structures:

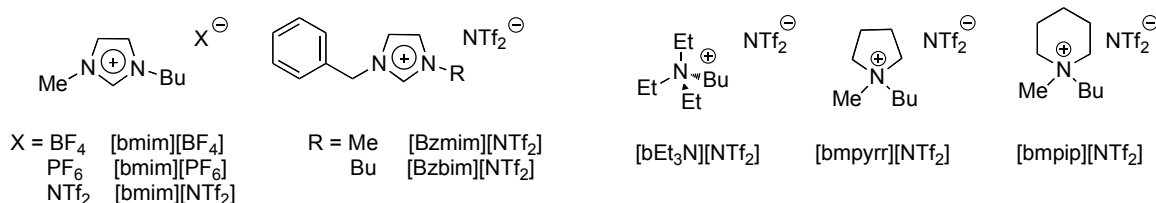


Figure 6: structures of functionalised OSs and ILs applied.

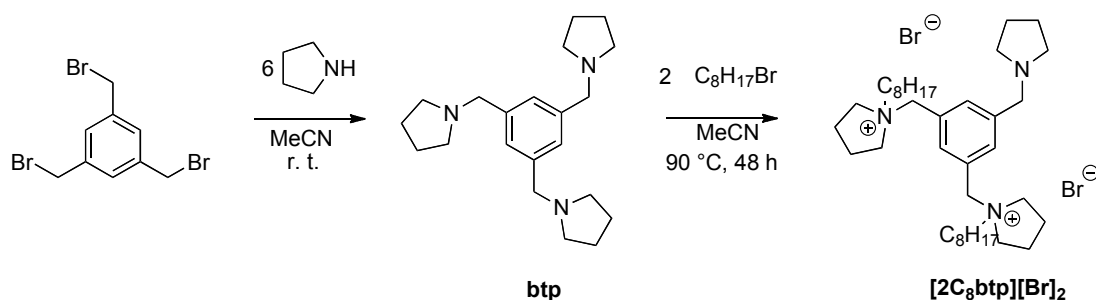
Several monocationic ILs, selected from the most studied ones, have been used to test gel formation. Regarding the cationic head, among the aromatic ones imidazolium based ILs such as [bmim][NTf₂], [Bzvim][NTf₂] and [Bzmim][NTf₂] have been chosen. The presence of the phenyl ring on the imidazolium might favour the formation of additional interactions such as π - π stacking (comparison between [bmim] and [Bzmim]), while a different length of the alkyl chain could explain if van der Waals interactions also play an important role in the gel formation (comparison between [Bzmim] and [Bzvim]). On the other hand, aliphatic cations such as ammonium, pyrrolidinium and piperidinium have been selected in order to compare the effect derived by an increase in the order degree of the cation. For cyclic structures, the effect exerted by the size and geometry of the ring has been also investigated.

Anions of ILs have been varied in terms of size, shape and coordination ability, *i.e.* [BF₄], [PF₆] and [NTf₂].

1. 1. Synthesis of OSs as gelators

The synthetic strategy to obtain diimidazolium functionalised organic salts has been previously discussed in Chapter 1 (par. 1.).

A similar approach has also been applied for the synthesis of the pyrrolidinium salts. Indeed, the bromide one has been synthesised after alkylation of the neutral precursor 1,3,5-trimethylenpyrrolidylbenzene (**btp**). The synthetic pathway is shown below and the experimental details are reported in the experimental section.



Scheme 1: two-step procedure for the synthesis of functionalised dipyrrolidinium salts.

The anion exchange of dipyrrolidinium bromide used for the synthesis of the corresponding naphthalendisulfonate salts has been performed with the basic resin Amberlite IRA-400, following the same procedure applied for diimidazolium salts.

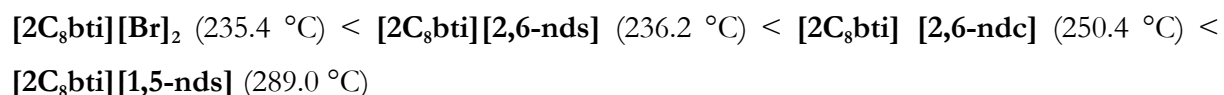
1. 2. Thermal stability of dipyrrolidinium salts

As previously ran over, an accurate analysis of thermal properties of salts used as gelators should be fundamental in order to have a complete knowledge of temperature ranges in which their gel or solutions obtained from their melting can be used. For this reason decomposition temperature of dipyrrolidinium salts have been studied using TGA analysis as previously performed for diimidazolium salts. Also in these cases the operational limit of the salts has been attributed to the temperature corresponding to the maximum of the derivative of TGA (DTG) of the first step, T_{d1} . Indeed, once again the salts present at least two degradation steps. Data obtained are shown in Table 1.

Table 1: decomposition temperature (T_d) and relative percentage of loss in weight in brackets determined by TGA; melting temperature (T_m) determined by Kofler.

Organic Salt	T_{d1} (°C)	T_{d2} (°C)	T_{d3} (°C)	T_m (°C)
[2C ₈ btp][Br] ₂	248 (39.5)	345 (30.3)	471 (11.0)	54.1
[2C ₈ btp][1,5-nds]	246 (11.3)	307 (52.7)	478 (12.4)	128.7-131.4
[2C ₈ btp][2,6-nds]		307 (65.0)	486 (6.8)	135.3-138.4

For dipyrrolidinium salts, the process is less affected by the anion than in the case of the diimidazolium salts where the trend is the following one:



With the only exception of [2C₈bti][1,5-nds], dipyrrolidinium salts presented higher decomposition temperatures than corresponding diimidazolium salts; results are in agreement with data reported for dicationic salts having a flexible spacer.⁴⁴ However, these functionalised salts presented a lower thermal stability than the one reported for unfunctionalised dicationic salts, as previously mentioned probably due to the presence of a different spacer and a higher substitution on it.⁴⁵

Differently from diimidazolium salts that can be all classified as TSILs thanks to their melting temperature below than 100 °C, dipyrrolidinium ones presenting dianions did not fall in this class. Only the bromide salt, indeed, could be considered as IL.

[44] J. L. Anderson, R. Ding, A. Ellern and D. W. Armstrong, *J. Am. Chem. Soc.* **2005**, *127*, 593-604.

[45] C. Chiappe and C. S. Pomelli, *Eur. J. Org. Chem.* **2014**, *2014*, 6120-6139.

1. 3. Gelation tests

The gelling ability of the salts synthesised has been tested in a wide range of organic solvents with different polarity, by the way they were not able to behave as organogelators. The formation of a gelatinous precipitate was only observed in glycerol but the material was not positive to “tube inversion” test that is the common method to assess the gel nature of the material.⁴⁶ In particular, dipyrrolidinium salts showed the lowest solubility, indeed, they were insoluble or only partially soluble in most of solvents used but they presented a good solubility in highly polar solvents such as glycols, DMSO and DMF. A different behaviour was detected for diimidazolium salts. In particular, the bromide one showed a high solubility in protic as well as in aprotic polar solvents. While, the corresponding [nds]-salts were soluble in protic polar solvents, such as alcohols, glycols and glycerol, but they were insoluble also at a low percentage weight in aprotic solvents.

Bearing in mind all the properties and applications that could characterize ionogels, we tested the gelling ability of the functionalised OSs in monocationic IL solution. Differently from what observed in organic solvents, the functionalised DOSs were able to trap ILs. Furthermore, gels obtained were stable to the tube inversion test for almost six months at 20 °C and they were opaque phases coloured in light yellow when formed by diimidazolium salts and in brown when formed by dipyrrolidinium salts (Figure 7).

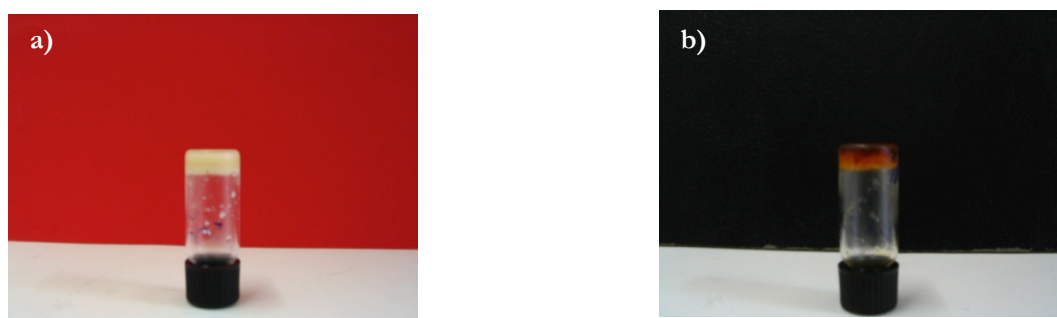


Figure 7: gel phases of **a)** $[2C_8bti][Br]_2/[bEt_3N][NTf_2]$ at 20% (w/w) and **b)** $[2C_8btp][1,5-nds]/[bmim][NTf_2]$ at 16 % (w/w).

[46] X. Huang, S. R. Raghavan, P. Terech and R. G. Weiss, *J. Am. Chem. Soc.* **2006**, *128*, 15341-15352.

Gelation tests performed in ILs of diimidazolium and dipyrrolidinium salts are reported in Tables 2. For gel phases, the CGC (*i.e.*, the critical gelation concentration allowing gel phase formation) and the corresponding T_{gel} (*i.e.*, the gel melting temperature measured by lead ball method or micro-DSC analysis) are reported.

Different methods of preparation of soft materials are also indicated in the Table. In general, gels were obtained by simply cooling at 4 °C the clear hot solution. However, in some cases, the cold solution was opaque and the gel phase occurred after magnetic stirring of the mixture at a constant rate, or with a combined action of ultrasound irradiation and magnetic stirring. It has been previously reported that these actions probably favour the entanglement of preformed fibers, giving rise to the gel phase formation.⁴⁷

Table 2: gelation tests for diimidazolium and dipyrrolidinium salts in different IL solutions.

Solvent	Range ^b	[2C ₈ bti][1,5-nds]			[2C ₈ bti][2,6-nds]			[2C ₈ bti][2,6-ndc]		
		CGC ^c	T_{gel} ^d	ΔC_p ^h	CGC ^c	T_{gel} ^d	ΔC_p ^h	CGC ^c	T_{gel} ^d	ΔC_p ^h
[bmim][NTf ₂]	4.0-16.1	OG ^e	10.6	23						
[bmim][BF ₄]	2.0-15.0	OG ^e	14.8	34						
[bmim][PF ₆]	4.0-15.0	S								
[bEt ₃ N][NTf ₂]	8.0-21.0	OG	16.1	37	16.1	34		11.6	SM	
				31 ^f		24 ^f			22 ^f	
				304 ^g	0.079	297 ^g	0.055		295 ^g	0.102
[bmpip][NTf ₂]	4.6-11.0	GP						8.7 ^c /3.2 ⁱ	SM	
									ns	
[bmpyrr][NTf ₂]	4.0-12.0	GP						8.3	SM	
									ns	
[Bzbim][NTf ₂]	4.0-13.0	GP							GP	
[Bzmim][NTf ₂]	4.0-13.0	GP							GP	

Solvent	Range ^b	[2C ₈ btp][1,5-nds]			[2C ₈ btp][2,6-nds]		
		CGC ^c	T_{gel} ^d	ΔC_p ^h	CGC ^c	T_{gel} ^d	ΔC_p ^h
[bmim][NTf ₂]	8.0-15.0	OG	15.0	73	S		
				ns			
[bmim][BF ₄]	7.0-15.0	OG ^e	10.0	35	OG	14.0	58
							28 ^f
							301 ^g
							0.075
[bmim][PF ₆]	8.0-15.0	OG ^e	11.6	43	OG ^e	10.5	SM
[bEt ₃ N][NTf ₂]	4.0-10.0	S			S		
[bmpip][NTf ₂]	1.0-8.0	S			S		
[bmpyrr][NTf ₂]	1.0-9.0	OG ^e	12.6	SM	S		
[Bzbim][NTf ₂]	7.0-17.0	PG			OG ^e	16.8	SM
[Bzmim][NTf ₂]	8.0-19.0	OG ^e	16.1	112	OG ^e	18.1	SM

^aS = soluble; OG = opaque gel; GP = gel-like precipitate; SM = soft material; ns = no μ -DSC signal. ^bInvestigated organogelator percentage range. ^c(%, w/w, organogelator/solvent). ^d T_{gel} (°C) values were reproducible within 1 °C. ^eThe gel phase was obtained after that the cold solution was magnetically stirred for 10 minutes at 1000 rpm. ^fDetermined by μ -DSC investigation (°C). ^gDetermined by μ -DSC investigation (K). ^hDetermined by μ -DSC investigation (J g⁻¹ K⁻¹). ⁱThe gel phase was obtained after ultrasound irradiation of the cold solution for 5 minutes at 200 W and 45 kHz and magnetic stirring for 10 minutes at 1000 rpm.

[47] M.-O. M. Piepenbrock, N. Clarke and J. W. Steed, *Soft Matter* **2010**, *6*, 3541-3547.

It is worth of noting that gelation tests performed for bromide salts gave rise to ionogel phase only for **[2C₈bti][Br]₂** in [bEt₃N][NTf₂] at a CGC value of 20.1% (w/w) ($T_{gel} = 75$ and 15 °C obtained with the lead-ball method and μ -DSC measurements respectively, $T_{gel} = 288$ K, $\Delta C_p = 0.114$ J g⁻¹ K⁻¹). The low ability to form gel of the bromide salts is evidenced also by their high solubility in organic solvents. Moreover, this result recalls the fact that formation of organogels formed by unfunctionalised dicationic salts is mostly favoured for salts with naphthalendisulphonate anions than with bromide.¹⁸

Analysis of data reported in Table 2 evidences a higher tendency of diimidazolium salts to form gel phases in respect to dipyrrolidinium ones. Indeed in the last case the gel formation was mostly observed after magnetic stirring of the mixture. This behaviour could be ascribed to the higher hydrogen bond donor ability of diimidazolium salts.

Interestingly, it can be noted that aliphatic and aromatic cations of ionogelators hardened different ILs, in particular a structural complementarity between the solvent and gelator was detected, for example aromatic ionogelators preferably gelled aliphatic ILs and *vice versa*. Indeed, among gelators presenting aromatic cations, only **[2C₈bti][1,5-nds]** was able to gel aromatic ILs such as [bmim][NTf₂] and [bmim][BF₄] with the assistance of magnetic stirring; on the other hand, among aliphatic ones, **[2C₈btp][1,5-nds]** was able to trap only [bmpyrr][NTf₂] as aliphatic IL. The gelation process seems positively affected by this complementarity between gelator and solvent and it can be explained in terms of cation- π interactions occurring between the two components of the material.

So, as already stressed the nature of the solvent is a key factor in gel formation, for this reason considering ILs as gelation solvents it is possible to analyse gelation tests as function of cation and anion properties of ILs used.

In particular, CGC of **[2C₈bti][1,5-nds]** in aromatic ILs increased from [bmim][NTf₂] to [bmim][BF₄], evidencing a negative effect deriving from the increase in the IL anion coordination ability ($\beta = 0.376$ and 0.243 for [bmim][BF₄] and [bmim][NTf₂] respectively)⁴⁸ and symmetry. Whereas considering aliphatic ILs, all diimidazolium salts were able to gel [bEt₃N][NTf₂], while only **[2C₈bti][2,6-ndc]** was able to form stable opaque gels in [bmpip][NTf₂] and in [bmpyrr][NTf₂]. Data reported in Table 2 evidenced

[18] F. D'Anna, P. Vitale, F. Ferrante, S. Marullo and R. Noto, *ChemPlusChem* **2013**, *78*, 331-342.

[48] L. Crowhurst, P. R. Mawdsley, J. M. Perez-Arlandis, P. A. Salter and T. Welton, *Phys. Chem. Chem. Phys.* **2003**, *5*, 2790-2794.

a correlation between the cation structure of the solvent and the CGC values. Indeed, the CGC decreased from [bEt₃N][NTf₂] to [bmpyrr][NTf₂]. Then, the arrangement of the solvent cation in a cyclic structure seems to make the ionogel fibers growth and entanglement easier. It is noteworthy that in [bmpip][NTf₂], the combined action of magnetic stirring and ultrasound irradiation of the cold solution induced a significant decrease in the CGC value.

In addition, gelation process of **[2C₈btp][1,5-nds]** in aromatic ILs evidences that the CGC value was affected by the anion symmetry and the cross-linking ability. Indeed, significant differences in CGC values (15 and 11.6% (w/w) for [bmim][NTf₂] and [bmim][PF₆] respectively) cannot be ascribed to the anion coordination ability in ($\beta = 0.243$ and 0.207 for [bmim][NTf₂] and [bmim][PF₆] respectively).⁴⁸ This hypothesis is also confirmed in the case of **[2C₈btp][2,6-nds]** that formed gel with the lowest CGC value in [bmim][PF₆] solution, having the lowest β value. Moreover, taking into account nature of aromatic cation of ILs, the presence of the benzylic group on the imidazolium ring instead of the butyl chain caused an increase in CGC value. On the other hand, the presence of a longer alkyl chain favoured the gelation process thanks to the ability of the cation to establish van der Waals interactions (CGC = 16.8 and 18.8 % (w/w) for **[2C₈btp][2,6-nds]** in [Bzmim][NTf₂] and [Bzbim][NTf₂] respectively).

Obviously, CGC values were affected also by anion nature of the gelator. For example, an increase in the anion basicity for diimidazolium salts gave rise to formation of gel at a lower CGC value (16.1 and 11.6% (w/w) for naphthalenedisulfonate salts and naphthalenedicarboxylate salt, presenting the following pK_a of the corresponding acids 0.60 for 1,5-nds, 0.41 for 2,6-nds and 3.60 for 2,6-ndc).⁴⁹ This explanation is also confirmed for differences in CGC values observed in naphthalendisulphonate salts. In addition this trend recalls the one previously reported about the hydrogen bond affinities of carboxylate and sulfonate anions.⁵⁰ Nevertheless, for both diimidazolium and dipyrrolidinium ionogelators, CGC values were barely affected by the different isomeric substitution on the anion.

[48] *ibid.*

[49] in *Development and Advanced Chemistry (ACD/Labs)*, Vol. 11.02 1994–2014.

[50] A. Onoda, Y. Yamada, M. Doi, T.-a. Okamura and N. Ueyama, *Inorg. Chem.* **2001**, *40*, 516-521.

Interestingly the majority of the materials obtained were formed by gelation of dicationic ILs in IL solution and it was the first example reported in literature. Indeed, only Dotz *et al.* synthesised pyridine-bridged bis(benzoimidazolylidene)-palladium complexes capable of gelling both organic solvents and different ILs. However, in that case, gel phase formation could also be a result of metal coordination.⁵¹

The gelling ability of the salts analysed in our case is probably favoured by the neutral functionality. Indeed, data previously collected using corresponding *m*-diimidazolium salts did not give rise to supramolecular gels.¹⁸

1. 4. Thermal stability of gel phases

The thermal stability of ionogels was evaluated determining the T_{gel} , *i.e.* the temperature at which the transition from gel to solution occurs. Values obtained for a concentration of gel equal to CGC are reported in Table 2. As previously pointed out, T_{gel} has been determined by the lead-ball method and, in all cases where the gel was obtained only upon heating and cooling, by micro-DSC measurements. The first method allows detecting the temperature at which a ball falls from the surface of the gel to the bottom of the vial. It is important to underline that in some cases it was not possible to measure T_{gel} by the lead-ball method, indeed as consequence of the soft texture of gel phases, the lead-ball slid downward before gel melting. These materials have been indicated as soft material (SM) in Tables 2.

On the other hand, calorimetry indicates the complete clarification of the gel, extrapolating from the process not only the T_{gel} but also a thermodynamic parameter such as ΔC_p . A representative thermogram is shown in Figure 8.

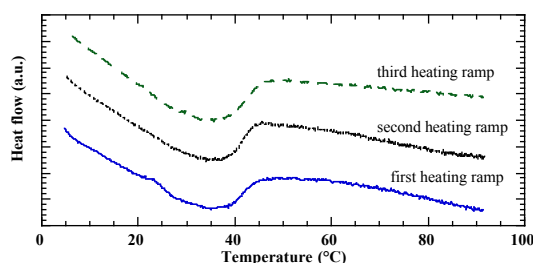


Figure 8: thermogram of ionogel $[2C_8bti][2,6-nds]/[bEt_3N][NTf_2]$.

[51] T. Tu, X. Bao, W. Assenmacher, H. Peterlik, J. Daniels and K. H. Dötz, *Chem. Eur. J.* **2009**, *15*, 1853-1861.

[18] F. D'Anna, P. Vitale, F. Ferrante, S. Marullo and R. Noto, *ChemPlusChem* **2013**, *78*, 331-342.

The thermograms showed a broad signal in the heat capacity that proves the occurrence of a second order phase transition in the systems. It is worth noting that the thermally induced process is reversible, in fact the signal is reproducible in a heating cooling cycle for 3 cycles at least. In particular, lower T_{gel} values were systematically detected from calorimetry than those from the lead-ball method. Such a difference can be explained considering that by calorimetry the onset of the process was monitored while the other method evidenced the full loss of gel consistency. Finally, in all cases the heat capacity change (ΔC_p) for the thermally induced gel rupturing is positive. This result evidences that some degree of freedom are gained into the system above the T_{gel} in agreement with the formation of a liquid mixture.

In general, T_{gel} collected at the CGC shows that the thermal stability of gel phases formed by dipyrrolidinium salts was higher than that detected for diimidazolium salts. For example the gel formed by **[2C₈btp][1,5-nds]** in [Bzmim][NTf₂] was stable until 112 °C. Taking into account gel formed by diimidazolium salts, analysis of values corresponding to T_{gel} determined by lead-ball method shows that thermal stability increased with the anion coordination ability of the IL (10.6 and 14.8 °C for **[2C₈bti][1,5-nds]** in [bmim][NTf₂] and [bmim][BF₄] solution respectively). Whereas the anion coordination ability of the ionogelator negatively affected this material properties as evidenced by data collected in [bEt₃N][NTf₂], indeed T_{gel} decreased from **[2C₈bti][Br]₂** to **[2C₈bti][2,6-ndc]**.

The trend is also opposite considering thermal stability of dipyrrolidinium salts as function of IL properties, indeed, it decreased with the increase in the anion symmetry of IL used, as accounted for by values collected for **[2C₈btp][1,5-nds]** in [bmim][BF₄] and [bmim][NTf₂].

1. 5. Kinetic of gel formation

To study the ionogel formation, RLS (Resonance Light Scattering) and UV-vis measurements were performed. RLS is a technique that allows detecting the presence of aggregates formed by different systems, especially chromophores, in solution.⁵² Interestingly RLS intensity can be related to the size of aggregates and in general, it

[52] J. Anglister and I. Z. Steinberg, *J. Chem. Phys.* **1983**, *78*, 5358-5368.

simultaneously increases with the size of aggregates.⁵³ One of the main advantages of this technique is that can be performed simply using a common spectrofluorometer. While UV-vis measurements, also easily accessible with a common spectrophotometer, are frequently used to evaluate the opacity of a gel phases that represents a measure of gel crystallinity.⁵⁴

Kinetic measurements were carried out evaluating the variation of RLS intensity or absorbance as function of time at 20 °C, that represents the lowest operational temperature of the instruments used. Unfortunately, it was possible to follow the gelation process only for gel of diimidazolium salts (Figure 9), as in the case of dipyrrolidinium salts the ionogel formation at the above temperature was too slow and did not allow having reproducible results.

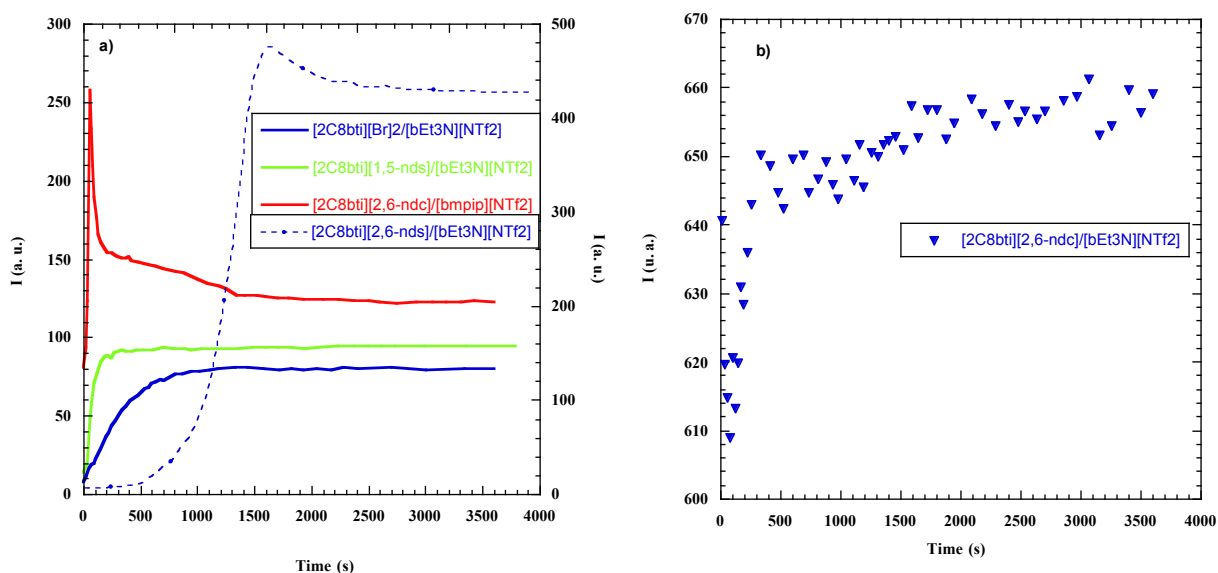


Figure 9: plots of RLS intensity (I_{RLS}) as a function of time for ionogels formed by diimidazolium salts in aliphatic ILs at 17% (w/w).

As shown in the graphs above, gelation processes in $[bEt_3N][NTf_2]$ solution were influenced by the anion nature of the gelator. First of all, for gelators $[2C_8bti][Br]_2$, $[2C_8bti][1,5-nds]$ (Figure 9a) and $[2C_8bti][2,6-ndc]$ (Figure 9b), gel phase formation occurred by a single step mechanism. Even if in the latter case, the gelation was very fast and it was possible to observe only the last part of the process. It is worth of noting how a different isomeric substitution on the anion plays a significant role in determining the

[53] R. Pasternack and P. Collings, *Science* **1995**, *269*, 935-939.

[54] P. Terech, D. Pasquier, V. Bordas and C. Rossat, *Langmuir* **2000**, *16*, 4485-4494.

mechanism of gel phase formation. Indeed, a completely different situation is depicted in the case of gel formed by **[2C₈bti][2,6-nds]** that reached the equilibrium after the formation of an intermediate in a two-step mechanism. This behaviour was previously observed for gel formed by 2,6-nds-salts and it was ascribed to a particular self-assembly process of gelator molecules that, in presence of this anion, might favour a previous formation of large aggregates, subsequently rearranging into smaller and more stable ones finally present in the gel network.¹⁸

Furthermore, the kinetic of gelation is also influenced by the nature of the IL cation used as solvent as evidenced from results of **[2C₈bti][2,6-ndc]** in [bEt₃N][NTf₂] and [bmpip][NTf₂]. Indeed, on going from acyclic to cyclic aliphatic cation a change from a single to a two-step process was observed.

In addition to this first qualitative analysis of the process, it is possible to compare gelation times and size of aggregates for the systems studied. To this aim, data of these parameters for nucleation (t_n), intermediate formation (t_m , I_m) and gelation, corresponding to an equilibrium situation (t_e , I_e), are reported in Table 3.

Table 3: time and I_{RLS} intensity values^a corresponding to gelation processes of in ILs solution.

Ionogel	^b t_n (s)	^b t_m (s)	^b I_m (a.u)	^b t_e (s)	^b I_e (a.u)
[2C₈bti][Br]₂ /[bEt ₃ N][NTf ₂]				540	80
[2C₈bti][1,5-nds] /[bEt ₃ N][NTf ₂]				130	90
[2C₈bti][2,6-nds] /[bEt ₃ N][NTf ₂]	300	970	480	1390	435
[2C₈bti][2,6-ndc] /[bEt ₃ N][NTf ₂]				260	640
[2C₈bti][2,6-ndc] /[bmpip][NTf ₂]		55	260	1470	125

^aTime and intensity values were reproducible within 5%.^b t_n = nucleation time; t_m = fibrillar intermediate formation time; I_m = fibrillar intermediate formation intensity; t_e = gel formation time; I_e = gel formation intensity.

Interestingly, data reported in the Table underline the influence of the ionogelator anion also in the rate of the gelation process. Indeed, gelation time (t_e) increased along the series: **[2C₈bti][1,5-nds]** < **[2C₈bti][2,6-ndc]** < **[2C₈bti][Br]₂** < **[2C₈bti][2,6-nds]**.

The highest time was observed for the ionogelator giving rise to the materials through a two-step mechanism, that in the case 2,6-naphthalene based anions gelators presented also an induction time attributed to the nucleation process. In addition, the latter ionogel phases showed the presence of more extended aggregates. Analysis of the above parameters once again shed light on the importance of the solvent in the material properties, so that in the case of **[2C₈bti][2,6-ndc]**, a change in the IL cation structure

[18] F. D'Anna, P. Vitale, F. Ferrante, S. Marullo and R. Noto, *ChemPlusChem* **2013**, 78, 331-342.

induced not only a change in the gelation mechanism, but also significant differences in the gelation time. Indeed, the gel phase in [bmpip][NTf₂] was formed more slowly and was characterized by the presence of less extended aggregates.

A further support to the RLS measurements was given by opacity ones obtained evaluating changes in the absorbance at 568 nm as a function of time. Plots corresponding to ionogel formation in [bEt₃N][NTf₂] from diimidazolium salts are reported in Figure 10.

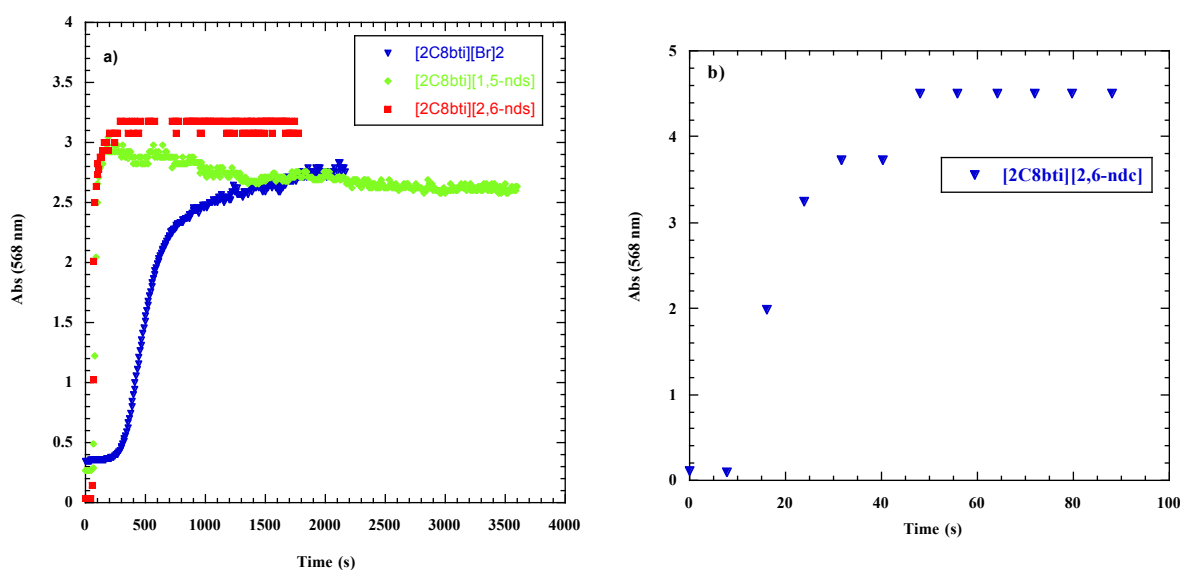


Figure 10: Plots of absorbance values at 568 nm as a function of time corresponding to gelation processes of diimidazolium salts in [bEt₃N][NTf₂].

Analysis of data reported in Figure 10 shows that opacity of gel phases increases along the following trend: [2C₈bti][Br]₂ ≈ [2C₈bti][1,5-nds] < [2C₈bti][2,6-nds] < [2C₈bti][1,5-ndc]. Gelation times obtained by UV-vis measurements perfectly recall the ones detected by RLS measurements, even if in this case understanding the differences of gelation rate among gels of dianionic ionogelators is more difficult.

1. 6. Self-healing ability of ionogels

One of the important properties of gels is their ability to self-repair after disruption caused by external stimuli such as magnetic stirring (thixotropy) and ultrasound irradiation (sonotropy). This property has been largely investigated in the case of

organogels,⁵⁵ on the contrary it has been analysed only in few cases of ionogels. In particular, the thixotropy of ionogels has been reported as advantage for quasi-solid-state DSSC performances^{1c} and for the obtainment of solid-like lubricants.³³

Results obtained after submission of ionogels studied to these external stimuli are reported in Table 4 in terms of thixotropic or sonotropic behaviour of the gel.

Table 4: thixotropic and sonotropic behavior of gel phases obtained.^a

Ionogel	Thixotropy	Sonotropy	Ionogel	Thixotropy	Sonotropy
[2C ₈ bti][Br] ₂ / [bEt ₃ N][NTf ₂]	Y	N	[2C ₈ btp][1,5-nds]/ [bmim][NTf ₂]	N	N
[2C ₈ bti][1,5-nds]/ [bEt ₃ N][NTf ₂]	Y	Y	[2C ₈ btp][1,5-nds]/ [bmim][PF ₆]	Y	Y
[2C ₈ bti][1,5-nds]/ [bmim][NTf ₂]	Y	N	[2C ₈ btp][1,5-nds]/ [bmim][BF ₄]	Y	S
[2C ₈ bti][1,5-nds]/ [bmim][BF ₄]	Y	S	[2C ₈ btp][1,5-nds]/ [bmpyrr][NTf ₂]	Y	S
[2C ₈ bti][2,6-nds]/ [bEt ₃ N][NTf ₂]	Y	Y	[2C ₈ btp][1,5-nds]/ [Bzmim][NTf ₂]	Y	Y
[2C ₈ bti][2,6-ndc]/ [bEt ₃ N][NTf ₂]	Y	Y	[2C ₈ btp][2,6-nds]/ [bmim][BF ₄]	N	N
[2C ₈ bti][2,6-ndc]/ [bmpyrr][NTf ₂]	Y	Y	[2C ₈ btp][2,6-nds]/ [Bzmim][NTf ₂]	Y	Y
[2C ₈ bti][2,6-ndc]/ [bmpip][NTf ₂]	Y	Y	[2C ₈ btp][2,6-nds]/ [Bzbim][NTf ₂]	Y	N
			[2C ₈ btp][2,6-nds]/ [bmim][PF ₆]	N	Y

^aY = the gel phase was able to self-repair after the action of external stimulus. N = the gel phase was not able to self-repair after the action of external stimulus. S = the gel phase was stable to the action of external stimulus.

Ionogels evidenced an enhanced thixotropic behaviour in almost all cases considered, with the only exception of the [2C₈btp][1,5-nds] in [bmim][NTf₂] and [2C₈btp][2,6-nds] in [bmim][BF₄] and [bmim][PF₆].

On the other hand the response to ultrasound irradiation showed three different situations: stable ionogels to ultrasound irradiation (S), like [2C₈bti][1,5-nds] and [2C₈btp][1,5-nds] in [bmim][BF₄] and [2C₈btp][1,5-nds] in [bmpyrr][NTf₂]; ionogels totally destroyed after the stimulus and finally ionogels with sonotropic behaviour.

[55] a) P. Mukhopadhyay, N. Fujita, A. Takada, T. Kishida, M. Shirakawa and S. Shinkai, *Angew. Chem., Int. Ed.* **2010**, *49*, 6338-6342, b) Y. Ohsedo, M. Miyamoto, A. Tanaka and H. Watanabe, *New J. Chem.* **2013**, *37*, 2874-2880.

[1c) Y. Fang, J. Zhang, X. Zhou, Y. Lin and S. Fang, *Electrochim. Acta* **2012**, *68*, 235-239.

[33] M. Cai, Y. Liang, F. Zhou and W. Liu, *J. Mater. Chem.* **2011**, *21*, 13399-13405.

Once again these data underline how imidazolium salts, exhibiting a better response to the action of external stimuli, formed soft material with enhanced properties than pyrrolidinium ones. In particular, six ionogels formed by diimidazolium salts presented both thixotropic and sonotropic behaviour.

1. 7. Conductivity of ionogels

As already pointed out, one of the main advantages in using these materials is their good conductivity. Indeed, usually they keep the same conductivity of the IL used as gelation solvent.

For this reason, we have determined this property by using dielectric spectroscopy. In particular the dissipation factor (D) has been measured as function of frequency (ν) at 25 °C for IL solutions and ionogels at the CGC value.

All ILs presented a monotonic change of the dissipation factor *vs.* ν that indicates the absence of relaxation phenomena in the investigated range. A similar result was found for ionogels that presented dielectric spectra almost coincident in shape with those of the solvent (Figure 11a). However, in general the absolute value of the dissipation factor is higher than the IL one, indeed the curve for the gels diverges from those of the corresponding IL solvent in the high frequency range. An interesting feature was found for the systems that provided a soft material (SM in Table 2) as they exhibited a peak in the dissipation factor *vs.* ν (Figure 11b). It should be noted that the relaxation phenomenon is due to the gelator, as the solvent did not show any peak in the same frequency range. Moreover the absence of relaxation in more rigid gels indicates that the gelator motions are strongly reduced in these systems.

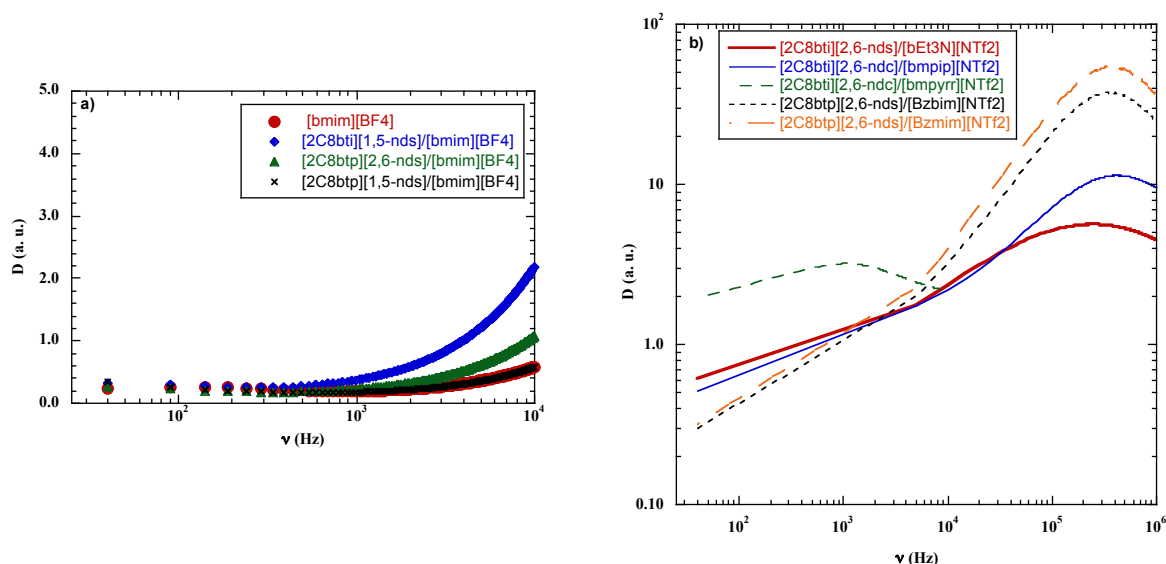


Figure 11: dissipation factor (D) *vs.* ν : **a)** for [bmim][BF₄] and ionogels in the same IL; **b)** for ionogels that present a maximum value of conductivity.

The ν at the maximum, maximum value of conductivity and the ratio between dissipation factor evaluated for gel and the one of the corresponding IL are given in Table 5.

Table 5: dielectric properties of ionogels at 25 °C.

IL	Gelator	ν_{\max} (kHz)	Conductivity at maximum ($\Omega^{-1} \text{ m}^{-1}$)	$D_{\text{gel}}/D_{\text{IL}}^{\text{a}}$
[bEt ₃ N][NTf ₂]	[2C ₈ bti][2,6-nds]	360	1.35×10^{-2}	1.05
[bmpip][NTf ₂]	[2C ₈ bti][2,6-ndc]	420	1.24×10^{-2}	2.61
[bmpyrr][NTf ₂]	[2C ₈ bti][2,6-ndc]	1.06	3.05×10^{-4}	6.69
[Bzbim][NTf ₂]	[2C ₈ btp][2,6-nds]	360	3.60×10^{-2}	3.04
[Bzmim][NTf ₂]	[2C ₈ btp][2,6-nds]	245	5.59×10^{-2}	5.55
[bmim][BF ₄]	[2C ₈ bti][1,5-nds]			3.78
[bmim][BF ₄]	[2C ₈ btp][2,6-nds]			1.78
[bmim][BF ₄]	[2C ₈ btp][1,5-nds]			1.00
[bEt ₃ N][NTf ₂]	[2C ₈ bti][Br] ₂			0.96
[bEt ₃ N][NTf ₂]	[2C ₈ bti][1,5-nds]			0.27
[bEt ₃ N][NTf ₂]	[2C ₈ bti][2,6-ndc]			0.27
[bmim][PF ₆]	[2C ₈ btp][2,6-nds]			1.11
[bmim][PF ₆]	[2C ₈ btp][1,5-nds]			1.16
[bmim][NTf ₂]	[2C ₈ bti][1,5-nds]			2.06
[bmim][NTf ₂]	[2C ₈ btp][1,5-nds]			5.98
[bmpyrr][NTf ₂]	[2C ₈ btp][1,5-nds]			3.28
[Bzmim][NTf ₂]	[2C ₈ btp][1,5-nds]			8.15

^aRatio of the gel dissipation factor with respect to those of IL solvent measured at 10 kHz.

As observed from the trend of the curves, the ratio $D_{\text{gel}}/D_{\text{IL}}$ calculated from values collected at 10 kHz shows that, with the only exception of gels formed in [bEt₃N][NTf₂], the dissipation factor of the gel is improved when compared to the corresponding IL.

Although a strict comparison is not possible due to frequency, temperature and concentration, we can state that the conductivity values found in the investigated gels are in the same order of magnitude of those reported in the literature (roughly $10^{-2} \Omega^{-1} \text{ m}^{-1}$).⁵⁶ Notwithstanding, it is interesting that most of the gels presented in the manuscript showed an increase of conductivity compared to the corresponding IL. This was surprising considering that, to the best of our knowledge, we observed this trend for the first time; indeed, generally an almost constant⁵⁷ or a slight decrease^{25a} of conductivity with ionogelator addition was detected. In our case, this behaviour could be attributed, as recently hypothesised, to the higher affinity of gelator molecules towards IL's anions.³¹ This affinity could reduce the electrostatic attraction between the ion pair of the IL and thus increases their mobility overcoming the higher viscosity of the gel in respect of the IL.

In this section the ability of aromatic and aliphatic functionalised DOSs has been demonstrated. Interestingly, they were able to gel ILs following a complementarity criterion between aromatic and aliphatic structure of gelators and IL cations.

The properties of the materials obtained are strongly dependent on the combination of cation and anion of salt used as gelator and on solvent nature. In particular, salt presenting aromatic cations and anions exhibit a higher tendency to gel and formed ionogel more responsive to external stimuli. All gels obtained have a high thermal stability and a peculiar conductivity surprisingly higher than the one of the ILs, so they can be considered as perfect candidates for their use in systems like DSSCs. Having also in mind the presence of the basic functionality tethered on the cationic unit these soft materials could be also applied as alternative media for catalytic studies.

[56] a) O. Cabeza, J. Vila, E. Rilo, M. Domínguez-Pérez, L. Otero-Cernadas, E. López-Lago, T. Méndez-Morales and L. M. Varela, *J. Chem. Thermodyn.* **2014**, *75*, 52-57, b) J. C. Ribot, C. Guerrero-Sanchez, T. L. Greaves, D. F. Kennedy, R. Hoogenboom and U. S. Schubert, *Soft Matter* **2012**, *8*, 1025-1032.

[57] Y. Ishioka, N. Minakuchi, M. Mizuhata and T. Maruyama, *ibid.* **2014**, *10*, 965-971.

[25] a) K. Hanabusa, H. Fukui, M. Suzuki and H. Shirai, *Langmuir* **2005**, *21*, 10383-10390.

[31] A. Maršavelski, V. Smrečki, R. Vianello, M. Žinić, A. Moguš-Milanković and A. Šantić, *Chem. Eur. J.* **2015**, *21*, 12121-12128.

2. Gel phases formed by non-stoichiometric OSs

Studying the gelling ability of diimidazolium OSs, we have demonstrated how small modifications in their structure lead to the formation of materials with different properties. In particular, to have further insights on the anion effect of the gelator we have taken into account both stoichiometric and non-stoichiometric organic salts. In particular, we have synthesised two isomeric diimidazolium organic cations, 3,3'-di-n-dodecyl-1,1'-(1,4-phenylenedimethylene) diimidazolium [*p*-C₁₂im] and 3,3'-di-n-dodecyl-1,1'-(1,3-phenylenedimethylene) diimidazolium [*m*-C₁₂im] in which the counter-ions are aliphatic or aromatic carboxylate anions that differ in the extension of their π -surfaces and the number of negative charges (1,4-benzendicarboxylate [1,4-bdc], 2,6-naphtalenedicarboxylate [2,6-ndc], trimesate [Trim], citrate [Cit], ethylenediaminetetracetate [EDTA] Figure 12).

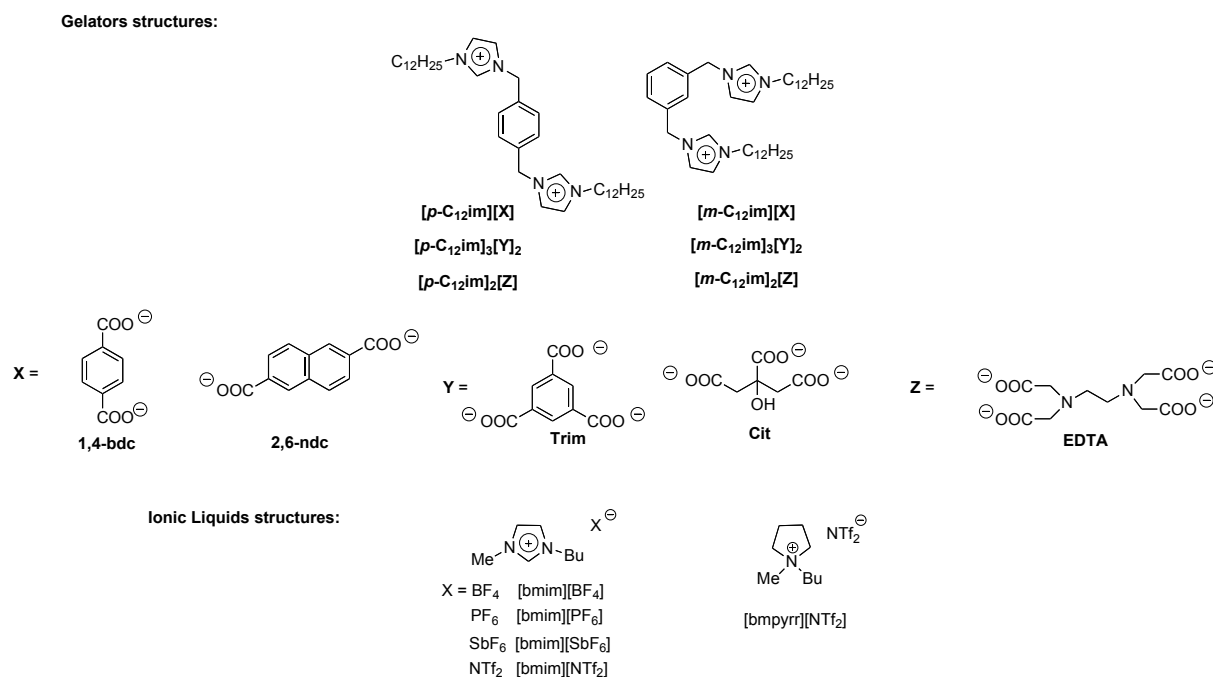


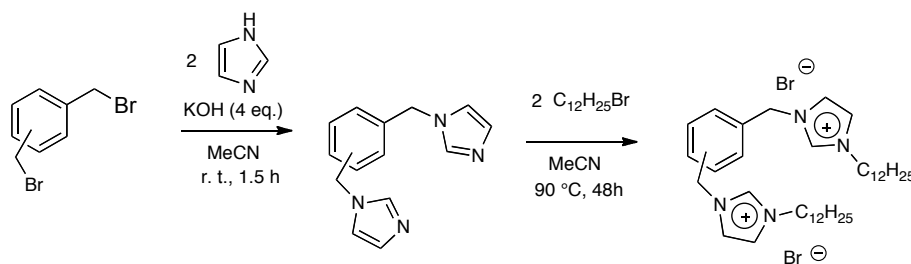
Figure 12: structures of diimidazolium salts used as gelators and ionic liquids used as the solvent components.

Carboxylate anions presenting good coordination ability should favour the formation of the three-dimensional network; in fact, 2,6-ndc-based functionalised DOSs exhibited the highest gelling ability. In this case, we have analysed how the combination of the two dications with di-, tri- or tetraanions influenced the gelling ability of the organic salts with several ILs and with conventional solvents. Indeed, the different stoichiometries between

the dications and their anions (1:1, 3:2, 2:1, respectively) can lead to different packing arrangements of the salts. More dications or more anions in the salt composition are expected to have important consequences on the favourability of interactions leading to gel formation. Furthermore, we hypothesized that the different (non 1:1) stoichiometries might increase the possibility of the *meta* dication salts becoming efficient gelators as well. In fact, it has been previously demonstrated by DFT calculations that the substitution pattern of the dications is a key factor in determining the efficiency of the gelation process due to the different packing modes that the *meta* and *para* isomers require, especially when paired with their anions. In particular, one more time it is important to focus on the fact that *meta* substitution of the benzene core gives rise to stronger interactions with the anion than does *para* substitution. Thus, the “close cage” formed by *meta* dications with anions limits ion pair interactions needed to form the gel networks.¹⁸ As in the case of functionalised organic salts, gelation tests were performed in several organic solvents and in ILs. Among the most commonly used ILs, imidazolium ones having anions that differ in size, symmetry, and coordinating ability, and a pyrrolidinium IL were examined as gelation solvents (Figure 12). Pyrrolidinium IL could give information about the role played by the cation ability to form π - π interactions. Also in this case we were interested in the analysis of the gelling ability of the salts and material properties as function of different solvent characteristics.

2. 1. Synthesis of DOSs

The synthetic approach was similar to the ones applied for the functionalised DOSs. In the first step we have obtained neutral diimidazole species *meta* or *para* substituted, that were subsequently alkylated with two equivalent of dodecylbromide to form the dibromide salts. The latter ones were finally submitted to the anion exchange protocol performed with the anionic resin.



Scheme 2: synthetic approach to obtain diimidazolium bromide salts.

[18] F. D'Anna, P. Vitale, F. Ferrante, S. Marullo and R. Noto, *ChemPlusChem* **2013**, 78, 331-342.

2. 2. Thermal stability of DOSs

Before testing the gelling ability of the salts, once again we have investigated their thermal properties evaluating the decomposition and melting process by TGA and DSC measurements.

Thermal parameters are reported in Table 6. In particular, decomposition temperature (T_d), melting temperature (T_m), variation of enthalpy corresponding to the melting process (ΔH_m) and temperature of glass transition (T_g) were determined as the maximum of TGA derivative, as the maximum of heat flow in the DSC trace, as the integral of the melting process calorimetric peak and as the onset point of the sigmoidal curve of heat flow in the DSC trace, respectively.

In all cases we observed single step decomposition processes and T_d values range from 206 °C for [*p*-C₁₂im]₃[Cit]₂ up to 245 °C for [*m*-C₁₂im][2,6-ndc]. Although it is high, thermal stability of these organic salts is lower than that reported by Armstrong *et al.* for some diimidazolium salts bearing aliphatic spacers.⁴⁴

Perusal of data reported in the Table evidences how thermal properties are significantly affected by both the isomeric substitution on the cation and anion nature.

In general, *para*-isomers show lower T_d values than the corresponding *meta*-ones. As for the anion nature, thermal stability decreases along the following order: [EDTA] > [1,4-bdc] > [2,6-ndc] > [Trim] > [Cit] for *para*-isomers and [2,6-ndc] > [1,4-bdc] > [Trim] > [EDTA] > [Cit] for *meta*-isomers. In general, T_d decreases on going from bivalent to trivalent anions and, in the latter case, they decrease on going from aromatic to aliphatic ones ([Trim] > [Cit]). However, between aliphatic anions, [EDTA] stabilizes the salts against decomposition process. Furthermore, in agreement with the thermal stability of the functionalised dioctylimidazolium salts,⁴² the increase in π -surface area of aromatic dianions positively affected T_d , as evidenced on going from [*m*-C₁₂im][1,4-bdc] to [*m*-C₁₂im][2,6-ndc].

[44] J. L. Anderson, R. Ding, A. Ellern and D. W. Armstrong, *J. Am. Chem. Soc.* **2005**, *127*, 593-604.

[42] F. D'Anna, C. Rizzo, P. Vitale, G. Lazzara and R. Noto, *Soft Matter* **2014**, *10*, 9281-9292.

Table 6: experimental decomposition temperatures (T_d) determined by TGA measurements, melting temperatures at heat flow maximum (T_m), enthalpy variation (ΔH_m) and glass transition (T_g) temperatures determined using DSC measurements.

Salts	T_d ($^{\circ}\text{C}$)	T_m ($^{\circ}\text{C}$) ^a	ΔH_m (J/g) ^a	T_g ($^{\circ}\text{C}$) ^b	T_m ($^{\circ}\text{C}$) ^b	ΔH_m (J/g) ^b
[<i>p</i> -C ₁₂ im][2,6-ndc]	231	142.2	2.6	-	115.7	1.9
[<i>p</i> -C ₁₂ im][1,4-bdc]	232	102.3	18.9	63.7		
[<i>p</i> -C ₁₂ im] ₃ [Trim] ₂	229	ns ^c		85.6		
[<i>p</i> -C ₁₂ im] ₃ [Cit] ₂	206	110.9	8.1	49.9		
[<i>p</i> -C ₁₂ im] ₂ [EDTA]	233	104.7	17.2	-	56.8	15.4
[<i>m</i> -C ₁₂ im][2,6-ndc]	245	139.4	21.3	45.7		
[<i>m</i> -C ₁₂ im][1,4-bdc]	237	91.9	45.2	41.5		
[<i>m</i> -C ₁₂ im] ₃ [Trim] ₂	235	ns ^c		64.3		
[<i>m</i> -C ₁₂ im] ₃ [Cit] ₂	219	ns ^c		62.8		
[<i>m</i> -C ₁₂ im] ₂ [EDTA]	234	71.1	12.5	ns ^c		

^amelting temperatures and enthalpy variations corresponding to the first heating cycles; ^bglass transition temperature, melting temperatures and enthalpy variations reported as average of second and third heating cycles; ^cns= no signal

It is worth of noting that analysis of DSC thermograms reveals the presence of polymorphism in the compounds.⁵⁸ Indeed, different transitions appear in the first heating cycle respect the ones shown in the second and third cycles. The last two cycles present reproducible transitions indicating the stability of the salts. Probably, this behaviour depends on the solvent of crystallization of the salt and on the time that the salt needs to return to the first morph. This is longer than crystallization process that occurs in the instrument.

In some cases, analysis of the first heating cycle of the thermograms reveals the occurrence of endothermic processes characterized by a modest transition enthalpy. It was ascribed to melting processes, as salts did not show mesophases using polarized optical microscopy. Differently, with the only exception of [*p*-C₁₂im][2,6-ndc], [*p*-C₁₂im]₂[EDTA] and [*m*-C₁₂im]₂[EDTA], in all the other cases in the second and third cycles we observed only glass transitions.

Taking into account DSC data, [*p*-C₁₂im]-isomers have higher T_m and T_g values than the corresponding [*m*-C₁₂im]-isomers, indicating a lower structural order degree for the latter ones, in agreement on what previously demonstrated for salts with similar structures.¹⁶

However, there is not a clear relationship between salts stoichiometry and thermal transitions. Only in the case of *meta*-isomers, salts having trivalent anions displayed higher T_g values than those bearing bivalent ones.

[58] M. H. Nielsen, S. Aloni and J. J. De Yoreo, *Science* **2014**, *345*, 1158-1162.

[16] F. D'Anna, F. Ferrante and R. Noto, *Chem. Eur. J.* **2009**, *15*, 13059-13068.

As for the effect of the anion nature, valence being the same, T_g or T_m values decreased along the following order: [2,6-ndc] > [1,4-bdc] and [Trim] > [Cit]. Trend observed seems to indicate once again that aromaticity and the larger π -surface extension of the anion, together with its symmetry and rigidity, award to the salts a higher structural order degree. Consequently, corresponding systems require more energy to melt the crystal.

2. 3. Gelation tests and thermal stability of DOSs

Gelation tests have been performed in organic solutions, water and ILs. When the self-assembly process occurred, we obtained white opaque gels, stable to the tube inversion test for almost three months (Figure 13).

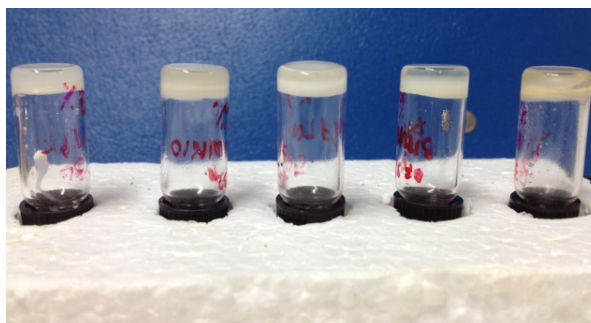


Figure 13: gel phases formed by $[p\text{-C}_{12}\text{im}][1,4\text{-bdc}]/\text{glycerol}$, $[p\text{-C}_{12}\text{im}]_2[\text{EDTA}]/\text{glycerol}$, $[p\text{-C}_{12}\text{im}][1,4\text{-bdc}]/[\text{bmim}][\text{BF}_4]$, $[p\text{-C}_{12}\text{im}]_3[\text{Trim}]_2/[\text{bmim}][\text{BF}_4]$ and $[p\text{-C}_{12}\text{im}]_3[\text{Cit}]_2/[\text{bmim}][\text{BF}_4]$ (from left to right).

Organic solvents

In general, salts were soluble in polar protic solvents and insoluble in polar aprotic ones. Some salts were able to gel in glycerol and only one, $[p\text{-C}_{12}\text{im}]_2[\text{EDTA}]$, also in octanol. Results obtained for these gels are reported in Table 7. In particular CGC, T_{gel} at CGC and at 5% (w/w) of gelator were determined.

Table 7: CGC, T_{gel} and ΔH_m for organogel obtained.^a

	solvents					
	glycerol			octanol		
	CGC ^b	T_{gel} ^c	T_{gel} ^d	ΔH_m ^g	CGC ^b	T_{gel} ^c
[<i>p</i>-C₁₂im][1,4-bdc]	3.2	37.2	36.2			
			42.6 ^e	1.785		
[<i>p</i>-C₁₂im][2,6-ndc]	2.3	31.9	33.8			
			57.0 ^f	-		
[<i>p</i>-C₁₂im]₂[EDTA]	2.0	SM	SM		5.0	33.0
			41.4 ^e	3.563		ns
[<i>m</i>-C₁₂im][1,4-bdc]	3.7	23.7	27.6			
			ns			
[<i>m</i>-C₁₂im]₂[EDTA]	2.0	24.0	27.3			
			29.3 ^e	0.542		

^aSM =soft material; ns = no DSC signal. ^bcritical gelation concentration (% w/w, organogelator/solvent). ^c T_{gel} values (°C) were reproducible within 1 °C; T_{gel} determined at CGC by lead-ball method. ^d T_{gel} values (°C) were reproducible within 1 °C; T_{gel} determined at 5 % of gelator by lead-ball method. ^e T_{gel} values (°C) determined by DSC investigation. ^f T_{gel} values (°C) determined by DSC investigation; the process consists of a glass transition. ^g ΔH_m (J/g) determined by DSC investigation.

CGC obtained for organogels was quite low evidencing the pronounced attitude of the salts to aggregate especially in glycerol. Indeed, CGC of [*p*-C₁₂im]₂[EDTA] in octanol slightly increased due to the decrease in both polarity and hydrogen bond donor ability of the solvent. In general, CGC values were affected by anion of gelators. Indeed, irrespective of the isomeric substitution on the cation, the above parameter decreased with the increase in the extension of π -surface area of the anion ([1,4-bdc] > [2,6-ndc]) and moving from the bivalent aromatic anions to the tetravalent aliphatic anion ([2,6-bdc] > [EDTA]).

T_{gel} results collected at 5% (w/w) gelator concentration (see Table 7) allowed having a comparison among different gelators and they were measured using both the lead-ball method and DSC measurements.

The thermograms showed a steep change in the heat capacity providing the occurrence of a second order phase transition in the systems as in ionogel phases obtained with functionalised DOSs (Figure 8 par. 1. 4.). Gels obtained were thermoreversible as all measurements were run three times with a good reproducibility. However, as the gel formation was slow, the subsequent heating cycles were measured after 24h to allow reformation of the gel phase. It is worth of noting that comparison among DSC traces of neat gelators in first cycle and organogels underlines that transitions occurred at significantly different temperatures; so that they are peculiar of the material.

Differently from what previously observed for ionogels first analysed (par. 1. 4.), lower T_{gel} values from lead-ball method than for calorimetry were systematically evidenced. The analysis of T_{gel} indicates that thermal stability decreased on going from *para*- to *meta*-isomers (see data for [EDTA]- and [1,4-bdc]-derivatives). This trend perfectly recalls the thermal stability of neat gelators (see Table 6), probably evidencing how differences in cation conformation affect not only the packing in the solid state, but also the organization of network in the gel phase. In the case of [EDTA]-derivatives, the above trend was also supported by significant differences detected in enthalpy values. Interestingly, the increase in π -surface area of the anion for *para*-isomers positively affected also the thermal stability of their gel phase in agreement with thermal stability of neat gelators and CGC values ($T_{gel} = 42.6$ and 57.0 °C for gels of [1,4-bdc]- and [2,6-ndc]-salt, respectively).

Ionic liquids

With the only exception of **[*m*-C₁₂im]₃[Cit]₂**, all DOSs hardened [bmim][BF₄] and in general *para*-isomers were able to gel in almost all the ILs taken into account; while, in some cases, *meta*-isomers precipitated or formed a gelatinous precipitate after the cooling of the hot solution. It is worth of noting that CGC obtained in IL solution are slightly higher than the ones collected in conventional organic solvent. Data of gelation tests in ILs and T_{gel} determined by lead-ball method at CGC are reported in Table 8.

As well as for functionalised diimidazolium salts, analysis of CGC data revealed a structural complementarity between gelator and IL structure, indeed, in imidazolium ILs it increased on going from [1,4-bdc] to [2,6-ndc] and from [Cit] to [Trim].

Once again the nature of IL used influenced the gelation process indeed, irrespective of the gelator considered, the largest CGC values were always observed in [bmim][BF₄], that presents the largest hydrogen bond acceptor ability among ILs used, β . Consequently, the result obtained seems to reflect a negative effect of the IL anion coordination ability on the gel phase formation. The decrease in the aromatic character of IL cation also negatively affected CGC (2.6 and 3.5% (w/w) for **[*p*-C₁₂im]₃[Cit]₂** and 2.1 and 5 % (w/w) for **[*p*-C₁₂im]₂[EDTA]** in [bmim][NTf₂] and [bmpyrr][NTf₂], respectively).

Table 8: CGC and T_{gel} at CGC for ionogel obtained.

Ionic liquids	[<i>p</i> -C ₁₂ im][1,4-bdc]		[<i>p</i> -C ₁₂ im][2,6-ndc]		[<i>p</i> -C ₁₂ im] ₃ [Trim] ₂		[<i>p</i> -C ₁₂ im] ₃ [Cit] ₂		[<i>p</i> -C ₁₂ im] ₂ [EDTA]	
	CGC ^b	T _{gel} ^c	CGC ^b	T _{gel} ^c	CGC ^b	T _{gel} ^c	CGC ^b	T _{gel} ^c	CGC ^b	T _{gel} ^c
[bmim][PF ₆]	I		I		G		G		G	
					2.0	SM	2.3	SM	2.1	SM
[bmim][NTf ₂]	P		I		G		G		G	
					3.9	40.1	2.6	42.4	3.2	34.7
[bmim][BF ₄]	G		G		G		G		G	
	3.4	53.0	4.3	SM	5.0	47.9	3.5	40.7	3.5	SM
[bmim][SbF ₆]	I		I		G		G		G	
					4.1	46.0	2.2	25.2	2.4	SM
[bmpyrr][NTf ₂]	G		P		I		G		G	
	1.8	SM					3.5	40.5	5	SM
Ionic liquids	[<i>m</i> -C ₁₂ im][1,4-bdc]		[<i>m</i> -C ₁₂ im][2,6-ndc]		[<i>m</i> -C ₁₂ im] ₃ [Trim] ₂		[<i>m</i> -C ₁₂ im] ₃ [Cit] ₂		[<i>m</i> -C ₁₂ im] ₂ [EDTA]	
	CGC ^b	T _{gel} ^c	CGC ^b	T _{gel} ^c	CGC ^b	T _{gel} ^c	CGC ^b	T _{gel} ^c	CGC ^b	T _{gel} ^c
[bmim][PF ₆]	I		I		G		G		G	
					2.9	SM	4.6	38.2	3.2	33.3
[bmim][NTf ₂]	P		I		GP		S		S	
[bmim][BF ₄]	G		G		G		S		G	
	3.3	24.3	4.8	29.1	4.0	22.2			5.0	SM
[bmim][SbF ₆]	I		I		P		S		GP	
[bmpyrr][NTf ₂]	GP		P		G		G		GP	
					6.3	39.1	5.9	SM		

^aS=soluble; I=insoluble; P=precipitate; G=gel; GP=gel-like precipitate; SM =soft material. ^bcritical gelation concentration (%o, w/w, organogelator/solvent). ^cT_{gel} values (°C) were reproducible within 1 °C; T_{gel} determined at CGC by lead-ball method.

Supramolecular gel formation is usually described as the result of gelator ability to entrap solvent within a three-dimensional network. Nevertheless, in systems like our ionogels, the ability to form this network could be due to a mix of ions of solvent and gelator. Indeed, during the mixing of IL and gelator, cation of gelator can interact with its own anion but also with the IL anion. This interaction should favour a mixed ionic network formation and should become more significant when less tight interactions occur between ions of solvent (lower β values).

This consideration poses a question on the nature of gelator in ionogels. In fact, each system was characterized by the presence of a couple of cations and a couple of anions that could cause exchange processes. To have information about the nature of the salt inducing gelation, we took into account the ionogel [*p*-C₁₂im]₃[Cit]₂/[bmim][NTf₂] (CGC = 2.6%) and we synthesised possible salts deriving from exchange processes ([*p*-C₁₂im][NTf₂]₂ and [bmim]₃[Cit]). So that, we prepared two mixtures [*p*-C₁₂im][NTf₂]₂/[bmim]₃[Cit] having the cations and anions mole ratios characterizing the ionogel ($n_{[bmim]^+}/n_{[p-C_{12}im_2]^+} = 506$ and $n_{[NTf_2]^-}/n_{[Cit]^-} = 72$). In both cases, heating and

subsequent cooling of the mixtures did not induce soft materials formation. In addition, we centrifuged (6000 rpm, 1 x 10 min; 6000 rpm, 4 x 40 min) the **[*p*-C₁₂mim]₃[Cit]₂/[bmim][NTf₂]** gel in order to check the occurrence of phase-separation between solid and liquid, method previously adopted to discriminate gelator nature in ionogels.⁵⁹ However, in all cases we obtained a gelatinous suspension that did not allow separating the components. This result and the non gelling ability of [*p*-C₁₂mim][NTf₂]₂ in [bmim][NTf₂] allowed us to identify **[*p*-C₁₂mim]₃[Cit]₂** as the gelator. Moreover, different transitions occurring in DSC traces of exchange salts ([*p*-C₁₂mim][NTf₂]₂, [*p*-C₁₂mim]₃[Cit]₂ and [bmim]₃[Cit]) in respect to the one corresponding ionogel (**[*p*-C₁₂mim]₃[Cit]₂/[bmim][NTf₂]**) further supported our hypothesis.

The knowledge of the gelator allowed investigating properties of the material, once again, as function of gelator and solvent properties. Table 9 summarizes thermal stability of ionogels at the same concentration 5 % (w/w).

According to data collected for organogels, T_{gel} values determined using DSC measurements resulted higher than those obtained by the lead-ball method. In general, thermal stability of ionogels resulted higher than the one of organogels and in particular, ionogels formed by *para*-isomers presented higher T_{gel} than the ones formed by *meta*-salts. While, the anion nature of the gelator did not strongly influence the thermal stability of ionogels in [bmim][BF₄] solution. In general, considering DSC data, T_{gel} values slightly increase on going from bivalent to trivalent anions.

Taking into account solvent properties, it seems that higher IL anion symmetry, positively affected T_{gel} . Indeed, for gels of [Trim] and [Cit]-based salts, T_{gel} decreased according to the following order: [bmim][BF₄] > [bmim][PF₆] > [bmim][SbF₆] > [bmim][NTf₂] > [bmpyrr][NTf₂]. While, it diverged from the one corresponding to the anion coordination ability of the IL ([BF₄] > [SbF₆] > [NTf₂] > [PF₆]).

In general, the complementarity between IL cation and anion of gelator, determining the CGC of ionogels, is pointed out also for thermal stability; indeed, ionogels of **[*p*-C₁₂mim]₃[Cit]** and **[*p*-C₁₂mim]₂[EDTA]** presented slightly higher thermal stability in [bmim][NTf₂] than in [bmpyrr][NTf₂] solution.

[59] J. Kagimoto, N. Nakamura, T. Kato and H. Ohno, *Chem. Commun.* **2009**, 2405-2407.

Table 9: T_{gel} and ΔH_m determined for ionogels obtained.^a

Ionic liquids	[<i>p</i> -C ₁₂ im] [1,4-bdc]		[<i>p</i> -C ₁₂ im] [2,6-ndc]		[<i>p</i> -C ₁₂ im] ₃ [Trim] ₂		[<i>p</i> -C ₁₂ im] ₃ [Cit] ₂		[<i>p</i> -C ₁₂ im] ₂ [EDTA]	
	T_{gel}^b	ΔH_m^e	T_{gel}^b	ΔH_m^e	T_{gel}^b	ΔH_m^e	T_{gel}^b	ΔH_m^e	T_{gel}^b	ΔH_m^e
[bmim][PF ₆]					41.4		SM		56.8	
					64.3 ^c	1.907	67.1 ^c	2.075	65.0 ^c	0.717
[bmim][NTf ₂]					41.7		42.4		42.0	
					44.2 ^c	2.668	49.5 ^c	5.152	45.3 ^c	2.867
[bmim][BF ₄]	53.4		SM		47.9		49.5		89.0	
	81.7 ^c	1.880	84.7 ^c	1.898	85.1 ^c	1.278	85.4 ^c	1.655	ns	-
[bmim][SbF ₆]					43.7		39.9		49.0	
					49.8 ^c	1.16	50.3 ^c	2.195	ns	-
[bmpyrr][NTf ₂]	36.3						42.8		47.0	
	39.2 ^d	-					49.1 ^c	2.554	44.6 ^c	1.718
Ionic liquids	[<i>m</i> -C ₁₂ im] [1,4-bdc]		[<i>m</i> -C ₁₂ im] [2,6-ndc]		[<i>m</i> -C ₁₂ im] ₃ [Trim] ₂		[<i>m</i> -C ₁₂ im] ₃ [Cit] ₂		[<i>m</i> -C ₁₂ im] ₂ [EDTA]	
	T_{gel}^b	ΔH_m^e	T_{gel}^b	ΔH_m^e	T_{gel}^b	ΔH_m^e	T_{gel}^b	ΔH_m^e	T_{gel}^b	ΔH_m^e
[bmim][PF ₆]					39.9		35.4		34.7	
					62.0 ^c	2.122	62.4 ^c	1.883	ns	
[bmim][NTf ₂]										
[bmim][BF ₄]	SM		28.4		SM				53.0	
	47.2 ^c	1.483	47.4 ^c	2.042	50.6 ^c	2.549			53.9 ^c	0.967
[bmim][SbF ₆]										
[bmpyrr][NTf ₂]					28.2		SM			
					65.9 ^d	-	60.5 ^d	-		

^aSM =soft material; ns = no DSC signal. ^b T_{gel} values (°C) were reproducible within 1 °C; T_{gel} determined at 5 % of gelator by lead-ball method. ^c T_{gel} values (°C) were reproducible within 1 °C; T_{gel} determined at 5 % of gelator by DSC investigation. ^d T_{gel} values (°C) determined by DSC investigation; the process consists of a glass transition. ^e ΔH_m (J/g) determined by DSC investigation.

Thermal stability of ionogels formed by functionalised DOSs was higher than the one of ionogels formed by DOSs, however the last ones generate the soft materials at a lower CGC.

2. 4. Morphology of gel phases

Morphology of both organo- and ionogels at 5 % (w/w) was analysed using POM measurements. This technique allowed having images comprehensive of three-dimensional structure of gelator and solvent. POM images were recorded observing soft materials casted between glass slides, unfortunately in some cases, the pressure of the glass caused the disruption of gel phases and did not allow obtaining gel morphology. POM images for some selected samples are reported in Figure 14.

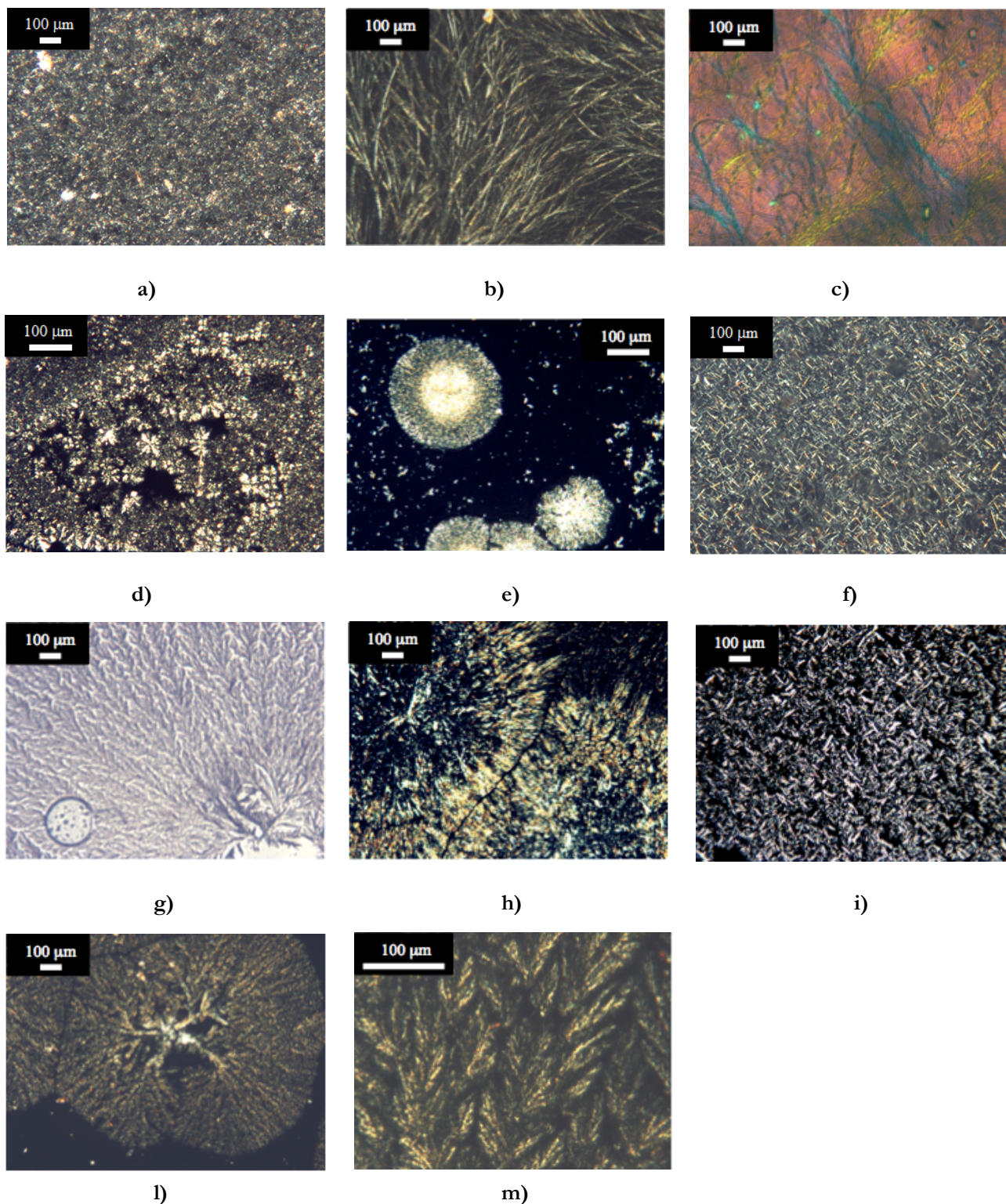


Figure 14: POM images of organogels and ionogels **a)** gel of $[p\text{-C}_{12}\text{im}]_2[\text{EDTA}]$ in glycerol at room temperature; **b)** gel of $[p\text{-C}_{12}\text{im}]_2[\text{EDTA}]$ in octanol at room temperature after first heating and cooling of the sample; **c)** gel of $[m\text{-C}_{12}\text{im}]_2[\text{EDTA}]$ in glycerol at room temperature after first heating and cooling of the sample; **d)** gel of $[p\text{-C}_{12}\text{im}]_3[\text{Cit}]_2$ in $[\text{bmim}][\text{PF}_6]$ at room temperature after first heating and cooling of the sample; **e)** gel of $[m\text{-C}_{12}\text{im}]_3[\text{Trim}]_2$ in $[\text{bmim}][\text{PF}_6]$ at 40 °C of cooling ramp of the sample after first heating; **f)** gel of $[p\text{-C}_{12}\text{im}][1,4\text{-bdc}]$ in $[\text{bmim}][\text{BF}_4]$ at room temperature; **g)** gel of $[p\text{-C}_{12}\text{im}]_3[\text{Trim}]_2$ in $[\text{bmim}][\text{BF}_4]$ at room temperature; **h)** gel of $[m\text{-C}_{12}\text{im}]_3[\text{Trim}]_2$ in $[\text{bmim}][\text{BF}_4]$ at room temperature after first heating and cooling of the sample; **i)** gel of $[p\text{-C}_{12}\text{im}]_3[\text{Cit}]_2$ in $[\text{bmim}][\text{BF}_4]$ at room temperature; **l)** gel of $[p\text{-C}_{12}\text{im}]_2[\text{EDTA}]$ in $[\text{bmim}][\text{BF}_4]$ at 40°C after first heating and cooling of the sample; **m)** gel of $[m\text{-C}_{12}\text{im}]_2[\text{EDTA}]$ in $[\text{bmim}][\text{BF}_4]$ at room temperature.

From pictures above, it is clear that morphology changes in dependence of organic solvents, ILs and of course gelators.

For example, comparison between results collected for $[p\text{-C}_{12}\text{im}]_2[\text{EDTA}]$ as a function of solvent shows that morphology significantly changed from a thick network in glycerol to a spherulitic one in octanol, where big spherulites are formed by a fibrous structure (Figures 14a-b). On the other hand, solvent and gelator anion being the same (glycerol and [EDTA]), change in the isomeric substitution on going from *para*- to *meta*-salt, induced the obtainment of a clearly tangled fibrous system (Figures 14 c).

In general, ionogels seems to assume three distinct morphologies: *i*) thick texture, *ii*) spherulitic network, *iii*) reticular texture. The occurrence of one or the other morphology seems to be mainly determined by the nature of gelator anion rather than the isomeric substitution on the cation. Indeed, differently from organogels, in most of cases morphology did not change on going from *meta*- to *para*-salt for the same anion (Figures 14g-h, Figures 14l-m).

Whereas, IL nature really influenced ionogels architectures, as detected in ionogels formed by $[p\text{-C}_{12}\text{im}]_3[\text{Cit}]_2$ in all five ILs. Data collected seem to indicate that the higher symmetry of IL anion gave rise to a structural ordering of the gel network. Indeed, change from tetrahedral $[\text{BF}_4]$ (Figure 14i) to octahedral $[\text{PF}_6]$ (Figure 14d) and $[\text{SbF}_6]$ anions gradually modified the morphology from a reticular to thick texture characterized by the presence of spherulitic domains. It is worth of noting that this principle governed also the thermal stability of ionogels, as already stated (T_{gel} reported in Table 9). So, probably the higher thermal stability could be a consequence of the higher ordering in ionogel architectures induced by the anion of the solvent.

Nevertheless, also the resulting morphology of ionogels is comprehensive of several factors. Indeed, considering the same IL ($[\text{bmim}][\text{BF}_4]$), reticular networks were detected for $[p\text{-C}_{12}\text{im}][1,4\text{-bdc}]$ and $[p\text{-C}_{12}\text{im}]_3[\text{Cit}]_2$ (Figures 14f-i), whereas spherulitic domains could be observed in all the other cases ($[2,6\text{-ndc}]$, $[\text{Trim}]$ and $[\text{EDTA}]$ -based salts, Figure 14g-l for the last two).

2. 5. Mechanical properties

Mechanical properties of both organo- and ionogels were investigated using rheology measurements. In all cases, measurements were performed at 5% (w/w) of gelator, at room temperature, using a frequency of 1Hz and varying the strain from 0.02% to 0.5% (values were chosen after determining the linear visco-elastic region of the gel). In all cases we detected a non-linear trend for the strain sweep. Indeed, storage modulus (G') was higher than loss modulus (G'') at low values of strain, indicating a solid-like behaviour, whereas with the increase in strain the trend was inverted and $G' < G''$ accounting for a liquid like behaviour. Furthermore, G' was always higher than G'' in the frequency sweep performed at the suitable yield of strain (γ). All the above observations support the gel nature of samples tested.⁶⁰

From the above measurements it was also possible to have a measure of the strength of the gels thanks to the crossover point of yield strain (γ) and loss of tangent ($\tan \delta = G''/G'$). In particular, they represent the level of stress needed to detect the flow of material and strength of colloidal forces operating in the gel network. In general, the increase in gel strength induces a decrease in $\tan \delta$ and a corresponding increase in γ values, respectively.

Organogels. Rheological measurements were not carried out for gels formed by [*p*-C₁₂im]₂[EDTA] and [*m*-C₁₂im][1,4-bdc] in glycerol. Indeed, in these cases, gels had a low thermal stability and one of them was a soft material (see Table 7). Consequently, we were not able to determine the linear viscoelastic region by strain and frequency sweep. G' and G'' at a fixed strain, loss of tangent ($\tan \delta = G''/G'$) and cross over point of yield strain (γ) are reported in Table 10.

[60] a) C. Daniel, C. Dammer and J.-M. Guenet, *Polymer* **1994**, *35*, 4243-4246, b) A. Garai and A. K. Nandi, *J. Polym. Sci., Part B: Polym. Phys.* **2008**, *46*, 28-40.

Table 10: values of G' , G'' at $\gamma = 0.05\%$, $\tan \delta = G''/G'$ and of γ at $G'' > G'$ for organogels at 5% (w/w) and 25 °C; T_{gel} were also included for comparison reason. Error limits are based on average of three different aliquots of the same gel.

salts	Gel in glycerol			Gel in octanol
	[p-C₁₂im][1,4-bdc]	[p-C₁₂im][2,6-ndc]	[m-C₁₂im]₂[EDTA]	[p-C₁₂im]₂[EDTA]
G' (Pa)	16900±400	3340±330	5350±650	9940±640
G'' (Pa)	6630±130	1830±70	4150±460	1850±370
$\tan \delta$	0.39±0.01	0.55±0.02	0.77±0.01	0.18±0.06
γ at $G'' > G'$	4.8±0.2 %	0.2±0.1%	4.6±0.2 %	2.2±0.1%
T_{gel} (°C)	36.2	33.8	27.3	27.6

In all cases, $\tan \delta$ were lower than 1, indicating that a strong association among particles characterized the materials. In particular, the strongest gel seems to be **[p-C₁₂im]₂[EDTA]**/octanol ($\tan \delta = 0.18$) and among gels in glycerol is the one formed by **[p-C₁₂im][1,4-bdc]** ($\tan \delta = 0.39$). On the other hand, taking into account the cross over point that should depend on the relaxation time of the material, results are different. Indeed, even if **[p-C₁₂im][1,4-bdc]**/glycerol presents a high γ value in agreement with a low $\tan \delta$ and **[p-C₁₂im][2,6-ndc]**/glycerol a low γ with a corresponding high $\tan \delta$, for the other gels the trend is not confirmed. However, it may indicate that even if the gels present a good strength their relaxation time is fast and they need a low strain to flow. Finally, the two parameters allow detecting a drop in the gel strength with the increase in π -surface area of the anion gelator on going from **[p-C₁₂im][1,4-bdc]** to **[p-C₁₂im][2,6-ndc]**. Taking into account that a further evaluation of gel strength can also derive from determination of T_{gel} values, we searched for a correlation among rheological parameters and T_{gel} values collected at 5% (w/w) of gelator using the lead-ball method. Interestingly, thermal stability of organogels in glycerol solution decreases with the raise in $\tan \delta$ values.

Ionogels. In ionogels a contribution to gelation could derive also from viscosity of ILs, for this reason rheological properties of the most viscous IL used, *i.e.* [bmim][PF₆], were determined. The IL showed the classical behaviour of the liquids presenting really low G' and G'' , so the mechanical properties measured for ionogels are consistent of a combination of both components of the supramolecular gels.

Mechanical properties were also influenced by gelator and IL structure, so they can be understood as function of these two effects on gel phases. To study properties dependent on gelator nature, gel phases formed in [bmim][BF₄] and [bmim][PF₆] were investigated,

as most of the DOSs were able to harden the above ILs. On the other hand, to have information about the influence exerted by structural properties of ILs, we analysed gels formed by $[\rho\text{-C}_{12}\text{im}]_3[\text{Cit}]_2$ in all five ILs considered. Plots of strain and frequency sweep for ionogels formed by both $[\rho\text{-C}_{12}\text{im}]_2[\text{EDTA}]$ and $[\text{m-C}_{12}\text{im}]_2[\text{EDTA}]$ in $[\text{bmim}][\text{PF}_6]$ are displayed in Figure 15, as example of typical rheological graphs. They allowed determining, firstly, the linear viscoelastic region of the gels and, subsequently, the strength parameters discussed.

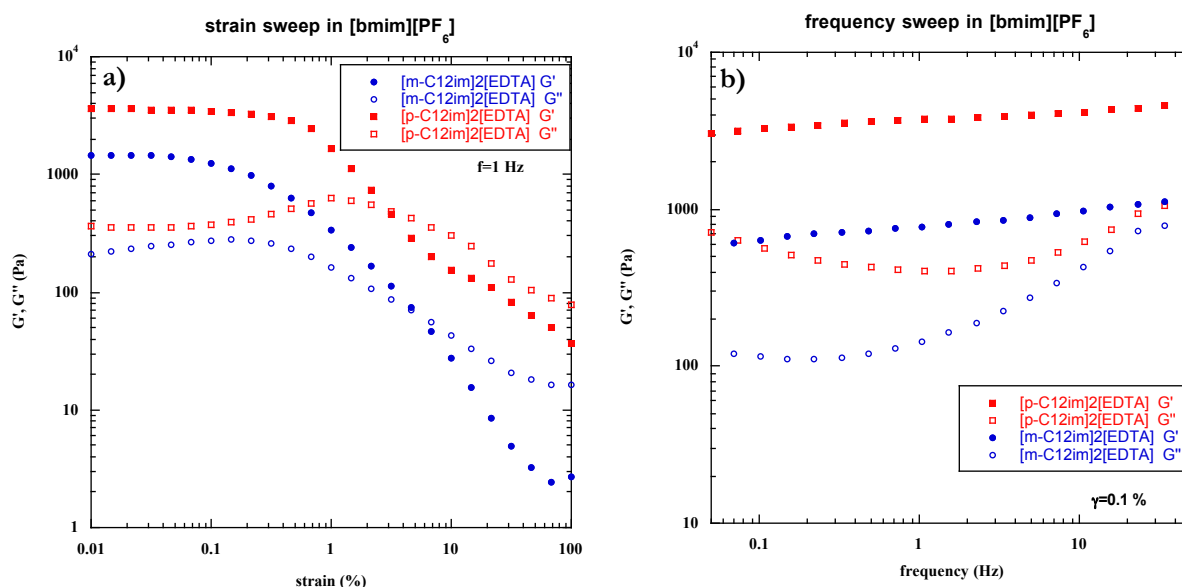


Figure 15: plots of **a)** strain sweep and **b)** frequency sweep performed using ionogels obtained in $[\text{bmim}][\text{PF}_6]$ at 5% (w/w) and 25 °C.

Strength parameters are reported as a function of gelator for ionogels formed in $[\text{bmim}][\text{BF}_4]$ and $[\text{bmim}][\text{PF}_6]$ in Table 11.

Table 11: G' , G'' at $\gamma = 0.05\%$, $\tan \delta = G''/G'$ and values of γ at $G'' > G'$ for ionogels formed in [bmim][BF₄] and [bmim][PF₆] at 5% (w/w) and 25 °C. Error limits are based on average of three different aliquots of the same gel.

salts	Gel in [bmim][BF ₄]			
	G' (Pa)	G'' (Pa)	$\tan \delta$	γ at $G'' > G'$
[<i>p</i> -C ₁₂ im][1,4-bdc]	4340±220	590±80	0.14±0.01	3.2±0.6 %
[<i>p</i> -C ₁₂ im][2,6-ndc]	2200±800	300±100	0.13±0.02	36±5 %
[<i>p</i> -C ₁₂ im] ₃ [Trim] ₂	840±50	120±10	0.14±0.01	21±2 %
[<i>p</i> -C ₁₂ im] ₃ [Cit] ₂	303±14	55±15	0.18±0.06	7.4±1.2 %
[<i>p</i> -C ₁₂ im] ₂ [EDTA]	1500±700	260±70	0.16±0.01	32±9 %
[<i>m</i> -C ₁₂ im][1,4-bdc]	20200±4700	4400±700	0.22±0.02	6.9±1.4 %
[<i>m</i> -C ₁₂ im][2,6-ndc]	19800±7500	5800±800	0.29±0.03	15±3 %
[<i>m</i> -C ₁₂ im] ₃ [Trim] ₂	28000±4600	4980±550	0.180±0.001	0.5±0.3 %
[<i>m</i> -C ₁₂ im] ₂ [EDTA]	3600±600	840±90	0.23±0.01	1.0±0.4 %
	Gel in [bmim][PF ₆]			
	G' (Pa)	G'' (Pa)	$\tan \delta$	γ at $G'' > G'$
[<i>p</i> -C ₁₂ im] ₃ [Trim] ₂	6630±870	850±120	0.13±0.02	6±1 %
[<i>p</i> -C ₁₂ im] ₃ [Cit] ₂	8400±900	1410±90	0.17±0.04	15±3 %
[<i>p</i> -C ₁₂ im] ₂ [EDTA]	3340±560	350±30	0.11±0.01	3.4±0.1 %
[<i>m</i> -C ₁₂ im] ₃ [Trim] ₂	3340±340	370±90	0.11±0.02	1.7±0.3 %
[<i>m</i> -C ₁₂ im] ₃ [Cit] ₂	1390±20	270±20	0.19±0.02	0.4±0.1%
[<i>m</i> -C ₁₂ im] ₂ [EDTA]	1400± 300	250±60	0.18±0.01	4.6±1.2%

Analysis of strength parameters of the above table clearly indicates that ionogels are stronger materials than organogels, indeed $\tan \delta$ is much lower -it ranged from 0.11 to 0.29- and the cross over yield strain is much higher with the maximum value at 35.9 %.

These results are in agreement on what previously observed for ionogels formed by crown-ether functionalised bisurea gelator.³⁰

Taking into account data collected for ionogels obtained in the same ILs, the strength of ionogels seems higher for gels formed by *para*-salts than for the one of *meta*-isomers. Indeed, even if small differences were detected as function of $\tan \delta$, values at crossover point clearly confirmed this trend. This is extremely evident, above all, for gels in [bmim][BF₄]; *para*-gelators in this IL solution probably possess longer relaxation times before flowing, consequently, higher stress should be applied to obtain the liquid phase. In addition, the increase in the aromatic character of the gelator, once again, positively influenced crossover point of yield strain in [bmim][BF₄]. Indeed, stronger gels were obtained on going from [1,4-bdc] to [2,6-ndc] and from [Cit] to [Trim], as gelator anions. In general, results collected about the effect of gelator structure on the gel strength seem

[30] Z. Qi, N. L. Traulsen, P. Malo de Molina, C. Schlaich, M. Gradzielski and C. A. Schalley, *Org. Biomol. Chem.* **2014**, *12*, 503-510.

to indicate that a higher rigidity and symmetry in both cation and anion structure of gelator induce the formation of stronger gels having also higher thermal stability. Indeed, similarly to what we have previously discussed about organogels, also for ionogels a certain correspondence between thermal stability, as accounted by DSC measurements (see Table 5) and rheological parameters can be detected with a raise in $\tan \delta$ values corresponding to a decrease in thermal stability.

On the other hand, the influence of IL on ionogels strength could be understood analysing data of Table 12, where rheological parameters of ionogels formed by [*p*-**C₁₂mim**]₃[**Cit**]₂ in five ILs are reported.

Table 12: G' , G'' at $\gamma = 0.05$ %, $\tan \delta = G''/G'$ and crossover point of γ for ionogels formed by [*p*-**C₁₂mim**]₃[**Cit**]₂ at 5% (w/w) and 25 °C as a function of IL. Error limits are based on average of three different aliquots of the same gel.

Ionic liquids	G' (Pa)	G'' (Pa)	$\tan \delta$	γ at $G'' > G'$
[bmim][PF ₆]	8400±900	1410±90	0.17±0.04	15±3 %
[bmim][NTf ₂]	3090±60	1610±10	0.52±0.01	0.5±0.3 %
[bmim][BF ₄]	303±14	55±15	0.18±0.06	7.4±1.2 %
[bmim][SbF ₆]	26400±14600	4000±1000	0.15±0.02	2.2±0.9 %
[bmpyrr][NTf ₂]	14100±900	3450±190	0.24±0.02	1.0±0.2 %

Taking into account the crossover point of γ , strength of ionogels decreased as function of the gelation solvent used in the following order: [bmim][PF₆] > [bmim][BF₄] > [bmim][SbF₆] > [bmpyrr][NTf₂] > [bmim][NTf₂]. This trend could be due to the different network flexibility of ionogels that was strongly affected also from the gelation solvent. Indeed, as discussed above, the increase of the anion symmetry of the IL gave rise to high ordered network of ionogels (spherulitic domains), which probably awarded higher strength to the material. In addition, considering solvent parameters of the ILs it is possible to assert that the mechanical strength is also affected by IL's viscosity. Trends of the two parameters are, in fact, in agreement, differently from polarity and hydrogen bond donor ability. Solvent parameters of ILs used as reference are reported in Table 13.^{48,61}

[48] L. Crowhurst, P. R. Mawdsley, J. M. Perez-Arlandis, P. A. Salter and T. Welton, *Phys. Chem. Chem. Phys.* **2003**, *5*, 2790-2794.

Table 13: solvent parameters of ionic liquids used.⁶¹

IL	E_T^N	$E_{T(30)}$	E_{NR}	π^*	α	β	η (cP)
[bmim][BF ₄]	0.670	52.5	217.2	1.047	0.627	0.376	233
[bmim][PF ₆]	0.669	52.3	218.5	1.032	0.634	0.207	450
[bmim][NTf ₂]	0.644	50.0	218.0	0.984	0.617	0.243	52
[bmim][SbF ₆]	0.673	52.5		1.039	0.639	0.146	108
[bmpyrr][NTf ₂]	0.544			0.954	0.427	0.252	85

Finally, comparison between data collected in [bmim][NTf₂] and [bmpyrr][NTf₂] evidences the positive effect on the mechanical properties of ionogels deriving from the aliphatic nature of IL used as solvent. Indeed, as accounted for by both $\tan \delta$ and γ values, the gel strength increases on going from [bmim][NTf₂] to [bmpyrr][NTf₂].

1. 6. Self-healing ability of gel phases

Thixotropy and sonotropy of gels obtained have been tested since it has been previously underlined the importance of self-repair ability of gels after disruption (par. 1. 6). Remembering also that these properties have been rarely analysed for ionogels.

As for ionogels formed by functionalised DOSs, they were qualitatively determined after external stimuli such as magnetic stirring and ultrasound irradiation. In addition, in some cases thixotropy has been analysed also using rheological measurements (all self-healing results are reported in Table 9). To this aim, samples, at 5 % (w/w) of gelator concentration, were subjected to initial conditions at which gel was stable ($\gamma = 0.05-0.1$ % and $f = 1$ Hz). Thereafter, strain was applied ($\gamma = 5-50$ % and $f = 1$ Hz) to induce the loss of gel properties (conditions were determined from the linear viscoelastic region of the gels). Graphs of G' and G'' after applying the strain for some ionogels are displayed in Figure 16. In general, at least two cycles on each sample were performed and when initial conditions were re-obtained, we measured G' higher than G'' values confirming the true nature of gel of our samples.

[61] a) A. J. Carmichael and K. R. Seddon, *J. Phys. Org. Chem.* **2000**, *13*, 591-595, b) J. G. Huddleston, A. E. Visser, W. M. Reichert, H. D. Willauer, G. A. Broker and R. D. Rogers, *Green Chem.* **2001**, *3*, 156-164, c) C. Reichardt, *ibid.* **2005**, *7*, 339-351.

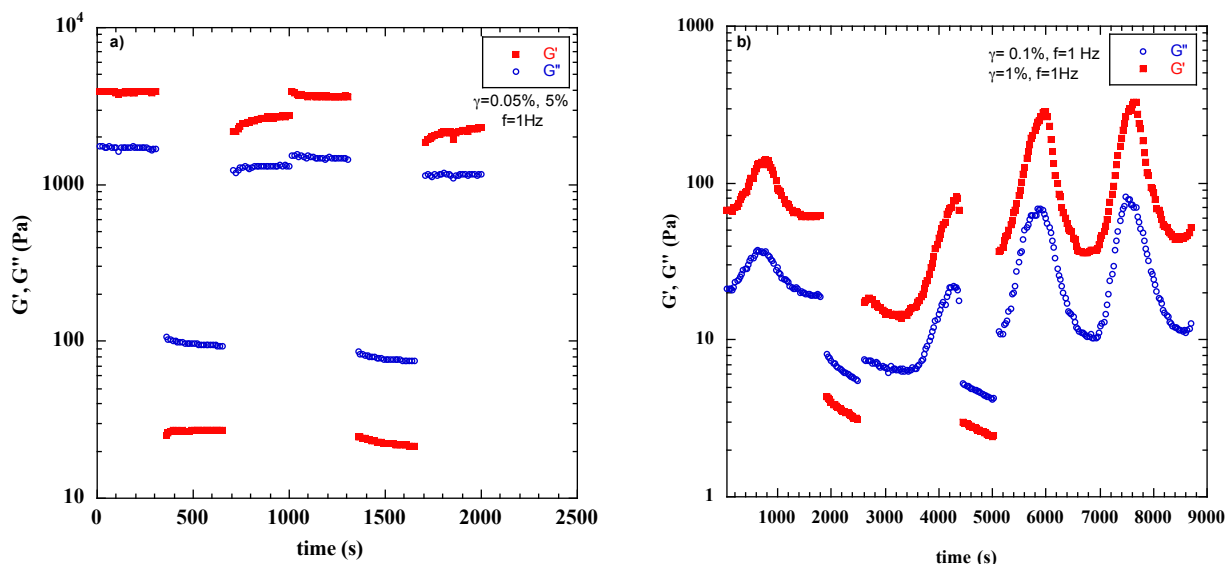


Figure 16: G' and G'' at 25 °C as a function of time and application of strain to a) $[p\text{-C}_{12}\text{im}]_3[\text{Cit}]_2/[\text{bmim}][\text{NTf}_2]$ and b) $[p\text{-C}_{12}\text{im}]_3[\text{Cit}]_2/[\text{bmim}][\text{BF}_4]$, both at 5 % (w/w) of gelator concentration.

Only in four cases a partial recovery of the original storage modulus of gels could be measured. Percentage of storage modulus recovery are indicated in Table 14 and they range from 15% ($[m\text{-C}_{12}\text{im}]_2[\text{EDTA}]/[\text{bmim}][\text{BF}_4]$) up to 73% ($[p\text{-C}_{12}\text{im}]_3[\text{Cit}]_3/[\text{bmim}][\text{NTf}_2]$).

In the other cases, after applying the initial conditions, an increase in G' values (labeled with G' increasing in Table 14) or the presence of peaks as a function of time (labeled with oscillations in Table 14 and an example is reported in Figure 16b) was observed. These behaviours did not allow determining the recovery of the initial values of rheological parameters, as they were not constant in time. The presence of oscillations in rheological studies was previously reported by Nandi *et al.*⁶² They ascribed the presence of peaks in the plateau region of rheological trace to a shear assisted re-aggregation process. According to this report, also in our case the occurrence of a similar event can be hypothesized. In fact, it could give rise to a different organization of the gel network. Similar considerations have been drawn taking into account also kinetic rheological investigation and opacity measurements (see later).

[62] B. Roy, P. Bairi, A. Saha and A. K. Nandi, *Soft Matter* **2011**, 7, 8067-8076.

Table 14: mechanical properties of ionogels at 5 % (w/w) determined by rheometer (Thixotropy R), ultrasound irradiation (Sonotropy) and magnetic stirring (Thixotropy MS).

<i>Gel</i>	Thixotropy R	Sonotropy	Thixotropy MS	$T_{gel} (^{\circ}\text{C})^g$
[<i>p</i> -C ₁₂ im][1,4-bdc]/[bmim][BF ₄]	Y (G' increasing) ^a	Y ^e	N	81.7
[<i>p</i> -C ₁₂ im][1,4-bdc]/[bmpyrr][NTf ₂]	Y (G' increasing)	S ^f	Y	39.2
[<i>p</i> -C ₁₂ im][2,6-ndc]/[bmim][BF ₄]	Y (oscillations) ^b	N	N	84.7
[<i>p</i> -C ₁₂ im] ₃ [Trim] ₂ /[bmim][PF ₆]	Y (25 %) ^c	S	Y	64.3
[<i>p</i> -C ₁₂ im] ₃ [Trim] ₂ /[bmim][BF ₄]	N ^d	S	N	85.1
[<i>p</i> -C ₁₂ im] ₃ [Cit] ₂ /[bmpyrr][NTf ₂]	N	S	N	49.1
[<i>p</i> -C ₁₂ im] ₃ [Cit] ₂ /[bmim][BF ₄]	Y (oscillations)	N	N	85.4
[<i>p</i> -C ₁₂ im] ₃ [Cit] ₂ /[bmim][PF ₆]	Y (oscillations)	S	Y	67.1
[<i>p</i> -C ₁₂ im] ₃ [Cit] ₂ /[bmim][NTf ₂]	Y (71 %)	S	Y	49.5
[<i>p</i> -C ₁₂ im] ₃ [Cit] ₂ /[bmim][SbF ₆]	Y (oscillations)	S	Y	50.3
[<i>p</i> -C ₁₂ im] ₂ [EDTA] / octanol	Y (64 %)	N	Y	ns ^h
[<i>p</i> -C ₁₂ im] ₂ [EDTA] / glycerol	-	N	Y	41.4
[<i>p</i> -C ₁₂ im] ₂ [EDTA] / [bmim][BF ₄]	N	N	N	49.0
[<i>p</i> -C ₁₂ im] ₂ [EDTA] / [bmim][PF ₆]	Y (31 %)	Y	Y	65.0
[<i>m</i> -C ₁₂ im][1,4-bdc]/[bmim][BF ₄]	Y (oscillations)	Y	Y	47.2
[<i>m</i> -C ₁₂ im][2,6-ndc]/[bmim][BF ₄]	Y (oscillations)	Y	Y	47.4
[<i>m</i> -C ₁₂ im] ₃ [Trim] ₂ /[bmim][BF ₄]	Y (oscillations)	Y	Y	50.6
[<i>m</i> -C ₁₂ im] ₃ [Trim] ₂ /[bmim][PF ₆]	Y (oscillations)	S	Y	62.0
[<i>m</i> -C ₁₂ im] ₃ [Cit] ₂ /[bmim][PF ₆]	Y (oscillations)	S	Y	62.4
[<i>m</i> -C ₁₂ im] ₂ [EDTA] / glycerol	Y	S	Y	29.3
[<i>m</i> -C ₁₂ im] ₂ [EDTA] / [bmim][BF ₄]	Y	S	Y	53.9
[<i>m</i> -C ₁₂ im] ₂ [EDTA] / [bmim][PF ₆]	Y (oscillations)	S	Y	ns

^aY (G' increasing) = yes; the gel phase was able to self-repair after the disruption but the storage modulus increased continuously as function of the time for a fixed strain; ^bY (oscillations) = yes; the gel phase was able to self-repair after the disruption but moduli, G' and G'' , oscillated as function of the time for a fixed strain; ^cY=yes (% recovery of storage modulus at the first cycle); ^dN = no; the gel phase was not able to self-repair after the action of external stimulus; ^eY = yes; the gel phase was able to self-repair after the action of external stimulus; ^fS = stable; the gel phase was stable to the action of external stimulus; ^g T_{gel} measured by DSC reported for comparison with self-healing properties of gels; ^hns = no signal at DSC thermogram.

Data obtained by rheological measurements are in agreement with the qualitative evaluation of thixotropy by magnetic stirring (at 1000 rpm for 5 minutes). Furthermore, with only few exceptions (6 cases out of 22), we observed gel formation afterwards materials were stored at 4 °C overnight. It is worth of mention that non thixotropic gels showed the highest thermal stability (see T_{gel} value in Table 14). This seems to indicate that more stable materials were less able to recover their properties after the action of magnetic stirring. It has been recently detected a similar behaviour studying self-healing ability of two component gels formed by some diimidazolium salts in the presence of aromatic guests.⁴¹ According to this report, we can suppose that the perturbing action of external stimuli is better counterbalanced if the gel has a less entangled network in which feebler interactions are operative.

[41] P. Vitale, F. D'Anna, S. Marullo and R. Noto, *ibid.* **2015**, *11*, 6652-6662.

Sonotropy was detected for five gels presenting aromatic anions in gelator structures, while in most cases (12 out of 22), gel phases resulted stable to ultrasound irradiation; this behaviour could be important for future applications of these gels as reaction media for ultrasound assisted processes. Finally, the complete loss of gel consistency induced by ultrasound irradiation was observed for gels of $[p\text{-C}_{12}\text{im}]_2[\text{EDTA}]$ in three solvents and for two *para*-gelators in $[\text{bmim}][\text{BF}_4]$. These behaviours could be due to the different networks of the gels awarded by gelators that are not able to rearrange after ultrasound irradiation.

2. 7. Kinetic formation of gel phases: rheology measurements

The variation of the mechanical properties of gels as function of time has been analysed to study the gel formation. In particular, at the beginning the instrument was set to 90 °C, temperature at which the liquid-like behaviour was detected; afterwards the temperature was gradually decreased to 25 °C. When this temperature was reached, we followed the kinetic formation of the gel.

The process has been studied at 5 % (w/w) of gelator, when the formation of gels occurred in reasonable times and within the linear viscoelastic region, using a low strain ($\leq 1\%$). Among organogels, only $[p\text{-C}_{12}\text{im}]_2[\text{EDTA}]/\text{octanol}$ could be analysed. Some typical kinetic traces are reported in Figure 17.

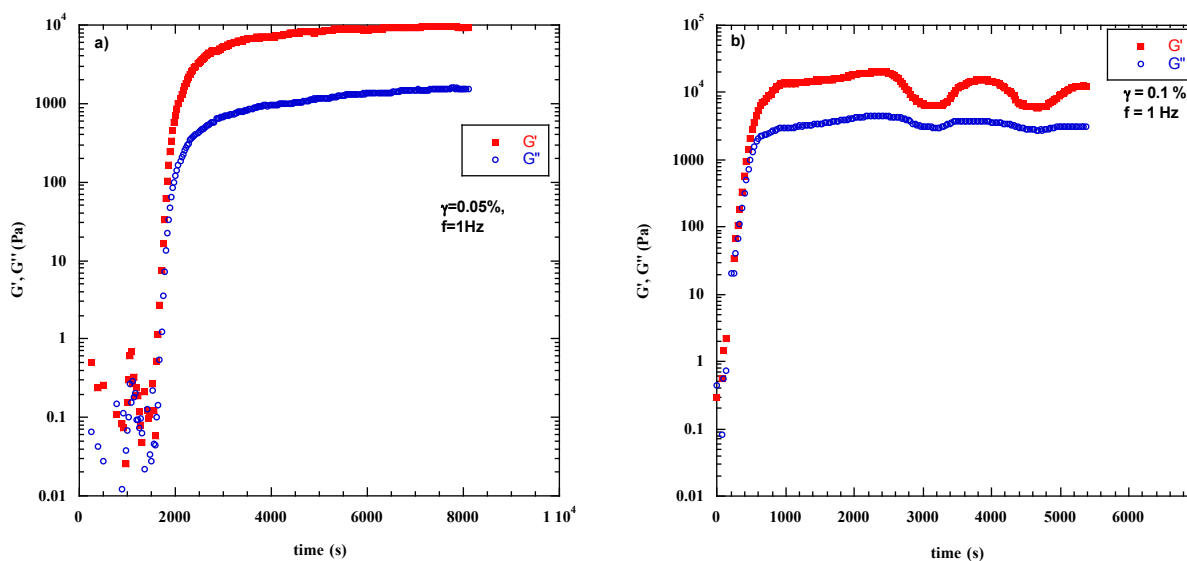


Figure 17: plots of G' and G'' as a function of time collected at 25 °C for gel phases: a) $[p\text{-C}_{12}\text{im}]_2[\text{EDTA}]/\text{octanol}$ and b) $[p\text{-C}_{12}\text{im}]_3[\text{Cit}]_2/[\text{bmim}][\text{PF}_6]$.

Most of kinetic traces presented an induction period, as already mentioned, that could be ascribed to the occurrence of elementary nucleation steps thereafter favouring network formation.⁴⁶ In some cases, the occurrence of an induction period was also detected performing RLS measurements to study gel phase formation (see later).

As for thixotropic measurements, also in this case, some ionogels presented oscillations in the plateau region (Figure 17b), probably ascribed to the shear assisted re-aggregation process; this behaviour was observed for most of ionogels obtained. Excluding these cases (in which a rheological parameter could not be determined at the equilibrium), for 6 gels it was possible to determine some kinetic constants applying the Avrami equation.⁶³ This equation was initially developed to describe the crystallization of polymer melts. However, it is frequently used in the log-log form (see eq. (1)) to study gelation processes:

$$\ln [-\ln(1-\Phi)] = [n (\ln k + \ln t)] \quad \text{eq. (1)}$$

where k is the rate constant, n is the so-called Avrami exponent that account for the type of growth leading to gel formation, t is the time and Φ is the volume fraction of gel and it is expressed as:

$$\Phi = (G(t) - G(0)) / (G(\infty) - G(0)) \quad \text{eq. (2)}$$

data obtained from the fit of eq. (1) are reported in Table 15.

Table 15: rate constant (k) expressed in (t^{-n}) and Avrami exponent (n) of gel formation, derived from Avrami equation (1) applied to rheology measurements.

Entry	Gel	$k(s^{-n})$	n
1	[<i>p</i> -C ₁₂ im] ₂ [EDTA] / octanol	0.70·10 ⁻³	1.89
2	[<i>p</i> -C ₁₂ im][1,4-bdc] / [bmpyrr][NTf ₂]	0.75·10 ⁻³	1.85
3	[<i>p</i> -C ₁₂ im][1,4-bdc] / [bmim][BF ₄]	1.13·10 ⁻³	2.02
4	[<i>p</i> -C ₁₂ im] ₃ [Trim] ₂ / [bmim][BF ₄]	0.89·10 ⁻³	1.59
5	[<i>p</i> -C ₁₂ im] ₃ [Cit] ₂ / [bmim][BF ₄]	1.98·10 ⁻³	2.09
6	[<i>p</i> -C ₁₂ im] ₃ [Cit] ₂ / [bmim][PF ₆]	1.95·10 ⁻³	3.00

Perusal of data reported in the Table indicates that, as anion of gelator is the same, the rate of gel phase formation increases on going from aliphatic to aromatic IL (see entries 2 and 3), but it is not affected by different nature of IL anion (see entries 5 and 6). On the other hand, IL being the same, formation of ionogel was faster in the presence of aliphatic anion in the gelator structure (see entries 4 and 5). Interestingly, comparison

[46] X. Huang, S. R. Raghavan, P. Terech and R. G. Weiss, *J. Am. Chem. Soc.* **2006**, *128*, 15341-15352.

[63] X. Y. Liu and P. D. Sawant, *Appl. Phys. Lett.* **2001**, *79*, 3518-3520.

between k and $\tan \delta$ values (Table 11) corresponding to the above ionogels reveals that a faster gel phase formation gives rise to less stable and strong gels.

With the only exception of $[p\text{-C}_{12}\text{im}]_3[\text{Cit}]_2/[\text{bmim}][\text{PF}_6]$ ionogel, Avrami exponent values forecast a rod-like or disk-like growth from sporadic or instantaneously nuclei and this perfectly agrees with morphologies detected using POM investigation (Figures 14f-g, i). In the above-mentioned case, Avrami exponent is equal to three and POM images (Figure 14d) accounts for a spherulitic growth.

2. 8. Kinetic formation of gel phases: RLS and UV-vis

Remembering the important information that RLS and UV-vis measurements can give about the gelation process (see par. 1. 5.), they were performed also in this case.

In order to compare results, in both cases, measurements were carried out at 5 % (w/w) of gelator, in all cases in which the rate of gelation process allowed obtaining soft materials at 25 °C. In Figure 18, some representative plots of I_{RLS} as a function of time are reported.

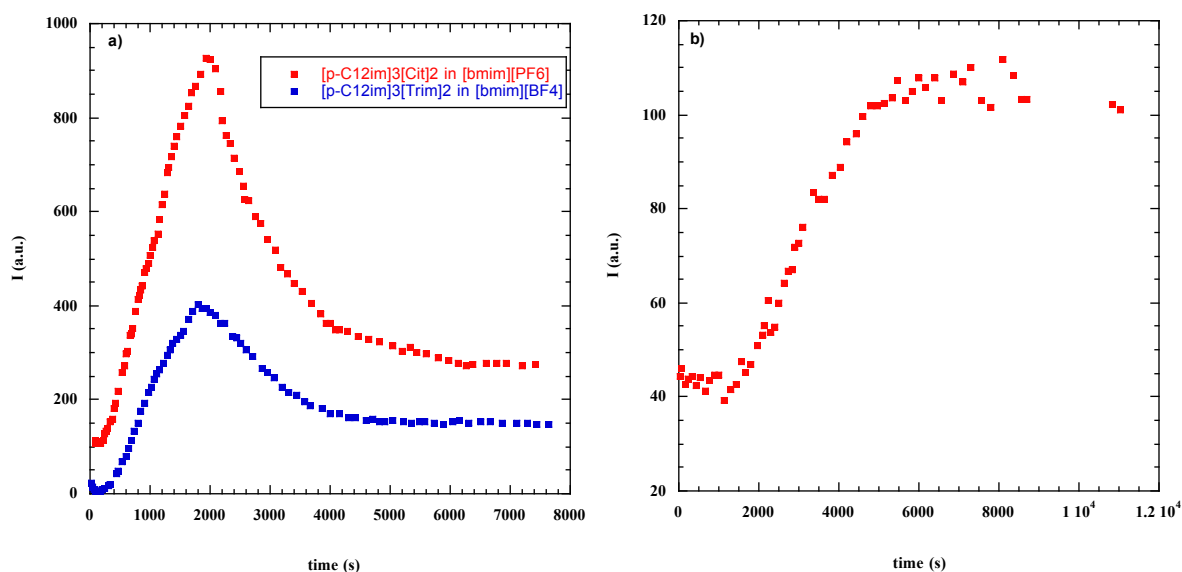


Figure 18: plots of I_{RLS} as a function of time collected at 25 °C and corresponding to a) $[p\text{-C}_{12}\text{im}]_3[\text{Cit}]_2/[\text{bmim}][\text{PF}_6]$, $[p\text{-C}_{12}\text{im}]_3[\text{Trim}]_2/[\text{bmim}][\text{BF}_4]$ and b) $[p\text{-C}_{12}\text{im}]_2[\text{EDTA}]/[\text{bmim}][\text{PF}_6]$ at 5% (w/w) of gelator.

As shown in Figure 18a, I_{RLS} values firstly increased as function of time to reach a maximum value (I_m) and after decreased until the equilibrium value (I_e), corresponding to gel phase formation. The drop of I_{RLS} should indicate the formation of intermediate aggregates that subsequently rearranged to form smaller and more stable ones present in

the gel network. This process could be seen as a two step mechanism and it was detected for ionogels by RLS and opacity measurements, with the exception of $[p\text{-C}_{12}\text{im}][1,4\text{-bdc}]/[\text{bmim}][\text{BF}_4]$, $[p\text{-C}_{12}\text{im}]_2[\text{EDTA}]/[\text{bmim}][\text{BF}_4]$, $[p\text{-C}_{12}\text{im}]_2[\text{EDTA}]/[\text{bmim}][\text{PF}_6]$ and $[p\text{-C}_{12}\text{im}]_3[\text{Cit}]_2/[\text{bmpyrr}][\text{NTf}_2]$. The occurrence of the above process, in addition to our previous observations (see par. 1. 5.), has been also recently detected for some tetrapeptides.⁶⁴

On the other hand, as shown in Figure 18b, some plots of I_{RLS} vs. time showed an induction period, in agreement with rheological kinetics. Comparison with data reported in literature allowed ascribing this induction period to elementary nucleation steps.⁴⁶

Before comparing results obtained, it is worth of mention that the process investigated was reversible, as shown in Figure 19. Indeed, after performing the kinetic of a model ionogel ($[p\text{-C}_{12}\text{im}]_3[\text{Cit}]_2/[\text{bmim}][\text{BF}_4]$) on the same sample for three-times, I_{RLS} value at equilibrium were constant irrespective of the cycle. This result, supported also by T_{gel}

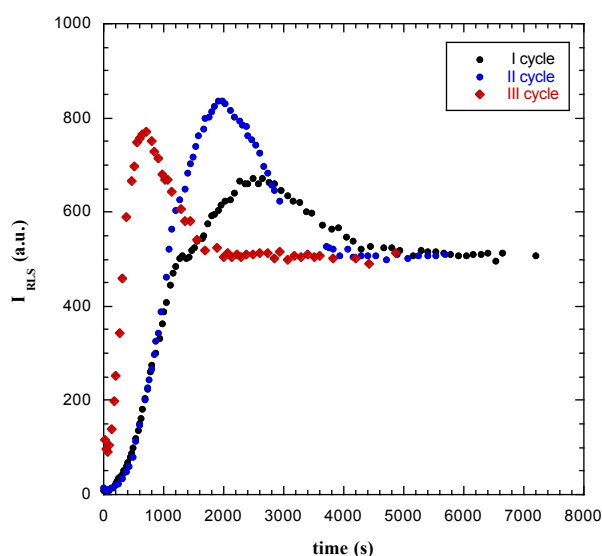


Figure 19: I_{RLS} plot of same ionogel repeated three times.

determination after each cycle (reproducible within experimental uncertainty, $T_{\text{gel}} = 49.5, 49.7$ and 47.9 °C for the first, second and third cycle, respectively) allowed hypothesizing the formation of comparable materials, even if, time corresponding to gel phase formation and the maximum of I_{RLS} gradually decreased on going from the first to the third cycle.

In order to understand effect of gelator and IL on gelation process, time and intensity of intermediate formation (t_m, I_m) and gelation (t_g, I_g) are reported in Table 16.

[64] M. Tena-Solsona, B. Escuder, J. F. Miravet, V. Castelleto, I. W. Hamley and A. Dehsorkhi, *Chem. Mater.* **2015**, *27*, 3358-3365.

[46] X. Huang, S. R. Raghavan, P. Terech and R. G. Weiss, *J. Am. Chem. Soc.* **2006**, *128*, 15341-15352.

Table 16: time and I_{RLS} intensity values^a corresponding to gelation processes.

Ionogel	^b t_n (s)	^b t_m (s)	^b I_m (a.u)	^b t_e (s)	^b I_e (a.u)
[<i>p</i> -C ₁₂ im][1,4-bdc]/[bmim][BF ₄]				644	344
[<i>p</i> -C ₁₂ im] ₃ [Trim] ₂ /[bmim][BF ₄]		1775	399	4070	155
[<i>p</i> -C ₁₂ im] ₃ [Cit] ₂ /[bmim][BF ₄]		2178	690	4530	523
[<i>p</i> -C ₁₂ im] ₃ [Cit] ₂ /[bmim][PF ₆]		1944	929	6185	275
[<i>p</i> -C ₁₂ im] ₃ [Cit] ₂ /[bmpyrr][NTf ₂]				1442	568
[<i>p</i> -C ₁₂ im] ₃ [Cit] ₂ /[bmim][SbF ₆]	2611	4618	360	7333	178
[<i>p</i> -C ₁₂ im] ₂ [EDTA] / [bmim][BF ₄]				1170	101
[<i>p</i> -C ₁₂ im] ₂ [EDTA] / [bmim][PF ₆]	1457			4921	105
[<i>m</i> -C ₁₂ im][1,4-bdc]/[bmim][BF ₄]	666	2557	497	4680	334

^aTime and intensity values were reproducible within 5%. ^b t_n = nucleation time; t_m = fibrillar intermediate formation time; I_m = fibrillar intermediate formation intensity; t_e = gel formation time; I_e = gel formation intensity.

Data collected for gels, in the same IL and presenting the same anion ([1,4-bdc] based salts), evidence that the different isomeric substitution on the cation was able to induce changes in gelation mechanism. Indeed, the gelation was faster for *para*-salts than for *meta*- ones ($t_e = 644$ and 4680 s for *para* and *meta*, respectively), in addition in the first case, it occurred in one step, while in the second case in a two steps mechanism.

The effect of the anion can be understood analysing data in [bmim][BF₄], which indicates how gelation time increases along the following order: [1,4-bdc] < [EDTA] < [Trim] < [Cit]. In particular, for trivalent anions, gel phase formation occurred faster in the presence of aromatic anion ([Trim]), but more extended aggregates were formed in the presence of the aliphatic anion ([Cit]). This latter result could also account for the different morphologies of gel phases obtained in these cases (Figures 14g and 14i).

On the other hand, IL nature did not affect gelation mechanism, as shown from two-step kinetics obtained for [*p*-C₁₂im]₃[Cit]₂ in all used imidazolium ILs. However, gelation time depends on IL anion cross-linking ability, increasing on going from [bmim][BF₄] to [bmim][SbF₆]. This result indicates that ionogel formation was favoured in a less reticulated solvent system, even if it caused a decrease in the size of gel's aggregates. This trend perfectly recalls considerations previously made about CGC values.

Differently from what observed in rheological and RLS measurements, kinetics performed by UV-vis did not show significant changes in the gels crystallinity considering effect of IL and gelator nature of ionogels. Indeed, similar maximum absorbance values (corresponding to the obtainment of gel phase) were detected for ionogels obtained in [bmim][BF₄] solution (Figure 20a). A slightly effect on crystallinity could derive only from

the different isomeric substitution on the cation of gelator, that decreased on going from $[p\text{-C}_{12}\text{im}][1,4\text{-bdc}]/[\text{bmim}][\text{BF}_4]$ to $[m\text{-C}_{12}\text{im}][1,4\text{-bdc}]/[\text{bmim}][\text{BF}_4]$ ionogels.

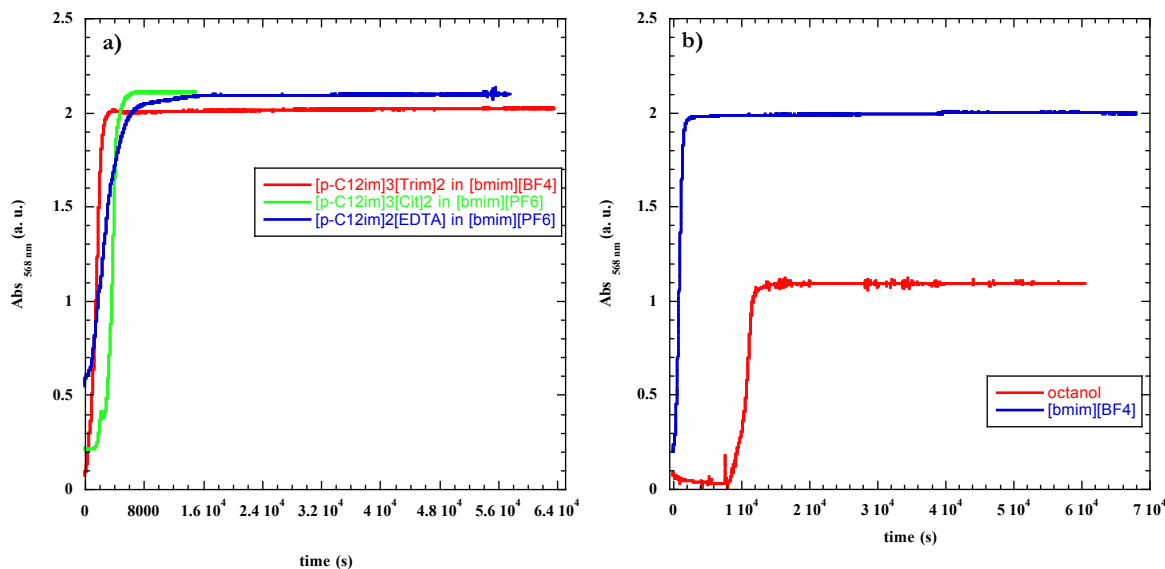


Figure 20: plot of absorbance values at 568 nm and at 25 °C as a function of time for a) $[p\text{-C}_{12}\text{im}]_3[\text{Trim}]_2/[\text{bmim}][\text{BF}_4]$, $[p\text{-C}_{12}\text{im}]_3[\text{Cit}]_2/[\text{bmim}][\text{PF}_6]$ and $[p\text{-C}_{12}\text{im}]_2[\text{EDTA}]/[\text{bmim}][\text{PF}_6]$ ionogels; b) $[p\text{-C}_{12}\text{im}]_2[\text{EDTA}]$ in octanol and $[\text{bmim}][\text{BF}_4]$.

On the other hand, ionogels presented a higher crystallinity than organogels (Figure 20b). Indeed, data collected show that Abs_{568 nm} values increase on going from octanol to IL for gels of $[p\text{-C}_{12}\text{im}]_2[\text{EDTA}]$.

2. 9. Powder X-ray diffraction (XRD)

Powder X-ray (PXRD) diffractograms of selected neat gelators and their 5 % (w/w) gels are compared in Figures 21. Ionogels formed in $[\text{bmim}][\text{PF}_6]$ by the gelator consisting of the *para* isomer of the cation and three different anions were investigated in order to gain insights into the influence of the anion on molecular packing within the self-assembled fibrillar networks (SAFINS). Also, the PXRD patterns for both $[p\text{-C}_{12}\text{im}]_2[\text{EDTA}]$ and $[m\text{-C}_{12}\text{im}]_2[\text{EDTA}]$ as neat solids and in $[\text{bmim}][\text{PF}_6]$ gels were compared to determine whether the neat solid and SAFIN morphs differ and the role of the cation of the gelator on molecular packing within the SAFINS. Finally, packing within SAFINS of gels with $[p\text{-C}_{12}\text{im}]_2[\text{EDTA}]$ as gelator and an IL ($[\text{bmim}][\text{PF}_6]$) or a ‘normal’ solvent (glycerol) were compared (Figure 21).

The 2θ values of the diffraction peaks demonstrate that molecular packing of $[p\text{-C}_{12}\text{im}]_2[\text{EDTA}]$ differs in its neat bulk solid, in its $[\text{bmim}][\text{PF}_6]$ ionogel and in its

glycerol organogel.⁶⁵ Also, the diffractograms of neat $[p\text{-C}_{12}\text{im}]_3[\text{Trim}]_2$, $[p\text{-C}_{12}\text{im}]_3[\text{Cit}]_2$, and $[m\text{-C}_{12}\text{im}]_2[\text{EDTA}]$ differ from those of their gels with $[\text{bmim}][\text{PF}_6]$ as the liquid. Thus, all the gelators investigated are polymorphic; the processes by which they aggregate and nucleate to form the 3D networks of their SAFINs depend acutely on the nature of the solvent-gelator interactions.

Although it was not possible to obtain diffraction quality single crystals of the gelators,^{65b} we were able to assign possible cell constants and lattice types in some cases by indexing the PXRD peaks for the gelators and their gels (Table 17).^{65a} At least 40 diffraction peaks were used to index each gelator, whereas 15-33 diffraction peaks were used for the gels. A few peaks with very low intensity could not be assigned; they may be from minor amounts of a different morph or trace impurities. Regardless, most of gelators and their gels pack in monoclinic lattices. As mentioned, the assigned unit cells for the gelators and those of the gels are different; the packing arrangements of the gelator molecules change significantly from the neat solid phase to their gel phases. Clearly, this observation constitutes a challenge to an even deeper understanding of how the SAFINs form from their sol phases, and points to an obvious direction for future investigations.

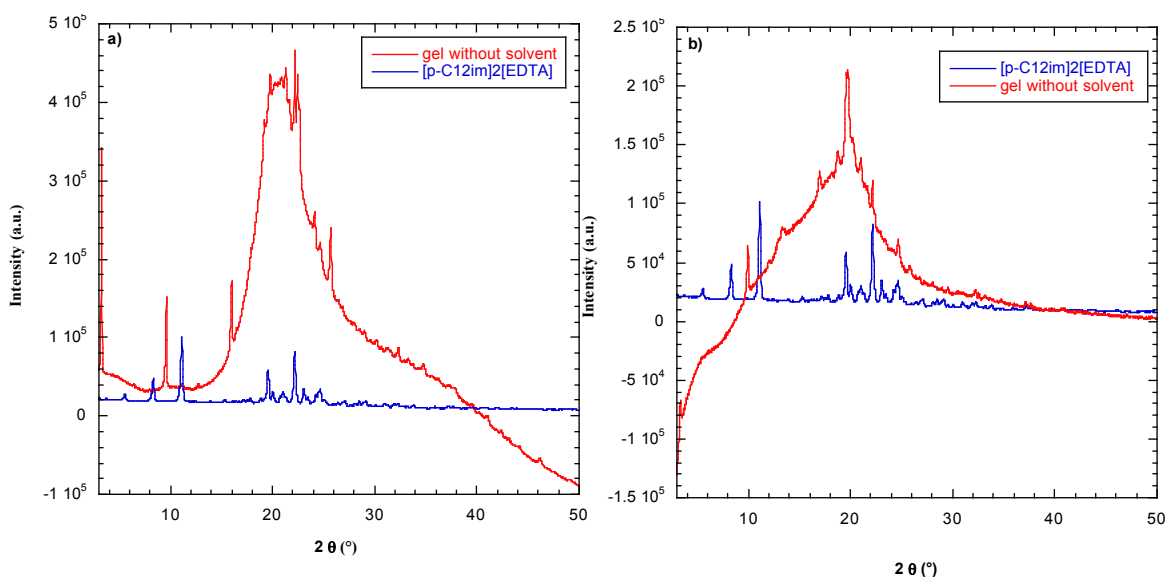


Figure 21: XRD diffractograms for neat gelator and gel: a) $[p\text{-C}_{12}\text{im}]_2[\text{EDTA}]/\text{glycerol}$ and b) $[p\text{-C}_{12}\text{im}]_2[\text{EDTA}]/[\text{bmim}][\text{PF}_6]$.

[65] a) E. Ostuni, P. Kamaras and R. G. Weiss, *Angew. Chem., Int. Ed. Engl.* **1996**, *35*, 1324-1326, b) M. Zhang, S. Selvakumar, X. Zhang, M. P. Sibi and R. G. Weiss, *Chem. Eur. J.* **2015**, *21*, 8530-8543.

Table 17: comparison of the proposed lattice types and unit cells of neat gelators and the SAFINs of their gels.

Sample		Total number of peaks /number of fitted peaks	Lattice type	Space group	Unit cell
Gelators ^a	[<i>m</i>-C₁₂im]₂[EDTA]	44/40	Monoclinic	Cc	$a = 86.9 \text{ \AA}, b = 28.9 \text{ \AA}, c = 15.5 \text{ \AA}, \alpha = 90^\circ, \beta = 123^\circ, \gamma = 90^\circ$
	[<i>p</i>-C₁₂im]₃[Cit]₂	48/45	Monoclinic	P2 ₁ /n	$a = 24.5 \text{ \AA}, b = 13.5 \text{ \AA}, c = 27.0 \text{ \AA}, \alpha = 90^\circ, \beta = 131.9^\circ, \gamma = 90^\circ$
	[<i>p</i>-C₁₂im]₃[Trim]₂	49/47	Monoclinic	P2 ₁ /n	$a = 24.5 \text{ \AA}, b = 13.5 \text{ \AA}, c = 27.0 \text{ \AA}, \alpha = 90^\circ, \beta = 131.9^\circ, \gamma = 90^\circ$
	[<i>p</i>-C₁₂im]₂[EDTA]	42/38	Monoclinic	C2/m	$a = 6.6 \text{ \AA}, b = 24.8 \text{ \AA}, c = 35.2 \text{ \AA}, \alpha = 90^\circ, \beta = 115^\circ, \gamma = 90^\circ$
Gels 5 % (w/w)	[<i>m</i>-C₁₂im]₂[EDTA] /[bmim][PF₆]	15/15	Monoclinic	P2/m	$a = 12.9 \text{ \AA}, b = 51.5 \text{ \AA}, c = 8.9 \text{ \AA}, \alpha = 90^\circ, \beta = 102^\circ, \gamma = 90^\circ$
	[<i>p</i>-C₁₂im]₃[Cit]₂ /[bmim][PF₆]	29/28	Monoclinic	P2/n	$a = 14.0 \text{ \AA}, b = 25.1 \text{ \AA}, c = 16.3 \text{ \AA}, \alpha = 90^\circ, \beta = 103^\circ, \gamma = 90^\circ$
	[<i>p</i>-C₁₂im]₃[Trim]₂ /[bmim][PF₆]	20/18	Monoclinic	C2/m	$a = 31.2 \text{ \AA}, b = 6.9 \text{ \AA}, c = 33.9 \text{ \AA}, \alpha = 90^\circ, \beta = 130^\circ, \gamma = 90^\circ$
	[<i>p</i>-C₁₂im]₂[EDTA] /[bmim][PF₆]	22/22	Orthorhombic	Pnnm	$a = 7.4 \text{ \AA}, b = 30.9 \text{ \AA}, c = 52.4 \text{ \AA}, \alpha = 90^\circ, \beta = 90^\circ, \gamma = 90^\circ$
	[<i>p</i>-C₁₂im]₂[EDTA] /glycerol	33/33	Monoclinic	Cc	$a = 5.7 \text{ \AA}, b = 25.1 \text{ \AA}, c = 64.9 \text{ \AA}, \alpha = 90^\circ, \beta = 124^\circ, \gamma = 90^\circ$

^[a] neat powders precipitated from diethyl ether.

All neat gelators show diffraction peaks that are consistent with (but not unique to) the presence of hydrogen bonding: $2\theta = 20.00^\circ$ (4.43 Å), 20.68° (4.29 Å), 20.14° (4.40 Å) and 20.92° (4.24 Å) for [*p*-C₁₂im]₂[EDTA], [*p*-C₁₂im]₃[Trim]₂, [*p*-C₁₂im]₃[Cit]₂ and [*m*-C₁₂im]₂[EDTA], respectively.⁶⁶ Also, a diffraction peak from [*p*-C₁₂im]₃[Cit]₂ at $2\theta = 25.08^\circ$ (3.63 Å) may be due to π - π stacking.^{3,67}

The diffractograms of the organo- and ionogels contain peaks that may be due to self-assembly through hydrogen bonding interactions as well. Previously reported DFT calculations on some diimidazolium salts¹⁸ indicate that the anions of the gelators may form bridges among diimidazolium cations.

As mentioned previously, the degree of additional stabilization of the gels by π - π interactions seems to depend on both the nature of the anion and the substitution pattern on the cation of the gelators. Indeed, irrespective of solvent nature, peaks at $2\theta = 25.70^\circ$ (3.46 Å) and 25.82° (3.54 Å) were observed for [*p*-C₁₂im]₂[EDTA] gels in both glycerol and [bmim][PF₆]. However, the gel of [*m*-C₁₂im]₂[EDTA] in [bmim][PF₆] lacks diffractions expected of π - π interactions and the gel of [*p*-C₁₂im]₃[Cit]₂ in

[66] S. Roy, A. Baral and A. Banerjee, *ibid.* **2013**, *19*, 14950-14957.

[3] M. George and R. G. Weiss, *Acc. Chem. Res.* **2006**, *39*, 489-497, [67] A. Ajayaghosh and V. K. Praveen, *ibid.* **2007**, *40*, 644-656.

[18] F. D'Anna, P. Vitale, F. Ferrante, S. Marullo and R. Noto, *ChemPlusChem* **2013**, *78*, 331-342.

[bmim][PF₆] exhibits diffraction peaks consistent with hydrogen bond formation only. Considering the non-aromatic nature of the [EDTA] anion, the occurrence of π - π interactions in [*p*-C₁₂im]₂[EDTA] must be ascribed to interactions among the cations. In general, the data indicate more facile bridging by [EDTA] than for the [Cit] anion. Also, DFT calculations¹⁶ suggest a higher propensity for π -stacking by [*p*-C₁₂im²⁺]. Finally, evidence for π - π interactions was also found in the diffraction peak of the [*p*-C₁₂im]₃[Trim]₂/[bmim][PF₆] ionogel at $2\theta = 25.83^\circ$ (3.53 Å), where both cation/cation and cation/anion interactions should be considered.

The use of these several techniques allowed having a deep insight on gel properties, like thermal stability, mechanical properties, self-healing ability and opacity. In particular, the wide range of gels obtained, especially in IL solutions, explained the strict relation among salts, solvent features and soft materials obtained. In particular, *meta*-salts were able to harden glycerol and ILs for the first time, probably thank to a positive effect exerted by a different stoichiometry between cation and anion. However, properties of gels formed by *para*-salts were in general better than the ones of materials formed by the corresponding *meta*-salts. In addition ionogels were stronger and more thermal stable than organogels, but the latter ones were obtained at lower CGC values. Interestingly, unexpected trends in kinetics of gel formation were observed and they probably indicate a rearrangement of the gel aggregate. The supramolecular interactions among gelator structures, that give rise to the gels, seem to be hydrogen bonds and π - π stacking.

3. Two-component hydrogels formed by cyclodextrins and DOSs⁶⁸

The gelling ability of some diimidazolium OSs has been tested also in water, but they resulted insoluble after cooling of the hot solution. So that, driven by this experimental observation and by the properties of two-component hydrogels, the gelling ability of some DOSs in presence of α -cyclodextrin (CD) has been investigated.¹⁷ Indeed, the low toxicity of such hydrogels should allow their application as soft materials in fields such as medicine, food, cosmetics, and the pharmaceutical industry.

[16] F. D'Anna, F. Ferrante and R. Noto, *Chem. Eur. J.* **2009**, *15*, 13059-13068.

[68] C. Rizzo, F. D'Anna, S. Marullo, P. Vitale and R. Noto, *Eur. J. Org. Chem.* **2014**, *2014*, 1013-1024.

[17] F. D'Anna, P. Vitale, S. Marullo and R. Noto, *Langmuir* **2012**, *28*, 10849-10859.

Furthermore, only a few cases of simple host-guest complexes with cyclodextrins, giving rise to gel-phase formation, have been studied.⁶⁹ In fact, these two-component gels are usually formed by the aggregation of complexes formed after the inclusion of polymers into the cyclodextrin cavity generating polyrotaxanes or polypseudorotaxanes.⁷⁰

Given that, to best of our knowledge the gel formation without functionalization of the cyclodextrin or addition of any polymer was obtained for the first time, using a highly efficient and versatile approach considering that the organic molecules can be structurally changed in a straightforward manner.¹⁷ For this reason, we were interested in studying the influence of structural modification of the organic salts on the formation of host-guest complexes with α - and β -cyclodextrin, varying also host-guest ratio. The dicationic imidazolium salts studied varied for length of alkyl chain and anions: 3,3'-di-*N*-decyl- ($[p\text{-C}_{10}\text{im}][\text{Br}]_2$) and 3,3'-di-*N*-dodecyl-1,1-(1,4-phenylenedimethylene) diimidazolium ($[p\text{-C}_{12}\text{im}][\text{Br}]_2$) dibromide, and 3,3'-di-*N*-dodecyl-1,1-(1,4-phenylenedimethylene)diimidazolium ditetrafluoroborate ($[p\text{-C}_{10}\text{im}][\text{BF}_4]_2$) and dihexafluorophosphate ($[p\text{-C}_{10}\text{im}][\text{PF}_6]_2$) and are shown in Figure 22.

We analysed in detail the formation of the host-guest complex and the properties of the two-component hydrogels, comparing the results also with those obtained in a previous work.¹⁷

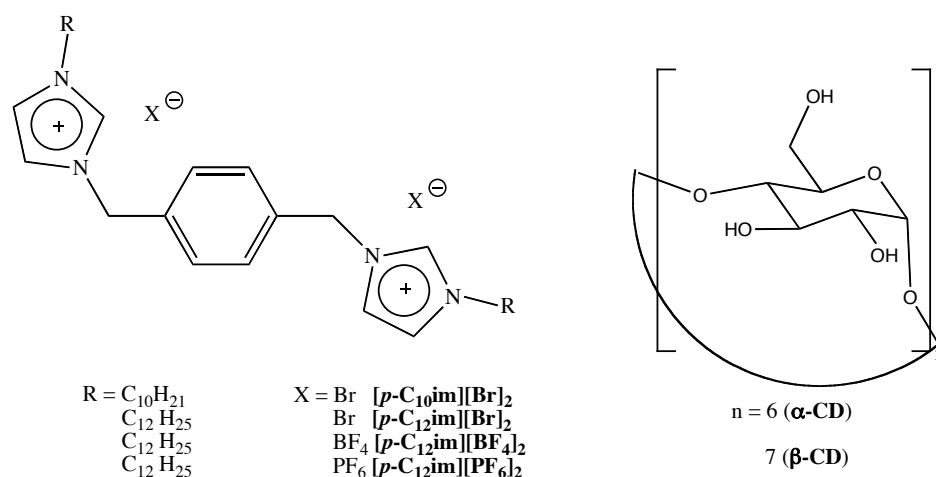


Figure 22: dicationic imidazolium salts and cyclodextrins used to form hydrogels.

[69] a) D. Rizkov, S. Mizrahi, J. Gun, R. Hoffman, A. Melman and O. Lev, *ibid.* **2008**, *24*, 11902-11910, b) Y. Suzuki, T. Taira and K. Osakada, *J. Mater. Chem.* **2011**, *21*, 930-938, c) T. Taira, Y. Suzuki and K. Osakada, *Chem. Eur. J.* **2010**, *16*, 6518-6529, d) L. Zhu, X. Ma, F. Ji, Q. Wang and H. Tian, *ibid.* **2007**, *13*, 9216-9222.

[70] a) E. Larrañeta and J. R. Isasi, *Langmuir* **2012**, *28*, 12457-12462, b) K. L. Liu, Z. Zhang and J. Li, *Soft Matter* **2011**, *7*, 11290-11297.

[17] F. D'Anna, P. Vitale, S. Marullo and R. Noto, *Langmuir* **2012**, *28*, 10849-10859.

3. 1. Gelation tests

Hydrogels formation was observed only upon addition of CD and gave rise to thermoreversible opaque gels (Figure 23).

In fact, we further confirmed that diimidazolium salts alone and native CDs do not undergo gelation in water. The results of gelation tests, as function of the different salts and CD/salt ratio, and T_{gel} , determined by lead-ball method, are reported in Table 18. For a useful comparison, data previously collected for $[p-C_{10im}][Br]_2$ and $[p-C_{12im}][Br]_2$ in the presence of α -CD are also shown.



Figure 23: opaque gel formed by $[p-C_{10im}][Br]_2$ (5%, w/w) in the presence of two equivalents of β -CD.

Table 18: critical gelation concentrations (CGC) at 25 °C and T_{gel} value (°C) at CGC, of gels formed by DOSs in presence of α -CD or β -CD in water.^a

Entry	Salt	CD/Salt ratio		Range ^b	CGC (%, w/w) ^c	T_{gel} (°C) ^d
1	$[p-C_{10im}][Br]_2$	1 (α -CD)	PG ^e	1.0-5.0		
2		2 (α -CD)	OG ^e	1.0-4.0	4.0	46.1
3		0.5 (β -CD)	P	1.0-5.0		
4		1 (β -CD)	OG	1.0-4.5	4.2	SM
5		2 (β -CD)	OG	1.0-4.5	4.2	33.3
6		3 (β -CD)	OG	1.0-5.0	2.0	SM
7		3.5 (β -CD)	I	1.0-5.0		
8	$[p-C_{12im}][Br]_2$	1 (α -CD)	OG ^e	1.0-4.0	3.7	37.0
9		2 (α -CD)	OG ^e	1.0-4.0	4.0	52.0
10		0.5 (β -CD)	P	1.0-5.0		
11		1 (β -CD)	OG	1.0-5.0	4.7	SM
12		2 (β -CD)	OG	1.0-5.0	4.4	SM
13		3 (β -CD)	OG	1.0-5.0	3.0	SM
14		3.5 (β -CD)	I	1.0-5.0		
15	$[p-C_{12im}][BF_4]_2$	2 (α -CD)	OG ^f	1.0-5.0	1.5	SM
16		3 (α -CD)	OG	0.5-1.0	1.0	SM
17		2 (β -CD)	I	0.5-2.0		
18	$[p-C_{12im}][PF_6]_2$	2 (α -CD)	OG ^g	0.05-3.0	2.6	SM ^g
19		3 (α -CD)	P	0.1-2.0		
20		4 (α -CD)	P	1.0-4.0		
21		2 (β -CD)	I	2.0-5.0		

^aPG=gel-like precipitate; P=precipitate; OG=opaque gel; I=insoluble; SM=soft material. ^bInvestigated salt percentage range. ^c%, w/w, salt/solvent. ^d T_{gel} values were reproducible within 1 °C. ^eSee ref. 17. ^fIn the hot solution, two components were only partially soluble. ^gIn the hot solution, two components were only partially soluble and T_{gel} of soft materials were not reproducible.

Analysis of data in the Table above clearly indicates that the ability to form hydrogels was heavily affected by the nature of the anion also in the presence of CD. Indeed, $[p-$

C_{12im}][Br]₂ was able to give hydrogels in the presence of either α - or β -CD, while, [**p-C_{12im}][BF₄]₂ and [**p-C_{12im}][PF₆]₂ induced the gelation only in the presence of α -CD, as they were insoluble in the presence of β -CD. In addition, the higher anion hydrophobicity of PF₆-based salt caused only a partial solubilisation of the salt in the presence of α -CD (2 equiv.). However, data obtained for this soft material were not reproducible, so they were not taken into account.****

In general, CGC slightly increased with increasing of alkyl chain length (see entries 4 and 11 or 5 and 12). Moreover, materials formed with β -CD were softer than those obtained with α -CD (see entries 2 and 9). In all the other cases, the gel phases obtained in the presence of β -CD and at the CGC were not measured, as gels were soft materials.

On the other hand, CGC decreased on going from [**p-C_{12im}][Br]₂ to [**p-C_{12im}][BF₄]₂ in the presence of α -CD, evidencing once again the positive role of the anion cross-linking ability.****

3. 2. Investigation on the role of CDs in hydrogel formation

In the gelation process, CDs might behave as simple additives, changing the solvent properties and favouring the self-assembly process, or they can form host-guest complexes with salts. In the latter case, the hydrogel formation could stem from pseudorotaxane formation and subsequent self-assembly. To discriminate between these hypotheses, we carried out polarimetric, spectrofluorimetric, and ¹H NMR spectroscopic investigations on the bromide salts.

Polarimetric measurements. The formation of host-guest complexes may be characterised by significant conformational changes of the CD that can be detected by means of polarimetric measurements.⁷¹ As this approach allowed demonstrating pseudorotaxane formation between [**p-C_{10im}][Br]₂ or [**p-C_{12im}][Br]₂ and α -CD, the same approach was carried out for the salts in β -CD water solution.¹⁷ Changes in molar optical rotation ($\Delta\theta$) of β -CD, as a function of the salt used at different β -CD/salt ratios, are reported in Table 19. It is worth of noting that the low solubility of [**p-C_{12im}][Br]₂ in water forced us to******

[71] a) P. Lo Meo, F. D'Anna, S. Riela, M. Gruttadauria and R. Noto, *Tetrahedron* **2009**, *65*, 2037-2042, b) W. Saenger, *Angew. Chem., Int. Ed. Engl.* **1980**, *19*, 344-362.

[17] F. D'Anna, P. Vitale, S. Marullo and R. Noto, *Langmuir* **2012**, *28*, 10849-10859.

carried out polarimetric measurements at low concentration, but even worse was the case $[p\text{-C}_{12}\text{im}][\text{BF}_4]_2$, which, due to its even lower solubility, did not allow obtaining reproducible measurements. Furthermore, we also performed polarimetric measurements with inorganic and organic bromides, such as sodium and tetrabutylammonium bromide, as the used guests are ionic species and changes in ionic strength of the solvent medium may affect the optical rotation values (θ).

Table 19: molar optical rotation (θ) and differential molar optical rotation ($\Delta\theta$) values collected at 25 °C in water solution.

$\beta\text{-CD/salt}$ ratio	$[\beta\text{-CD}]$ (M)	Salt	θ (deg dm ⁻¹ M ⁻¹) ^a	$\Delta\theta$ (deg dm ⁻¹ M ⁻¹)
	0.004		178.8	
1:1	0.004	$[p\text{-C}_{10}\text{im}][\text{Br}]_2$ (0.004 M)	172.8	-6.0
	0.004	NaBr (0.008 M)	182.5	3.7
	0.004	Bu ₄ NBr (0.008 M)	181.5	2.7
1.5:1	0.004	$[p\text{-C}_{10}\text{im}][\text{Br}]_2$ (0.003 M)	172.1	-6.8
	0.004	NaBr (0.005 M)	182.8	4.0
	0.004	Bu ₄ NBr (0.005 M)	181.4	2.6
2:1	0.004	$[p\text{-C}_{10}\text{im}][\text{Br}]_2$ (0.002 M)	171.5	-7.3
	0.004	NaBr (0.004 M)	181.0	2.2
	0.004	Bu ₄ NBr (0.004 M)	180.3	1.4
3:1	0.004	$[p\text{-C}_{10}\text{im}][\text{Br}]_2$ (0.0013 M)	171.2	-7.6
	0.004	NaBr (0.0026 M)	181.0	2.2
	0.004	Bu ₄ NBr (0.0026 M)	180.6	1.8
	0.001		180.3	
1:1	0.001	$[p\text{-C}_{12}\text{im}][\text{Br}]_2$ (0.001 M)	168.4	-11.9
	0.001	NaBr (0.002 M)	183.7	3.4
	0.001	Bu ₄ NBr (0.002 M)	177.8	2.5
1.5:1	0.001	$[p\text{-C}_{12}\text{im}][\text{Br}]_2$ (0.0007 M)	165.1	-15.2
	0.001	NaBr (0.00135 M)	174.7	5.6
	0.001	Bu ₄ NBr (0.0014 M)	176.7	3.6
2:1	0.001	$[p\text{-C}_{12}\text{im}][\text{Br}]_2$ (0.0005 M)	171.3	-9.0
	0.001	NaBr (0.001 M)	177.1	3.2
	0.001	Bu ₄ NBr (0.001 M)	182.2	1.9
3:1	0.001	$[p\text{-C}_{12}\text{im}][\text{Br}]_2$ (0.0003 M)	173.1	-8.1
	0.001	NaBr (0.0006 M)	178.6	1.4
	0.001	Bu ₄ NBr (0.0006 M)	187.2	2.4

^aMolar optical rotations were reproducible within ± 2.0 deg dm⁻¹M⁻¹.

First of all, it is clear from data in the table above that the addition of inorganic or organic salts different from DOSs did not affect the molar optical rotation of the $\beta\text{-CD}$ solution. Indeed, the effect of changes in ionic strength induced only a slight increase in θ value that frequently fell within the reproducibility range. On the other hand, in the case of diimidazolium salts, irrespective of the $\beta\text{-CD/salt}$ ratio, changes in $\Delta\theta$ values were more significant than those collected by using NaBr or [Bu₄N][Br]. Furthermore, in contrast to

the addition of NaBr or [Bu₄N][Br], the addition of DOSs caused a decrease in θ values. These results allowed hypothesising that the effect on the variation of θ should be due to the formation of a host-guest complex and a subsequent CD conformational change rather than to the different ionic strength of the media.

Interestingly, keeping the β -CD/salt ratio constant, more significant changes in $\Delta\theta$ values were detected for [*p*-C₁₂im][Br]₂, probably due to the higher hydrophobicity awarded from the longer alkyl chain length. In addition, the polarimetric effect of diimidazolium salts appears to be a function of the β -CD/salt ratio. In fact, in both cases, the $\Delta\theta$ values gave a non monotonic trend with the host-guest ratio. The highest change was detected at different stoichiometric ratio (3:1 and 1.5:1 for [*p*-C₁₀im][Br]₂ and [*p*-C₁₂im][Br]₂, respectively). The latter result could further support the hypothesis that the more hydrophobic salt [*p*-C₁₂im][Br]₂ has a more pronounced tendency to interact with the host cavity. Indeed, larger conformational changes and, consequently, stronger interactions should indicate an equilibrium displacement towards host-guest complex formation.

Fluorescence measurements. To determine the inclusion constant of the host-guest complexes, spectrofluorimetric measurements were carried out using a competitive method. Indeed, the imidazolium salts did not show significant changes in the UV/vis spectra after the inclusion in the β -CD cavity. In addition, their low solubilities did not allow studying the process by polarimetric measurements. Even if, the information gained from this investigation cannot be directly related to the gel phase, as a consequence of the different concentration ranges, it can give an insight on the interaction that occur between the two gelator components of the gel.

To carry out the spectrofluorimetric measurements, we used xanthone as fluorescent probe. For this guest, inclusion in the β -CD cavity induces a decrease in the fluorescence intensity.⁷² The thermodynamic stability constant, determined by the Benesi–Hildebrand method,⁷³ was very close to the one previously determined in buffer solution ($K = 1230 \text{ M}^{-1}$ in water solution determined by us, and $K = 1100 \text{ M}^{-1}$ in borate buffer at pH 9.0⁷⁴).

[72] M. Barra, C. Bohne and J. C. Scaiano, *J. Am. Chem. Soc.* **1990**, *112*, 8075-8079.

[73] H. A. Benesi and J. H. Hildebrand, *J. Am. Chem. Soc.* **1949**, *71*, 2703-2707.

[74] F. D'Anna, S. Riela, P. L. Meo and R. Noto, *Tetrahedron* **2004**, *60*, 5309-5314.

Nevertheless, the subsequent addition of DOSs caused a significant increase in the fluorescence intensity, probably indicating the gradual displacement of the fluorescent probe from the β -CD cavity to water solution. The emission spectra recorded at increasing concentrations of $[p\text{-C}_{10}\text{im}][\text{Br}]_2$ for binary systems β -CD/xanthone and fluorescence intensity at 395 nm as a function of the diimidazolium salt concentration are reported in Figure 24.

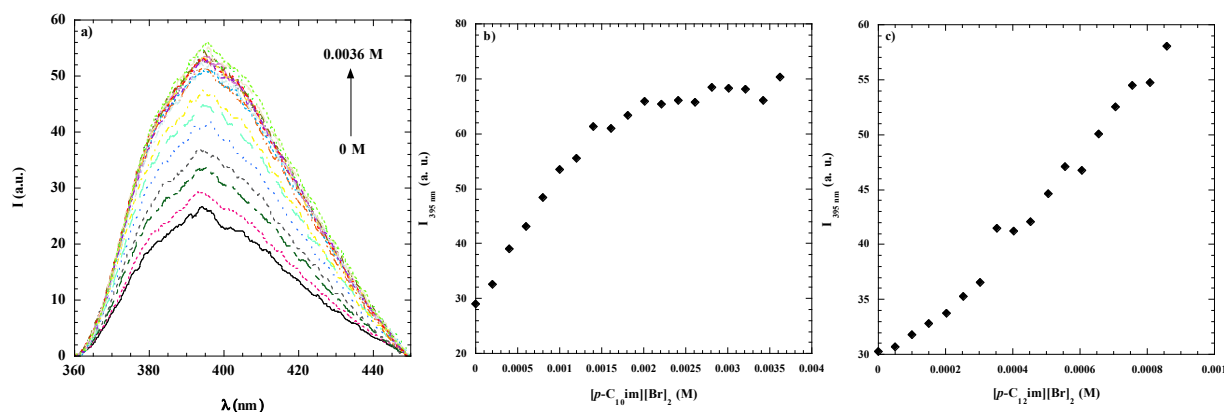
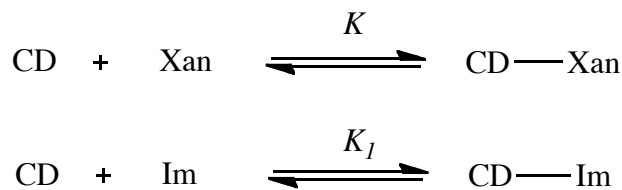


Figure 24: a) fluorescence spectra of the binary complex xanthone/ β -CD recorded at 25 °C in the presence of increasing concentration of $[p\text{-C}_{10}\text{im}][\text{Br}]_2$ ($[\text{Xan}] = 3 \cdot 10^{-6}$ M and $[\beta\text{-CD}] = 1.5 \cdot 10^{-3}$ M); b) trend of fluorescence intensity at 395 nm as a function of increasing concentration of $[p\text{-C}_{10}\text{im}][\text{Br}]_2$; c) trend of fluorescence intensity at 395 nm as a function of increasing concentration of $[p\text{-C}_{12}\text{im}][\text{Br}]_2$.

Fluorescence spectra of xanthone in the presence of increasing concentrations of $[\text{NaBr}]$ and $[\text{Bu}_4\text{N}][\text{Br}]$ were recorded, once again, to verify that fluorescence changes were not due to changes in the ionic strength. On the other hand, spectra of xanthone at increasing concentration of $[p\text{-C}_{10}\text{im}][\text{Br}]_2$ and $[p\text{-C}_{12}\text{im}][\text{Br}]_2$, without CD, were carried out to rule out the formation of a complex between the imidazolium ring of the salts and the electronically complementary phenyl ring of the xanthone. However, in all these cases, the fluorescence intensity remained constant.

So, having demonstrated the inclusion of DOSs into CD cavity, stability constants of the complexes were determined. However, it is noteworthy that, for $[p\text{-C}_{12}\text{im}][\text{Br}]_2$, a narrower concentration range of the dicationic salt was investigated. Indeed, as the concentration of $[p\text{-C}_{12}\text{im}][\text{Br}]_2$ was increased beyond 0.001 M, the measurement solutions became opalescent, probably as a consequence of precipitation of the complex.

The difference between the fluorescence intensity of xanthone in water and in the β -CD cavity was used to calculate the stability constant of complexes formed by diimidazolium salts and β -CD. We took into account the following two competitive equilibria in the measurement solutions:



where Xan, CD and Im represent the xanthone, β -CD and imidazolium salt concentration. It could be possible that, as a consequence of the presence of two imidazolium heads bearing long alkyl chains, salts might also form a 1:2 salt/ β -CD complex. However, under our experimental conditions ($[\beta\text{-CD}] = 0.0015 \text{ M}$, $[\textit{p}\text{-C}_{10}\text{im}][\text{Br}]_2 = 0\text{-}0.003 \text{ M}$ and $[\textit{p}\text{-C}_{12}\text{im}][\text{Br}]_2 = 0\text{-}0.0009 \text{ M}$) it could be conceivable that the formation of lower stoichiometry complexes is favoured.

Stability constants of the inclusion complexes, K_I , (Table 20) were calculated using previously reported methods.⁷⁵

Table 20: stability constants (K_I) corresponding to complexes formed by dicationic imidazolium salts $[\textit{p}\text{-C}_{10}\text{im}][\text{Br}]_2$ and $[\textit{p}\text{-C}_{12}\text{im}][\text{Br}]_2$ in presence of β -CD in water solution at 25 °C.

Salt	$K_I \text{ (M}^{-1}\text{)}$
$[\textit{p}\text{-C}_{10}\text{im}][\text{Br}]_2$	1240
$[\textit{p}\text{-C}_{12}\text{im}][\text{Br}]_2$	3020

^aStability constant values were reproducible within 10%.

A longer alkyl chain seems to increase the complex stability, result in agreement with previous reports on host-guest complex stability.⁷⁶ In addition, the higher stability of the complex formed by $[\textit{p}\text{-C}_{12}\text{im}][\text{Br}]_2$ could also explain the more significant changes in $\Delta\theta$ detected in the presence of this salt. Indeed, a tighter host-guest interaction should induce more significant conformational changes in the host. Clearly, if hydrogel formation follows host-guest complex formation, such as a pseudorotaxane, the differences discussed above should have significant repercussions on the properties of the soft materials obtained.

[75] a) S. Cui, J. Du, T. Wang and X. Hu, *Spectrochim. Acta, Part A* **2012**, *96*, 188-192, b) M. Megyesi, L. Biczók and I. Jablonkai, *J. Phys. Chem. C* **2008**, *112*, 3410-3416.

[76] M. V. Rekharsky and Y. Inoue, *Chem. Rev. (Washington, DC, U. S.)* **1998**, *98*, 1875-1918.

¹H-NMR measurements. NMR spectroscopic investigation can give information on the arrangement of salts in the CD cavity. The ¹H-NMR spectra for [p-C₁₀im][Br]₂, [p-C₁₂im][Br]₂ and [p-C₁₂im][BF₄]₂ were recorded at 25 °C both in water solution and with increasing concentration of CD (β-CD for the bromide salts and α-CD for the tetrafluoroborate one). It is worth noting that the low solubility of [p-C₁₂im][BF₄]₂ in water did not allow to record the spectrum. For this reason, it was not possible to hypothesise a geometry inclusion for this salt in α-CD. However, after α-CD addition, the measurement solutions became clearer, allowing spectra to be recorded. The above evidence points to a host-guest interaction between α-CD and the used salt.

On the other hand, for bromide salts, significant changes in the chemical shifts of signals corresponding to protons of the alkyl chain were detected upon β-CD addition. The Δδ values [Δδ = δ_{CD(3 equiv.)} - δ_{H₂O} or Δδ = δ_{CD(2 equiv.)} - δ_{H₂O}] for the bromide salts corresponding to protons of the alkyl chain, are reported in Figure 25.

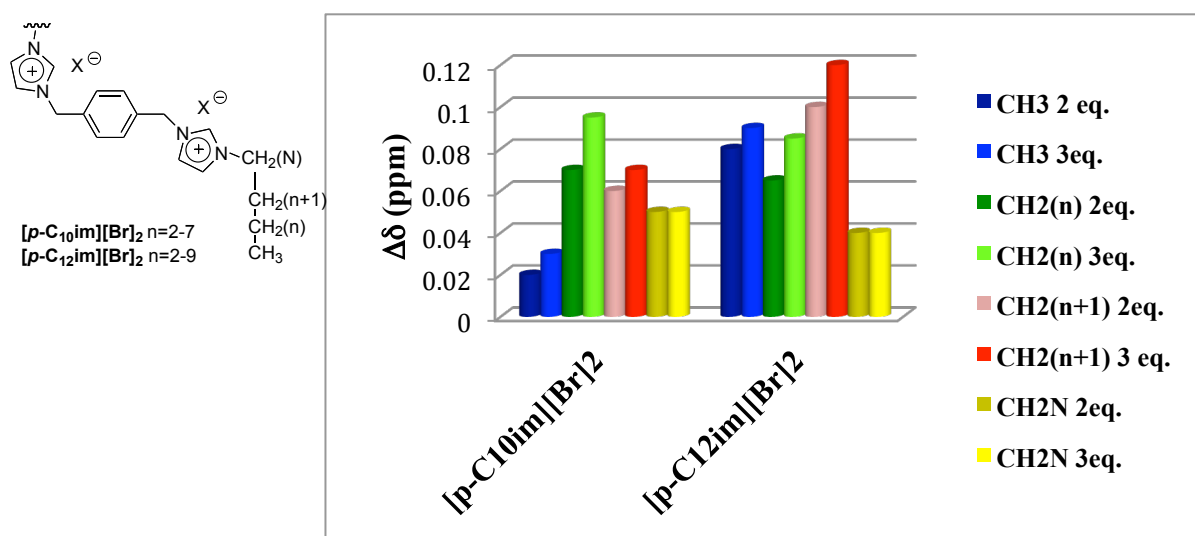


Figure 25: schematic representation of alkyl chain structure for the used salts and histogram of Δδ values as a function of alkyl chain protons.

In both cases, CD addition induced a downfield shift of the analysed signals. In general, the change of chemical shift signals increased on going from 2 to 3 equiv. of β-CD and it was slightly higher in the case of [p-C₁₂im][Br]₂. Furthermore, in this case, the β-CD cavity seems to include a larger portion of the alkyl chain, as revealed by the significant chemical shift variations detected for signals corresponding to CH₃ and CH₂₍₂₎-CH₂₍₁₁₎. These results are consistent with those previously reported for the inclusion of

imidazolium salts with long alkyl chains in CDs.⁷⁷ On the basis of these results, the formation of pseudorotaxanes between the organic salt and β -CD can be hypothesised. As a consequence of the hydrophobic interactions it is fair to suppose a partial tangle of the alkyl chain in water solution. Probably, the main role of the CD cavity, subsequent to the inclusion process, is to favour the elongation of the alkyl chain, allowing the formation of the tectons that are involved in the self-assembly process.

Considering all the above information and taking into account that host-guest complex formation might be a necessary condition for the gelation process, a study of the properties of the obtained soft materials was carried out.

3. 3. Thermal stability of hydrogels

The thermal stability of the obtained soft materials was studied, using the lead-ball method, as a function of the gelator concentration, keeping the β -CD/salt ratio constant. In particular, a β -CD/salt ratio of 2:1 was used for gels of bromide salts and a α -CD/salt ratio of 3:1 for gels of tetrafluoroborate salt. Unfortunately, keeping constant the salt concentration, it was not possible to obtain a reasonable trend of T_{gel} as function of CD concentration. Plots of T_{gel} as function of salt concentration are reported in Figure 26. For clarity, now on gel phases formed will be indicated as **10Br β** , **12Br β** and **12BF α** .

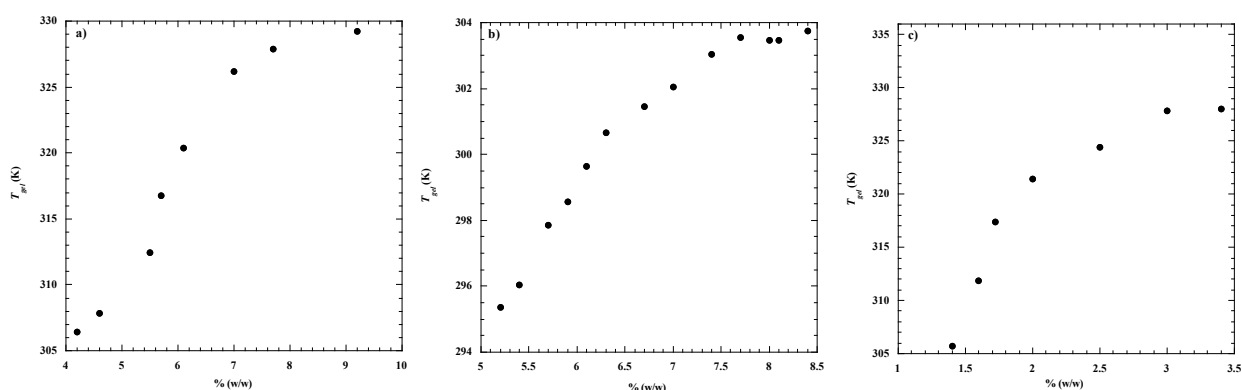


Figure 26: plots of T_{gel} as a function of salt concentration for gels of: a) β -CD/[*p*-C₁₀im][Br]₂ (2:1); b) β -CD/[*p*-C₁₂im][Br]₂ (2:1); c) α -CD/[*p*-C₁₂im][BF₄]₂ (3:1).

Figures above show how higher T_{gel} were detected for gels formed by [*p*-C₁₀im][Br]₂ than for those detected for gels of [*p*-C₁₂im][Br]₂. In addition, data can be investigated also

[77] a) Y. He, Q. Chen, C. Xu, J. Zhang and X. Shen, *J. Phys. Chem. B* **2009**, *113*, 231-238, b) D. Ondo, M. Tkadlecová, V. Dohnal, J. Rak, J. Kvičala, J. K. Lehmann, A. Heintz and N. Ignatiev, *ibid.* **2011**, *115*, 10285-10297.

evaluating the enthalpy variation of the melting process, ΔH_m , which was determined by using van't Hoff Equation (3) previously reported in literature:⁷⁸

$$\ln C = \text{const} + \Delta H_m / RT_m \quad (3)$$

in fact, this parameter can give some information about the thermodynamic stability of the gel and it was calculated from the plots of $\ln C$ (M) as a function of $1/T_{gel}$ (K). In Equation (3), C represents the molar gelator concentration, which, in our case, involves both diimidazolium salt and CD. However, because in each measurement sample the CD/salt ratio remained constant and this term can be validly represented by salt concentration (for example in the case of **10Br β** or **12Br β** , $C_{gelator} = C_{salt} + 2 C_{CD} = 3 C_{salt}$). Analysis of the results once more highlights the influence of the alkyl chain length on the calculated thermodynamic parameter. Indeed, ΔH_m increases with increasing alkyl chain length ($\Delta H_m = 6.0 \pm 0.6$ and 10.2 ± 0.8 kcal/mol for **10Br β** and **12Br β** , respectively). The increasing thermodynamic stability of the gels as function of the alkyl chain of the salt can be probably related also to the higher inclusion constant of the host-guest complex formed by the bromide salt with a longer alkyl chain. Indeed, a more stable complex could also affect the thermodynamic stability of the material obtained.

On the other hand, with the cation being the same, we detected a significant decrease in ΔH_m on going from **12Br β** to **12BF $_4\alpha$** system ($\Delta H_m = 8.0 \pm 0.6$ kcal/mol). Even if, the gels are not directly comparable as the CD is different, more stable gel phases were obtained in the latter case.

3. 4. Kinetic of formation of hydrogels

Kinetic investigations, performed by RLS and UV-vis measurements, revealed that the formation of the gels occurred after consecutive steps, including the nucleation, the formation of an intermediate and the final rearrangement of the aggregates in an equilibrium state (Figure 27).

Analysis of the gel formation was performed at 5 % (w/w) of bromide salt using 1, 2 and 3 equivalents of β -CD, while a concentration of 2 % (w/w) of salt and 3 equivalents of α -CD were used for gels of tetrafluoroborate salt.

[78] A. Takahashi, M. Sakai and T. Kato, *Polym J* **1980**, *12*, 335-341.

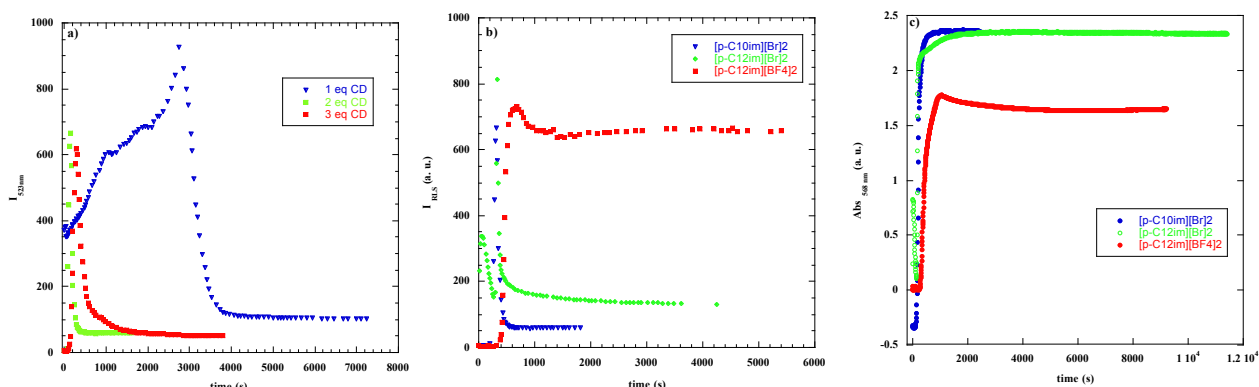


Figure 27: a) plot of I_{RLS} for **10Brβ** as function of time varying CD eq; b) plot of I_{RLS} for gels of the three different salts in presence of 2 eq. of β -CD and 3 of α -CD; c) plot of Abs at 568 nm for gels of the three different salts in presence of 2 eq. of β -CD and 3 of α -CD.

As shown in Figure 27a, the formation of intermediate aggregates and the gel phase occurred faster with increased β -CD concentration. Whereas, the size of the intermediate and gel-phase aggregates significantly decreased on going from a 1:1 to a 2:1 β -CD/salt ratio, but it remained constant when this ratio was further increased. The increase of β -CD concentration caused also an increase in the opacity of the gels.

The length of salt alkyl chain did not significantly affect both RLS and opacity measurement, even if **12Brβ** presented a faster kinetic and more extended aggregates; on the other hand, the different anion of the salt affected both (Figure 27b-c). In fact, for **12BF₄α**, the kinetic of formation followed again consecutive steps, but it gave rise to more extended aggregates on respect of gels formed by bromide salts, probably thanks to higher cross-linking ability of the anion salt. By the way, **12BF₄α** was less opaque than **10Brβ** and **12Brβ**.

Finally, gel formation is also influenced by the CD used, indeed comparison with the data previously collected for bromide salts in the presence of α -CD¹⁷ shows that an increase in the CD cavity size induced an increase in the gelation rate ($t_e = 8420$ and 540 s for **10Bra** and **10Brβ**, respectively) and the formation of less extended aggregates ($I_e = 450$ and 62 for **10Bra** and **10Brβ**, respectively).

[17] F. D’Anna, P. Vitale, S. Marullo and R. Noto, *Langmuir* **2012**, *28*, 10849-10859.

3. 5. Self-healing ability of hydrogels

The gel phases were also investigated for their ability to respond to external stimuli such as magnetic stirring and ultrasound irradiation. We analysed the gel phases **10Br β** and **12Br β** at 5% (w/w) of salts varying β -CD/salt ratios and **12BF $_4\alpha$** at 2% (w/w) of salt in presence of three equivalents of α -CD (Table 21).

Table 21: thixotropic and sonotropic behaviour of gels formed by the DOSs in the presence of increasing concentration of CDs.

Gel	CD (eq.)	% (w/w)	Sonotropy	Thixotropy
10Brβ	1	5.0	N	N
	1.5	5.0	N	N
	2	4.9	N	N
	3	5.7	S	N
12Brβ	1	5.0	Y	Y
	1.5	5.1	Y	Y
	2	4.9	Y	Y
	3	5.1	S	Y
12BF$_4\alpha$	3	2.0	S	Y

Y = gel phase was reformed after standing at 4 °C; N = gel phase was not reformed after standing at 4 °C; S = the gel phase was stable to the action of external stimulus.

Analysis of the above data showed that the gelators exhibited very different behaviours as a function of the different alkyl chain length. Indeed, none of the gel phases formed by **[*p*-C $_{10}$ im][Br] $_2$** were able to repair after the action of external stimuli, irrespective of the nature of the stimuli. It is noteworthy that these materials were also the most thermodynamically stable as in the case of ionogels and organogels formed by DOSs (see par. 2.6.). In contrast, the increase in alkyl chain length seems to play a positive role. Indeed, all gel phases formed by dodecylimidazolium-based salts showed thixotropic and sonotropic behaviour. It is noteworthy that **12Br β** (3 equiv.) and **12BF $_4\alpha$** (3 equiv.) were stable to the action of ultrasound irradiation.

3. 6. Morphology of hydrogels

SEM measurements allowed obtaining hydrogel morphology from xerogels formed by **10Br β** and **12Br β** at 5% (w/w) and **12BF $_4\alpha$** at 2% (w/w) (Figure 28). Even if, morphology might change on going from the xerogels to wet gels, however, generally, differences in xerogel morphologies parallel those occurring in wet gels.

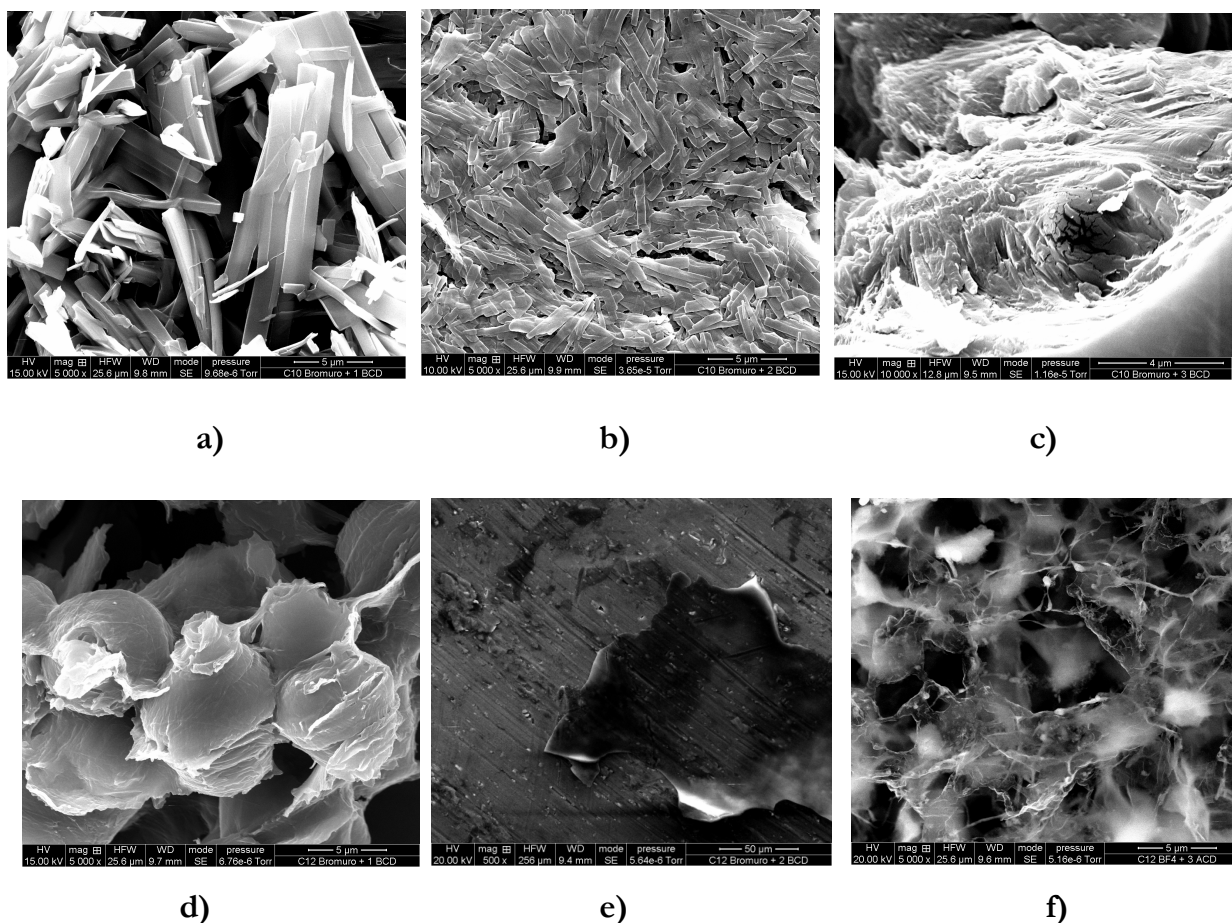


Figure 28: SEM images of xerogels prepared from a) **10Brβ** with 1 equiv. β -CD and $[p\text{-C}_{10}\text{im}][\text{Br}]_2$ (5%, w/w); b) **10Brβ** with 2 equiv. β -CD and $[p\text{-C}_{10}\text{im}][\text{Br}]_2$ (5%, w/w); c) **10Brβ** with 3 equiv. β -CD and $[p\text{-C}_{10}\text{im}][\text{Br}]_2$ (5%, w/w); d) **12Brβ** with 1 equiv. β -CD and $[p\text{-C}_{12}\text{im}][\text{Br}]_2$ (5%, w/w); e) **12Brβ** with 2 equiv. β -CD and $[p\text{-C}_{12}\text{im}][\text{Br}]_2$ (5%, w/w); f) **12BF₄α** with 3 equiv. α -CD and $[p\text{-C}_{12}\text{im}][\text{BF}_4]_2$ (2%, w/w).

First of all, it is important to underline that SEM images recorded from water solutions of the individual components evidence a different morphology with respect to one of xerogels. So, the morphology of the xerogels can be ascribed to the two-component system.

Morphologies of gel-phases, as well the other properties analysed until now, were significantly affected by both the CD/salt ratio and by the nature of the salt used. In fact, the increase in the CD/salt ratio for **10Brβ** (Figure 28, a–c) gave rise to thicker materials. A gradual change was detected on going from one to three equivalents of β -CD, aggregates varied from a fibrous (medium fibre width 1.14 μm) to lamellar (medium width 438 nm) up to a thicker morphology that did not allow identifying the constituents. While, in the case of **12Brβ**, further increases in the CD/salt ratio, did not give good

SEM images at 5000x magnification. However, at 500x magnification, this xerogel in the presence of two equivalents β -CD seems to display a lamellar morphology (Figure 28d-e). On the other hand, xerogel of **10Br β** gave rise to a fibrous structure, whereas the one of **12Br β** was characterised by the presence of spherical aggregates with a diameter in the range 8–8.5 μm (Figure 28a and 28d). Furthermore, analysis of SEM images collected from the xerogel formed by **12BF α** in the presence of 3 equiv. of α -CD shows that, in this case, the gel morphology looks like a “cob-web” in which more extended aggregates are distributed (Figure 28f).

Properties of two-component hydrogels analysed vary in relation of DOSs, CDs and their ratio. It has been demonstrated that a necessary condition allowing the self-assembly process is the formation of host-guest complexes, such as pseudorotaxanes. The supramolecular complexes organize to give fibrous aggregates that subsequently rearrange to form the typical three-dimensional network of the soft materials. This hypothesis perfectly agrees with the picture frequently reported in literature concerning the hierarchical organisation that allows gel-phase formation through a self-assembly process giving fibres prior to gel formation (Figure 29).^{1a}

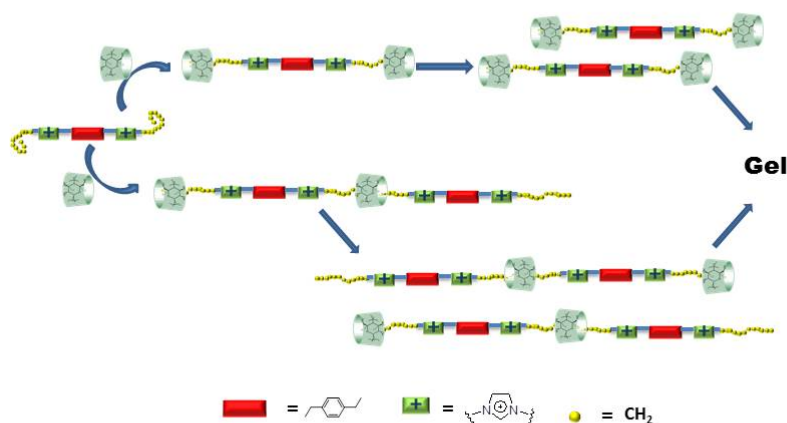


Figure 29: schematic representation of self-assembly process.

An innovative formation of two-component gels formed by CD not involving polymers as guest molecules and CD derivatisation have been performed. Indeed, data collected showed that LMWGs might also favour the gelation of native CDs, simply changing the features of soft materials by the introduction of minor structural changes, such as

[1] a) B. Escuder, F. Rodriguez-Llansola and J. F. Miravet, *New J. Chem.* **2010**, *34*, 1044-1054.

lengthening the alkyl chain of the cation or increasing the coordination ability of the anion.

4. DOSs and gels exerting antimicrobial activity

Gels formed in biocompatible solvents can be applied in biological and pharmaceutical fields. Many polymer gels have been used to this aim, even if, recently, the application of supramolecular gels in these fields is growing rapidly. For example, supramolecular gels based on a geminal imidazolium amphiphile have been used as molecular material for drug delivery of anti-inflammatory agents.¹⁹ While a supramolecular hydrogel, based on benzylidene sorbitol gelator, was able to extract acid functionalised anti-inflammatory drugs through directed interactions with the self-assembled gel nanofibres. In addition, upon simple mixing of the components, hydrogel-drug hybrid materials can be formed and they have also exhibited pH controlled drug release.⁷⁹ Furthermore, some organo- and ionogels nanocomposites have exhibited an antimicrobial activity,⁸⁰ tested on Gram-positive, Gram-negative bacterial strains and fungal strains on the basis of their involvement in skin infection and the possible topical application of the gels.

In this framework, we were interested in testing the gelling ability of some new diimidazolium salts and the antimicrobial activity of the salts and of the corresponding materials. DOSs presenting as cationic head the previously studied 3,3'-di-*N*-dodecyl-1,1-(1,4-phenylenedimethylene) diimidazolium [**p-C₁₂im**] and some aminoacid derivatives as anions have been synthesised. So that, we have combined a cation with a proved gelling ability and biocompatible anions such as L-isoleucinate [**L-Ile**], L-phenylalaninate [**L-Phe**] and a dipeptide derivative, D-alanyl-D-alaninate [**D-Ala-D-Ala**] (Figure 30). In particular, we were interested in studying also the gelling ability of salts presenting the protected aminoacids derivatives, such as 9-fluorenylmethoxycarbonyl-L-isoleucinate and 9-fluorenylmethoxycarbonyl-L-phenylalaninate, as it has been recently reported their combined action as antimicrobial agents and hydrogelators.⁸¹ However, the salts obtained,

[19] M. Rodrigues, A. C. Calpena, D. B. Amabilino, M. L. Garduno-Ramirez and L. Perez-Garcia, *J. Mater. Chem. B* **2014**, 2, 5419-5429.

[79] E. J. Howe, B. O. Okesola and D. K. Smith, *Chem. Commun.* **2015**, 51, 7451-7454.

[80] a) K. Pandurangan, J. A. Kitchen, S. Blasco, F. Paradisi and T. Gunnlaugsson, *ibid.* **2014**, 50, 10819-10822, b) A. Sharma, P. Prakash, K. Rawat, P. Solanki and H. B. Bohidar, *Appl. Biochem. Biotechnol.* **2015**, 177, 267-277.

[81] I. Irwansyah, Y.-Q. Li, W. Shi, D. Qi, W. R. Leow, M. B. Y. Tang, S. Li and X. Chen, *Adv. Mater.* **2015**, 27, 648-654.

resulted totally insoluble in all solvents tested. On the other hand, the choice of the dipeptide stands on its biological activity importance, as it represents the final part of the penta-peptide moiety, which is involved in the biosynthesis and maturation of prokaryotic cell walls. If opportunely modified, D-Ala-D-Ala also exhibited an antibacterial activity.⁸²

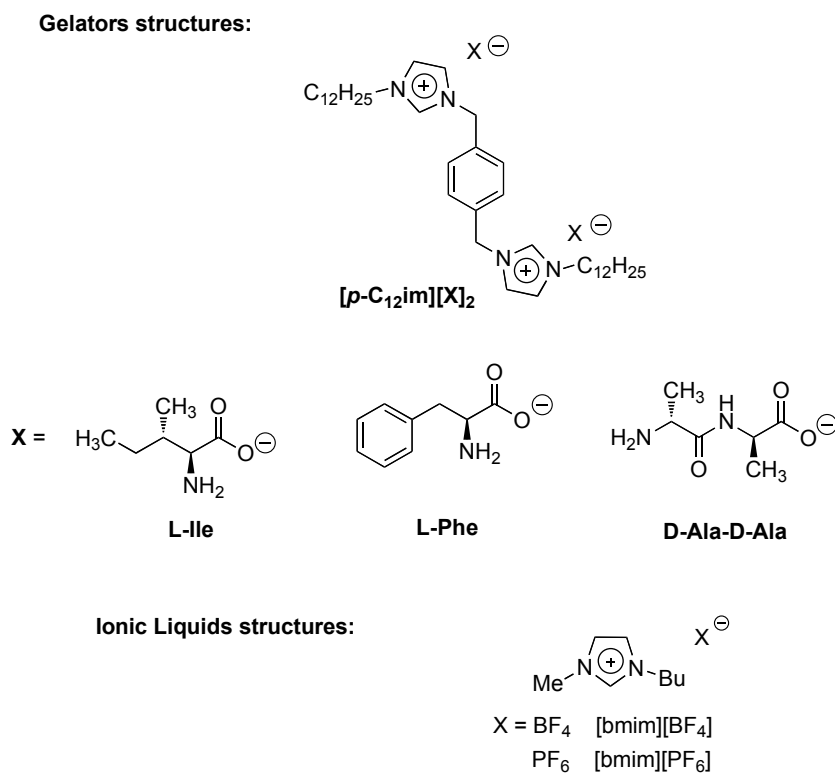


Figure 30: DOSs used as gelators and structure of ILs.

Salts have been synthesised through anion exchange protocol on resin of the corresponding dibromide diimidazolium salt. The gelling ability of these salts has been tested in biocompatible organic solvents, water, phosphate-buffered saline solution (PBS) and ILs, such as [bmim][BF₄] and [bmim][PF₆], that resulted biocompatible from previous studies.⁸³

[82] S. S. Azam, S. W. Abbasi, A. S. Akhtar and M. Mirza, *Med. Chem. Res.* **2014**, *23*, 4108-4137.

[83] a) H. Pfruender, R. Jones and D. Weuster-Botz, *J. Biotechnol.* **2006**, *124*, 182-190, b) F. Zhang, L.-H. Cheng, X.-H. Xu, L. Zhang and H.-L. Chen, *Process Biochem. (Amsterdam, Neth.)* **2011**, *46*, 1934-1941.

4. 1. Melting process of DOSs

Melting process of salts has been studied by DSC, in some cases more than one transition has been detected, probably due to the presence, also in this case, of polymorphs of the salts. All measurements were repeated twice to assure their reproducibility. Table 22 summarizes results obtained.

Table 22: melting temperature (T_m), enthalpy variation of melting process (ΔH_m) or glass transition temperature of melting process (T_g) and crystallization temperature (T_c), enthalpy variation of crystallization process (ΔH_c) of DOSs.

salts	T_m (°C)	ΔH_m (J/g)	T_g (°C)	T_c (°C)	ΔH_c (J/g)
[<i>p</i> -C ₁₂ im][L-Ile] ₂	73.2	4.9			
[<i>p</i> -C ₁₂ im][L-Phe] ₂			79.9		
[<i>p</i> -C ₁₂ im][D-Ala-D-Ala] ₂	41.5 ^b	23.0			
	105.3 ^a	1.3		88.2 ^c	0.8

^atemperature obtained from a second transition of the salts in the heating cycle; ^btransition not reproducible in the second heating cycle; ^ctemperature of crystallization reproducible for two cycles.

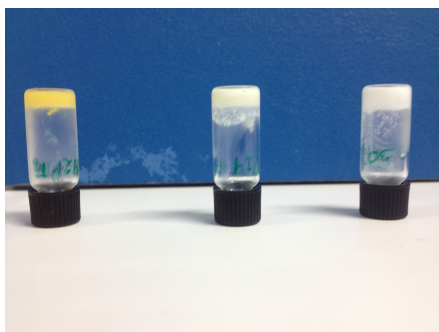
Melting temperature of the salts does not significantly vary in relation to the different anion used. However, the melting process was different, as in one case a glass transition instead of a melting temperature has been observed and in one case two transitions have been detected in the melting process. Considering the second melting temperature of [*p*-C₁₂im][D-Ala-D-Ala]₂, as the first one was not reproducible, the trend is the following one: [L-Ile] < [L-Phe] < [D-Ala-D-Ala].

The lowest melting temperature of the salts seems the one detected for the aliphatic aminoacid based salt. Indeed, the presence of aromatic rings in the anion awards to the salt a more packed structure, probably, as a consequence of the occurrence of cation-anion π -interactions, which requires higher energy to melt. The above hypothesis is well supported by T_g determined for the [L-Phe] derivative.

Finally, melting temperature increased on going from aminoacid to dipeptide anion, probably thanks to the presence of multiple sites in the anion that can further interact with the cation through hydrogen bonds conferring to the salt a higher degree of crystallinity.

4. 2. Gelation tests and thermal stability of gel phases

In general, salts were soluble in biocompatible organic solvents tested and in water. On the other hand, they were able to gel some ILs or PBS (1 x).



White opaque gels were obtained, with the only exception of the one formed by **[p-C₁₂im][L-Phe]₂**, which was a yellow opaque material (Figure 31).

All gels were stable for almost three months, in particular ionogels at room temperature and hydrogels formed in PBS at 4 °C.

Figure 31: gels at 7 % (w/w) of gelator, on going from left to right, formed by: **[p-C₁₂im][L-Phe]₂** in [bmim][PF₆]; **[p-C₁₂im][L-Ile]₂** in [bmim][PF₆] and **[p-C₁₂im][D-Ala-D-Ala]₂** in PBS (1 x).

CGC and T_{gel} , determined at CGC and at the common concentration of 7 % (w/w) of gelator, are reported in Table 23. T_{gel} at CGC was obtained by lead-ball method, while T_{gel} , at 7 % (w/w) of gelator, was obtained by the falling drop method or DSC. Indeed some of the gels were too soft to support the weight of the ball; for this reason, to analyse results homogeneously, the falling drop method has been applied, instead of the lead-ball one. It is noteworthy that, when it was possible to apply both methods, values were coincident. For the falling drop method, the vial containing the gel was immersed, turned upside down, in a water and ice bath and T_{gel} was determined when the first drop of gel fell.

Table 23: CGC, T_{gel} and ΔH_m for gels obtained.^a

salts	solvents										
	PBS (1 x)				[bmim][BF ₄]			[bmim][PF ₆]			
	CGC ^b	T_{gel}^c	T_{gel}^d	ΔH_m^g	CGC ^b	T_{gel}^c	T_{gel}^d	CGC ^b	T_{gel}^c	T_{gel}^d	ΔH_m^g
[p-C₁₂im][L-Ile]₂	2.8	25.7	29.9		6.3	SM	49.5	2.3	SM	51.5	
[p-C₁₂im][L-Phe]₂			ns				ns	2.4	43.7	53.1	
[p-C₁₂im][D-Ala-D-Ala]₂	2.8	36.6	41.8	10.0						66.5 ^e	1.6

^aSM =soft material; ns = no DSC signal. ^bcritical gelation concentration (% w/w, gelator/solvent). ^c T_{gel} values (°C) were reproducible within 1 °C; T_{gel} determined at CGC by lead-ball method. ^d T_{gel} values (°C) were reproducible within 1 °C; T_{gel} determined at 7 % of gelator by falling drop method. ^e T_{gel} values (°C) determined by DSC investigation. ^g ΔH_m (J/g) determined by DSC investigation.

Data reported in Table 23 evidence that **[*p*-C₁₂im][L-Ile]₂** is the best gelator among salts tested, as it hardened three different solvents; on the other hand, two salts were able to gel in [bmim][PF₆] solution, which seems the best solvent to our aim.

Taking into account results in the same gelator, **[*p*-C₁₂im][L-Ile]₂**, CGC increases, as function of gelation solvent, in the following order: [bmim][PF₆] < PBS (1 x) < [bmim][BF₄]. The CGC drastically increased in presence of [bmim][BF₄], this seems to indicate that the highest viscosity, awarded from the anion of the IL, facilitated the gelation process ($\eta = 239$ and 450 cP for [bmim][BF₄] and [bmim][PF₆], respectively).^{61b} In addition, the same consideration can be applied to the thermal stability of the gels, as gels obtained in [bmim][PF₆] presented a higher T_{gel} at 7 % (w/w). On the other hand, gel formed in PBS (1 x) was the least thermal stable, so that, it can be stated, once again, that ionogels present higher thermal stability than organo- or hydrogels, as in this case.

Furthermore, considering gels formed in [bmim][PF₆], both CGC and T_{gel} at 7 % (w/w) increased as function of the anion of gelators following this trend: [L-Ile] \leq [L-Phe]. Probably, the π surface of the anion favoured gel formation awarding also a higher thermal stability to the material. Data are in agreement on what previously observed for ionogels obtained from functionalised and unfunctionalised DOSs. Interestingly, as for the ionogels previous obtained from unfunctionalised DOSs, T_{gel} observed by DSC are higher than the one collected by lead-ball method, however they perfectly recall the trend just discussed.

Finally, gels formed in PBS (1 x) presented the same CGC, however the one formed by **[*p*-C₁₂im][D-Ala-D-Ala]₂** is more stable than the one formed by **[*p*-C₁₂im][L-Ile]₂**, indicating that the higher degree of crystallinity of the salt influenced also the property of the material. Indeed, if, as hypothesised above, this effect is due to the possibility of the salt to establish additional hydrogen bonds, thanks to the presence of multiple sites in the dipeptide anion, a thicker network is probably formed in the soft material.

[61] b) J. G. Huddleston, A. E. Visser, W. M. Reichert, H. D. Willauer, G. A. Broker and R. D. Rogers, *Green Chem.* **2001**, *3*, 156-164.

4. 3. Self-healing ability of gel phases

The ability of self-repair after magnetic stirring or ultrasound irradiation has been determined also for these gels using the procedure previously described. Table 24 summarizes data obtained at a concentration of gels equal to 7 % (w/w) of gelator.

Table 24: results of self-healing ability of the gels in terms of sonotropy and thixotropy.

gels	sonotropy	thixotropy
[p-C₁₂im][L-Ile]₂ /PBS (1 x)	N	N
[p-C₁₂im][L-Ile]₂ / [bmim][BF ₄]	N	N
[p-C₁₂im][L-Ile]₂ / [bmim][PF ₆]	Y	Y
[p-C₁₂im][L-Phe]₂ / [bmim][PF ₆]	Y	N
[p-C₁₂im][D-Ala-D-Ala]₂ /PBS (1 x)	N	N

Y = gel phase was reformed after standing at 4 °C; N = gel phase was not reformed after standing at 4 °C.

It is worth of noting that only gels formed in [bmim][PF₆] solution exhibited sonotropic and thixotropic behaviour. Even if, **[p-C₁₂im][L-Phe]₂** / [bmim][PF₆] was sonotropic but did not reform after mechanical disruption. Gel formed both in PBS (1 x) and [bmim][BF₄] solutions did not exhibit neither sonotropy nor thixotropy. So, probably, self-healing ability of the gels depends on solvent properties.

4. 4. Morphology of gel phases

Gel morphology has been analysed using POM measurements. Samples at 7 % (w/w) have been casted between two glass slides and images were recorded for the heating and the cooling cycles of the gels. A characteristic image for each gel is shown in Figure 32.

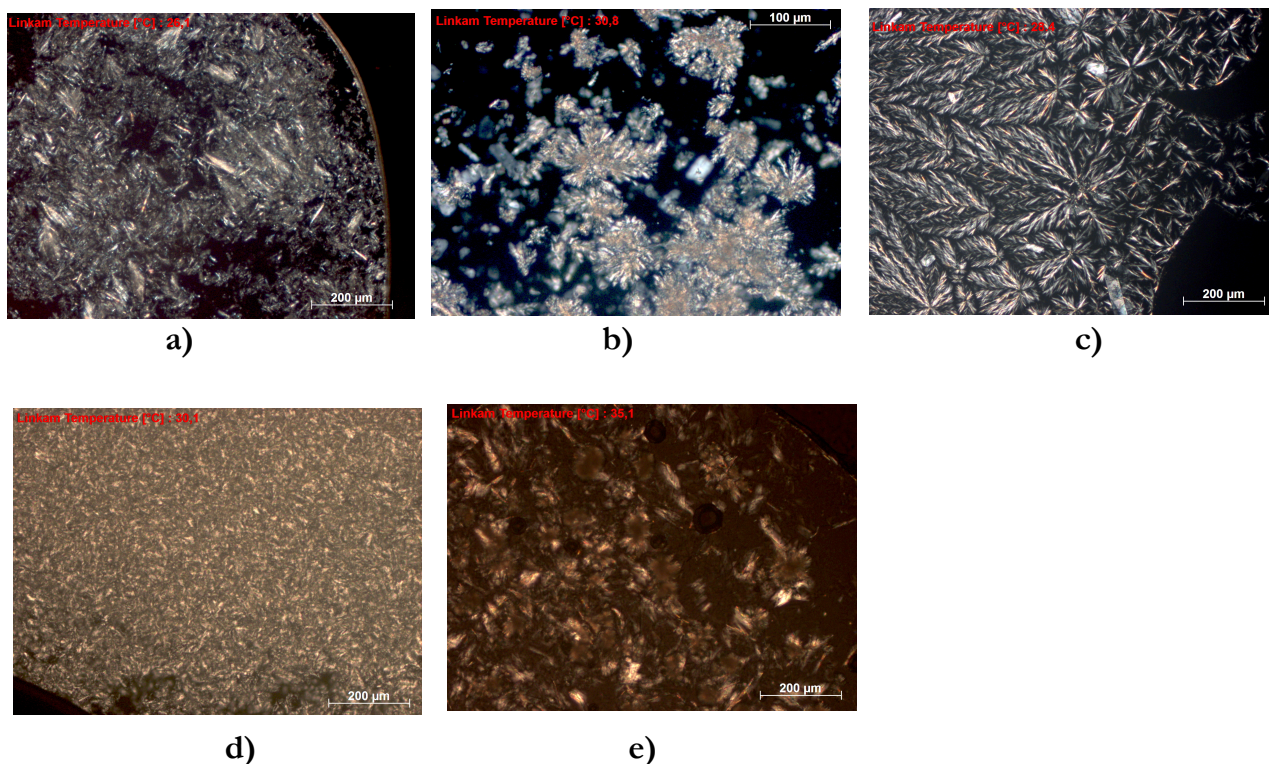


Figure 32: POM images of gels at 7 % (w/w): **a)** $[p\text{-C}_{12}\text{im}][\text{L-Ile}]_2/\text{PBS}$ (1 x); **b)** $[p\text{-C}_{12}\text{im}][\text{L-Ile}]_2/[\text{bmim}][\text{BF}_4]$; **c)** $[p\text{-C}_{12}\text{im}][\text{L-Ile}]_2/[\text{bmim}][\text{PF}_6]$; **d)** $[p\text{-C}_{12}\text{im}][\text{L-Phe}]_2/[\text{bmim}][\text{PF}_6]$; **e)** $[p\text{-C}_{12}\text{im}][\text{D-Ala-D-Ala}]_2/\text{PBS}$ (1 x).

It is worth of mention that POM allowed obtaining better images for ionogels than for hydrogels, nevertheless they can be discussed as well.

Also in this case, morphology is affected by the small modification generated in the system, such as anion of the gelator and gelation solvent. In general, gels seem characterised by spherulitic or thick texture morphology.

Taking into account gels formed by $[p\text{-C}_{12}\text{im}][\text{L-Ile}]_2$, it is clear the difference between hydrogel and ionogels, as the first one showed a thick texture (Figure 32a) while in the second case a spherulitic network can be easily recognised (Figure 32b-c). Ionic liquids, being highly organized systems, probably award also a higher structural order in the formation of the three-dimensional network.

On the other hand, considering the same gelation solvent $[\text{bmim}][\text{PF}_6]$, there is not a clear trend explaining gel morphology, indeed $[p\text{-C}_{12}\text{im}][\text{L-Ile}]_2$ showed a spherulitic morphology (Figure 32c), while $[p\text{-C}_{12}\text{im}][\text{L-Phe}]_2$ a thick texture (Figure 32d). Probably in this case the discriminant factor could be the nature of aminoacid anion.

Finally, results obtained in PBS (1 x) underline, once again, how the higher thermal stability of the gel could be a consequence of the higher ordering in gel architectures

induced by the anion of gelator. In fact, the more thermal stable gel, formed by $[p\text{-C}_{12}\text{im}][\text{D-Ala-D-Ala}]_2$ (Figure 32e), presented a spherulitic texture while the less thermal stable, formed by $[p\text{-C}_{12}\text{im}][\text{L-Ile}]_2$, showed a thick texture (Figure 32a).

4. 5. Kinetic of gel formation

When it was possible, gel formation has been analysed by means of RLS and UV-vis measurements for gels at 7 % (w/w), but unfortunately only for three gels RLS experiment could be carried out, as in the other cases the process was too slow to be followed.

RLS traces revealed, also in these cases, a consecutive process leading to gel phase; indeed, as shown in Figure 33a, the equilibrium state, corresponding to gel formation, is subsequent to an intermediate formation.

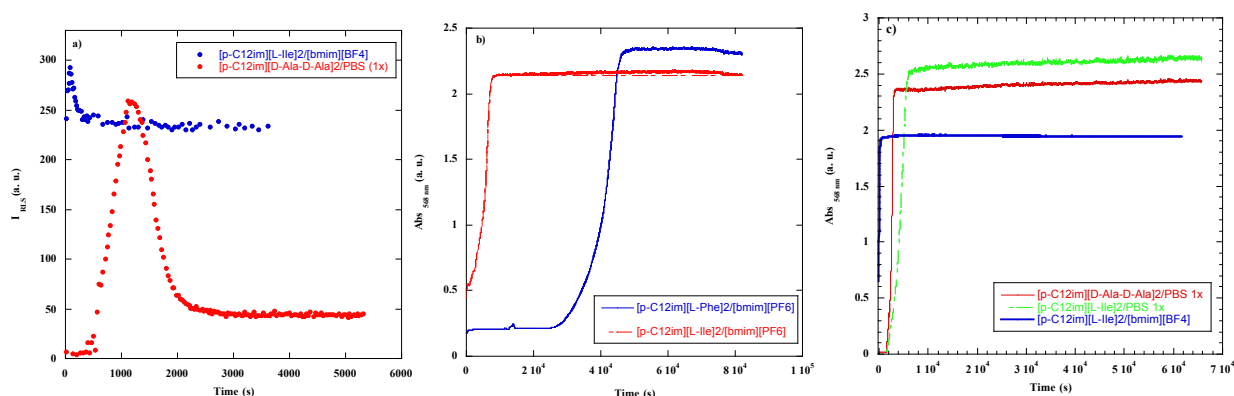


Figure 33: kinetic trace of gels: **a)** RLS intensity as function of time; **b-c)** absorbance as function of time.

Even if, RLS data are not directly comparable as they were obtained only for gels such as, $[p\text{-C}_{12}\text{im}][\text{L-Ile}]_2/[\text{bmim}][\text{BF}_4]$ and $[p\text{-C}_{12}\text{im}][\text{D-Ala-D-Ala}]_2/\text{PBS}(1x)$, that differ for gelators and solvent, it is possible to assert that ionogel formation is faster than hydrogel one. Indeed, the only exception to this trend was observed for the ionogel formed by $[p\text{-C}_{12}\text{im}][\text{L-Phe}]_2$, which formation is too slow to be followed. In addition, intensity values are higher for ionogel ($I_{\text{RLS}} = 230$ for $[p\text{-C}_{12}\text{im}][\text{L-Ile}]_2/[\text{bmim}][\text{BF}_4]$, while $I_{\text{RLS}} = 50$ a.u. for $[p\text{-C}_{12}\text{im}][\text{D-Ala-D-Ala}]_2/\text{PBS}(1x)$). As previously evidenced, these values can give a qualitative indication of aggregates size, so that, the presence of larger aggregates in ionogel phases could explain their higher thermal stability in respect of hydrogels one.

Kinetic of gel formation can be better analysed considering UV-vis measurements. Figure 33b displays the different effect exerted on the process by the anion of the gelator. In [bmim][PF₆] the trend is the following one: [L-Phe] < [L-Ile].

While the comparison of data for gels, formed by the same gelator, confirmed what previously observed by RLS, as ionogels kinetic is faster than hydrogel one. The kinetic trend as function of gelation solvent is: PBS (1x) < [bmim][PF₆] < [bmim][BF₄]. Probably the higher hydrogen bond acceptor ability of the anion of the IL favours the gel formation. Interestingly, the trend of the opacity, that indicates the crystallinity of gel phases, is completely inverted.

Kinetic trends, observed as function of both gelator and solvent, revealed an interesting correlation with gel morphology, as the slowest systems presented in both cases a thick texture instead of a spherulitic one. This consideration is valid also for the comparison between gels formed in PBS (1x), as the faster gel formation was obtained for gel of [**p-C₁₂im**][**D-Ala-D-Ala**]₂ presenting a spherulitic texture, on the contrary the one of [**p-C₁₂im**][**L-Ile**]₂ showed a thick texture.

4. 6. *Application of the gels: test of antimicrobial activity*

Before evaluating the antimicrobial activity of gel phases, the one of their single components, such as gelators and ILs, has been firstly tested in solutions of DMSO.

The activity was evaluated taking into account Gram-negative (*Escherichia coli*) and Gram-positive (*Kocuria rhizophila*) bacterial strains, knowing that their different composition of cell walls could influence the antibacterial activity of the systems.

Microbiological assays were carried out directly spotting on bacterial tester overlays different volumes ranging from 1 to 10 μL of DMSO solutions containing 1 and 10 μg of salts or 1, 10 and 25 μg of ILs. An amount of 10 μL of pure DMSO was used as control.

The antibacterial activity was, qualitatively, evaluated measuring the diameter of the inhibition zone circumference (Figure 34).

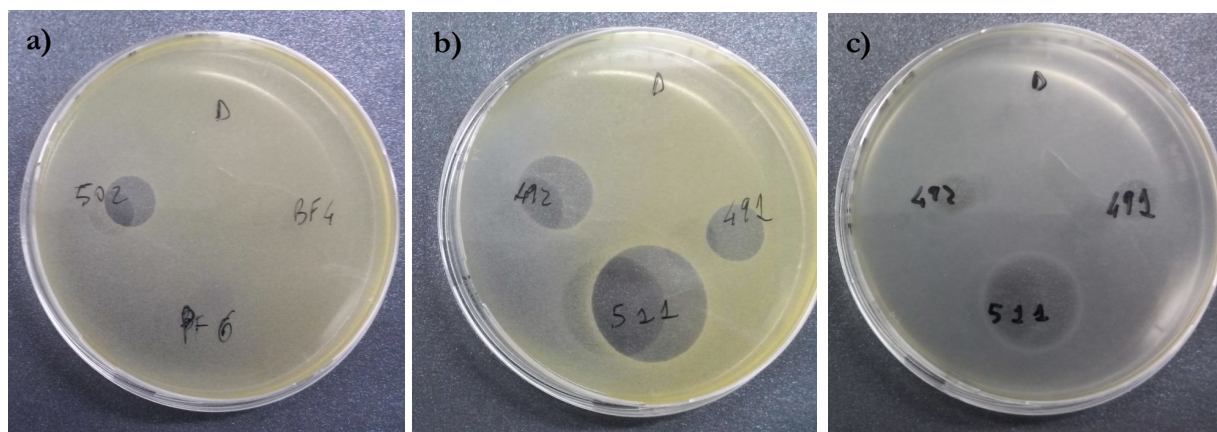


Figure 34: evaluation of antimicrobial activity by agar-diffusion test performed using a), b) *K. rhizophila* and c) *E. coli* as testers. Clear halos indicate inhibition of bacterial growth after an overnight incubation at 37 °C.

Results obtained have demonstrated the antimicrobial efficiency of the DOSs; on the contrary ILs, used as gelation solvents, did not exert any effect on both bacterial strains. The antimicrobial activity could be favoured by the presence of long alkyl chain on the cationic structure, indeed, previous studies on ILs activity demonstrated that a longer alkyl chain of the cation enhanced the antimicrobial activity.^{81b} This behaviour could be explained considering that the cationic components can interact with the bacterial cell envelope by displacing cations. Subsequent interactions with the cytoplasmic membrane components can result in membrane disruption and leakage of cytoplasmic material. The hydrophobic chain has the important function of adsorbing into the surface of the microbial cell, and eventually, cells die.

Activity of DOSs was slightly higher in *K. rhizophila* than in *E. coli*; however, at 10 µg of salts, the same trend of efficiency as function of DOS anions has been detected for both bacterial strains: [D-Ala-D-Ala] < [L-Ile] < [L-Phe]. This trend indicates that aromatic anion exerted a higher efficiency than the other ones. Furthermore, an antimicrobial activity has been detected also for 1 µg of salts, but it did not change in relation of salt used.

This preliminary analysis gave a first indication of the salts antimicrobial activity and allowed performing a subsequent quantitative analysis on LB-liquid culture. In this case, the turbidimetric evaluation of concentration of bacterial suspension, OD₆₀₀, allowed determining the percentage of vitality of bacteria and the Minimal Inhibitory

81b) A. Sharma, P. Prakash, K. Rawat, P. Solanki and H. B. Bohidar, *Appl. Biochem. Biotechnol.* **2015**, *177*, 267-277.

Concentration, MIC. In particular, the first one has been calculated as ratio between OD in presence of salts and the one of control, *i.e.* DMSO, while the second parameter was determined as MIC90, which represents the minimal concentration inhibiting at least the 90 % of bacterial growth in respect of control cultivations. Results are reported in Table 25.

Table 25: OD and % OD determined at different concentrations of the salts; MIC90 against *K. rhizophila* and *E. coli* of tested salts.

bacterial strain	salt	concentration (µg/mL)	OD	%OD ^a	MIC90
<i>E. coli</i>	[<i>p</i> -C ₁₂ im][L-Ile] ₂	10	0.15	5	3 µg/mL
		5	0.15	5	
		3	0.14	5	
		1.5	2.73	97	
		0.5	2.88	100	
	[<i>p</i> -C ₁₂ im][L-Phe] ₂	10	0.20	7	3 µg/mL
		5	0.15	5	
		3	0.09	3	
		1.5	2.47	87	
		0.5	2.62	93	
	[<i>p</i> -C ₁₂ im][D-Ala-D-Ala] ₂	10	0.16	5	3 µg/mL
		5	0.15	5	
		3	0.13	5	
		1.5	2.67	95	
		0.5	2.49	88	
<i>K. rhizophila</i>	[<i>p</i> -C ₁₂ im][L-Ile] ₂	5	0.15	1	0.5 µg/mL
		0.5	0.17	2	
		0.1	7.82	98	
	[<i>p</i> -C ₁₂ im][L-Phe] ₂	5	0.14	2	0.5 µg/mL
		0.5	0.16	2	
		0.1	6.51	82	
	[<i>p</i> -C ₁₂ im][D-Ala-D-Ala] ₂	5	0.15	2	0.5 µg/mL
		0.5	0.18	2	
		0.1	7.11	89	

^apercentual ratio calculated between OD of bacterial culture in presence of salts and the one of control.

Data obtained, clearly, indicate that Gram-positive strains are much more sensitive to the action of our salts than Gram-negative, indeed, in the first bacterial strain a MIC90 equal to 0.5 µg/mL has been detected for every salt, while in the second one it increased to 3 µg/mL. This comparison can be better understood, analysing graphs in Figure 35. Probably, DOSs can better interact with the outer peptidoglycan, located in Gram-positive cell wall, than with the outer membrane of Gram-negative cell wall.⁸⁴

[84] Thomas J. Silhavy, Daniel Kahne and S. Walker, *Cold Spring Harb Perspect Biol* **2010**, *1*, 1-16.

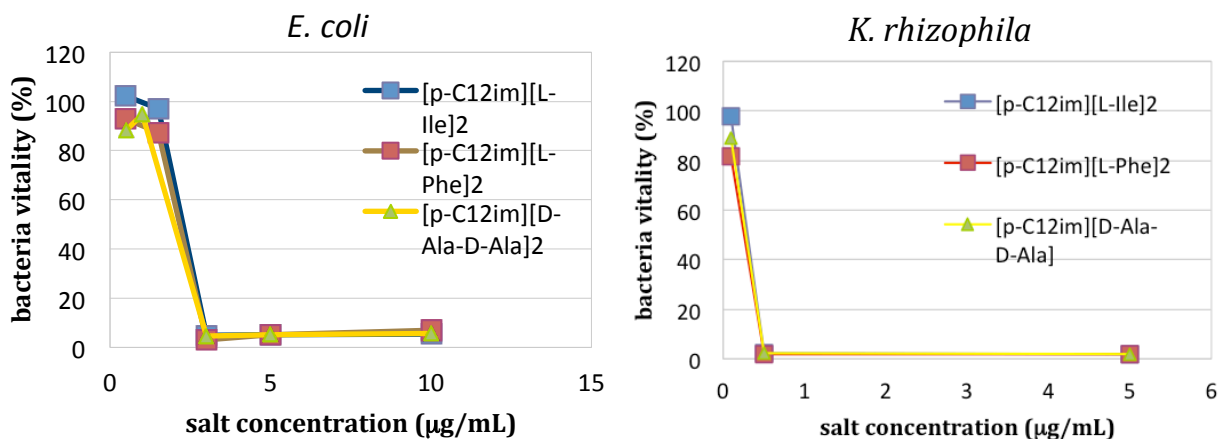


Figure 35: percentage of bacteria vitality as function of salt concentration for *E. coli* and *K. rhizophila*.

The evaluation of %OD, at concentration of 1.5 μg/mL for *E. coli* and 0.1 μg/mL for *K. rhizophila*, confirmed the better antimicrobial activity of **[p-C12im][L-Phe]₂** in both bacterial strains. On the other hand, in respect to the preliminary results from agar-diffusion test, a comparable activity to the one of **[p-C12im][L-Phe]₂** has been detected also for **[p-C12im][D-Ala-D-Ala]₂**, this data is not surprising taking into account the nature of the dipeptide anion. Encouraged by these results obtained for gelators, we studied the activity on gel phases.

Tests on gel phases. As previously stated, we were interested in analysing the antimicrobial activity of the gel phases obtained in IL solutions and PBS (1 x). So that, also in this case biological agar-diffusion test and test on liquid growth medium have been carried out. However, in order to use gels for example for future topical applications, we had to test the activity of the soft material in its form and not the one of the solution derived from the gel. For this reason experimental conditions were adapted for the new system. In particular, biological agar-diffusion tests were carried out inserting 10 and 50 μl of gels (spot 1-3 and 2-4 in Figure 36, respectively) into holes previously formed on the bacterial overlay on LB agar plate. In this way, diffusion problems were limited and inhibition circumference should be determined. All gels exhibited antimicrobial activity as shown in Figure 36. Even gels were more efficient in Gram-positive culture than in Gram-negative.

This result perfectly recalls what observed for gelators and what previously reported in literature for hydrogels of aminoacid derivative.⁸²

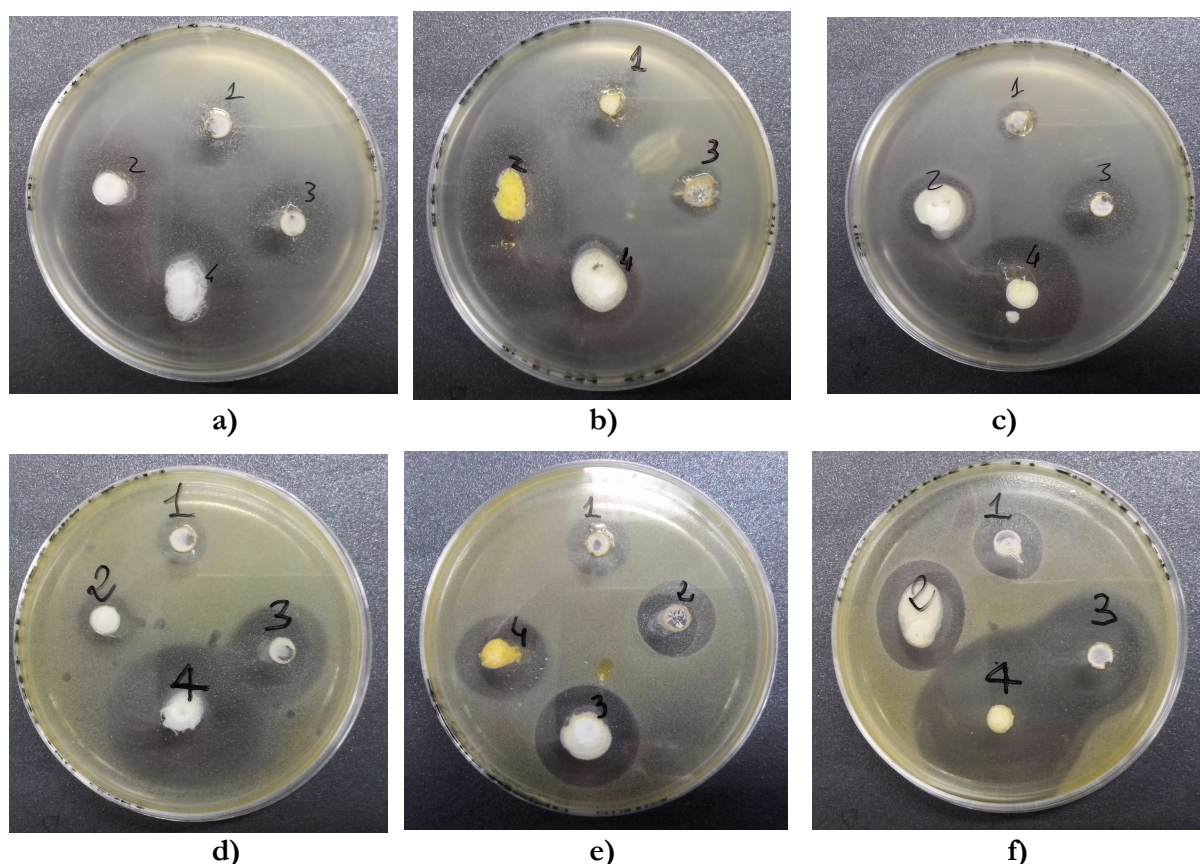


Figure 36: first row antimicrobial activity of gels on *E. coli* strain, second row on *K. rhizophila* strain; spot 1-3 10 μL of gel, spot 2-4 50 μL of gel. **a), d)** Spot 1 and 2 of $[\text{p-C}_{12}\text{im}][\text{L-Ile}]_2/[\text{bmim}][\text{PF}_6]$, spot 3 and 4 of $[\text{p-C}_{12}\text{im}][\text{L-Ile}]_2/[\text{bmim}][\text{BF}_4]$; **b), e)** spot 1 and 2 of $[\text{p-C}_{12}\text{im}][\text{L-Phe}]_2/[\text{bmim}][\text{PF}_6]$, spot 3 and 4 of $[\text{p-C}_{12}\text{im}][\text{L-Ile}]_2/\text{PBS}$ (1 x); **c), f)** spot 1 and 2 of $[\text{p-C}_{12}\text{im}][\text{D-Ala-D-Ala}]_2/\text{PBS}$ (1 x).

The highest antimicrobial activity, qualitatively observed by the quantification of the radii of the inhibition zone circumference, has been observed for $[\text{p-C}_{12}\text{im}][\text{L-Ile}]_2/[\text{bmim}][\text{BF}_4]$ (spot 3 and 4 of Figure 36a and d).

In general, the inhibition zones observed in 50 μL of gel are slightly larger than the one observed in 10 μL of gel. However, trend of antimicrobial activity is almost coincident for both concentrations. Considering results obtained in *E. coli*, ionogels exhibited higher activity than hydrogels, while in *K. rhizophila*, gels formed in PBS (1 x) showed a slight larger inhibition zone than $[\text{p-C}_{12}\text{im}][\text{L-Ile}]_2$ and $[\text{p-C}_{12}\text{im}][\text{L-Phe}]_2$ in $[\text{bmim}][\text{PF}_6]$.

[81] I. Irwansyah, Y.-Q. Li, W. Shi, D. Qi, W. R. Leow, M. B. Y. Tang, S. Li and X. Chen, *Adv. Mater.* **2015**, 27, 648-654.

Furthermore, we have demonstrated that ionogels, differently from hydrogels, resisted to the LB-liquid culture medium. In Figure 37, different aliquots of medium (100, 250, 500 μL) were casted on gel phase; as they resisted, 500 μL of medium and the bacterial suspension were casted on them, the system was then incubated overnight at 37 $^{\circ}\text{C}$. Even if, the day after, the medium solution was clear indicating the death of bacteria, unfortunately, OD could not be measured as the medium could present some remains of gels. By the way, a qualitative investigation of bacteria vitality was performed by plating on LB-agar 10 μL of bacterial suspensions which were exposed overnight to gels and incubating the plates overnight at 37 $^{\circ}\text{C}$. Bacterial suspensions from vials without gels were used as control. After another night of incubation we have detected the bacterial growth on the control plate (Figure 37c) and the complete absence of bacteria in the plate where 10 μL of bacterial culture were casted after being in contact with the gel phase (Figure 37b).

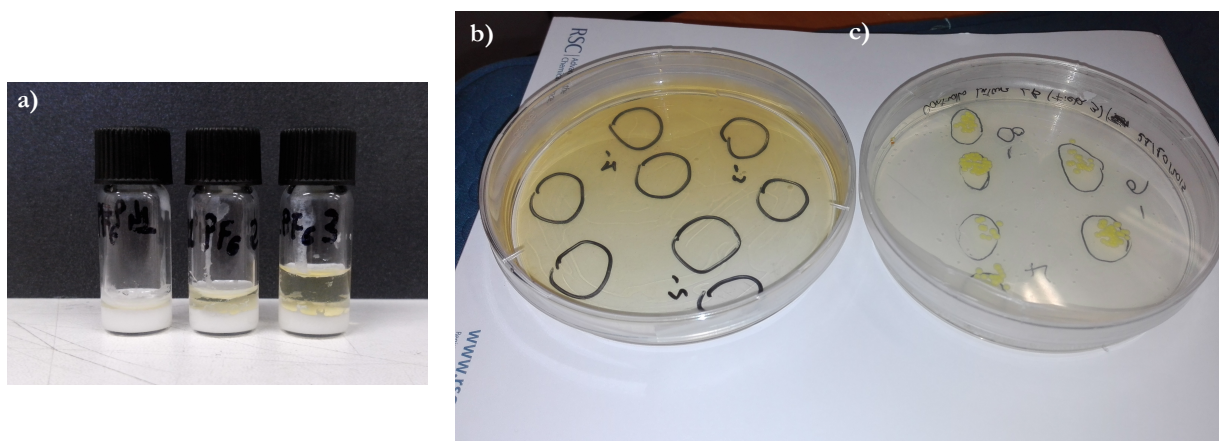


Figure 37: a) gels of $[\text{p-C}_{12}\text{im}][\text{L-Ile}]_2/[\text{bmim}][\text{PF}_6]$ at 7 % (w/w) with different aliquots of LB-liquid bacterial cultivations as overlay; b) LB-agar plates where 10 μl of bacterial suspensions previously exposed to gels have been spotted and then incubated to assess bacterial viability. c) LB-agar plates where 10 μl of bacterial suspensions from unexposed cultivations have been deposited and incubated as controls; in the last case the bacterial growth is evident.

The most resistant gels to the LB-liquid culture were the ones formed in $[\text{bmim}][\text{PF}_6]$ solution, as the ones formed in $[\text{bmim}][\text{BF}_4]$ showed a slight decrease of gel volume. We knew from tests on ILs that the activity could not be due to the gelation solvents, however, gelators exhibited a good antimicrobial activity. So that, in order to understand if the antibacterial activity was only due to the release of the gelator from the gel matrix into the culture, a kinetic experiment, evaluating the presence of the gelator in solution of LB, has been performed. This experiment was carried out by NMR investigation using a

reference compound with certain concentration, which NMR signals did not influence gelator spectrum in D₂O. 500 µL of LB-liquid culture dissolved in D₂O were added to four different gels and the systems were thermostated at 37 °C, 250 µL of culture were taken from the gels at interval of time equal to 0.1, 1, 2 and 24 h. All the spectra showed really low intensity peaks corresponding to gelator, that were not possible to integrate and correlate with the ones of the reference compound. This analysis clearly evidences how the antimicrobial activity is totally dependent on the gel and not on the gelator. A similar result have been reported by Gunnlaugsson *et al.*, indeed they have observed an enhanced activity on gel phases in respect of gelator one. So, they have hypothesised that the overall supramolecular structure can give rise to multiple hydrogen bonding interactions that can interact with the bacterial cell wall and possibly disrupt it or prevent its formation.^{81a}

Studies on antimicrobial activity of gel phases are still in progress in order to deeper analyse the influence of gelator and solvent also on this property of the materials. Results obtained are really encouraging for both ionogels and hydrogels. Indeed, even if, in the last case is more difficult to evaluate the activity in liquid culture, hydrogels have also exhibited an activity on bacterial overlay on LB agar plate and, having in mind topical application, they might be used as well. In fact, the soft-matter is easily applicable and as such highly attractive for use in coating implants to prevent the onset of bacterial infection.⁸⁵

In this chapter, the application of functionalised and unfunctionalised diimidazolium salts as LMWGs has been deeply investigated. It is clear how material properties are strongly dependent on combination of cation and anion of the salts and on the gelation solvent property. Gels in organic solutions, ILs, water and water buffer solution have been obtained. These materials present different properties and could be applied in several fields: ionogels for example can be used as electrolyte media for DSSCs; gels formed by functionalised DOSs, as confined reaction media; two-component hydrogels and gels formed by aminoacid based salts could be applied in biological and pharmaceutical fields.

[80] a) K. Pandurangan, J. A. Kitchen, S. Blasco, F. Paradisi and T. Gunnlaugsson, *Chem. Commun.* **2014**, 50, 10819-10822.

[85] a) A. M. Klibanov, *J. Mater. Chem.* **2007**, 17, 2479-2482, b) P. Li, Y. F. Poon, W. Li, H.-Y. Zhu, S. H. Yeap, Y. Cao, X. Qi, C. Zhou, M. Lamrani, R. W. Beuerman, E.-T. Kang, Y. Mu, C. M. Li, M. W. Chang, S. S. Jan Leong and M. B. Chan-Park, *Nat. Mater.* **2011**, 10, 149-156.

In addition, supramolecular gels formed by organic salts are not widely studied, even less ionogels, however, our results indicate a new emerging class of LMWGs and gels widely tuneable for several purposes.

Experimental section

1. *Materials and methods*

1,3,5-Tris(bromomethyl)benzene, 1-bromooctane, imidazole, sodium hydroxide, Amberlite IRA 400 resin (chloride form), 1,5-naphthalenedisulfonic-4H₂O acid, 2,6-naphthalenedicarboxylic acid, Amberlite IR 120 PLUS resin (sodium form), sodium 2,6-naphthalenedisulfonate, α,α' -*p*-dibromoxylene, α,α' -*m*-dibromoxylene, 1-bromododecane, 1,4-benzendicarboxylic acid, trimesic acid, citric acid, ethylenediaminetetraacetic acid, N-decylimidazole, N-dodecylimidazole, anhydrous acetonitrile, acetone, methanol, HBF₄ solution in water (50:50, w/w), HPF₆ solution (65% in water), L-isoleucine, L-phenylalanine, Fmoc-L-isoleucine, D-alanyl-D-alaninate, 5-hydroxy-methyl-furfural and all organic solvents used for gelation tests were analytical reagents purchased from commercial sources and used as received.

ILs as [bmim][NTf₂], [bmim][BF₄], [bmim][PF₆] were analytical reagents purchased from commercial sources and used as received, while [bmim][SbF₆], [bmpyrr][NTf₂], [bmpip][NTf₂], [bEt₃N][NTf₂], [Bzmim][NTf₂] and [Bzbim][NTf₂] were prepared and purified according to the reported procedures.¹ Pyrrolidine and dichloromethane were distilled before use.

α -CD and β -CD were dried in a desiccator in vacuo over phosphorus pentoxide at 90 °C for at least 24 h, and then used as such.

Functionalised diimidazolium salts were synthesized as previously reported in Chapter 1.² While, compounds [*p*-C₁₀im][Br]₂, [*p*-C₁₂im][Br]₂ and [*p*-C₁₂im][BF₄]₂ were prepared as previously reported.³

NMR studies. ¹H-NMR, ¹³C-NMR, spectra were recorded using Bruker 250, 300 and 400 MHz nuclear magnetic resonance spectrometers.

[1] a) L. Cammarata, S. G. Kazarian, P. A. Salter and T. Welton, *Phys. Chem. Chem. Phys.* **2001**, *3*, 5192-5200, b) F. D'Anna, S. La Marca, P. Lo Meo and R. Noto, *Chem. Eur. J.* **2009**, *15*, 7896-7902.

[2] F. D'Anna, H. Q. N. Gunaratne, G. Lazzara, R. Noto, C. Rizzo and K. R. Seddon, *Org. Biomol. Chem.* **2013**, *11*, 5836-5846.

[3] F. D'Anna, P. Vitale, S. Marullo and R. Noto, *Langmuir* **2012**, *28*, 10849-10859.

TGA analysis. Thermal gravimetric analyses (TGA) were performed on a TA 2910 differential scanning calorimeter interfaced to a TA Thermal Analyst 3100 controller while a slow stream of nitrogen flowed through the instrument cell. TGA Measurements were performed equilibrating the sample at 25 °C, isothermal 0.1 min, afterwards using a temperature ramp with a rate of 10 °C/min from 25 °C to 300 °C. The maximum values of the DTGA curves of each thermogram were used as a measure of the decomposition temperature.

Melting points. When melting points are indicated as range of temperature, they were determined with a Kofler. In all other cases DSC measurements were performed to obtain melting points of compounds.

DSC measurements. Differential scanning calorimetry (DSC) was carried out on a DSC Q200 calorimeter (TA Instruments, New Castle, DE) interfaced to a TA Thermal Analyst 3100 controller connected to an RCS90 cooling system. Heating and cooling cycles were done in a 50 mL/min stream of nitrogen. Samples were weighed (≈ 5 mg for salts, ≈ 15 mg for gels) in T-zero aluminum pans. Transition temperatures from DSC are reported at the point of maximum heat flow.

After equilibration of the sample at 25 °C, DSC measurements of organic salts were performed heating the sample with a rate of 20 °C/min from 25 °C to 180 °C and cooling it with the same rate ramp to 0 °C. DSC measurements of gel phases were performed equilibrating the sample at 25 °C and using a temperature ramp with a rate of 10 °C/min from 25 °C to 100 °C and a cooling ramp to 0 °C.

μ -DSC measurements. For gel formed by functionalised DOSs, in all cases in which gel phases were formed by simply cooling the hot solution, the sol–gel transitions were also recorded on a micro-DSC III (SETARAM) under nitrogen flow in the range from 0 to 70 °C with a scan rate of 0.3 K min⁻¹. The stainless steel (1 cm³) sample cell was filled with ca. 250 mg of ionogel and the reference cell with the corresponding amount of IL. The calibration was performed by using naphthalene.

Polarimetric Measurements. Solutions of DOSs and β -cyclodextrin were prepared in volumetric flasks. Optical rotations were measured using a glass polarimetric cell (light path 1 dm) and obtained as the average value over 50 readings.

Preparation of gels and T_{gel} determination. Gels were prepared by weighing into a screw-capped sample vial (diameter 1 cm) the amount of salt and solvent (\sim 250 mg). The sample vial was heated in an oil bath at 85-90°C (130 °C for gels of functionalised DOSs) until a clear solution was obtained. The vial was then cooled and stored at 4 °C overnight. The tube inversion test method was used to examine gel formation.

To determine the T_{gel} values, a lead ball (weighing 46.23 mg and 2 mm of diameter) was placed on the top of the gel and the vial was put into a water bath. The bath temperature was gradually increased until the gel melted and the lead ball reached the bottom of the vial (T_{gel}). The T_{gel} values were reproducible within 1 °C.

When, T_{gel} could not be determined by lead-ball method, the falling drop one has been used. In this case, the vial containing the gel was immersed, turned upside down, in a water and ice bath and T_{gel} was determined when the first drop of gel fell.

Dielectric spectroscopy. A Hewlett-Packard impedance analyzer (HP 4294A) equipped with HP 16451B dielectric test fixtures was used at 298 K. The dielectric constant and the dispersion factor were measured as a function of frequency.

POM measurements. Samples were casted between two glasses to record POM (Polarizing Optical Microscope) images. The samples were heated to their sol phases and cooled. The instrument used is a Leitz 585 SM-LUX-POL microscope equipped with crossed polarizers, a Leitz 350 heating stage, a Photometrics CCD camera interfaced to a computer, and an Omega HH503 microprocessor thermometer connected to a K (Chrome-Alome) thermocouple (Omega Engineering, Inc.).

Rheological measurements. Rheology measurements were recorded on an Anton Paar MCR 302 strain-controlled rheometer using a Peltier temperature controller and a cone plate (CP 25-2) tool, the sample was placed between the shearing plates of the rheometer. Rheological properties, such as strain sweep and frequency sweep, were recorded before

and after heating the sample. Kinetics were performed, in the linear visco-elastic region, heating the sample to 90 °C for 30 min to ensure the formation of solution, then it was cooled at ~20 °C/min to 22 °C. When the moduli presented a plateau, indicating the reformation of the gel, strain sweep and frequency sweep were performed again to compare the results with the previous ones.

Self-healing properties of gel phases were also tested by rheometer. They were carried out at room temperature and at a frequency of 1 Hz, varying the strain from low to high percentage values for fixed time intervals of 5 minutes (values were chosen from the strain sweep graph that indicates the percentage of strain needed for the disruption of the gel). When the gel was restored, it was possible to calculate the percentage of recovery of the initial G' value. In some cases even if the G' values were restored, they were oscillating or increasing continuously, so the measure of G' and G'' at a fix strain and frequency was carried out for longer time.

RLS Measurements. RLS measurements were carried out with a spectrofluorophotometer using a synchronous scanning mode in which the emission and excitation monochromators were preset to identical wavelengths. The RLS spectrum was recorded from 300 to 600 nm with both the excitation and emission slit widths set at 1.5 nm. We chose as working wavelength the one corresponding to the intensity maximum of the emission spectrum. Samples for a typical kinetic measurement were prepared by injecting into a quartz cuvette (light path 0.2 cm) the limpid hot solution of salt. The measurements were carried out at 20 °C. Spectra were recorded until gel formation. The gel phase obtained at the end of the measurement was stable after the tube inversion test.

Opacity Measurements. Opacity measurements were recorded with a spectrophotometer. The opacity of the gel phases was determined with UV/Vis measurements as a function of time, at a wavelength of 568 nm and a temperature of 20 °C. As described for RLS measurements, samples for a typical measurement were prepared by injecting into a quartz cuvette (light path 0.2 cm) the limpid hot solution of salt. Spectra were recorded until gel formation. The gel phase obtained at the end of the measurement was stable after the tube inversion test.

Thixotropic and Sonotropic Behaviour. The gel phases obtained were subjected to two different external stimuli. The mechanical stimulus involved stirring the gel phase at 1000 rpm for 5 min, using a stirring bar (length 8 mm, height 3 mm). The sonotropic behaviour of the gel phases was tested by irradiating in an ultrasound water bath for 5 min with a power of 200 W and a frequency of 45 kHz. Thereafter, the materials were stored at 4 °C overnight. When the samples were stable to the tube-inversion test, the gels were defined as thixotropic or sonotropic.

Powder X-ray diffraction. (XRD) patterns of samples were obtained on a Rigaku Ultima IV X-Ray diffractometer with Cu K α X-rays ($\lambda = 1.54 \text{ \AA}$) generated by a Rigaku generator operating at 40 kV and 30 mA with the collimator at 0.5 mm and a D/Tex dectector. Salts, solvents and gels were doped on the sample holder as thin films, measurements were recorded overnight from 3 to 50 ($^{\circ}$) of 2θ .

Fluorescence Measurements. Fluorescence measurements were carried out with a spectrofluorophotometer using an emission mode. The fluorescence spectrum was recorded from 360 to 450 nm with the excitation slit widths set at 1.5 nm and emission slit at 3 nm.

We chose as excitation wavelength 348 nm, corresponding to the intensity maximum of the xanthone. Water was used as blank. In all cases, xanthone aqueous solutions were prepared by injecting a guest solution (MeOH; ca. 10^{-3} M) in water. Measurement solutions were prepared by adding increasing volumes of β -CD to guest solution (1 mL) in a volumetric flask. In these solutions, the concentration of guest was constant and equal to $3 \cdot 10^{-6}$ M. In the case of binary complex xanthone/ β -CD, the β -CD concentration ranged from 0 to $1.5 \cdot 10^{-3}$ M.

For competitive measurements, the xanthone concentration was $3 \cdot 10^{-6}$ M, the β -CD concentration was $1.5 \cdot 10^{-3}$ M and the salt concentration ranged from 0 to $3.6 \cdot 10^{-3}$ M in the case of **[*p*-C₁₀im][Br]₂** and from 0 to $9 \cdot 10^{-4}$ M in the case of **[*p*-C₁₂im][Br]₂**. All measurements solutions were removed from air before use, insufflating Ar for 12 min. A quartz cuvette with a 1 cm light path was used. The fluorescence intensity was reported as an average value over 50 readings.

Scanning Electron Microscopy. SEM images were recorded with an instrument with 20 kV operating voltage. The gel was placed on the stub and the solvent was evaporated under vacuum to form a xerogel. The dry sample thus obtained was shielded by gold.

Biological test of antimicrobial activity. Gram-negative *Escherichia coli* K12 and Gram-positive *Kocuria rhizophila* ATCC 9341 bacteria, stored as bacterial suspension in water solution of glycerol 20 %, were used in our experiments as tester strains. For each strain, an aliquot of 10 μ l of bacterial suspension was incubated overnight 37 °C in using *Luria–Bertani* agar broth medium (LB agar, Invitrogen) in Petri disk and then harvested. The bacterial biomass was re-suspended in sterile distilled water. The concentration of bacterial suspension was photometrically measured as optical density (OD) at wavelength of 600 nm (OD_{600}). Before performing the antibacterial experiments, the OD_{600} values of bacterial suspension were adjusted to 1, which corresponded to the concentrations of 10^9 colony forming units (CFU) *per* 1 mL based on the bacterial colony-counting method. All the procedures were performed under sterile conditions.

Agar diffusion test method. For each tester strain, a bacterial suspension of 10^8 CFU was inoculated into 5 ml of LB soft-agar (i.e. 0.7 % agar) to obtain a uniform bacterial overlay on LB agar plates. For the antibacterial assays, salt powders were dissolved in DMSO (C = 1 mg/mL for DOSs and 25 mg/mL for ILs). Gels were used at 7 % (w/w). Volumes of 5 μ L and 10 μ L of stock solutions of salts were directly spotted on bacterial overlay to assess their antibacterial activity; while, volumes of 10 μ L and 50 μ L of gels were spotted in holes previously formed in LB-agar culture. After an overnight incubation at 37 °C, the radii of observed bacterial growth inhibition halos were measured in centimetres. All the procedures were performed under sterile conditions.

Turbidity test for salt solutions against tester strain cultivations. Strain cultivations were incubated overnight in presence of an opportune amount of salt solutions (ranging from 0 to 10 μ g/mL as final concentrations) using 24-well tissue culture plates on a orbital shaker (180 r.p.m.) at 37 °C. Subsequently, OD_{600} values of bacterial tester cultivations were determined. The bacterial cultivations without salt addition were used as control ones.

Liquid turbidity test against Gram-positive and Gram-negative on gel phases. For each bacterial tester a total of 10^6 /mL bacteria in 500 μ L of LB medium was placed into vials over different gels, and then incubated overnight at 37 °C. The visual inspection of turbidity assesses antibacterial activity using i) uninoculated amounts of LB medium and ii) bacterial cultivations unexposed to gels as negative (i.e. no growth) and positive (i.e. observed bacterial growth) as controls, respectively. To confirm bactericidal activity, aliquots of exposed and unexposed bacterial cultivation serial dilutions were plated on LB agar and incubating overnight at 37 °C for CFU counting.

Kinetic of gelator release from gel phase to LB-liquid culture by NMR. As reference gel [**p-C₁₂mim**][**L-Ile**]₂/[bmim][BF₄] has been taken into account as during the antimicrobial tests a slight decrease of gel phase was observed. Prior carrying out the kinetic of release, spectra of gelator, LB, 5-hydroxy-methyl-furfural -used as reference compound to determine quantity of gelator- and mixtures of gelator and 5-hydroxy-methyl-furfural in different ratios have been recorded in D₂O. Knowing that the reference compound shows ¹H NMR peaks at different chemical shifts in respect of gelator ones, we were able to perform the kinetic study.

500 μ L of LB-culture dissolved in D₂O have been casted on the surface of four different samples of gel previously formed. The vials were kept at 37 °C and 250 μ L of LB-culture have been taken at 0.17, 1, 2, and 24 h. The LB-culture taken was then added to a proper amount of reference compound (3 mg) and diluted until a volume of 750 μ L of D₂O was reached. The samples, so prepared, were used to record ¹H NMR spectra.

2. 1. General procedure for the synthesis of the neutral precursor btp

1,3,5-Tris(pyrrolidinemethylen)benzene (btp). The compound was obtained by modifying a procedure reported in the literature.⁴

Pyrrolidine (5.98 g; 0.084 mol) was dissolved in CH₃CN (360mL) at room temperature. Then 1,3,5-tris(bromomethyl)benzene (5 g, 0.014 mol) was added to the solution. The reaction mixture was stirred at room temperature for 3 h under Ar atmosphere.

[4] M. Komiyama, S. Kina, K. Matsumura, J. Sumaoka, S. Tobey, V. M. Lynch and E. Anslyn, *J. Am. Chem. Soc.* **2002**, *124*, 13731-13736.

The mixture was concentrated in vacuo and the residue was dissolved in CHCl_3 (1 L) and it was washed with water (6 x 100 mL) until the neutrality of the pH. The organic layer was dried with Na_2SO_4 and it was concentrated in vacuo.

Yield 72%. Brown oil. $^1\text{H-NMR}$ (300 MHz; CD_3OD); δ (ppm) = 1.81 (dd, $J^1_{\text{H-H}} = 3.3$ Hz, $J^2_{\text{H-H}} = 6.6$ Hz, 12 H); 2.55 (t, $J_{\text{H-H}} = 5.1$ Hz, 12 H); 3.64 (s, 6 H); 7.25 (s, 3 H). $^{13}\text{C-NMR}$ (250 MHz; CD_3OD); δ (ppm) = 24.1; 54.9; 61.3; 130.5; 139.7. Elemental anal. calcd (%) for $\text{C}_{21}\text{H}_{33}\text{N}_3$ (327.51): C, 77.01; H, 10.16; N, 12.83. Found: C, 76.82; H, 10.19; N, 12.87%.

2. 2. General procedure for the synthesis of the dipyrrolidinium dibromide salt

To a stirred solution of 1,3,5-tris(pyrrolidinemethyl)-benzene (3.29 g; 0.01 mol), in CH_3CN (150 mL) a solution of 1-bromooctane (3.5 mL; 0.02 mol) in CH_3CN (30 mL) was added dropwise. The reaction mixture was stirred at 90 °C for 48 h under Ar atmosphere.

Then the solvent was concentrated in vacuo. The residue was washed with diethyl ether (4 x 100 mL) under ultrasound irradiation.

1-[N-Pyrrolidylmethyl]-3,5-di-[N,N-octylpyrrolidylmethyl]-benzene dibromide [2C₈btp][Br]₂. (Yield 97%. Brown solid. m. p.: 54.1 °C. $^1\text{H-NMR}$ (300 MHz; $\text{DMSO} [d_6]$); δ (ppm) = 0.87 (m, 6 H); 1.30 (m, 18 H); 1.96 (m, 8 H); 2.28 (m, 6 H); 2.69 (m, 4 H), 3.22 (m, 6 H); 3.66 (m, 6 H); 3.88 (m, 2 H); 4.67 (m, 4 H); 4.92 (m, 4 H); 7.67 (m, 2 H); 7.94 (m, 1 H). $^{13}\text{C-NMR}$ (400 MHz; $\text{DMSO} [d_6]$); δ (ppm) = 13.9; 20.9; 22.0; 22.4; 22.5; 22.9; 23.1; 25.9; 26.1; 28.5; 31.2; 53.4; 58.4; 60.3; 60.7; 116.2; 129.6; 130.2; 138.2. ESI-MS: m/z (+): 553; m/z (-): 79, 81. Elemental anal. calcd (%) for $\text{C}_{37}\text{H}_{67}\text{Br}_2\text{N}_3$ (713.76): C, 62.26; H, 9.46; N, 5.89. Found: C, 62.15; H, 9.43; N, 5.92%.

2. 3. General procedure for anion exchange on resin as reported in Chapter 1

1-[N-Pyrrolidylmethyl]-3,5-di-[N,N-octylpyrrolidylmethyl]-benzene-1,5-naphthalenedisulfonate [2C₈btp][1,5-nds]. Yield 97%. Orange solid. m. p.: 128.7–131.4 °C. $^1\text{H-NMR}$ (300 MHz; $\text{DMSO} [d_6]$); δ (ppm) = 0.94 (t, $J_{\text{H-H}} = 6.3$ Hz, 6 H); 1.34 (m, 20 H); 1.79 (m, 8 H); 2.09 (m, 10 H); 2.61 (m, 4 H); 3.07 (m, 4 H); 3.48 (m, 8 H); 3.76 (m, 2 H); 4.53 (m, 4 H); 7.44 (d, $J_{\text{H-H}} = 7.2$ Hz, 2 H); 7.69 (m, 3 H); 7.98 (d, $J_{\text{H-H}} = 7.2$ Hz, 2 H); 8.93 (d, $J_{\text{H-H}} = 8.4$ Hz, 2 H). $^{13}\text{C-NMR}$ (250 MHz; $\text{DMSO} [d_6]$); δ (ppm) = 14.3; 21.2; 22.4; 22.7; 23.4; 26.2;

26.4; 29.0; 31.1; 31.6; 53.8; 60.7; 61.1; 71.2; 116.2; 122.9; 123.2; 123.3; 123.4; 124.2; 124.3; 129.4; 129.9. ESI-MS: m/z (+): 840; total mass = 840.5034; calculated mass = 840.5019. Elemental anal. calcd (%) for $C_{47}H_{63}N_3O_6S_2$ (840.23): C, 67.18; H, 8.76; N, 5.00. Found: C, 67.02; H, 8.73; N, 5.03%.

1-[N-Pyrrolidylmethyl]-3,5-di-[N,N-octylpyrrolidylmethyl]-benzene *2,6-naphthalenedisulfonate*
[2C₈btp][2,6-nds]. 2,6-Naphthalenedisulfonic acid was obtained by elution of a water solution of the corresponding sodium salt through an Amberlite IR 120 plus column. Yield 98%. Orange solid. m. p.: 135.3–138.4 °C. ¹H-NMR (300 MHz; DMSO [d₆]); δ (ppm) = 0.92 (t, J_{H-H} = 4.8 Hz, 6 H); 1.31 (m, 20 H); 1.82 (m, 6 H); 2.12 (m, 8 H); 2.61 (m, 4 H); 3.11 (m, 4 H); 3.41 (m, 8 H); 3.55 (m, 2 H); 4.59 (m, 4 H); 7.74 (m, 5 H); 7.76 (d, J_{H-H} = 8.4 Hz, 2 H); 7.93 (d, J_{H-H} = 8.7 Hz, 2 H); 8.15 (s, 2 H). ¹³C-NMR (250 MHz; DMSO [d₆]); δ (ppm) = 14.3; 21.3; 22.4; 22.7; 23.4; 26.3; 28.9; 29.0; 31.0; 31.6; 53.8; 58.7; 60.6; 61.0; 116.2; 122.9; 123.3; 123.5; 124.1; 124.6; 128.4; 132.2; 146.3. ESI-MS: m/z (+): 840; m/z (-): 143; total mass = 840.5021; calculated mass = 840.5019. Elemental anal. calcd (%) for $C_{47}H_{63}N_3O_6S_2$ (840.23): C, 67.18; H, 8.76; N, 5.00. Found: C, 67.05; H, 8.74; N, 5.05%.

3. 1. Procedure for the synthesis of neutral precursors diimidazole-methylenbenzene

Imidazole (3.67 g, 0.054 mol) and potassium hydroxide (6.0 g, 0.11 mol) were dissolved in acetonitrile (400 mL) and stirred for 2 h at room temperature. Then α,α' -*p*-dibromoxylene or α,α' -*m*-dibromoxylene (7.0 g, 0.027 mol) was added to the mixture. The reaction mixture was stirred at room temperature for 1.5 h. The mixture was filtered through a Hirsch funnel to remove insoluble salts and the filtrate was concentrated in vacuo at 40 °C. The residue was dissolved in $CHCl_3$ (1 L) and was washed with water (4×150 mL) until the aqueous layer was neutral to pH paper. The organic layer was dried over anhydrous Na_2SO_4 and was concentrated in vacuo.

1,4-bis[(1H-imidazol-1-yl)methylene]benzene: yield 88%; white powder; m.p. = 148-150 °C; ¹H NMR (300 MHz; DMSO [d₆]): δ = 5.22 (s, 4 H); 6.94 (s, 2 H); 7.21 (s, 2 H); 7.29 (s, 4 H); 7.79 (s, 2 H). ¹³C NMR (300 MHz, DMSO [d₆]): δ = 48.9; 118.7; 127.1; 127.1; 127.2; 136.7. Elemental Anal. Calcd (%) for $C_{14}H_{14}N_4$ (238.29): C, 70.57; H, 5.92; N, 23.51. Found: C, 70.52; H, 5.96; N, 23.43.

1,3-bis[(1H-imidazol-1-yl)methylene]benzene: yield 56%; light yellow powder; m.p. = 85-87 °C; ¹H NMR (300 MHz, DMSO [d₆]): δ = 5.23 (s, 4 H); 6.95 (s, 2 H); 7.21 (m, 5 H); 7.38 (m, 1 H); 7.78 (s, 2 H). ¹³C NMR (300 MHz, DMSO [d₆]): δ = 49.5; 119.6; 126.8; 126.9; 128.9; 129.2; 137.5; 138.4. Elemental Anal. Calcd (%) for C₁₄H₁₄N₄ (238.29): C, 70.57; H, 5.92; N, 23.51. Found: C, 70.62; H, 5.92; N, 23.42.

3. 2. Procedure for the synthesis of bromide salts precursors

To a stirred solution of neutral precursor, (2.85 g; 0.012 mol) in CH₃CN (150 mL) was added drop-wise a solution of 1-bromododecane (6 g; 0.024 mol) in CH₃CN (30 mL). The reaction mixture was stirred at 90 °C for 48 h under Ar atmosphere. After concentration in vacuo, the residue was washed with diethyl ether (4 × 100 mL) under sonication.

3,3'-di-n-dodecyl-1,1' [1,4-phenylenedimethylene]diimidazolium dibromide: yield: 75%; white solid. m. p.: 163.4-169.8 °C. ¹H NMR (300 MHz, DMSO [d₆]): δ (ppm) = 0.84 (t, J = 5.73 Hz, 6 H); 1.23 (m, 36 H); 1.77 (m, 4 H); 4.16 (t, J = 7.0 Hz, 4 H); 5.44 (s, 4 H); 7.47 (s, 4 H); 7.83 (s, 4 H); 9.44 (s, 2 H). ¹³C NMR (300 MHz, DMSO [d₆]): δ (ppm) = 14.3; 22.5; 25.9; 28.7; 29.1; 29.2; 29.3; 29.4; 29.6; 31.1; 31.6; 49.3; 51.7; 122.9; 123.2; 129.3; 135.6; 136.3. Anal. Calcd. for C₃₈H₆₄Br₂N₄ (736.75) C, 61.93; H, 8.76; N, 7.61. Found: C, 61.80; H, 8.72; N, 7.64.

3,3'-di-n-dodecyl-1,1' [1,3-phenylenedimethylene]diimidazolium dibromide: yield: 82%; light yellow waxy solid. ¹H NMR (300 MHz, DMSO [d₆]): δ (ppm) = 0.90 (t, J = 7.52 Hz, 6 H); 1.29 (m, 36 H); 1.85 (m, 4 H); 4.24 (t, J = 8.64 Hz, 4 H); 5.52 (s, 4 H); 7.50 (m, 4 H); 7.91 (s, 4 H); 9.50 (s, 2 H). ¹³C NMR (300 MHz, DMSO [d₆]): δ (ppm) = 19.8; 28.0; 31.4; 34.3; 34.6; 34.7; 34.7; 34.9; 34.9; 35.2; 37.2; 54.9; 57.5; 126.5; 128.4; 128.7; 134.4; 135.6; 141.5; 142.2. Anal. Calcd. for C₃₈H₆₄Br₂N₄ (736.75) C, 61.93; H, 8.76; N, 7.61. Found: C, 62.10; H, 8.73; N, 7.53.

3. 3. General procedure for anion exchange on resin as reported in Chapter 1

3,3'-di-n-dodecyl-1,1' [1,4-phenylenedimethylene]diimidazolium 1,4-benzendicarboxylate [p-C₁₂im][1,4-bdc]: yield 96%; white solid; m. p. = 102 °C. ¹H NMR (300 MHz, DMSO

[d₆]: δ = 0.90 (t, J = 6.6 Hz, 6 H); 1.30 (m, 36 H); 1.83 (m, 4 H); 4.24 (t, J = 7.2 Hz, 4 H); 5.54 (s, 4 H); 7.51 (s, 4 H); 7.79 (s, 4 H); 7.91 (dd, 4 H, J = 9.9 Hz); 10.01 (s, 2 H) ppm. ¹³C NMR (300 MHz; DMSO [d₆]): δ = 14.0; 22.2; 25.6; 28.4; 28.8; 28.8; 28.9; 29.0; 29.1; 29.4; 31.4; 49.0; 51.4; 122.6; 122.9; 127.9; 128.9; 135.7; 137.2; 169.2; 191.2 ppm. Anal. Calcd. for C₄₆H₆₈N₄O₄ (740.52) C, 74.55; H, 9.25; N, 7.56. Found: C, 74.63; H, 9.21; N, 7.59.

3,3'-di-n-dodecyl-1,1'[1,4-phenylenedimethylene]diimidazolium 2,6-naphthalendicarboxylate [p-C₁₂im][2,6-ndc]: yield 98%; light yellow solid; m. p. = 142 °C. ¹H NMR (300 MHz, DMSO [d₆]): δ = 0.89 (t, J = 6 Hz, 6 H); 1.25 (m, 36 H); 1.82 (m, 4 H); 4.23 (t, J = 6.9 Hz, 4 H); 5.55 (s, 4 H); 7.53 (s, 4 H); 7.88 (dd, J¹_{H-H} = 13.8 Hz, J²_{H-H} = 2.7 Hz, 6 H); 8.04 (d, J = 8.4 Hz, 2 H); 8.45 (s, 2 H); 9.99 (s, 2 H) ppm. ¹³C NMR (300 MHz; DMSO [d₆]): δ = 14.0; 22.2; 25.6; 28.4; 28.8; 28.9; 29.4; 28.9; 29.1; 29.4; 31.4; 49.1; 51.5; 122.6; 122.9; 126.8; 127.6; 128.3; 129.0; 133.3; 135.6; 136.8; 168.6 ppm. Anal. Calcd. for C₅₀H₇₀N₄O₄ (790.54) C, 75.91; H, 8.92; N, 7.08. Found: C, 75.83; H, 8.95; N, 7.10.

tri[3,3'-di-n-dodecyl-1,1'[1,4-phenylenedimethylene]diimidazolium] ditrimesate [p-C₁₂im]₃[Trim]₂: yield 83%; white powder; m. p. = 86 °C. ¹H NMR (250 MHz, CD₃OD [d₄]): δ = 0.89 (t, J = 3.1 Hz, 18 H); 1.28 (m, 108 H); 1.88 (m, 12 H); 4.21 (t, J = 7.4 Hz, 12 H); 5.37 (s, 12 H); 7.35 (s, 12 H); 7.59 (dd, J¹ = 12.4 Hz, J² = 1.6 Hz, 12 H); 8.52 (s, 6 H) ppm. ¹³C NMR (250 MHz; CD₃OD [d₄]): δ = 14.4; 23.7; 27.3; 30.1; 30.4; 30.5; 30.6; 30.7; 30.8; 31.1; 33.1; 51.0; 53.5; 123.8; 124.1; 130.4; 130.4; 132.8; 136.3; 139.0; 174.7 ppm. Anal. Calcd. for C₁₃₂H₁₉₈N₁₂O₁₂ (2145.06) C, 73.91; H, 9.30; N, 7.84. Found: C, 73.78; H, 9.24; N, 7.81.

tri[3,3'-di-n-dodecyl-1,1'[1,4-phenylenedimethylene]diimidazolium] dicitrate [p-C₁₂im]₃[Cit]₂: yield 87%; white powder; m. p.: 111 °C. ¹H NMR (300 MHz, CD₃OD [d₄]): δ = 0.89 (t, J = 7.38 Hz, 18 H); 1.32 (m, 108 H); 1.90 (m, 12 H); 2.66 (dd, J¹ = 21.4 Hz, J² = 17.9 Hz, 8 H); 4.21 (t, J = 7.4 Hz, 12 H); 5.46 (s, 12 H); 7.50 (s, 12 H); 7.64 (dd, J¹ = 6.5 Hz, J² = 1.75 Hz, 12 H) ppm. ¹³C NMR (250 MHz, CD₃OD [d₄]): δ = 14.4; 23.7; 27.3; 30.1; 30.3; 30.5; 30.5; 30.7; 30.7; 31.1; 33.0; 51.0; 53.6; 75.0; 123.8; 124.0; 130.6; 136.5; 178.1; 181.1; 193.5 ppm. Anal. Calcd. for C₁₂₆H₂₀₂N₁₂O₁₄ (2107.03) C, 71.76; H, 9.65; N, 7.97. Found: C, 71.95; H, 9.62; N, 7.95.

di[3,3'-di-n-dodecyl-1,1' [1,4-phenylenedimethylene]diimidazolium] ethylenediaminetetraacetate [p-C₁₂im]₂[EDTA]: yield 98%; white solid; m. p. = 105 °C. ¹H NMR (400 MHz, DMSO [d₆]): δ = 0.82 (t, J = 6.8 Hz, 12 H); 1.20 (m, 72 H); 1.75 (m, 8 H); 2.74 (s, 4 H); 3.36 (s, 8 H); 4.13 (t, J = 7.2 Hz, 8 H); 5.41 (s, 8 H); 7.44 (s, 8 H); 7.78 (s, 8 H); 9.36 (s, 4 H) ppm. ¹³C NMR (400 MHz; DMSO [d₆]): δ = 14.4; 22.5; 25.9; 28.8; 29.1; 29.2; 29.3; 29.4; 29.7; 31.7; 49.4; 51.6; 51.7; 51.8; 56.6; 122.9; 123.3; 129.3; 135.8; 136.6; 172.8 ppm. Anal. Calcd. for C₈₆H₁₄₀N₁₀O₈ (1442.09) C, 71.63; H, 9.79; N, 9.71. Found: C, 71.75; H, 9.81; N, 9.68.

3,3'-di-n-dodecyl-1,1' [1,3-phenylenedimethylene]diimidazolium 1,4-benzendicarboxylate [m-C₁₂im][1,4-bdc]: yield 96%; white solid; m. p. = 92 °C. ¹H NMR (300 MHz, DMSO [d₆]): δ = 0.90 (t, J = 7.4 Hz, 6 H); 1.27 (m, 36 H); 1.83 (m, 4 H); 4.22 (t, J = 8.6 Hz, 4 H); 5.51 (s, 4 H); 7.48 (s, 4 H); 7.78 (s, 1 H); 7.87 (s, 5 H); 7.94 (s, 2 H); 9.89 (s, 2 H) ppm. ¹³C NMR (250 MHz; DMSO [d₆]): δ = 14.1; 22.2; 25.7; 28.5; 28.9; 29.0; 29.1; 29.1; 29.2; 29.5; 31.5; 49.1; 51.7; 122.7; 122.8; 128.4; 128.8; 129.1; 129.7; 135.9; 137.0; 139.3; 168.8 ppm. Anal. Calcd. for C₄₆H₆₈N₄O₄ (740.52) C, 74.55; H, 9.25; N, 7.56. Found: C, 74.50; H, 9.27; N, 7.58.

3,3'-di-n-dodecyl-1,1' [1,3-phenylenedimethylene]diimidazolium 2,6-naphthalendicarboxylate [m-C₁₂im][2,6-ndc]: yield 98%; light yellow solid; m. p. = 140 °C. ¹H NMR (300 MHz, DMSO [d₆]): δ = 0.89 (t, J = 7.4 Hz, 6 H); 1.67 (m, 36 H); 1.80 (m, 4 H); 4.20 (t, J = 8.5 Hz, 4 H); 5.52 (s, 4 H); 7.48 (s, 2 H); 7.91 (dd, J¹=24.5 Hz, J²=13.6 Hz, 8 H); 8.05 (d, J = 10.7 Hz, 2 H); 8.46 (s, 2 H); 9.99 (s, 2 H) ppm. ¹³C NMR (300 MHz; DMSO [d₆]): δ = 14.1; 22.2; 25.7; 28.6; 28.8; 29.0; 29.1; 29.2; 29.5; 29.4; 31.4; 49.1; 51.8; 122.7; 122.8; 126.9; 127.6; 128.4; 128.9; 129.3; 133.4; 136.0; 137.2; 169.0 ppm. Anal. Calcd. for C₅₀H₇₀N₄O₄ (790.54) C, 75.91; H, 8.92; N, 7.08. Found: C, 75.85; H, 8.89; N, 7.11.

tri[3,3'-di-n-dodecyl-1,1' [1,3-phenylenedimethylene]diimidazolium] ditrimesate [m-C₁₂im]₃[Trim]₂: yield 86%; yellow solid; m. p. = 64 °C. ¹H NMR (250 MHz, CD₃OD [d₄]): δ = 0.90 (t, J = 6.5 Hz, 18 H); 1.30 (m, 108 H); 1.88 (m, 12 H); 4.20 (t, J = 7.4 Hz, 12 H); 5.37 (s, 12 H); 7.37 (m, 9 H); 7.48 (s, 3 H); 7.60 (m, 12 H); 8.58 (s, 6 H) ppm. ¹³C NMR (250 MHz;

CD₃OD [d₄): δ = 17.5; 26.8; 30.4; 33.2; 33.5; 33.6; 33.7; 33.8; 33.9; 34.2; 36.1; 54.1; 56.87; 126.9; 127.1; 131.8; 133.3; 133.4; 134.1; 134.4; 139.6; 142.7; 177.6 ppm. Anal. Calcd. for C₁₃₂H₁₉₈N₁₂O₁₂ (2145.06) C, 73.91; H, 9.30; N, 7.84. Found: C, 73.85; H, 9.34; N, 7.82.

tri[3,3'-*di-n-dodecyl-1,1'*[1,3-*phenylenedimethylene*]diimidazolium] dicitrate [***m*-C₁₂im**]₃[Cit]₂: yield 73%; yellow solid; m. p. = 63 °C. ¹H NMR (250 MHz, CD₃OD [d₄): 0.89 (t, J = 6.4 Hz, 18 H); 1.27 (m, 108 H); 1.90 (m, 12 H); 2.80 (dd, J¹ = 17.4 Hz, J² = 15 Hz, 8 H); 4.24 (t, J = 7.3 Hz, 12 H); 5.45 (s, 12 H); 7.45 (s, 9 H); 7.64 (m, 12 H); 7.82 (s, 3 H) ppm. ¹³C NMR (250 MHz; CD₃OD [d₄): δ = 14.4; 23.7; 27.4; 30.2; 30.5; 30.5; 30.6; 30.7; 31.2; 33.1; 50.9; 53.6; 76.8; 123.7; 123.7; 129.5; 130.3; 131.1; 137.0; 179.9; 192.9 ppm. Anal. Calcd. for C₁₂₆H₂₀₂N₁₂O₁₄ (2107.03) C, 71.76; H, 9.65; N, 7.97. Found: C, 71.89; H, 9.67; N, 7.99.

di[3,3'-*di-n-dodecyl-1,1'*[1,3-*phenylenedimethylene*]diimidazolium] ethylenediaminetetraacetate [***m*-C₁₂im**]₂[EDTA]: yield 97%; light yellow waxy solid; m. p. = 71 °C. ¹H NMR (400 MHz, DMSO [d₆): δ = 0.82 (t, J = 6.8 Hz, 12 H); 1.20 (m, 72 H); 1.76 (m, 8 H); 2.75 (s, 4 H); 3.36 (s, 8 H); 4.15 (t, J = 7.2 Hz, 8 H); 5.42 (s, 8 H); 7.40 (m, 8 H); 7.81 (s, 8 H); 9.44 (s, 4 H) ppm. ¹³C NMR (400 MHz; DMSO [d₆): δ = 14.4; 22.5; 26.0; 28.8; 29.1; 29.3; 29.4; 29.4; 29.5; 29.7; 31.7; 49.4; 51.5; 52.0; 56.7; 123.0; 123.2; 128.9; 130.1; 136.0; 136.7; 172.8 ppm. Anal. Calcd. for C₈₆H₁₄₀N₁₀O₈ (1442.09) C, 71.63; H, 9.79; N, 9.71. Found: C, 71.73; H, 9.80; N, 9.67.

tri[1-*butyl-3-methylimidazolium*] citrate [**bmim**]₃[Cit]: yield 96%; light yellow oil; ¹H NMR (400 MHz, CDCl₃ [d₁): 0.95 (t, J = 8 Hz, 9 H); 1.37 (sext, J = 8 Hz, 6 H); 1.87 (q, J = 4 Hz, 6H); 2.73 (s, 4 H); 4.09 (s, 9 H); 4.32 (t, J=8 Hz, 6 H); 7.23 (s, 3 H); 7.24 (s, 3 H); 7.28 (s, 3 H) ppm. ¹³C NMR (400 MHz; CDCl₃ [d₁): δ = 13.7; 19.2; 332.0; 36.0; 47.3; 48.7; 74.4; 122.5; 123.8; 138.2; 175.3; 178.9 ppm. Anal. Calcd. for C₃₀H₅₀N₆O₇ (606.75) C, 59.39; H, 8.31; N, 13.85. Found: C, 58.53; H, 8.34; N, 13.89.

3,3'-di-n-dodecyl-1,1' [1,4-phenylenedimethylene]diimidazolium di-bistrifluoromethanesulfonylimide [p-C₁₂im][NTf₂]₂: The product was obtained according the classical anion exchange reported procedure.^{1a}

Yield 45%; white solid; m. p. = 73 °C. ¹H NMR (400 MHz, DMSO [d₆]); δ (ppm): 0.83 (t, J = 4 Hz, 6 H); 1.24 (m, 36 H); 1.75 (m, 4 H); 4.14 (t, J = 8 Hz, 4 H); 5.40 (s, 4 H); 7.44 (s, 4 H); 7.77 (d, J = 12 Hz, 4 H); 9.27 (s, 2 H). ¹³C NMR (400 MHz; DMSO [d₆]); δ (ppm): 14.4; 22.5; 25.9; 28.8; 29.2; 29.2; 29.3; 29.4; 29.4; 29.8; 31.7; 49.4; 51.9; 123.0; 123.3; 129.3; 135.8; 136.6 ppm. Anal. Calcd. for C₄₂H₆₄F₁₂N₆O₈S₄ (1136.35) C, 44.36; H, 5.67; N, 7.39. Found: C, 44.23; H, 5.65; N, 7.37.

4. 1. Salt for two-component hydrogels

3,3'-di-n-dodecyl-1,1' [1,4-phenylenedimethylene]diimidazolium di-hexanfluorophosphate [p-C₁₂im][PF₆]₂: yield 55 %; white solid; m. p. = 117.1–121.8 °C. ¹H NMR (300 MHz, CD₃OD [d₄]): δ = 0.90 (t, J = 6.6 Hz, 6 H); 1.31 (m, 36 H); 1.88 (m, 4 H); 4.22 (t, J = 7.2 Hz, 4 H); 5.44 (s, 4 H); 7.49 (s, 4 H); 7.60 (dd, J = 11.7, 1.8 Hz, 4 H) ppm. ¹³C NMR (250 MHz, CD₃OD [d₄]): δ = 15.1; 24.4; 27.9; 30.8; 31.1; 31.2; 31.3; 31.4; 31.8; 33.7; 51.7; 54.3; 124.4; 124.7; 131.4; 131.6; 137.1 ppm. C₃₈H₆₄F₁₂N₄P₂ (866.87): Anal. Calcd. for: C, 52.65; H, 7.44; P, 7.15; F, 26.30; N, 6.46. Found: C, 52.85; H, 7.50; P, 7.05; F, 26.00; N, 6.40.

5. 1. Aminoacid based DOSs

3,3'-di-N-dodecyl-1,1-(1,4-phenylenedimethylene) diimidazolium di-L-isoleucinate [p-C₁₂im][L-Ile]₂: yield 97 %; hygroscopic white solid; m.p.: 73.2 °C. ¹H-NMR (300 MHz; DMSO [d₆]); δ = 0.72 (m, 12 H); 0.78 (t, J_{H-H}=6 Hz, 6 H); 0.98 (m, 4 H); 1.24 (m, 36 H); 1.35 (m, 2 H); 1.78 (m, 4 H); 2.77 (m, 2 H); 4.17 (t, J_{H-H}=9 Hz, 4 H); 5.48 (s, 4 H); 7.49 (s, 4 H); 7.83 (d, J_{H-H}=6 Hz, 4 H); 9.89 (s, 2 H) ppm. ¹³C-NMR (300 MHz; DMSO [d₆]); δ = 11.3, 14.1, 15.0, 22.7, 25.1, 27.1, 29.3, 29.6, 30.1, 31.9, 36.1, 50.2, 52.7, 59.1, 120.9, 122.1, 127.2, 134.3, 138.1, 174.7 ppm. Elemental Anal. Calcd (%) for C₅₀H₈₈N₆O₄ (837.3): C, 71.73; H, 10.59; N, 10.04. Found: C, 71.55; H, 10.54; N, 9.99.

[1] a) L. Cammarata, S. G. Kazarian, P. A. Salter and T. Welton, *Phys. Chem. Chem. Phys.* **2001**, *3*, 5192-5200.

3,3'-di-N-dodecyl-1,1-(1,4-phenylenedimethylene) diimidazolium di-L-phenylalaninate [p-C₁₂im][L-Phe]₂: yield 95 %; waxy orange solid; m.p.: 79.9 °C. ¹H-NMR (300 MHz; DMSO [d₆]); δ = 0.85 (t, J_{H-H}=9 Hz, 6 H); 1.23 (m, 36 H); 1.77 (m, 4 H); 2.97 (m, 4 H); 4.15 (t, J_{H-H}=6 Hz, 4 H); 4.45 (m, 2 H); 5.42 (s, 4 H); 7.17 (m, 10 H); 7.40 (s, 4 H); 7.81 (s, 4 H); 9.53 (s, 2 H) ppm. ¹³C-NMR (300 MHz; DMSO [d₆]); δ = 14.1, 22.7, 27.1, 29.3, 29.6, 30.1, 31.9, 37.3, 50.2, 52.7, 56.7, 121.4, 122.3, 125.9, 127.3, 127.7, 128.6, 134.3, 138.1, 140.8, 175.2 ppm. Elemental Anal. Calcd (%) for C₅₆H₈₄N₆O₄ (905.3): C, 74.30; H, 9.35; N, 9.28. Found: C, 74.21; H, 9.32; N, 9.25.

3,3'-di-N-dodecyl-1,1-(1,4-phenylenedimethylene) diimidazolium di-D-alanyl-D-alaninate [p-C₁₂im][D-Ala-D-Ala]₂: yield 96 %; white solid; m.p.: 105.3 °C. ¹H-NMR (300 MHz; DMSO [d₆]); δ = 0.84 (m, 6 H); 1.12 (m, 12H); 1.24 (m, 36 H); 1.78 (m, 4 H); 3.20 (m, 2 H); 3.61 (m, 2 H); 4.17 (t, J_{H-H}=6 Hz, 4 H); 5.45 (s, 4 H); 7.48 (s, 4 H); 7.82 (d, J_{H-H}=6 Hz, 4 H); 9.56 (s, 2 H) ppm. ¹³C-NMR (300 MHz; DMSO [d₆]); δ = 14.5, 19.8, 22.1, 22.4, 26.0, 28.5; 29.2, 29.33, 29.45, 29.6, 29.7, 31.4, 49.0, 50.8, 50.13, 51.8, 122.9, 123.2, 129.4, 135.6, 137.0, 174.1 ppm. Elemental Anal. Calcd (%) for C₅₀H₈₆N₈O₆ (895.3): C, 67.08; H, 9.68; N, 12.52. Found: C, 66.96; H, 9.65; N, 12.47.

Conclusions

Several policationic organic salts have been taken into account in this dissertation, the wide range of cation and anion combinations allowed modulating their properties in order to apply in different fields.

DOSs have been synthesised in not more than three synthetic steps, obtaining good yields in each step. In particular, the wide variety of DOSs was given by varying the anions, this procedure involved an anion exchange on a basic resin, procedure in agreement with Green Chemistry principles as it required the use of water and did not generate by-products.

All DOSs synthesised presented good thermal stability in terms of decomposition temperature, and the complexity of their structure led to peculiar melting processes that sometimes clearly indicated the presence of polymorphs.

The dissertation is mainly focused on two different classes of DOSs, the functionalised and the unfunctionalised ones.

The first class includes DOSs with melting temperature below 100 °C, that can be defined as TSILs. An aromatic spacer bearing diimidazolium dications and a neutral imidazole as basic functionality characterized them. The higher flexibility of the cationic structure leads to three conformational isomers in solution. Interestingly, their presence in solution could be varied as function of counter anion used. Indeed, monoanions and flexible dianions favour the interchange from one isomer to another, awarding a degree of freedom to the cationic structure. On the other hand, aromatic and rigid dianions seem to limit the flexibility of the cationic structure avoiding the presence of conformers in solutions. In addition, different anions used modulate also thermal properties of the TSILs, determined by TGA and DSC measurements.

The catalytic ability of these salts has been tested applying them as reaction media in the study of two base-catalysed organic reactions: the mononuclear rearrangement of heterocycles of (*Z*)-phenylhydrazone of 3-benzoyl-5-phenyl-1,2,4-oxadiazole into the corresponding triazole and the Michael addition of malonitrile to *t*-chalcone.

The catalytic and the recycling ability of the TSILs have been proved for the first reaction. Therefore the mononuclear rearrangement of heterocycles has been performed with good yields and reaction times using only TSILs as solvent and catalyst reaction. This represents a great challenge in terms of chemical sustainability to perform organic reactions. Interestingly, the higher catalytic activity is not only due to the presence of the basic functionality, but is probably due to a combined action of neutral functionality and high structural order of the cationic structure. Furthermore, the catalytic ability of TSILs confirmed the influence of anion, in terms of flexibility, coordination ability or aromaticity, on the ILs properties. Indeed, monoanions and flexible dianions were the best reaction media as they favoured the interactions between the cationic unit and the transition state of the reaction. On the other hand, rigid dianions limited this interaction, leading to really low reaction yields also in long reaction times.

Having in mind results obtained for the mononuclear rearrangement of heterocycles, we further analysed the catalytic ability of TSILs carrying out the Michael addition. For this study, TSILs that exerted the best catalytic activity in the previous reaction and TSILs presenting chiral mono- and dianions have been tested. Also in this case, surprising results have been obtained in terms of reaction times and reaction yields, evidencing the importance of the catalyst directly linked to the IL. Indeed, some TSILs allowed the outcome of the reaction in just 10 minutes, following the atom-economy of the reaction and utilizing the same solvent and catalyst. The systems studied can be considered a great challenge for the Michael addition taken into account, as results reported in literature in terms of reaction times (average of 72 h), addition of catalyst and additive are worst compared to our less reactive TSIL. Unfortunately, our systems did not allow studying stereochemical aspects of the reaction, probably due to the higher polarity of ILs.

As stated above, DOSs presenting aromatic dianions did not exert a good catalytic activity, so that, having in mind the strict interaction that occurs between these dianions and the cationic unit (NOESY experiments), we demonstrated their ability to gel in IL solutions. In this case, we were also interested in evaluating how a different cationic unit could influence the gelation process, for this reason we have synthesised dipyrrolidinium salts bearing pyrrolidine as basic functionality. Interestingly, DOSs were able to gel ILs following a complementarity criterion between aromatic and aliphatic structure of gelators and IL cations.

The properties of the materials obtained were strongly dependent on the combination of cation and anion of salt used as gelator and on solvent nature. In particular, salt presenting aromatic cations and anions exhibited a higher tendency to gel, forming more responsive ionogels to external stimuli. All gels obtained present high thermal stability and a peculiar conductivity, surprisingly higher than the one of the ILs, so they can be considered as perfect candidates for their use in systems like DSSCs. Having also in mind the presence of the basic functionality tethered on the cationic unit, these soft materials could be also applied as alternative media for catalytic studies.

Furthermore, the class of unfunctionalised DOSs has been taken into account in order to further study the gelling ability of diimidazolium organic salts that differ for the isomeric substitution on the spacer (*para* or *meta*). In particular, to have further insights on the anion effect of the gelator we have considered both stoichiometric and non-stoichiometric organic salts.

These salts were able to gel in organic and IL solutions, and the properties of the material were, once again, dependent on the nature of gelator and solvents. The use of several techniques allowed having a deep insight on gel properties, like thermal stability, mechanical properties, self-healing ability and opacity. In particular, *meta*-salts were able to harden glycerol and ILs for the first time, probably thank to a positive effect exerted by a different stoichiometry between cation and anion. However, properties of gels formed by *para*-salts were in general better than the ones of materials formed by the corresponding *meta*-salts. In addition ionogels were stronger and more thermal stable than organogels, but the latter ones were obtained at lower CGC values. Interestingly, unexpected trends in kinetics of gel formation were observed and they probably indicate a rearrangement of gel aggregates. The supramolecular interactions among gelator structures, that give rise to the gels, seem to be hydrogen bonds and π - π stacking.

The gelling ability of *para*-diimidazolium salts presenting monoanions has been also studied in CD's solutions. In this case, the gel formation seems due to a previous host-guest interaction between salt and CD. So that, firstly, a deep study on the formation of the complex has been carried out, subsequently, properties of gels were analysed as well. In this case, properties of two-component hydrogels vary in relation of DOSs, CDs and their ratio. It has been demonstrated that the gel formation occurred after the formation

of the pseudo-rotaxane complex formed between salt and CD. These supramolecular complexes organize to give fibrous aggregates that subsequently rearrange to form the typical three-dimensional network of the soft materials.

An innovative formation of two-component gels formed by CD not involving polymers as guest molecules and CD derivatisation has been performed. Indeed, data collected showed that LMWGs might also favour the gelation of native CDs, simply changing the features of soft materials by the introduction of minor structural changes, such as lengthening the alkyl chain of the cation or increasing the coordination ability of the anion.

Finally, we have demonstrated the gelling ability of some aminoacid based diimidazolium salts in ILs and buffer saline water solution. Interestingly, the antimicrobial activity of the salts themselves and of the corresponding gel phases has been proved. Properties of these gels changed also in relation of anion of gelator and solvent used, it is worth of noting that the antimicrobial activity of gel is characteristic of the supramolecular soft-material and it is not due only to the activity of the gelator.

In general, we have synthesised and characterised several policationic organic salts and we have demonstrated how, upon small modifications, they can be applied in fields that extend from catalysis, to electrolyte systems or biological and pharmaceutical applications.

List of abbreviations and acronyms

<i>Abbreviations or acronyms</i>	<i>Full names</i>
1-PrOH	1-Propanol
ACN	Acetonitrile
CD	Cyclodextrin
CGC	Critical Gelation Concentration
D	Dissipation factor
DILs	Dicationic Ionic Liquids
DMF	Dimethylformamide
DMSO	Dimethyl sulfoxide
DOSs	Dicationic Organic Salts
DSC	Differential Scanning Calorimetry
DSSCs	Dye-Sensitized-Solar-Cells
DTG	Derivative of Thermogram
<i>E. coli</i>	<i>Escherichia coli</i>
ESI-MS	Electro-Spray Mass Spectrometry
G'	Storage modulus
G''	Loss modulus
H_-	Basicity function
HPLC	High Performance Liquid Chromatography
I_c	Gel formation intensity
ILs	Ionic Liquids
I_m	Fibrillar intermediate formation intensity
LB	<i>Luria-Bertani</i>
LMWGs	Low Molecular Weight Gelators
<i>M. luteus</i>	<i>Micrococcus luteus</i>
MeOH	Methanol
MIC	Minimal Inhibitory Concentration
NHCs	N-heterocyclic carbenes
NMR	Nuclear Magnetic Resonance
NOESY	Nuclear Overhauser Effect Spectroscopy
OD ₆₀₀	Turbidimetric evaluation of bacteria concentration in solution
OSs	Organic Salts
PBS	Phosphate-buffered saline water solution
POM	Polarizing Optical Microscopy
RLS	Resonance Light Scattering
RTILs	Room Temperature Ionic Liquids
SAFIN	Self-Assembled Fibrillar Network
SEM	Scanning Electron Microscopy
SM	Soft Material
T_d	Decomposition temperature
t_e	Gel formation time
T_g	Temperature of glass transition

TEM	Transmission Electron Microscopy
TGA	Thermogravimetric Analysis
T_{gel}	Melting temperature of gels
THF	Tetrahydrofuran
TLC	Thin Layer Chromatography
T_m	Melting temperature
t_m	Fibrillar intermediate formation time
t_n	Nucleation time
TOSs	Tricationic Organic Salts
TSILs	Task-Specific Ionic Liquids
XRD	X-Ray Diffraction
β	Anion coordination ability
γ	Yield strain
ΔC_p	Heat capacity change
ΔH_m	Variation of enthalpy of melting process
ΔS_m	Variation of entropy of melting process
η	Viscosity
θ	Optical rotation

Abbreviations of compounds

	<i>IUPAC name</i>
[bmim]	1-butyl-3-methylimidazolium
[bmpyrr]	1-butyl-3-methylpyrrolidinium
[bmpip]	1-butyl-3-methylpiperidinium
[bEt ₃ N]	butyltriethylammonium
[Bzmim]	1-benzyl-3-methylimidazolium
[Bzbim]	1-benzyl-3-butylimidazolium
[BF ₄]	tetrafluoroborate
[PF ₆]	hexafluorophosphate
[SbF ₆]	hexafluoroantimonate
[NTf ₂]	<i>N</i> -bis(trifluoromethylsulfonyl)imide
[<i>m</i> -C _n im]	3,3'-di- <i>n</i> -alkyl-1,1'-(1,3-phenylenedimethylene) diimidazolium
[<i>p</i> -C _n im]	3,3'-di- <i>n</i> -alkyl-1,1'-(1,4-phenylenedimethylene) diimidazolium
bti	trisimidazolylbenzene
[2C ₈ bti]	1-(1-imidazolylmethyl)-3,5-di[1-(3'-octylimidazolylmethyl)]benzene
[1,5-nds]	1,5-naphthalendisulfonate
[2,6-nds]	2,6-naphthalendisulfonate
[1,4-bdc]	1,4-benzendicarboxylate
[2,6-ndc]	2,6-naphtaledicarboxylate
[ad]	adipate
[sub]	suberate
[R-binaphtylphosphate]	(<i>R</i>)-(-)-1,1'-binaphtyl-2,2'-diyl phosphate
btp	trimethylenpyrrolylbenzene
[2C ₈ btp]	1-(<i>N</i> -pyrrolidylmethyl)-3,5-di(<i>N,N</i> -octylpyrrolidylmethyl)-benzene
[Trim]	Trimesate

[Cit]	Citrate
[EDTA]	Ethylenediaminetetraacetate
10Br β	Gel of 3,3'-di-n-decyl-1,1'-(1,4-phenylenedimethylene) diimidazolium dibromide and β -cyclodextrin in water
12Br β	Gel of 3,3'-di-n-dodecyl-1,1'-(1,4-phenylenedimethylene) diimidazolium dibromide and β -cyclodextrin in water
12BF $_4\alpha$	Gel of 3,3'-di-n-dodecyl-1,1'-(1,4-phenylenedimethylene) diimidazolium di-tetrafluoroborate and α -cyclodextrin in water
Fmoc	9-fluorenylmethoxycarbonyl
[L-Ile]	L-isoleucinate
[L-Phe]	L-phenylalaninate
[D-Ala-D-Ala]	D-alanyl-D-alaninate

Acknowledgements

First of all, I want to thank my advisors, Prof. Noto and Prof. D'Anna. They have always believed in me and guided me from the beginning of this experience. It was a pleasure for me being part of their research group and learning what the research is. Their experience has helped me growing professionally and personally.

A particular thank to my labmates, colleagues and friends Dr. Salvatore Marullo, Dr. Paola Vitale and Dr. Floriana Billeci. All difficulties and successes in these years have always been shared. Being in the same research group and staying together the majority part of the day has connected us every day more.

I would like to thank also all the students that during these years have attended the lab for their thesis, all technicians of STEBICEF for their kindness and patience and in particular Dr. Marco Cascino for NMR measurements.

I am grateful to Prof. Kenneth Seddon for hosting me and for giving me the possibility to collaborate with his research group at Queen's University of Belfast. In addition, the supervision of Dr. Nimal Gunaratne in Belfast gave me an important scientific support for the study of ILs.

A special thank to Prof. Richard Weiss who hosted me and gave me the possibility to closely work with him, discussing together my scientific results and teaching me new techniques and theories applied to gel studies. I want to thank also Ms. Mohan Zhang and Mr. Pasha Tabatabai for the important scientific support and in general, I am really grateful to all components of Weiss's group for the friendship reserved for me in all circumstances during my research period at Georgetown University in Washington, DC.

My acknowledgements go also to Prof. Giuseppe Lazzara for his support and collaboration for some chemical-physical measurements; to Prof. Anna Maria Puglia, Dr. Giuseppe Gallo and Dr. Alberto Sutura for performing and providing me antimicrobial tests on salts and gels; to Prof. Andrea Pace who allowed the use of some instruments obtained with project: PONA3_00053 and to Dr. Alessio Riccobono for some measurements.

Thanks to University of Palermo (2012-ATE-0405) and MIUR (FIRB2010RBFR10BF5V) for financial supports that allowed the progress of the research and my participation to PhD's Schools and Congresses, highly important for my education.

Curriculum vitae

General information: Rizzo Carla; address: via F. Lo Jacono, 10, 90144, Palermo; mail: carla.rizzo03@unipa.it; rizzo.carla@gmail.com; nationality: italian; data of birth: 15/05/1988.

Education:

August – December 2014: research period at Georgetown University, Washington, DC, U.S.A. under the supervision of Prof. Richard G. Weiss. Synthesis and properties of policationic organic salts used as LMWGs (Low-Molecular Weight Gelators) in the formation of supramolecular gels in organic solvent and ionic liquid solutions.

1 January 2013 - on going PhD Student in Chemistry: supervision of Prof. Francesca D'Anna and Prof. Renato Noto at University of Palermo, research project: "Synthesis and properties of policationic organic salts used as reaction media." Several types of dicationic organic salts have been synthesized and applied as catalysts and LMWGs.

April – November 2012: training period at Department STEMBIO Section Organic Chemistry "E. Paternò" of the University of Palermo under the supervision of Prof. Francesca D'Anna and Prof. Renato Noto. Synthesis and study of organic salts applied for the formation of supramolecular gel in ionic liquid solutions.

27 June 2012: qualifying examination to chemistry register obtained at University of Palermo.

September – December 2011: research period at QUILL (Queen's University Ionic Liquid Laboratories) of Queen's University of Belfast under the supervision of Prof. Kenneth R. Seddon and Dr. H. Q. Nimal Gunaratne. Synthesis and characterization of task specific ionic liquids.

January 2010 - March 2012: master's degree in Chemistry, curriculum "advanced methodologies of synthesis and characterization of new organic molecules", obtained the 27/03/2012 at University of Palermo with 110/110 & lode. Thesis title: "Synthesis and properties of some policationic organic salts".

June – August 2009: training period at ARPA Sicilia (Azienda Regionale Protezione Ambiente- Regional Institute for Environmental Protection)

October 2006 - February 2010: bachelor's degree in Chemistry obtained on the 25/02/2010 at University of Palermo with 104/110. Thesis title: "Dicationic Ionic

Liquids: a medium to conduct organic reactions”, developed in the Department of Organic Chemistry “E. Paternò”.

June 2005: First Certificate in English, English as a Foreign Language, Level B2 of the Common European Framework of Reference for Languages. Esol Examinations, University of Cambridge

September 2001 - June 2006: high school leaving certificate in Humanities Liceo Classico “G. Meli”, Palermo, 100/100.

Publications

1. Paola Vitale, Francesca D'Anna, Francesco Ferrante, Carla Rizzo and Renato Noto, “ π -conjugated diimidazolium salts: rigid structures to obtain organized materials”, *Phys. Chem. Chem. Phys.*, **2015**, *17*, 26903-26917.
2. Salvatore Marullo, Francesca D'Anna, Carla Rizzo, Renato Noto, “The ultrasounds–ionic liquids synergy on the copper catalysed azide–alkyne cycloaddition between phenylacetylene and 4-azidoquinoline”, *Ultrasonics Sonochem.*, **2015**, *23*, 317–323.
3. Francesca D'Anna, Carla Rizzo, Paola Vitale, Giuseppe Lazzara, Renato Noto, “Dicationic organic salts: gelators for ionic liquids”, *Soft Matter*, **2014**, *10*, 9281-9292.
4. Carla Rizzo, Francesca D'Anna, Salvatore Marullo, Renato Noto, “Task Specific Dicationic Ionic Liquids: Recyclable Reaction Media for the Mononuclear Rearrangement of Heterocycles”, *J. Org. Chem.*, **2014**, *79*, 8678-87683.
5. Francesca D'Anna, Salvatore Marullo, Paola Vitale, Carla Rizzo, Paolo Lo Meo, Renato Noto “Ionic liquid binary mixtures: Promising reaction media for carbohydrate conversion into 5-hydroxymethylfurfural”, *Appl. Cat. A: General*, **2014**, *482*, 287–293.
6. Carla Rizzo, Francesca D'Anna, Salvatore Marullo, Paola Vitale and Renato Noto, “Two-component Hydrogels formed by Cyclodextrins and Dicationic Imidazolium Salts”, *Eur. J. Org. Chem.*, **2014**, 1013-1024.
7. Francesca D'Anna, H. Q. Nimal Gunaratne, Giuseppe Lazzara, Renato Noto, Carla Rizzo and Kenneth R. Seddon, “Solution and thermal behaviour of novel dicationic imidazolium ionic liquids”, *Org. Biomol. Chem.*, **2013**, *11*, 5836-5846.

Conference communications

1. Oral communication to *Supramol 2015, XII Italian Congress of Supramolecular Chemistry, Giardini Naxos, 27-30 September 2015*: C. Rizzo, F. D'Anna, R. Noto, R. G. Weiss, “Non-stoichiometric dicationic organic salts form supramolecular gels”.
2. Poster communication to *Supramol 2015, XII Italian Congress of Supramolecular Chemistry, Giardini Naxos, 27-30 September 2015*: F. D'Anna, S. Marullo, C. Rizzo, P. Vitale, R. Noto, “Host-guest interactions between DMpillar[5]arene and fluorescent imidazolium salts”.
3. Poster communication to *Supramol 2015, XII Italian Congress of Supramolecular Chemistry, Giardini Naxos, 27-30 September 2015*: P. Vitale, F. D'Anna, S. Marullo, C. Rizzo, R.

Noto, "Two-component chiral gels: a study of properties and behaviour as recognition systems".

4. Poster communication to *Supramol 2015, XII Italian Congress of Supramolecular Chemistry, Giardini Naxos, 27-30 September 2015*: S. Marullo, F. D'Anna, C. Rizzo, P. Vitale, R. Noto, "Fully ionic metallogels from dicationic diimidazolium salts".

5. Poster communication to *XXXVI Italian National Congress of Organic Chemistry, Bologna, 13-17 September 2015*: C. Rizzo, F. D'Anna, S. Marullo, P. Vitale, R. Noto, "Task-specific dicationic ionic liquids used as reaction media for Michael addition".

6. Oral and Poster communication to *40th "A. Corbella" International Summer School on Organic Synthesis, 14-18 June 2015*: C. Rizzo, F. D'Anna, S. Marullo, P. Vitale, R. Noto, "Functionalized dicationic ionic liquids applied to the study of Michael addition".

7. Oral communication to *Sicily and Calabria Congress of Organic Chemistry, Palermo, 1 - 2 December 2014*: P. Vitale, F. D'Anna, S. Marullo, C. Rizzo, R. Noto, "Organic salts: tectons to study self-assembly processes in organic solvents".

8. Poster communication to *5th EuCheMS Chemistry Congress, Istanbul, 31 August - 4 September 2014*: F. D'Anna, P. Vitale, S. Marullo, C. Rizzo, R. Noto, "Self-assembly process of diimidazolium salts: the effect of the alkyl chain length and isomeric substitution".

9. Oral communication to *14th Anglo-Italian Meeting on Heterocyclic Chemistry, Windsor, 29 June-1 July 2014*: S. Marullo, F. D'Anna, C. Rizzo, P. Vitale, R. Noto, "Supramolecular aggregation of bis-imidazolium functionalised perylene bisimides".

10. Poster communication to *E-WISPOC (European Winter School of Physical Organic Chemistry) 2014, Bressanone, 2-7 February 2014*: C. Rizzo, F. D'Anna, S. Marullo, P. Vitale, R. Noto, "Functionalised Dicationic Imidazolium Ionic Liquids used as reaction media for base catalysed reactions".

11. Poster communication to *1^o EuChemS Congress on Green and Sustainable Chemistry, Budapest, 13-15 October 2013*: F. D'Anna, S. Marullo, C. Rizzo, P. Vitale, R. Noto, "Ionic liquids binary mixtures: promising reaction media for carbohydrates conversion in 5-HMF".

12. Oral communication to *Suprachem 2013, Italian Congress on Supramolecular Chemistry, Padova, 24-27 September 2013*: C. Rizzo, F. D'Anna, S. Marullo, P. Vitale, R. Noto, "Two-component hydrogels formed by host-guest interactions".

13. Poster communication to *XXXV Italian National Congress of Organic Chemistry, Sassari, 9-13 September 2013*: F. D'Anna, H. Q. N. Gunaratne, G. Lazzara, C. Rizzo, K. R. Seddon and R. Noto, "NMR Spectroscopic Characterization and Thermal Behaviour of a New Class of Dicationic Imidazolium Ionic Liquids".

14. Oral communication to *XXXVIII "A. Corbella" Summer School on Organic Synthesis, Gargnano (BS), 17-21 June 2013*: P. Vitale, F. D'Anna, S. Marullo, C. Rizzo, R. Noto, "Two components organogels as molecular recognition systems: properties, behavior and future applications".

15. Poster communication to *E-WISPOC (European Winter School of Physical Organic Chemistry) 2013, Bressanone, 27 January - 1 February 2013*: P. Vitale, F. D'Anna, S.

Marullo, C. Rizzo, R. Noto, “Diimidazolium-based Organic Salts as Low Molecular Weight Hydro- and Organogelators”.

16. Poster & flash communication to *12° SAYCS (Sigma Aldrich Young Chemists Symposium), Riccione, 1-3 October 2012*: C. Rizzo, F. D’Anna, G. Lazzara, S. Marullo, P. Vitale, R. Noto, “Properties study of ionogels formed by dicationic organic salts”.

17. Poster communication to *XXXIV Italian National Congress of Organic Chemistry, Pavia, 10-14 September 2012*: F. D’Anna, C. Rizzo, S. Marullo, P. Vitale, R. Noto, “Anion and ionic liquid effects on ionogel phases formation”.

18. Oral communication to *XIII RSC-SCI Joint Meeting on Heterocyclic Chemistry, Catania, 10-12 May 2012*: F. D’Anna, C. Rizzo, S. Marullo, P. Vitale, R. Noto, “Ionogels formed by geminal imidazolium salts: a preliminary investigation”.